CLOSED-FORM BACKCALCULATION ALGORITHMS FOR PAVEMENT ANALYSIS

BAGUS HARIO SETIADJI

NATIONAL UNIVERSITY OF SINGAPORE

2009

CLOSED-FORM BACKCALCULATION ALGORITHMS FOR PAVEMENT ANALYSIS

BAGUS HARIO SETIADJI

(B.Eng. (Hons.), ITB, Indonesia)

(M.Eng., ITB, Indonesia)

A THESIS SUBMITTED

FOR THE DEGREE OF DOCTOR OF PHILOSOPHY

DEPARTMENT OF CIVIL ENGINEERING

NATIONAL UNIVERSITY OF SINGAPORE

2009

ACKNOWLEDGEMENTS

In the name of Allah, the Most Gracious, the Most Merciful. All praises and thanks be to Allah who has provided the knowledge and guidance to the author in finishing this research work.

A deepest appreciation is expressed to the author's thesis advisor Professor Fwa Tien Fang for his invaluable assistance, supervision, and advice throughout the duration of the research. The author would also like to express his gratitude to National University of Singapore (NUS) for providing him the Research Scholarship and the opportunity to pursue the Doctoral degree program in Department of Civil Engineering.

The author would like to thank all my friends, Dr. Ong Ghim Ping Raymond, Dr. Lee Yang Pin Kelvin, Mr. Joselito Guevarra, Mr. Hendi Bowoputro, Mr. Kumar Anupam, Mr. Srirangam Santosh Kumar, Mr. Farhan Javed, Mr. Wang Xinchang, Mr. Qu Xiaobo, Ms. Yuan Pu, Ms. Ju Fenghua, Mr. Hadunneththi Rannulu Pasindu, Mr. Cao Changyong, and Mr. Yang Jiasheng for the support and friendship.

Gratitude is also extended to Mr. Goh Joon Kiat, Mr. Mohammed Farouk, Mr. Foo Chee Kiong, Mrs. Yap-Chong Wei Leng and Mrs. Yu-Ng Chin Hoe of the Transportation Engineering Laboratory.

A special appreciation is expressed to the author's parents, lovely wife, Amelia Kusuma Indriastuti, and sons, Bagus Jati Pramono and Bagus Dwisatyo Nugroho, for their patience, devotion and understanding given when the author was finishing the study in National University of Singapore (NUS).

TABLE OF CONTENTS

SUMMARY

Many backcalculation algorithms based on multi-layer elastic theory and plate theory were developed to backcalculate the layer moduli of a flexible and rigid pavement system, respectively. Unfortunately, they do not always give the unique answer due to the use of iterative trial and error approach in developing the algorithms. In this study, a development and evaluation of closed-form backcalculation algorithms was proposed. The aims of this research were to examine the merits of currently available closed-form backcalculation algorithms, and develop a procedure to derive the composite modulus of subgrade reaction (composite *k* value) for a rigid pavement with a subbase layer using a suitable closed-form backcalculation algorithm; and to develop a closed-form backcalculation algorithm for multi-layer flexible pavement system. The results showed that the closed-form backcalculation algorithm, NUS-BACK, was suitable to evaluate the layer moduli of an infinite- and finite-slab rigid pavement system. The next result produced was the relationship of two radius of relative stiffness of different foundation model, namely ℓ_k-ℓ_{Es} and ℓ_k-$\ell_{Es/sb}$ relationship, was suitable to determine *k* and composite *k* values from their respective layer moduli E_s; and E_s and E_{sb}. Another important achievement was the proposed closed-form backcalculation algorithms for three- and four-layer flexible pavement developed in this study, 3L-BACK and 4L-BACK, could produce slightly more accurate backcalculated moduli than those of other iterative-based backcalculation programs.

LIST OF TABLES

LIST OF FIGURES

NOMENCLATURE

a	Radius of loaded area
CBR	California Bearing Ratio
D	Flexural rigidity
E_c	elastic modulus of concrete slab
E_s	Elastic modulus of subgrade
E_{sb}	Elastic modulus of subbase
E_i	Elastic modulus of i^{th} layer (in flexible pavement system)
F	Deflection factor or Error function
FWD	Fallingweight Deflectometer
h	Layer thickness
k	modulus of subgrade reaction (for rigid pavement system) or ratio of layer moduli (ratio of E2 to E1 for flexible pavement system)
LTPP	Long term pavement performance
M_R	Resilient modulus
n	Ratio of layer moduli (ratio of E4 to E3 for four-layer flexible pavement system)
P	load
r	Distance of FWD sensor from the center of load
RMSE	Root mean square errors
RMSPE	Root mean square percentage errors
q	Ratio of layer moduli (ratio of E2 to E1 for three-layer flexible pavement or ratio of E3 to E2 for four-layer flexible pavement)
u	horizontal displacement
w_m	Measured deflection
w_c	Computed deflection

ℓ	Radius of relative stiffness
μ	Poisson's ratio
σz	Normal stress
τrz	Shear stress

CHAPTER 1

INTRODUCTION

1.1 Definition of Pavement Systems

Most pavements could be broadly classified into two categories, namely flexible and rigid pavements. A rigid or concrete pavement consists of a rigid slab typically designed based on a theoretically related analysis involving some empirical modifications to the Westergaard (1925) approach. Flexible pavements are represented by a pavement structure having a relatively thin asphalt wearing course overlying layers of granular base and subbase which are installed to protect the subgrade from being overstressed.

1.2 Rigid Pavement System

1.2.1 Background

A rigid pavement is in practice commonly constructed of Portland cement concrete slabs supported on a granular subbase overlying the subgrade soil. It is designed to withstand heavy axle-loads over a relatively long service life of as much as 40 years. The subgrade is an important part of the rigid pavement system having a major influence on the level of performance of the pavement, and how long the pavement can last without major repairs.

There are two approaches that are commonly used to model the subgrade soil, namely the dense liquid model and the elastic solid model. These two models represent the two extreme ends of the spectrum of behavior of the real soil. The liquid foundation, also called Winkler foundation, assumes that the vertical displacement of

the subgrade surface at any point is proportional to the vertical stress at that point, without shear transmission to its adjacent areas. The elastic solid model, first proposed by Boussinesq in 1885 (Huang, 2003), considers the soil as an elastic, homogenous and isotropic material. According to this model, a load applied to the surface of the foundation produces a continuous and infinite deflection basin.

In 1925, Westergaard introduced the term "modulus of subgrade reaction", widely known as the *k* value today, which is equal to the applied pressure required to produce a uniform unit deflection under a specified loaded area (Westergaard, 1925). In the early years, *k* was only used to represent the elastic characteristics of subgrade. However, after the first full-scale road test conducted in Arlington, USA, in 1930s, *k* was also used to characterize other layers above the subgrade, such as the subbase and base layers (Darter et al., 1995).

1.2.2 Significance of k Values in Design and Evaluation of Rigid Pavements

The concrete slab of a rigid pavement system is stiff and can distribute the applied load over a wide area. Because of its rigidity and ability to distribute the applied load effectively, structurally no additional layer is required between the slab and the subgrade.

In the early days of applications of rigid pavement systems, the design of the rigid pavement generally only consisted of two layers, i.e. concrete slab and subgrade soil. However, because of the joint pumping problem, this design became uncommon later. All rigid pavements today are practically constructed with a subbase layer to serve as a drainage layer and to protect the subgrade soil against pumping and other moisture-related distresses. Therefore, to take into account the contribution of the subbase layer in a rigid pavement system, the use of composite *k* value in pavement

design, instead of using only the k value of the subgrade soil, becomes a necessity today. Several major design methods in highway pavement, such as the AASHTO (1972) and PCA (1984), have used composite *k* values for the purpose of either new structural design or rehabilitation and overlay design (AASHTO, 1972, 1986, 1993; PCA, 1984). This indicates that the concept of composite *k* value is quite important in those types of design.

Because of the simplicity in its use and the input data required, the employment of the k value-based design methods are very popular. Generally, only two or three input parameters are required: some require only the modulus of subgrade reaction and the thickness of subbase (AASHTO, 1972; PCA, 1984); while others also require the modulus of subbase (AASHTO, 1986, 1993). For new construction design, the determination of the input data could be conducted by destructive methods (field test or laboratory test) and nondestructive methods (by measuring the responses of the pavement system under a test load). However, the results of composite *k* value determination using the different design methods are not consistent since each method only developed based on experimental experience for specific locations and for certain material types.

For rehabilitation and overlay design, the use of nondestructive test to determine the composite *k* value is more popular than destructive tests, because destructive tests are not practical for this type of design. In this type of design, the responses of the pavement under a test load will be employed as input to backcalculation analysis for the determination of the composite *k* value. Many backcalculation procedures and algorithms are available today. However, they tend to give different answers because of different simplifications and assumptions made in the modeling of the real pavement system.

1.3 Flexible Pavement System

1.3.1 Background

Boussinesq in 1885 introduced a theory of flexible pavement structure which was considered as a homogenous half-space. It means that the pavement system is only consisted of one layer which is infinite in its vertical and horizontal directions. The original theory by Boussinesq (1885) was based on a concentrated load applied on the system.

In 1943, Burmister developed a solution for multi-layer system by introducing a two-layer system (surface layer and subgrade) to represent a more appropriate model for flexible pavements that have more than one layer with better materials in the upper layers.

In 1945, Burmister extended the concept of multi-layer system by introducing a three-layer system (Burmister, 1945b). The system has an intermediate layer, namely base layer, between the surface layer and subgrade in order to construct economically a sufficiently thin thickness of surface layer and to provide adequate support against heavy loads by spreading the pressure over a weaker subgrade.

1.3.2 Multi-layered System in Design and Evaluation of Flexible Pavements

Theoretically, the assumptions mentioned in the previous section are only used to simplify the structural model of flexible pavement. It is known that the materials of base layer and subgrade are not homogenous and also nonlinear. It is also true that the surface layer should have weight, and not weightless at all. However, the use of those assumptions has a merit in developing the flexible pavement structure model. In contrast to rigid pavement system, all layers in flexible pavements are characterized by the same engineering parameter, i.e. the modulus of elasticity, E, rather than two

different parameters, that is, elastic modulus of concrete slab (E_c) and k, in rigid pavement systems.

Today, a flexible pavement consisted of three- or four-layer is used extensively. The use of three-layered models in pavement design can represent three layers with different ranges of elastic moduli, that is, surface layer (commonly contains asphalt materials), base layer (contains granular material) and subgrade (contains fine-grained soils). The use of an intermediate layer, which represents two layers, i.e. base layer and the subbase layer, in a three-layer model is also applicable. The second layer in the intermediate layer contains a lower-quality granular material and has purposes similar to the subbase layer in a rigid pavement system, that is, to minimize the intrusion of fines from subgrade into upper layer and to act as a drainage layer.

The four-layered system is more preferable to represent a multi-layer flexible pavement in practice. For new construction, the four-layer model is better than a three-layer one to represent the four layers commonly found in practice, i.e. surface layer, base layer, subbase layer and subgrade. Furthermore, a four-layer model is also more suitable to be used in overlay design, by assigning the overlay layer as top layer, followed by existing asphaltic-material layer as second layer, combination of base and subbase layers as the third layer and subgrade as the last layer.

Similar to the determination of composite k value in rigid pavement design, there are two methods to determine the layer elastic modulus E, i.e. destructive and nondestructive methods. For the destructive method, two tests are commonly used, namely triaxial compression test (for granular materials and fine-grained soils) and indirect tensile test (for asphaltic materials), while the deflection-based backcalculation algorithm is the most popular method to determine E in a nondestructive manner. Many backcalculation algorithms based on multi-layer elastic

theory have been used to backcalculate the layer moduli. Unfortunately, similar to the case of backcalculation analysis for rigid pavements, they do not always give the same answer due to the use of different approaches in developing the algorithms.

1.4 Objectives and Scope of Work

The main objectives of this research are: (a) to examine the merits of currently available closed-form backcalculation algorithms, and develop a backcalculation-based procedure to derive the composite *k* value for a rigid pavement with a subbase layer using a suitable closed-form backcalculation algorithm; and (b) to develop a closed-form backcalculation algorithm for a three-layer flexible pavement system, and another for a four-layer flexible pavement system.

The scope of work consists of the following components:

1. To evaluate the available existing closed-form and non-closed-form backcalculation algorithms for rigid pavements and assess their suitability for nondestructive determination of composite *k* value, addressing the issues of slab size, the choice of seed modulus values, and the choice of the forward deflection computation method.
2. To propose a procedure based on the backcalculation approach to determine the composite *k* value of a rigid pavement by means of deflection matching of equivalent pavement systems.
3. To perform a validation of the computed composite *k* value by the proposed procedure against actual measured field data reported in the literature.
4. To develop a forward calculation program for three- and four-layer flexible pavements respectively and perform a verification to examine the robustness of the program using hypothetical data.

5. To develop closed-form backcalculation methods of three- and four-layer flexible pavement systems respectively.
6. To perform verification of the proposed backcalculation algorithms of three- and four-layer flexible pavements using hypothetical data.

1.5 Organization of Thesis

Chapter 1 presents the background of the study highlighting the need for a rational analytical procedure to determine the composite *k* value of a rigid pavement and elastic modulus *E* of a multi-layer flexible pavement. The objectives and the main scope of work of this research are also presented.

Chapter 2 reviews the existing literature on *k* and *E* values, such as its definition, the methods of determination and factors affecting their determination. Special focus is placed on the determination of composite *k* value of rigid pavements and backcalculated *E* values of multi-layer flexible pavements, and the issues involved.

Chapter 3 presents comparisons of several closed-form backcalculation computer programs of concrete pavement using measured deflections from the database of the USA Long Term Pavement Performance (LTPP) Project (Elkin et al., 2003). The effect of finite slab size in backcalculation analysis of concrete pavement using the selected closed-form backcalculation program and four other different backcalculation programs are evaluated.

Chapter 4 presents the examination of existing k-E_s (E_s stands for elastic modulus of subgrade) relationships on rigid pavement system used in practice and the development of proposed k-E_s relationship by means of equivalent concepts, i.e.

equivalent *k*-model and equivalent E_s-model, and also equivalent *k*-model and equivalent E_s-model with subbase.

Chapter 5 presents the derivation of forward calculation solution for the determination of deflections of the three- and four-layer flexible pavement system, addressing the issue of robustness of the solution and comparing the results of the solution with that of other similar forward calculation programs.

Chapter 6 reviews the development of backcalculation algorithms for the determination of elastic moduli of the three- and four-layer flexible pavement system, respectively, addressing the issue of robustness of the program and comparing the results of the program with that of other backcalculation programs.

Chapter 7 presents the summary of research findings and recommendations for further research works.

CHAPTER 2

LITERATURE REVIEW

2.1 Introduction

In 1867, Winkler provided the conceptual model of a plate supported by a dense liquid foundation, with the assumption that this foundation will deflect under an applied vertical force in direct proportion to the force, without shear transmission or deflection to adjacent areas of the foundation not covered by the loaded area (Darter et al., 1995). The deflection under the load is assumed to be constant over the loaded area (see Figure 2.1).

The behavior of this type of foundation under a load is similar to that of a slab that is placed on an infinite number of spring, or that of water under a boat. According to Archimedes's principle, the weight of the boat is equal to the weight of water displaced. In other words, the total volume of displacement is proportional to the total load applied.

Using the analogy of this elastic spring behavior, Westergaard (1925) introduced the term "modulus of subgrade reaction", *k*, as the spring constant in the relationship between the contact pressure *p* at the bottom surface of the slab and the deflection of the foundation surface *w*, as given in Equation (2-1).

$$p = k \cdot w \qquad (2\text{-}1)$$

Because of the simplicity of the concept *k* value and its ability to simulate the actual behavior of rigid pavements with sufficient accuracy adequate for practical applications, liquid foundation is still being used widely today by pavement engineering practitioners and researchers. Researchers (Darter et al., 1995,

Khazanovich and Ioannides, 1993) have reported that for slabs on a natural soil subgrade or a granular subbase, the model can calculate accurately the responses of slab at its edges and corners, which are where the most critical stresses in the pavement would be located.

In the event that a subbase layer is provided, the use of Equation (2-1) in pavement design or overlay design requires that a composite *k* value that combines the structural response of the subgrade and the subbase layer to be evaluated. Practically all concrete pavements constructed today comprise a subbase layer to facilitate subsurface drainage and prevent joint pumping. The determination of composite *k* values is an important element of the concrete pavement design process.

On the other hand, the concept of elastic layered theory was introduced by Burmister (Burmister, 1943) as an improvement to the theory of flexible pavement as a homogenous half-space by Boussinesq (Boussinesq, 1885). The elastic layered theory is more appropriate to represent the actual pavement system since a flexible pavement system should not be consisted of only one layer of a homogenous mass, but should have multi layers with better materials on top because the intensity of stress is high on the upper layer of the pavement system, and inferior materials at the bottom where the intensity is low.

Firstly, Burmister introduced a concept of a pavement system with two layers in 1943 (Burmister 1943; 1945a), and then the concept was extended to a three-layer pavement system in 1945 (Burmister 1945b). The concept of the three-layer flexible pavement system could be extended to *n*-layer pavement system, but the following basic assumptions of the multi-layer pavement system should be satisfied (Burmister, 1943; 1945a):

a. each layer is homogenous, isotropic, and linearly elastic with an elastic modulus E and a Poisson ratio μ;

b. the surface layer is weightless and infinite in extent in the horizontal direction, but finite in vertical direction. The subgrade is infinite in extent in both horizontal and vertical directions;

c. the surface layer should be free of shearing stress and normal stress beyond the surface loading. The subgrade should be free of stress and displacement at infinite depth; and

d. continuity conditions at layer interfaces are satisfied.

The use of an assumption that layered elastic theory is infinite in the horizontal direction means that this theory cannot be applied to evaluate the rigid pavement system with transverse joint. This theory is also inapplicable to rigid pavement when the loads are less than 0.6 or 0.9 m from the pavement edge (Huang, 2003).

2.2 Determination of Layer Moduli

2.2.1 Direct Test Methods

2.2.1.1 *k* and Composite *k* Value of Rigid Pavement System

Destructive methods are the earliest approach used to measure the modulus of pavement layer, especially the modulus of subgrade reaction, i.e. the *k* value. By these methods, all layers above the subgrade must be removed to form an open pit before a measurement can be made. A common procedure used in the early days is the plate load test that includes the non-repetitive static plate load test (ASTM D1196-93 and AASHTO T222-81) and the repetitive static plate load test (ASTM D1195-93 and AASHTO T221-90). One main drawback of these methods is that a simulation of

subgrade at various moisture contents and densities to find out the worst condition of subgrade is almost impossible.

Besides *k* value, the composite *k* value also can be determined using these two tests, particularly for the design of new road construction. There are several methods used to determine composite *k* value based on the measured layer moduli, such as the AASHTO (American Association of State Highway and Transportation Officials) and PCA (Portland Cement Association) methods described in the following paragraphs.

The AASHTO method is one of the most widely used methods in pavement design today. The early version of AASHTO method (the 1972 AASHTO Interim Guide) provided a procedure to determine composite *k* value using a nomograph with subbase stiffness and modulus of subgrade reaction as its input values (see Figure 2.2). The later version of the AASTHO method (the 1986 Design Guide and then replaced by the 1993 Design Guide) modified the nomograph by replacing one input value, that is, the modulus of subgrade reaction with the subgrade resilient modulus (M_R), and adding a new input value, thickness of subbase layer (Figure 2.3). The resilient modulus used to compute the composite *k* value is based on a plate load test using a base of 30-in (762 mm) diameter. Huang (2003) stated that this procedure is misleading and will result in stresses and deflections that are too small.

The PCA procedure expresses the composite *k* value as a function of the subgrade soil *k* value, base thickness, and base type (granular or cement treated) (PCA, 1984). Tables 2.1 and 2.2 list the PCA recommended composite *k* values for untreated base and cemented treated base respectively. The values shown in Table 2.1 were derived by applying the Burmister (1943) theory of two-layer systems to the results of plate load tests on subgrades and sub-bases of full-scale test slabs (Childs, 1967).

This method has a main drawback in that the accuracy of the composite *k* values interpolated from the values in the tables is not known, and extrapolation beyond the range of the given values is questionable. Another disadvantage of this method is that the modulus of subbase is unknown for both types of subbase (untreated and cemented treated subbase).

2.2.1.2 Elastic Layer Moduli of Flexible Pavement System

All materials in a flexible pavement system are typically characterized by elastic modulus or resilient modulus. The resilient modulus (M_R) is the elastic modulus based on the recoverable strain under repeated loads (Huang, 2003), defined as

$$M_R = \frac{\sigma_d}{\varepsilon_r} \tag{2-2}$$

in which σ_d is the deviator stress and ε_r is the recoverable strain.

Under traffic loading, most pavement materials are considered to behave elastically since the deformation under the small load (compared with the strength of material) and repeatable loading is nearly completely recoverable. This is the reason why the term elastic modulus is more frequently used than resilient modulus.

Different procedures are adopted to measure the elastic moduli of different materials, such as the resilient modulus test for unbound granular base/subbase materials and subgrade soils using the repeated load triaxial test (AASTHO T 294-92 or known as SHRP Protocol P46), and the resilient modulus test for asphalt mixtures using indirect tension test (ASTM D4123-82 and the revised ASTM WK3751).

The use of elastic modulus to characterize pavement materials has practical benefits, especially for determining the elastic modulus of the subgrade. The resilient modulus test is faster and less expansive than plate loading test. In addition, the same

sample of the layer materials can be used for many tests under different loading and environmental conditions. This might be the reason for the AASHTO method to replace the use of the modulus of subgrade reaction in the 1972 Interim Guide with resilient modulus in the 1986 and 1993 Design Guide.

2.2.2 Correlation with Other Engineering Properties

Since the destructive methods are time-consuming and expensive, nowadays the *k* value is generally estimated by correlation to properties that can be determined by simpler tests. These include such the California Bearing Ratio (*CBR*) (Darter, 1995; Hall et al., 1995), the elastic modulus (*E*) and resilient modulus of the subgrade (M_R).

The correlation between *k* value and *CBR* developed by the Corps of Engineers, USA, was first published by Middlebrooks and Bertram (1942). Approximate relationships between the *k* value and *CBR* were also provided by PCA (1966), as seen in Figure 2.4. The relationships between *k* value and other soil properties are also depicted in the figure.

The correlation between the modulus of subgrade reaction (*k* value) and the elastic modulus of subgrade (*E*) is practically useful. For instance, *k* value can be related to elastic modulus and Poisson's ratio of the solid foundation (E_f and μ_f) so that the property of a liquid foundation can be derived from elastic analysis, thus resulting in a simplification in calculation and saving of computational time. Vesic and Saxena (1974) suggested the use of the following correlation:

$$k = \left(\frac{E_f}{E_c} \right)^{1/3} \frac{E_f}{\left(1-\mu_f^2\right)h} \tag{2-3}$$

in which E_c is the elastic modulus of concrete and *h* is the thickness of the slab. This equation is applicable only to loads in the interior of a slab (Huang and Sharpe, 1989).

For computing deflections, Vesic and Saxena (1974) suggested that the *k* value be taken as 42% of the value obtained from Equation (2-3).

The correlation between *k* value and the resilient modulus of subgrade can be derived using the definition of *k* value, that is, the ratio between an applied pressure (*p*) and the deflection (*w*) as shown by Equation (2-4).

$$k = \frac{p}{w} \tag{2-4}$$

The deflection of a plate on a solid foundation at the center of the slab (w_0) can be determined by the following equation:

$$w_0 = \frac{\pi\left(1-\mu^2\right)pa}{2E} \tag{2-5}$$

Substituting Equation (2-5) into (2-4) and replacing E with M_R will yield the following equation:

$$k = \frac{2M_R}{\pi\left(1-\mu^2\right)a} \tag{2-6}$$

in which μ is the Poisson's ratio of the foundation and a is the radius of the plate.

Another important correlation is one between resilient modulus and other engineering properties, as developed by Van Til et al. (1972) (see Figure 2.5). This correlation is important especially if only empirical tests, such as CBR test, stabilometer test, and so forth, are available. However, great care should be exercised since such empirical tests measure the strength of the materials and not their elastic properties. In addition, this empirical correlation is derived based on local conditions.

2.2.3 Non-destructive Test (NDT) Methods

NDT methods, as the name implies, leave the pavement structurally intact. Deflection based methods are by far the most commonly adopted approach today. In

these methods, deflection basins could be produced using NDT equipment such as steady-state vibratory devices or falling load deflectometers that produce impulse loads (Fwa, 2006). With the measured deflection basins, appropriate backcalculation algorithms can be employed to estimate the engineering properties of various pavement layers, including the subgrade soil. A detailed description of the different backcalculation approaches in use today is presented in Section 2.3. NDT methods have been used to evaluate the structural capacity of in-situ pavements (Pradhan, 1999), the load transfer efficiency across joints and cracks in concrete pavements (Jackson et al., 1994; McCullough and Taute, 1982), layer properties of in-service concrete pavements (Li et al., 1996), and to detect the locations and extents of voids under concrete slabs (Crovetti and Darter, 1985).

Past studies have indicated that the results of NDT in the determination of the layer moduli could be affected by the rate of loading, as well as other loading conditions such as the magnitude and duration of loading. The moduli in certain soil types, such as cohesive saturated soils, may be substantially higher under rapid loading (e.g. moving vehicle) than under slow loading. This is because under rapid loading, pore water pressure is not fully dissipated. In NDT methods, the application of inappropriate loading rate may occur and yield unexpected results. For instance, the modulus of subgrade reaction determined from static load tests may not adequately represent the actual condition under moving traffic (Darter et al, 1995). Hall and McCaffrey (1994) applied NDT at an airport and indicated that failure in the pavement evaluated was due to the application of a faster rate of loading on the pavement used as a parking area. Matsui et al. (2000) found that the measured data based on static and dynamic loads actually were not significantly different although this finding was contrary to what they obtained using numerical simulations. Roesset and Shao (1985)

reported that differences produced by static and dynamic loadings were insignificant when the subgrade thickness was more than 11.48 m.

Under the real condition, pavement structures are subjected to different magnitudes of loads. However, under different loading, the layer moduli would not be significantly different if the pavement system was truly linear elastic (Grogan et al., 1998). Grogan et al. (1998) stated that for rigid pavements, the layer moduli tend to be independent of load level, but not for flexible pavement. Similar results are also found by Hall et al. (1996) that if the load level is sufficiently large, *k* value usually does not depend on the load level.

The measured layer moduli may also be dependent on the duration of loading. Subgrade deformation may be time-dependent. Teller and Sutherland (1943) observed that for a given load applied to the bearing plate of the load testing apparatus, the displacement of the plate continued for a long time before a complete equilibrium was reached. It follows then that in reality, the selection of the duration of the test load must be carefully made in order to obtain an appropriate evaluation of the *k* value.

It is important for a NDT device to apply a loading condition (magnitude and duration) similar to that of the actual traffic. It is generally agreed that among all the currently available NDT devices, the Falling Weight Deflectometer (FWD) is the best device developed so far to simulate the magnitude and duration of actual moving loads (Lytton, 1989).

2.3 Backcalculation Algorithms for Layer Moduli

One of the most useful applications of NDT testing is to backcalculate the elastic moduli of pavement components. Backcalculation analysis can be classified into several categories, depending on the type of load representation and the type of

material characterization. Among all the types of backcalculation methods, the static linear backcalculation is generally preferred in the majority of pavement backcalculation studies because of its simplicity and acceptable error ranges (Goktepe et al., 2006).

Fwa (1998), Harichandran et al. (1994) and Goktepe et al. (2006) provided detailed descriptions of the various approaches of the static linear backcalculation currently available for the purpose of backcalculation analysis. One approach makes use of theoretical closed-form solutions to directly compute the elastic modulus of each layer by using layer thickness and deflections from one or more sensors (Li et al., 1996; Fwa et al., 2000). Another approach of backcalculation applies some form of iterative process that varies the various pavement layer moduli until a sufficiently close match between the computed and measured deflections is obtained (Hall et al., 1996; Khazanovich et al., 2000; Almedia et al., 1994). A third approach relies on an appropriate database that pre-calculates solutions based on measured deflections for a large number of pavement sections, and stores them in an organized database. The pavement structure in the database that has its deflection basin that best matches the measured deflection basins is picked as the solution. This approach is often termed as database search algorithm (Lytton, 1989; Uzan, 1994; Tia et al., 1989). The fourth approach is regression-equation based methods that relate surface deflections to pavement layer moduli using statistical regression techniques (Fwa and Chandrasegaran, 2001; Harichandran et al., 1994).

Huang (2003) commented that most of the second and third approaches of the backcalculation programs generally calculate the elastic modulus of the subgrade first using the outer sensor deflections, as it is known that the subgrade properties affect almost entirely the deflection measured by the sensor farthest from the load (Irwin et

al., 1989; Almedia et al., 1994). Once the elastic modulus of the subgrade is calculated, it is used as an input for the backcalculation of the moduli of the overlying layers.

Brief descriptions of backcalculation algorithms for both rigid and flexible pavements are given in the following sub-sections.

2.3.1 Closed-form Algorithms

2.3.1.1 ILLI-BACK

ILLI-BACK is a closed-form algorithm proposed by Hoffman and Thompson (1981) for calculation of pavement properties of an infinite rigid pavement slab supported directly on the subgrade. It is also known as the AREA method. *AREA* is a parameter defined by following equation:

$$AREA = \frac{1}{2\,w_0}\left[w_0\,r_1 + \left(\sum_{i=1}^{n-1} w_i\,(r_{i+1} - r_i)\right) + w_n\,(r_n - r_{n-1})\right] \quad (2\text{-}7)$$

in which w_i is the measured deflection at point i (i = 0, n), n is the number of FWD sensors minus one, and r_i is the distance between the center of the load plate and the sensor at point i. The *AREA* parameter is not truly an area, but has a dimension of length since it is normalized with respect to one of the measured deflections in order to remove the effects of load magnitude. Ioannides et al. (1989) found the following unique relationship between *AREA* and the radius of relative stiffness (ℓ),

$$\ell = \left(\frac{\ln\left(\frac{A - AREA}{B}\right)}{C}\right)^{D} \quad (2\text{-}8)$$

in which the values for *A*, *B*, *C* and *D* are given in Table 2.3.

Using this relationship, the layer moduli (E_c and k values) can be calculated using the following formulas,

$$k = \left(\frac{P d_r^*}{d_r \ell^2} \right) \tag{2-9}$$

$$d_r^* = x e^{\left(-y e^{(-z\ell)}\right)} \tag{2-10}$$

$$\ell = \left[\frac{E_c \, h^3}{12\left(1 - \mu^2\right)k} \right]^{0.25} \tag{2-11}$$

in which P is the applied NDT load; d_r is the measured deflection at radial distance r; d_r* is a non-dimensional deflection coefficient for radial distance r; μ is the Poisson's ratio of the concrete slab; and x, y and z are numerical constants as shown in Table 2.4.

Using a four-sensor configuration, Ioannides et al. (1989) developed a closed-form backcalculation computer program known as ILLI-BACK for a two-layer concrete pavement system. Hall et.al. (1996) applied the same approach using both a four- and a seven-sensor configuration to backcalculate pavement layer moduli for rigid pavements. The Strategic Highway Research Program (SHRP) (Hall et al., 1995) adopts a seven-sensor configuration with sensors located at 0, 203, 305, 457, 610, 914 and 1524 mm from the center of load and a four-sensor configuration with sensors located at 0, 305, 610 and 914 mm from the center of load. For convenience, ILLI-BACK4 and ILLI-BACK7 are used to denote the ILLI-BACK computer programs based on the four- and seven-sensor configuration, respectively. The ILLI-BACK7 based on the seven-sensor configuration has been adopted by the 1993 AASHTO Guide (AASHTO, 1993).

The ILLI-BACK algorithm offers a straight-forward computation for backcalculation of rigid pavement properties and gives good results in conditions similar to that established for the algorithm. However, several limitations related to its

rigid solution scheme and its inability to handle measurement errors effectively were identified by Li et al. (1996) as follows:

a. Equation (2-7) shows that the parameter *AREA* is normalized by deflection w_0. The reason for ILLI-BACK to choose w_0 as the normalizing deflection value is unclear. Li et al. (1996) has demonstrated that the selection of other deflection as normalizing deflection value could affect the computed results.

b. The use of equations in ILLI-BACK algorithm, such as Equations (2-8) and (2-10), is limited to certain sensor locations, as shown in Table 2.3 and 2.4. Any interpolation to estimate non-dimensional deflection coefficients for radial distances not listed in Table 2.4 is not advisable.

c. ILLI-BACK formulation has a built-in weighting scheme represented by the deviation of sensor offset from the center of the load plate (see Equation (2-7)). In real-life situations where measurement errors are involved in deflection input, it is unlikely that the scheme of weighting factors used by ILLI-BACK would always produce the best results (Li et al., 1996).

2.3.1.2 NUS-BACK

NUS-BACK is another closed-form solution for backcalculation of rigid pavement properties (Li et al., 1996). Like ILLI-BACK, it considers a two-layer system of an infinite slab supported on either a Winkler or a solid foundation. The Poisson's ratio and layer thicknesses of the pavement system are assumed to be known. The two remaining unknowns, the elastic modulus of the pavement slab and the *k* value, can be calculated using any two measured deflections provided by a NDT device, as shown in the following equations,

$$w_{mi} = f_i(k, E_c) \quad \text{(2-12a)}$$

$$w_{mj} = f_j(k,E_c) \qquad (i \neq j) \tag{2-12b}$$

in which w_{mi} and w_{mj} are surface deflections measured by sensors i and j respectively.

To backcalculate the pavement layer properties, the following two equations are considered,

$$w_{mi} - w_{ci} = 0 \quad 1 \leq i \leq N \tag{2-13a}$$

$$w_{mj} - w_{cj} = 0 \quad 1 \leq j \leq N, \; i \neq j \tag{2-13b}$$

in which w_{ci} and w_{cj} are the calculated deflections for points i and j, respectively. The formulas for computing w_{ci} and w_{cj} are as follows,

$$w_{ci} = \frac{P}{k\,\pi\,a^2} F_{ki} \tag{2-14a}$$

$$w_{cj} = \frac{P}{k\,\pi\,a^2} F_{kj} \tag{2-14b}$$

$$F_{ki} = \frac{a}{\ell} \int_0^\infty \frac{J_0\left(\frac{r_i}{\ell} t\right) J_1\left(\frac{a}{\ell} t\right)}{1+t^4} dt \tag{2-15a}$$

$$F_{kj} = \frac{a}{\ell} \int_0^\infty \frac{J_0\left(\frac{r_j}{\ell} t\right) J_1\left(\frac{a}{\ell} t\right)}{1+t^4} dt \tag{2-15b}$$

in which P is the applied load; a is the radius of loading plate; r_i and r_j are the horizontal distances of sensor i and j respectively from the load; F_{ki} and F_{kj} are the deflection factors; J_0 and J_1 are the Bessel functions of the first kind of order zero and order one, respectively; ℓ is the radius of relative stiffness; and t is a dummy variable.

For N number of sensors, Equation 2.13 gives $N(N\text{-}1)/2$ number of independent nonlinear equations as follows,

$$w_{mi}F_{kj} - w_{mj}F_{ki} = 0 \tag{2-16}$$

Solving these nonlinear equations will give $N(N\text{-}1)/2$ numbers of ℓ values. $N(N\text{-}1)/2$ pairs of k and E_C can be calculated using Equation (2-11). The last step is to calculate the mean values of backcalculated k and E_C, respectively.

It is important to note that, even though it is possible to use $N(N\text{-}1)/2$ number of two-sensor configurations, the choice of sensor configuration becomes important when errors are involved in the deflection measurements. Two different two-sensor configurations are introduced in backcalculating moduli using NUS-BACK. The first configuration is the use of deflections from a combination of the first sensor and any other sensor to backcalculate slab modulus. This configuration is proposed because the deflections measured by sensors closer to the load are dominated by the effect of slab properties. On the other hand, for the sensor furthest away from the load, the deflection depends almost entirely on the subgrade properties (Irwin et al., 1989; Almedia et al., 1994). Hence a combination of the last sensor and any other sensor is often used to backcalculate the k value.

NUS-BACK offers speedy computation for backcalculation rigid pavement properties by solving directly two unknowns in the deflection equation shown in Equations (2-12a) and (2-12b). It always gives a unique solution. However, due to the flexibility of the algorithm to use any two-sensor configuration, engineering judgment of the user is sometimes required to select a two-sensor configuration that provides the best result among $N(N\text{-}1)/2$ combinations.

2.3.1.3 2L-BACK

The backcalculation program 2L-BACK (Fwa and Rani, 2005) gives closed-form backcalculated solutions of layer moduli of a two-layer flexible pavement. It is based on the forward solution developed by Burmister (1943; 1945a) that permits one to

compute the deflection, w_i, of a point i in the pavement surface at the radial distance, r_i, from the center of the loaded area by the following expression,

$$w_i\, r_i\, E_1 = \frac{3P}{4\pi} F_i \qquad (2\text{-}17)$$

where E_1 is the elastic modulus of the surface layer of the pavement, P the total applied load, and F_i a deflection factor which is a function of the thickness of the surface layer, the radial distance r_i, and the ratio of the elastic moduli of the pavement surface layer and the subgrade, as given by the equation below,

$$F_i = \int_{x=0}^{\infty} \left(\frac{1 + 4Nme^{-2m} - N^2 e^{-4m}}{1 - 2N(1+2m^2)e^{-2m} + N^2 e^{-4m}} \right) J_o(x)\, dx \text{ , with } x = \frac{m\, r_i}{h} \text{ and } N = \frac{1-\theta}{1+\theta} \qquad (2\text{-}18)$$

where $J_o(x)$ is the Bessel function of the 0^{th} order, m is a continuous variable of integration, h the thickness of the surface layer, and θ the ratio given by (E_2/E_1), E_2 and E_1 are respectively the elastic moduli of the subgrade and the overlying pavement structure.

The program 2L-BACK solves for the two unknown E_1 and E_2 by considering the deflection equations at any two points i and j as follows,

$$w_i\, r_i\, E_1 = \frac{3P}{4\pi} F_i \qquad (2\text{-}19)$$

$$w_j\, r_j\, E_1 = \frac{3P}{4\pi} F_j \qquad (2\text{-}20)$$

Combining the two equations, we have

$$w_i\, F_j - w_j\, F_i = 0 \qquad (2\text{-}21)$$

It is noted that in the above equation, θ is the only unknown which can be solved by the bisection method (Matthews and Fink, 2004). Once θ is known, E_1 can be computed from either Eq. (2-19) or Eq. (2-20), and E_2 is given by θ times E_1. The

execution time of the backcalculation analysis on personal computer Pentium 4 with a clock speed of 2.4 GHz is less than one second.

The 2L-BACK program is applied for analysis of pavement by representing a typical multi-layer flexible pavement as an equivalent equal-thickness two-layer system as shown in Figure 2.6. While the subgrade representation is identical to that in the actual pavement, the overlying pavement structure is now represented in the equivalent pavement system by an equivalent structural layer with an elastic modulus of E_e, a Poisson's ratio of μ_e and equivalent thickness (h_t). The thickness h_t of the equivalent pavement structure is equal to the sum of the layer thicknesses of the actual pavement, i.e. $h_t = (h_1 + h_2 + h_3)$. In a similar manner, to evaluate the surface layer, the surface representation is identical to that in the actual pavement and the underlying pavement structure is represented by an equivalent pavement layer with characterized by equivalent elastic modulus E_e, a Poisson's ratio of μ_e, and infinite thickness. As a two-layer pavement model, 2L-BACK cannot be used to estimate the moduli of intermediate layers between surface and subgrade.

2.3.2 Trial-and-Error Best Fit Algorithms

The trial-and-error best fit method is an iterative optimization backcalculation method with an objective function to minimize an error function. Equation (2-22) shows a common form of error function used in backcalculation of rigid pavement properties.

$$F\left(\ell_k, k, E_c\right) = \sum_{i=0}^{n} \alpha_i \left(w_{ci} - w_{mi}\right)^2 \qquad (2\text{-}22)$$

where α_i are weighting factors, w_{ci} is the calculated deflection for point i, w_{mi} is the measured deflection at point i, and n is the total number of sensors. Different best fit

backcalculation algorithms have been used by highway agencies and researchers. The following subsections highlight three such algorithms.

2.3.2.1 ERESBACK

ERESBACK is computer program that solves for a combination of the radius of relative stiffness of the pavement slab and the modulus of subgrade reaction that produces the best possible agreement between the predicted and measured deflections at each sensor (Hall et al. 1996, Khazanovich et al., 2000).

ERESBACK sets the weighting factors defined in Equation (2-22) equal to 1 or $(1/w_{mi})^2$. Using the relationship between the calculated deflection, w_c, and load, p, an error function F of the following form was adopted:

$$F\left(\ell_k, k\right) = \sum_{i=0}^{n} \alpha_i \left(\frac{p}{k} f_i\left(l_k\right) - w_{mi} \right)^2 \tag{2-23}$$

To obtain the minimum value of the error function F, the following conditions should be satisfied:

$$\frac{\partial F}{\partial k} = 0 \tag{2-24a}$$

$$\frac{\partial F}{\partial \ell_k} = 0 \tag{2-24b}$$

Substitution of the error function equation into Equations (2-24a) and (2-24b) yields the following equation for the k value and the radius of relative stiffness,

$$k = p \frac{\sum_{i=0}^{n} \alpha_i \left(f_i\left(l_k\right)\right)^2}{\sum_{i=0}^{n} \alpha_i W_i f_i\left(l_k\right)} \tag{2-25}$$

$$\frac{\sum_{i=0}^{n} \alpha_i \, f_i\,(l_k) f_i^{'}(l_k)}{\sum_{i=0}^{n} \alpha_i \, (f_i(l_k))^2} = \frac{\sum_{i=0}^{n} \alpha_i \, w_{mi} \, f_i^{'}(l_k)}{\sum_{i=0}^{n} \alpha_i \, w_{mi} \, f_i \,(l_k)} \quad (2\text{-}26)$$

Hall et al. (1996) and Khazanovich et al. (2000) found that the best fit algorithm based on four sensors (0, 305, 610 and 914 mm) was better than other sensor configurations. Hall et al. (1996) compared the results produced by ERESBACK, and those by the two AREA backcalculation algorithms, ILLI-BACK4 and ILLI-BACK7 (see Section 2.3.1). In all the cases analyzed, it was found that the AREA methods produced slightly higher *k* values than the best fit method. Between the results by the two AREA-based backcalculation algorithms, those produced by ILLI-BACK7 exhibited closer relationship with those by ERESBACK. ILLI-BACK7 was recommended to be used if the ERESBACK program is not available.

ERESBACK developed the backcalculation method with a sound theoretical basis. However, the use of four sensor configuration in this program becomes an important issue. It is not proved yet that the use of four sensor configurations in this program is rigorous enough to handle the deflection basins that are not following the gradually decreasing pattern. Therefore, the users have to examine the pattern of the deflection basins before using this method.

2.3.2.2 MICHBACK

MICHBACK is a multi-layer elastic theory backcalculation program developed by Michigan State University. It adopts CHEVRONX (an enhanced version of the widely-used CHEVRON program) as its forward-calculation program and uses a modified Newton's method to improve the speed of convergence (Harichandran et al., 1994). The modification of the Newton's method consists of a logarithmic

transformation of the surface deflections and layer moduli. In this method, the i^{th} incremental corrections to the logarithm of the unknown moduli and layer thicknesses are obtained by computing the least-squares solution of the over-deterministic system of linear equations as follows.

$$[G]^i \begin{Bmatrix} \{\Delta(\log E)\}^i \\ \{\Delta t\}^i \end{Bmatrix} = \{\log w\} - \{\log \hat{w}\}^i \tag{2-27}$$

where:

$$[G]^i = \begin{bmatrix} \frac{\partial(\log w_1)}{\partial(\log E_1)} \cdots \frac{\partial(\log w_1)}{\partial(\log E_n)} & \frac{\partial(\log w_1)}{\partial t_1} \cdots \frac{\partial(\log w_1)}{\partial t_p} \\ \vdots \quad \vdots & \vdots \quad \vdots \\ \frac{\partial(\log w_m)}{\partial(\log E_1)} \cdots \frac{\partial(\log w_m)}{\partial(\log E_n)} & \frac{\partial(\log w_m)}{\partial t_1} \cdots \frac{\partial(\log w_m)}{\partial t_p} \end{bmatrix} \quad \{E\} = \{\hat{E}\}^i, \ \{t\} = \{\hat{t}\}^i \tag{2-28}$$

= gradient matrix of partial derivatives of the logarithm of the *m* surface deflections, with respect to the logarithm of the *n* unknown moduli and *p* unknown layer thickness; evaluated using the current moduli, $\{\hat{E}\}^i$, and thicknesses, $\{\hat{t}\}^i$;

$\{\Delta(\log E)\}^i$ = vector of corrections to the logarithm of the i^{th} estimate of the moduli;

$\{\Delta t\}^i$ = vector of corrections to the i^{th} estimate of the thicknesses;

$\{\log w\}$ = vector of logarithm of measured surface deflection;

$\{\log \hat{w}\}^i$ = vector of logarithm of surface deflections computed by a mechanistic analysis program using the i^{th} estimate of the moduli and thicknesses.

One technique for solving the least-squares problem is to solve the *n* x *n* normal equations.

$$[G]^T [G] \begin{Bmatrix} \{\Delta(\log E)\}^i \\ \{\Delta t\}^i \end{Bmatrix} = [G]^T \left[\{\log w\} - \{\log \hat{w}\}^i \right] \quad (2\text{-}29)$$

The gradient matrix is computed numerically and requires ($n + p + 1$) calls to the forward calculation program during each iteration. The iteration is terminated when the changes in the layer moduli are sufficiently small.

MICHBACK program requires seed moduli to initiate the backcalculation process. The program has two options regarding with the determination of the seed moduli, that is, by internal program or by user-input. A minimum of five deflections is required by MICHBACK program for backcalculation process

The use of modified Newton method is easy to be developed for any type of problems to optimize the objective function. The main shortcoming of this method is that the multi-dimensional surface represented by the objective function may have many local minima, and as a result the minimum to which a numerical procedure converges may depend on the selection of the initial seed moduli (Harichandran et al., 1994)

2.3.2.3 EVERCALC

EVERCALC is a backcalculation program using a nonlinear least-squares optimization technique with CHEVRONX as the forward calculation program. An efficient and general minimization method (Levenberg-Marquardt algorithm) has been implemented in EVERCALC, which makes it converge quickly with only a small number of calls to the mechanistic analysis program (Sivaneswaran et al., 1991). The algorithm of EVERCALC program is as follows.

If the relative error at location *i* is represented by

$$r_i(E,h) = \frac{d_i^c(E,h) - d_i^m}{d_i^m} \tag{2-30}$$

where $d_i^c(E,h)$ is the calculated deflection at location *i* based on *E* and *h*, *E* is the unknown layer moduli, *h* is the unknown layer thicknesses, and d_i^m is the measured deflection at location *i*. After multiplying by the constant *n* for convenience, the criterion function can be expressed as:

$$f(E,h) = \sum_{i=1}^{n} [r_i(E,h)]^2 = r^T r \tag{2-31}$$

in which *r* is the relative error (residual) or $\{r_1, r_2, r_3, \ldots, r_n\}$. Then the gradient of the criterion function is given by

$$\nabla f(E,h) = 2Ar \tag{2-32}$$

where A = $\{\nabla r_1, \nabla r_2, \nabla r_3, \ldots, \nabla r_n\}$, and the Hessian can be expressed by

$$H = \nabla^2 f(E,h) = 2AA^{\mathrm{T}} + 2\sum_{i=1}^{n} r_i \nabla^2 r_i \tag{2-33}$$

As the second part of the Hessian may be negligibly small, Equation (2-33) could be approximated by

$$H \approx 2AA^{\mathrm{T}} \tag{2-34}$$

A solution can be obtained by incorporating the approximated Hessian into the Levenberg-Marquardt algorithm (Lavenberg, 1944; Marquardt, 1963).

The program produces a solution when the summation of the absolute values of the discrepancies between the measured and theoretical surface deflection falls within a predetermined allowable tolerance. Similar to the MICHBACK backcalculation program, a set of seed moduli is required to start the backcalculation analysis. The seed moduli may be determined by internal program or by user-input. However, EVERCALC only permits user to generate the seed moduli using the internal program

if the number of pavement layer in the backcalculation process equals or less than three layers.

The drawbacks of this program are as follows.

a. Like most of other iterative optimization method, the results produced by this method are sometimes not the global optimal solution.

b. Engineering judgment is required to determine the seed moduli if the pavement system consists of more than three layers.

2.3.3 Regression Method

The use of regression method to backcalculate *k* value allows almost instantaneous computation of the moduli once the measured deflections are known (Fwa and Chandrasegaran, 2001; Harichandran et al., 1994).

In their application of the regression technique to backcalculate *k* value, Fwa and Chandrasegaran (2001) employed the NUS-BACK algorithm to backcalculate the radius of relative stiffness (ℓ) based on the dimensionless ratios of measured deflections at different points of the deflection basins. Having computed ℓ, the *k* value was determined as a function of ℓ, the measured deflections, and the applied load, *P* as follows,

$$\ell = f_1(d_1, d_2, d_3, d_4, d_5, d_6, d_7) \quad \text{(2-35a)}$$

$$k = f_2(\ell, P, d_1, d_2, d_3, d_4, d_5, d_6, d_7) \quad \text{(2-35b)}$$

in which d_1, d_2, d_3, d_4, d_5, d_6 and d_7 are the measured deflections at radial distances of 0, 300, 600, 900, 1200, 1500 and 1800 mm respectively from the center of loading.

The database for the development of the regression model was established by forward computation of deflections for the practical ranges of the various pavement properties. The final regression models take the following forms,

$$\log \ell = 0.023 - 0.251\log(d_2/d_1) - 0.003\log(d_3/d_1) + 0.030\log(d_4/d_1) + 0.429\log(d_5/d_1) - 0.003\log(d_6/d_1) - 1.360\log(d_7/d_1) \quad \text{(2-36a)}$$

$$\log k = -0.902 - 2.001\log \ell + 0.999\log \text{P} - 0.413\log d_1 - 0.319\log d_2 - 0.363\log d_3 - 0.136\log d_4 + 0.128\log d_5 + 0.136\log d_6 - 0.033\log d_7 \quad \text{(2-36b)}$$

The statistical coefficients of multiple determinations R^2 for these two models are 0.986 and 0.999, respectively.

Although the regression method is one of the fastest methods to backcalculate pavement layer moduli, this method has several drawbacks. It achieves high accuracy only for the materials and sites for which the method is developed. Its transferability to other regions with different site conditions is questionable.

2.3.4 Database Search Algorithm (DSA) Method

The DSA method matches the measured deflection basin with those in a database of deflection basins computed in advance for a variety of layer moduli. The application of this method was demonstrated by Tia et al. (1989) who developed the program DCONPAS (Data Base for Concrete Pavement Systems) using a database of analytical results generated by the forward-calculation computer program FEACONS (Finite Element Analysis of Concrete Slabs). MODULUS is another DSA based program, but it is for flexible pavement (Scullion et al., 1990). This program uses a forward calculation BISAR to generate the database. The main functions in the DSA method are as follows,

a. It collects and stores computed FWD deflections together with pavement properties in the database. In certain DSA programs such as DCONPAS, a regression analysis is performed by relating the deflections to the pavement properties stored in the database.

b. It generates analytical deflection basins using the pavement parameters in the database.

c. It estimates pavement properties by comparing the measured FWD deflection data with the analytical deflections stored in the database.

The use of database in backcalculation method is very convenient since the database could be expanded and updated easily. To expand the database, it is important to know the range of pavement properties (thickness and moduli values), since the backcalculated results are valid only within the range of pavement properties used to develop the database. Another advantage of this method is its efficiency in terms of computation time. However, the accuracy of the backcalculated pavement moduli depends on the quality of regression equation and the prediction model used in the program. The application of a database to pavement structures of a different pavement design or of different material types is not advisable.

2.3.5 Summary

An ideal backcalculation procedure is one which has a sound theoretical basis, and provides an accurate estimation of the pavement layer properties efficiently with a relatively short computation time. Computational time can be reduced by either developing a database or using a regression equation based on known spectrum of pavement properties. But the results produced by these methods sometimes cannot match closely with the actual values. In addition, the use of these methods is only applicable for the locality where the data were collected to develop the database or the regression equation. In general, they cannot be transferred to another region with different pavement conditions.

In terms of transferability over different sites and pavement conditions, the closed-form and best-fit methods are the preferred methods. The closed-form method can produce a unique solution and no iterative process is required. However, closed-form solutions are usually available only for relatively simple systems. For systems having many pavement layers and complex material properties, the use of closed-form method might not be possible. To overcome this difficulty, the best fit method offers an alternative solution to handle the problem by performing iterative search of a good solution to minimize a predetermined error function between the measured and computed deflections. However, more than one solution is possible with this method, depending on the choice of seed layer moduli that are used to start the search process. Therefore, the selection of seed moduli becomes an important aspect of this method.

In the best fit method, the more number of deflections used in the method, the longer is the time needed to back-calculate the layer moduli, although with the advancement in computer technology, computational time in the iterative process is no longer an important issue anymore.

2.4 Research Issues in Determination of Layer Moduli

The literature review presented in this chapter highlights several research issues that need to be addressed in the determination of the composite *k* value of a rigid pavement system and the layer moduli of a multi-layer flexible pavement system.

a. The use of plate load test to determine composite *k* value is possible and has been conducted by PCA and AASHTO using full-scale tests. However, this approach has obvious limitations in practical applications, such as the high cost and the long time required. Because of these two reasons, this test is seldom conducted in actual construction projects. For in-service roads, this test also

requires the surface layer of the road to be removed before the test can be performed.

The determination of resilient moduli by means of laboratory or field tests becomes more popular as another method to characterize the layer moduli. Although this procedure also can be used to determine the subgrade modulus as another alternative to the conventional plate load test, the relationship between *k* value and the resilient modulus is still difficult to be established due to the difference of the characteristics of the parameters measured.

NDT methods have become a logical choice in the determination of pavement layer moduli today. This method can be used for either new road construction or in-service pavements. The selection of the method to evaluate nondestructive test result is an important decision. There exist many nondestructive evaluation methods based on backcalculation analysis. However, because of the complexity of the characteristic of pavement systems to be modeled, the performance of the backcalculation methods could vary considerably. A careful analysis is necessary to identify the best method that can produce backcalculated layer moduli which matches closely with measured layer moduli.

b. The AASHTO and PCA methods have simplified the process of determination of composite *k* value for easy application in pavement design. However, the recommended charts or tables of values are not accurate enough for the purpose of condition evaluation of pavement sections. It needs an analytical method that can give better accuracy, offer important information such as the factor of safety, load transmission and its mechanism; and take into account the interaction of subgrade, subbase and pavement slab.

c. The regression method is also not an ideal backcalculation approach because the method lacks theoretical mechanistic basis. It depends on the correlation among various problem parameters. A regression model is only applicable for environment in which the model is developed. It does not provide any insight into the mechanism involved.

In summary, there is a need to develop an analytical procedure with sound theoretical basis for determining the layer moduli for the design of new pavements as well as the rehabilitation design of existing in-service pavements. This is in line with the latest research trend towards establishing a mechanistic design for new and rehabilitated pavements. Nondestructive evaluation techniques based on FWD tests and backcalculation analysis appear to be the most promising approach in this regard. This is the approach to be adopted in the present research to establish a theoretically sound analytical procedure for the determination of the composite *k* value of a concrete pavement with a subbase layer, and the determination of layered moduli of a flexible pavement system.

Table 2.1: Effect of Untreated Subbase on *k* Values (PCA, 1984)

Subgrade *k* value, MN/m^3 (pci)	Subbase *k* value, MN/m^3 (pci)			
	0.102 m (4 in.)	0.152 m (6 in.)	0.203 m (8 in.)	0.254 m (10 in.)
13.5 (50)	17.6 (65)	20.3 (75)	23.0 (85)	29.7 (110)
27 (100)	35.1 (130)	37.8 (140)	43.2 (160)	51.3 (190)
54 (200)	59.4 (220)	62.1 (230)	72.9 (270)	86.4 (320)
81 (300)	86.4 (320)	89.1 (330)	99.9 (370)	116.1 (430)

Table 2.2: Design *k* Values for Cement Treated Subbases (PCA, 1984)

Subgrade *k* value, MN/m^3 (pci)	Subbase *k* value, MN/m^3 (pci)			
	0.102 m (4 in.)	0.152 m (6 in.)	0.203 m (8 in.)	0.254 m (10 in.)
13.5 (50)	45.9 (170)	62.1 (230)	83.7 (310)	105.3 (390)
27 (100)	75.6 (280)	108.0 (400)	140.4 (520)	172.8 (640)
54 (200)	126.9 (470)	172.8 (640)	224.1 (830)	-

Table 2.3: Values for coefficient A, B, C and D in Equation (2-8)
(Ioannides et al., 1989)

AREA	A	B	C	D
A7	60	289.708	-0.698	2.566
A5	48	158.40	-0.476	2.220
A4	36	1812.279	-2.559	4.387
A3	24	662.272	-2.122	4.001

Remark: A7, A5, A4 and A3 are AREA parameter with 7, 5, 4 and 3 sensor configurations, respectively.

Table 2.4: Values for coefficient x, y and z in Equation (2-10) (Ioannides et al., 1989)

Radial Distance (m / in.)	x	y	z
0 / 0	0.12450	0.14707	0.07565
0.203 / 8	0.12323	0.46911	0.07209
0.305 / 12	0.12188	0.79432	0.07074
0.457 / 18	0.11933	1.38363	0.06909
0.610 / 24	0.11634	2.06115	0.06775
0.914 / 36	0.10960	3.62187	0.06568
1.524 / 60	0.09521	7.41241	0.06255

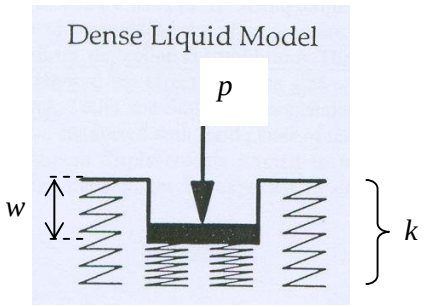

Figure 2.1: Representation of Dense Liquid Foundation

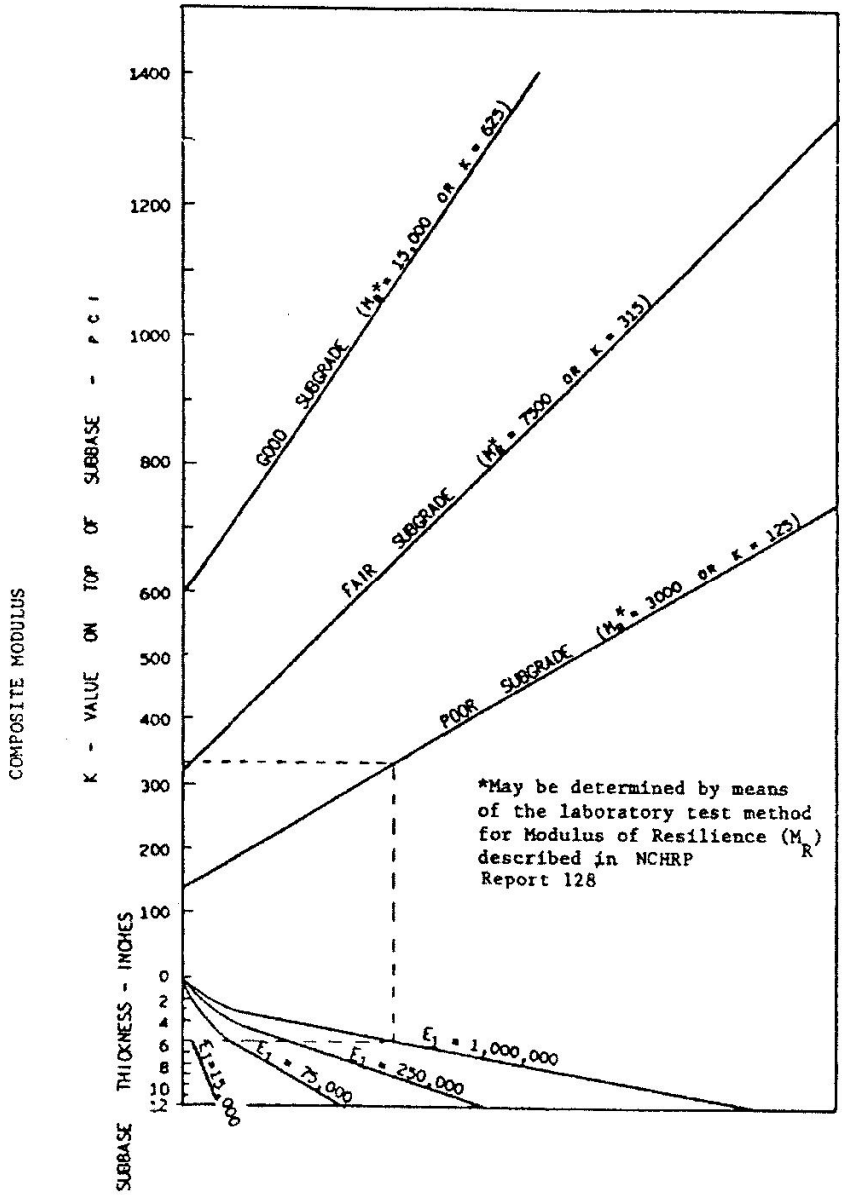

Figure 2.2: Chart for Estimating Composite *k* value Based on 1972 AASHTO Interim Guide (AASHTO 1972)

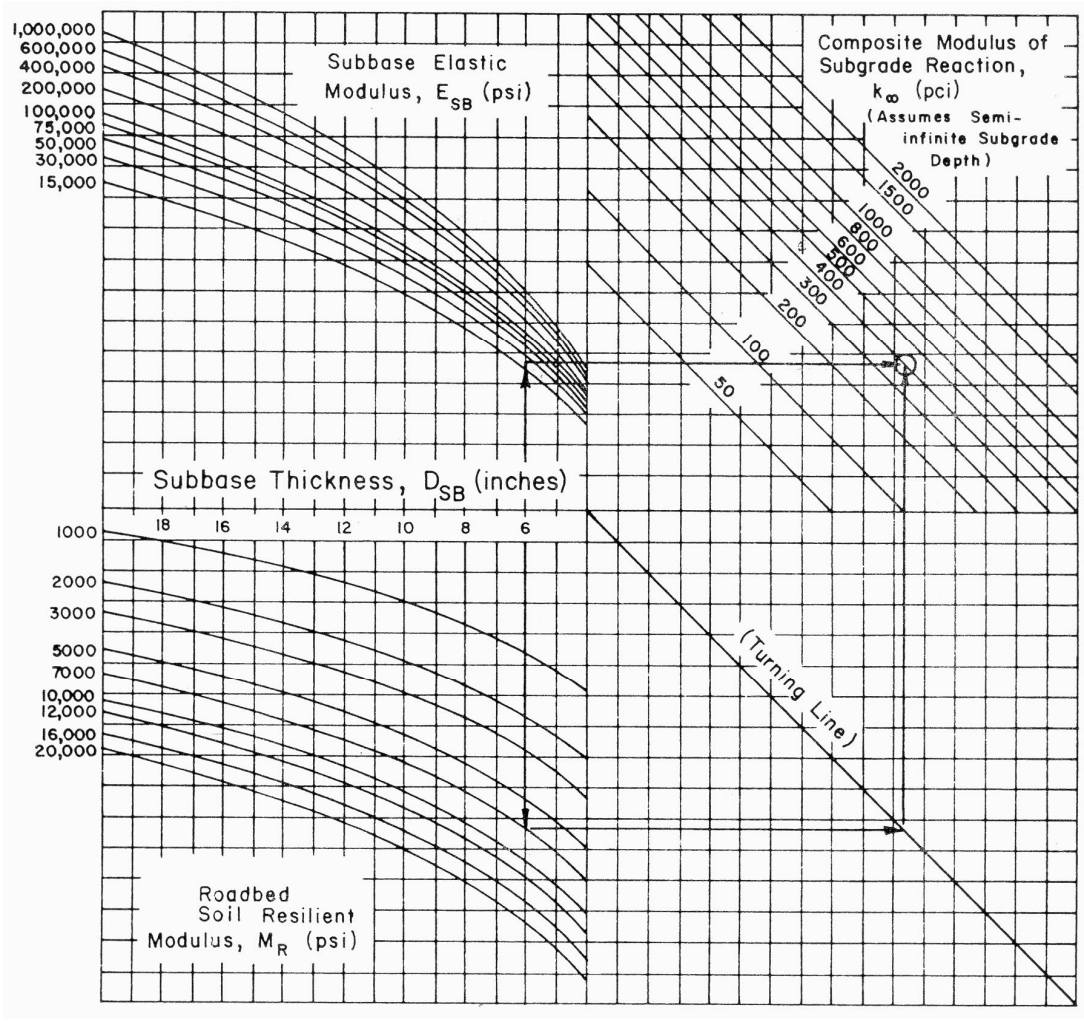

Figure 2.3: Chart for Estimating Composite *k* value Based on 1993 AASHTO Guide (AASHTO, 1993)

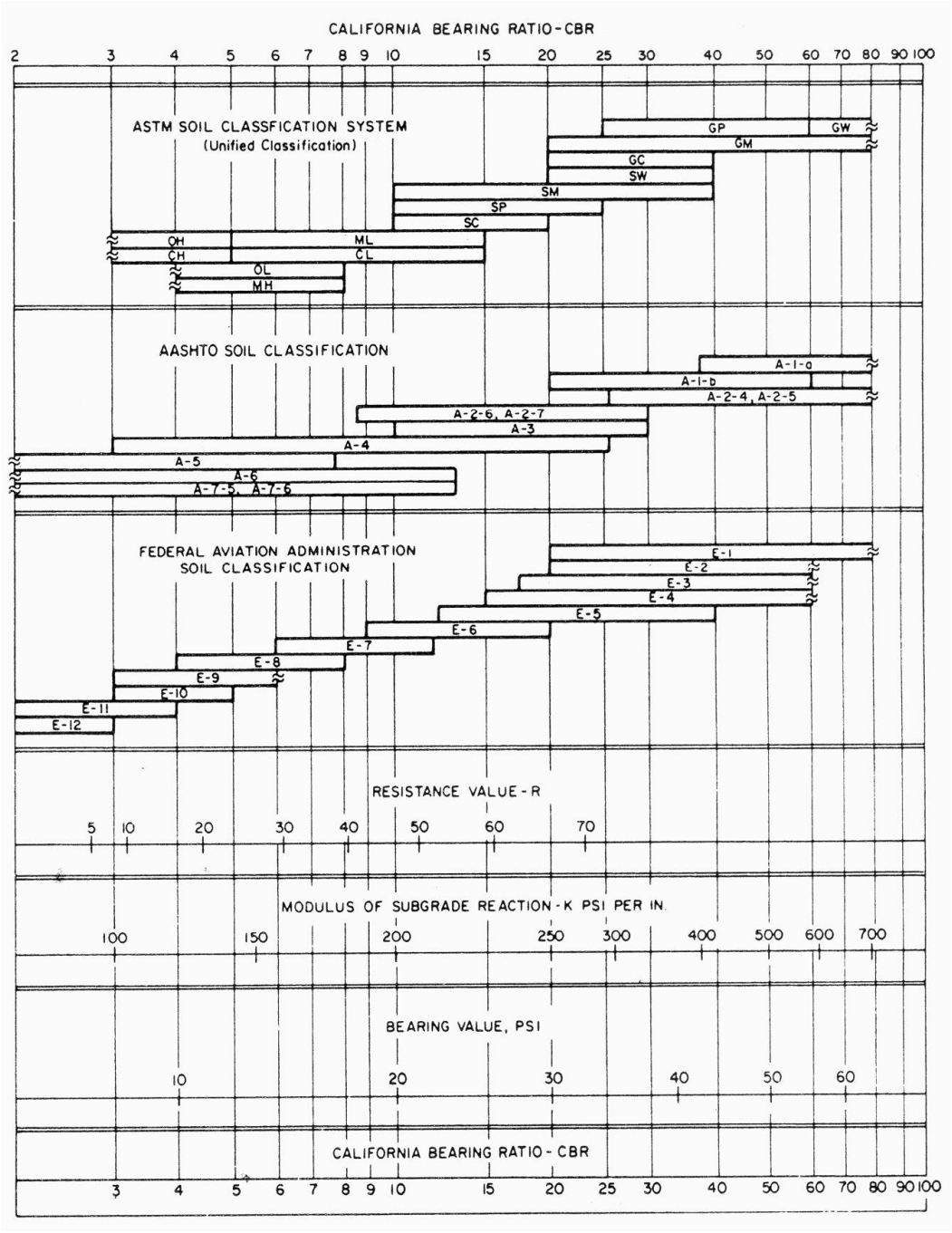

Figure 2.4: Approximate Relationship between *k* values and Other Soil Properties (PCA, 1966)

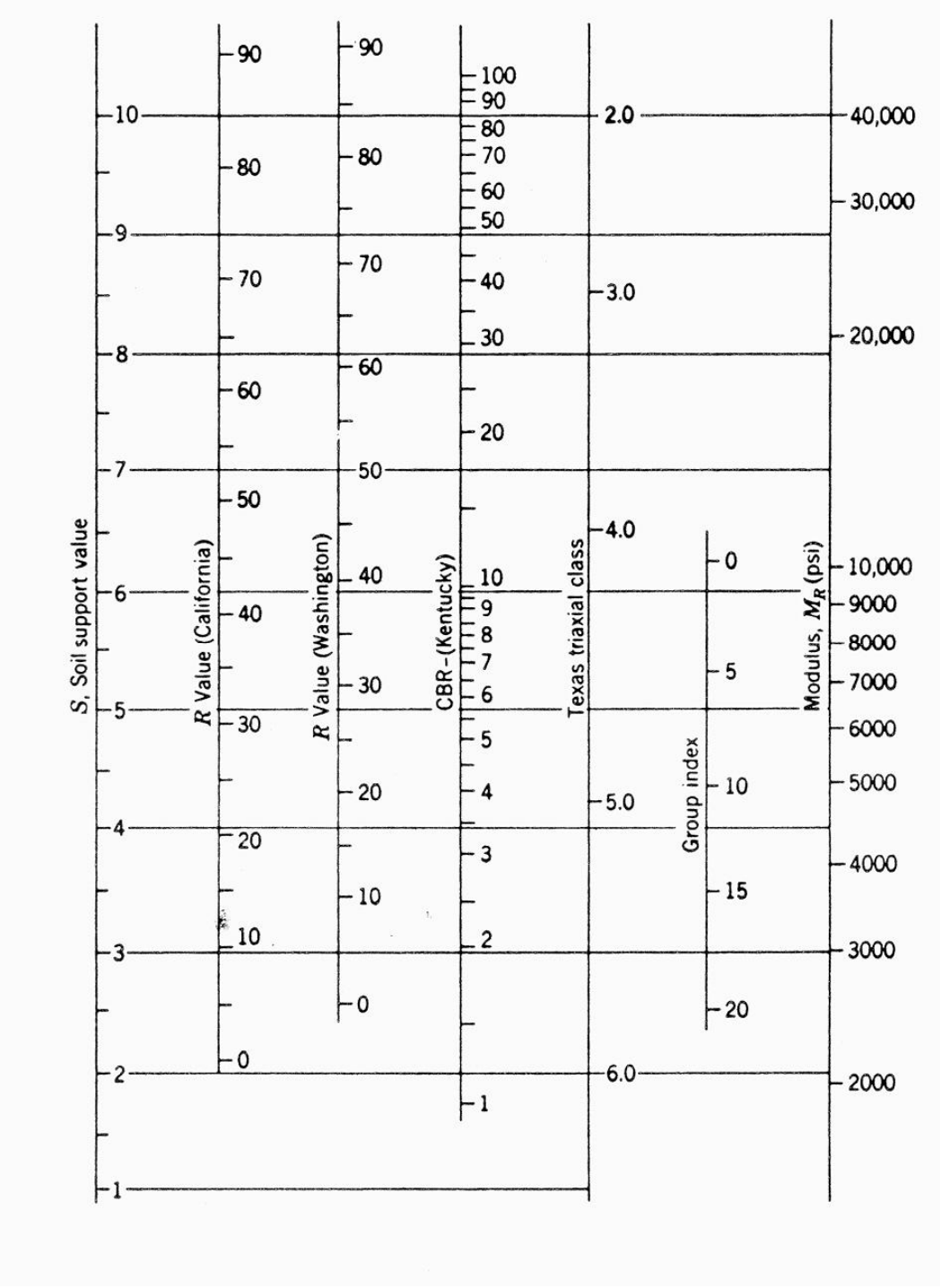

Figure 2.5: Approximate Relationship between M_R and Other Soil Properties (Van Til et al., 1972)

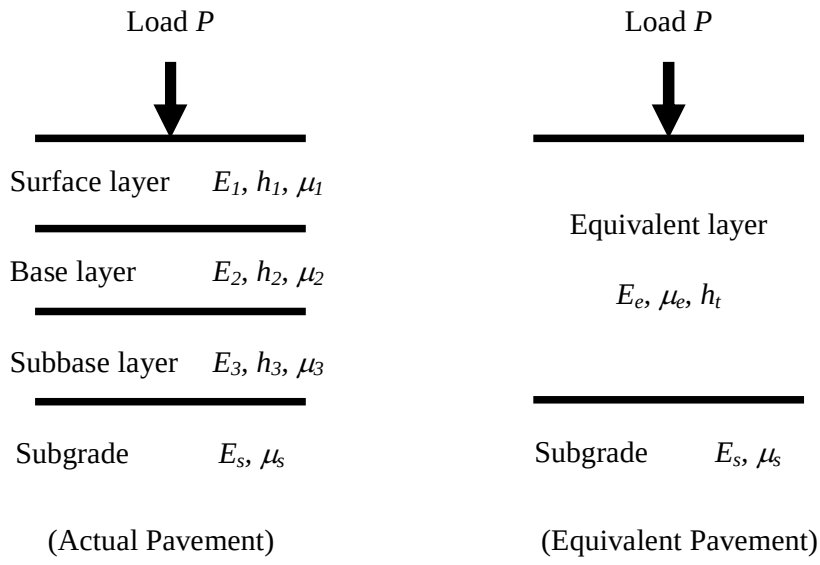

(a) Subgrade as the layer of interest in calculation

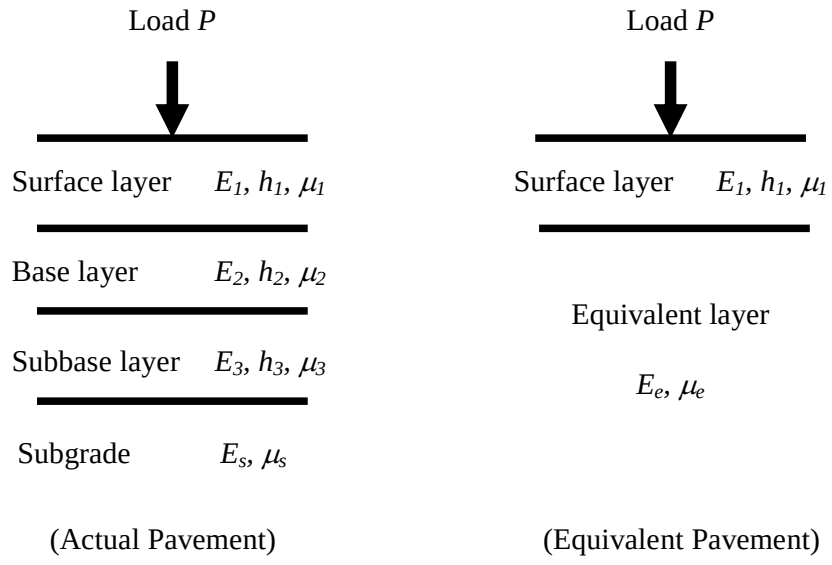

(b) Surface layer as the layer of interest in calculation

Figure 2.6: Representation of multi-layer pavement structure as equivalent two-layer system

CHAPTER 3

EVALUATION OF BACKCALCULATION ALGORITHMS FOR RIGID PAVEMENT SYSTEM

3.1 Introduction

In this chapter, two main aspects of pavement analysis using backcalculation algorithms for rigid pavement system are examined. The first aspect concerns with the selection of the most appropriate backcalculation algorithm for evaluating infinite rigid pavement systems. This is presented under Section 3.2. The second aspect, presented in Section 3.3, addresses the issue of the effect of finite slab size in backcalculation analysis of concrete pavements.

3.2 Selection of Backcalculation Algorithm for Rigid Pavements

3.2.1 Background

In the nondestructive determination of pavement properties by means of backcalculation algorithms based on deflection measurements, different answers can be obtained depending on the backcalculation algorithm employed. This is because of the differences in (a) the theoretical models employed to represent the pavement system and its structural behavior under load, (b) the search algorithms applied in the backcalculation analysis, and (c) the criteria of matching the computed and measured deflections. This presents a problem to pavement researchers and engineers alike on how one should go about selecting the most suitable backcalculation algorithm for their applications.

Regardless of the theory applied and the backcalculation algorithm adopted, a logical basis of selection of the backcalculation procedure for practical applications would be to assess if the backcalculated pavement properties provide good estimates of the actual pavement properties. Today, the ease and convenience of access to the Long-Term Pavement Performance (LTPP) database (Elkins et al., 2003) of actual measured data enables a highway agency to adopt this approach to select a backcalculation algorithm that meets its needs. This section presents a demonstration on how this approach was applied to evaluate the relative merits of different backcalculation algorithms for concrete pavements by comparing the computed concrete pavement properties, namely the elastic modulus of concrete pavement slab and the modulus of subgrade reaction, against the LTPP measured values.

3.2.2 Evaluation Procedure of Backcalculation Algorithms

The evaluation of backcalculation algorithms consists of the following main steps:

a. Identify suitable pavement sections that have the required pavement data and deflection test measurements, as well as appropriate measured pavement properties;
b. Select backcalculation algorithms to be evaluated;
c. Perform backcalculation analysis using the backcalculation algorithms selected;
d. Assess the relative performance of different backcalculation algorithms by comparing their respective computed pavement properties with the corresponding measured values.

Practically all the common design methods for rigid pavements today employ the Westergaard model that assumes the support to be a Winkler foundation (i.e. liquid

foundation). In this model, the structural behavior of rigid pavements under vertical loads are dependent mainly on two key structural pavement properties, namely the elastic modulus of the concrete slab, and the effective modulus of subgrade reaction. The effective modulus of subgrade reaction refers to the total composite modulus of subgrade reaction of the pavement foundation. The Poisson's ratio of the concrete slab and that of the foundation material usually do not have much influence on the structural response of the pavement system.

For backcalculation analysis to estimate the elastic modulus of the concrete slab and the effective modulus of subgrade reaction, the required data are pavement slab thickness, deflection test parameters and deflection measurements. The deflection test parameters include the magnitude and location of the applied load, the diameter of the loading plate, and the number and positions of deflection sensors.

The backcalculation algorithms to be evaluated are ILLI-BACK4, ILLI-BACK7, NUS-BACK, and the LTTP best-fit method. The theoretical basis and backcalculation procedure adopted in each of these four algorithms have been described in detail in chapter 2.

Except for NUS-BACK, the other three backcalculation algorithms employ measured deflections given by a prescribed sensor configuration. ILLI-BACK4 and LTTP best-fit method selected D_1, D_3, D_5, and D_6, whereas ILLI-BACK7 used deflections measured by all 7 sensors. The deflection data selected by NUS-BACK depend on the pavement layer for which the properties are to be backcalculated. It is known that the influence of the properties of the subgrade on measured deflections increases at points further away from the center of loading plate, while the elastic modulus of the pavement slab has relatively more important effects on measured deflections at points nearer to the center of loading plate. It is thus appropriate to

identify the best pair of measured deflections to be used in NUS-BACK analysis to backcalculate E_c and k respectively.

The selection of the best pair of sensor deflections can be made by performing a deflection-pair backcalculation sweep using NUS-BACK. For a given deflection basin with 7 sensor deflection readings, there are 21 possible pairs of deflection combinations and the backcalculation sweep involves analyzing each using NUS-BACK. The backcalculation sweep to select the best pair of measured deflections for NUS-BACK backcalculation of E_c and k respectively is conducted using the 26 pavement sections listed in Table 3.1. To analyze the results, two root-mean-square percent errors (*RMSPE*) are computed for each according to the following formulas.

$$RMSPE_1 = \sqrt{\frac{1}{N}\sum_{i=1}^{N}\left[\frac{X_i - x_i}{x_i}.100\right]^2} \qquad (3\text{-}1)$$

$$RMSPE_2 = \sqrt{\frac{1}{m}\sum_{i=1}^{N}\sum_{j=1}^{n(i)}\left[\frac{X_{ij} - x_i}{x_{ij}}.100\right]^2} \qquad (3\text{-}2)$$

where x_i is the measured property value for pavement section i, X_i in Equation (3-1) is the average backcalculated property value of pavement section i which is the mean of the backcalculated values obtained from all the measured deflection basins of the pavement section, X_{ij} in Equation (3-2) is the backcalculated property value for deflection basin j of pavement section i, $n(i)$ is the total number of measured deflection basins in pavement section i, N is the total number of pavement sections studied, and m is the total number of deflection basins analyzed.

Based on the *RMSPE* values computed as summarized in Table 3.2, the results suggest that deflections D_4 and D_7 produce the lowest *RMSPE* for the estimated k values; while deflections D_1 and D_3 produce the lowest *RMSPE* for the estimated E_c values. Hence, for the NUS-BACK backcalculation analysis performed in this study, k

is estimated based on the measured deflections D_4 and D_7, and E_c is computed based on the measured deflections D_1 and D_3.

3.2.3 Long-Term Pavement Performance (LTPP) Program

The LTPP program was one of six strategic research areas recommended by a Strategic Highway Research Program (SHRP) in 1984 (Elkins et al., 2003). Since mid-1992, the Federal Highway Administration (FHWA), USA, has assumed the management and funding of the LTPP program (Jiang and Tayabji, 1998). The main objective of the LTPP program is to assess the long-term performance of pavements under various loading and environmental conditions over a period of 20 years.

The LTPP program includes two fundamental classes of studies: the General Pavement Studies (GPS) and the Specific Pavement Studies (SPS). The GPS experiments are a series of selected in-service pavement studies structured to develop a comprehensive national pavement performance database. These studies are restricted to pavements that incorporate materials and designs representing good engineering practice and that are in common use across the United States and Canada. The GPS program includes experiments on all pavement system types, such as on Asphalt Concrete (AC) on Granular Base (GPS-1) and on Bound Base (GPS-2), Jointed Concrete Pavements (JCP) (GPS-3 and GPS-4) and Continuously Reinforced Concrete Pavement (CRCP) (GPS-5). The SPS program involves the study of specially constructed, maintained, or rehabilitated pavement sections incorporating a controlled set of experimental design and construction features. The category of SPS experiments includes pavement maintenance (SPS-3 and SPS-4), pavement rehabilitation (SPS-5 to SPS-7) and environmental effects (SPS-8) (Elkins et al., 2003).

Generally, each GPS and SPS test section consists of a 152-meter (500-ft) monitoring portion with transition zones between two test sections. For jointed rigid pavements, the number of panels in those sections can vary from as few as 9 or 10 to as many as 35 or more (Jiang and Tayabji, 2000).

As will be demonstrated through the analysis presented in this study, the LTPP database offers an excellent source of information and data for the selection of suitable backcalculation algorithm for an intended application.

3.2.4 Input Parameter and Assumptions Used in Analysis

As the purpose is to evaluate backcalculation algorithms by comparing the backcalculated and measured values of E_c and k, only pavement sections that contain measured values of E_c or k, or both are considered. As it turned out, only 26 JCP pavement sections in the LTPP database contain k values measured directly using plate loading test, as listed in Table 3.1. The data for these JCP pavement sections also contain measured E_c values, which are listed in Table 3.3 together with another 24 randomly selected JCP pavement sections for the purpose of backcalculation evaluation of E_c. In addition, 76 CRCP sections listed in Table 3.4 were randomly selected from the LTPP database for the purpose of backcalculation evaluation of E_c. There are altogether 281 deflection tests recorded in the 26 pavement sections in Table 3.1, 746 deflection basins in the 50 pavement sections in Table 3.3, and 1,437 deflection basins in the 76 pavement sections in Table 3.4.

The measured deflection data for all the pavement sections selected were obtained by falling weight deflectometers (FWD). However, only the average of the deflection data is employed, since averaging the results of multiple drops at a

particular point will enhance the accuracy of the deflection data (Irwin et al., 1989) and can minimize random errors on measurements (Fwa, 1998).

There were seven deflection readings per deflection basin, $D_1, D_2, D_3, D_4, D_5, D_6,$ and D_7 measured at 0, 203, 305, 457, 610, 914 and 1524 mm, respectively, from the center of a loading plate of 300-mm diameter. Three load levels of the FWD tests (40, 53.3 and 71.1 kN) are considered, and all the deflection basins recorded are obtained for the condition where the load was applied on the interior of the slab.

3.2.5 Comparison of Backcalculation Algorithms

3.2.5.1 Basis of Comparison

Each of the measured deflection basins of the LTPP pavement sections listed in Tables 3.1, 3.3 and 3.4 is analyzed by the backcalculation algorithms ILLI-BACK4, ILLI-BACK7 and NUS-BACK. The E_c and k values backcalculated by the LTPP best-fit method are obtained from the LTPP database directly. The relative performance of the four backcalculation algorithms with respect to their ability to predict the measured E_c and k values satisfactorily is assessed based on the following comparisons:

(a) The *RMSPE* for E_c and k, respectively, computed using the pavement-section average backcalculated property values, as defined by $RMSPE_1$ of Equation (3-1);

(b) The *RMSPE* for E_c and k, respectively, computed using the backcalculated property values from individual deflection basins, as defined by $RMSPE_2$ in Equation (3-2);

(c) Frequency distribution of absolute percent errors computed using the pavement-section average backcalculated property values; and

(d) Frequency distribution of absolute percent errors computed using the backcalculated property values from individual deflection basins.

(e) Coefficient of correlation between the calculated and measured deflections

The absolute percent errors in items (c) and (d) refer to the absolute difference between the computed and measured pavement property, as a percentage of the measured value.

3.2.5.2 Results of Comparative Analysis

A summary of the results of backcalculation analysis by the four backcalculation algorithms for different applied load levels is given in Tables 3.5(a) and 3.5(b). Since the trends of variation of backcalculated properties with respect to their corresponding measured properties are similar for the three load levels analyzed, only the results for the 71.1 kN load level are plotted. Figure 3.1 plots the backcalculated k against the measured k for the JCP sections of Table 3.1, Figure 3.2 plots the backcalculated E_c against the measured E_c for the JCP sections of Table 3.3, and Figure 3.3 plots the backcalculated E_c against the measured E_c for the CRCP sections of Table 3.4. Table 3.5(a) summarizes the $RMSPE_1$ and $RMSPE_2$ for the backcalculated E_c and k. Figure 3.4 presents the frequency plot of the absolute percent errors of backcalculated k for the JCP sections of Table 3.1, Figure 3.5 presents the frequency plot for the absolute percent errors of backcalculated E_c of the JCP sections of Table 3.3, and Figure 3.6 presents the frequency plot of the absolute percent errors of backcalculated E_c for the CRCP sections of Table 3.4.

Comparison Based on *RMSPE*

The *RMSPE* values in Table 3.5(a) represent quantitatively the deviations of the backcalculated E_c or k from their corresponding measured values. The following observations may be made:

a. For all load levels, NUS-BACK yielded the lowest *RMSPE* values. The LTPP best-fit method produced the next lower *RMSPE* values. Between the ILLI-BACK7 and ILLI-BACK4, the former performed better for k, but poorer for E_c. The following paragraphs provide possible reasons for these differences.

   A basic difference in the four backcalculation algorithms lies with their deflection matching criteria. The LTPP best-fit method seeks to minimize a pre-defined error function between the set of measured point deflections and the corresponding computed deflections, while ILLI-BACK4 and ILLI-BACK7 compute the estimated E_c and k by matching weighted cross-sectional area of the deflection basin. On the other hand, NUS-BACK derived the backcalculated pavement properties based on two selected measured deflections of the deflection basin. Theoretically speaking, the four backcalculation algorithms should give the same answers if the following conditions are met: (i) the real pavement behaves as a perfect elastic system in the manner described by the elastic theory adopted by the backcalculation algorithms, and (ii) there are no measurement errors in the measured deflections. Unfortunately, both conditions are known not satisfied in the real world.

   For instance, it is known that the theoretical deflection basin of a rigid slab resting on a liquid foundation is different from that of a rigid slab resting on an ideal solid foundation, and the actual deflection basin of a real pavement differs from both. It is for this reason that one may not obtain better results in

backcalculation analysis by imposing a stricter requirement on conformance of the measured deflection shape with a theoretical deflection shape. ILLI-BACK4 and ILLI-BACK7 have the strictest deflection basin conformance requirement by matching of the cross-sectional area of the deflection basin. The LTPP best-fit method is next with the criterion of matching all the measured deflection points, while NUS-BACK has the least conformance control by relying on matching of two most relevant deflection points. In other words, NUS-BACK offers the flexibility to choose the best pair of sensor deflections (among 21 possible pairs out of the 7 sensor deflections) that would produce the backcalculated pavement property closest to the corresponding measured value.

b. The magnitudes of *RMSPE* of the backcalculated k are larger than the corresponding *RMSPE* of the backcalculated E_c, regardless of the backcalculation algorithm adopted. This could possibly be attributed to two reasons:

- The times of measurements of k and E_c were different from the times of deflection tests. k values are affected more because compared to E_c, they tend to vary more with the environmental factors which often change with the season and climate.
- The locations of k or E_c measurements were likely to be different from the points of deflection tests. This location effect would have a higher impact on k than E_c because k varies with the soil condition along the pavement section while E_c of the concrete slab does not vary significantly within a pavement section.
- The models employed in the backcalculation algorithms did not give exact representations of the actual pavement (systematic error) in terms of

material model, response characteristics under loads, etc. (Fwa, 1998; Stoelle and Parvini, 2001).

c. The magnitude of percent errors of E_c for either CRCP or JCP are of the same order of magnitude. It appears that the four backcalculation algorithms, which were all developed based on the infinite slab theory, were also applicable to JCP as long as the deflection test was conducted at an interior point of the slab.

Comparison Based on Frequency Distribution of Percent Errors

The frequency distribution plots of percent errors are presented in Figures 3.4, 3.5, and 3.6 for k, E_c of JCP, and E_c of CRCP respectively. A backcalculation algorithm that produces more cases of percent errors in the lower range is preferred. The relative performance of the four backcalculation algorithms derived from these figures supports the assessment based on *RMSPE* presented in the preceding sub-section:

a. Based on percent errors of backcalculated k, the ranking that places the best performing algorithm first is: NUS-BACK, LTTP best-fit method, ILLI-BACK7, and ILLI-BACK4.

b. Based on percent errors of backcalculated E_c, the ranking that places the best performing algorithm first is: NUS-BACK, LTTP best-fit method, ILLI-BACK4, and ILLI-BACK7.

Comparison Based on Coefficient of Correlation

Because of the rather narrow ranges of the values of pavement properties (i.e. k and E_c) concerned, and the relatively wide deviations of the calculated properties from the measured values, the values of the coefficient of correlation between calculated

and measured properties are known to be low (Hall et al., 1996; Rufino et al., 2002), and are generally not used as a main criterion for comparison of backcalculation algorithms. Nevertheless, for completeness sake, the coefficients of correlation are also presented here for the four algorithms. Based on the average backcalculated *k* and E_c for each pavement section (see Figures 3.1, 3.2 and 3.3), the coefficients of correlation between the calculated and measured properties are summarized in Table 3.5(b).

Comments on Effect of Load Level

Khazanovich et al. (2001) stated that the result of backcalculation for concrete pavements usually did not depend on load level if the load level was sufficiently large. Kim and Park (2002) reported that it was necessary to apply a load level more than 53.3 kN (12 kip) to cause significant non-linearity in the behavior of subgrade soils.

The results of the presented study as presented in Table 3.5(a) appear to provide some indirect support to their observations. The tendency of the *RMSPE* for *k* values to increase with the load level was probably caused by the increasing deviation of the soil behavior from linearity as indicated by Kim and Park (2002) and Stubstad et al. (1994). On the other hand, the *RMSPE* for E_c values did not follow the same trend. The *RMSPE* for E_c values in fact showed a tendency to decrease with load level. Besides the fact that concrete exhibited less nonlinear behavior at the load range analyzed, another possible contributing factor is the decreasing influence of measurement errors at higher load levels which generated larger deflections.

Comment on Effect of Sensor Configuration

The analysis of this study clearly shows the significant effects of (i) the choice of the number of sensor used in the backcalculation analysis, and (ii) the locations of sensors selected. The following points may be noted:

a. Comparison between ILLI-BACK4 and ILLI-BACK7

ILLI-BACK7 performed better in estimating k, but not so in estimating E_c. Several factors may have contributed to the seemingly conflicting results. The inclusion of sensor deflections D_4 and D_7 (best for estimating k as indicated in Table 3.2) in ILLI-BACK7 may have led to its better performance in estimating *k*. On the other hand, the less stringent deflection basin matching requirement of ILLI-BACK4 could be the reason for its better performance in estimating E_c.

b. Comparison between ILLI-BACK and LTPP best-fit method

The main difference between the LTPP best-fit method and the two ILLI-BACK algorithms is their deflection matching criteria. With the less stringent point matching of deflections, as opposed to area matching of the two ILLI-BACK algorithms, the LTPP method yielded lower percent errors than ILLI-BACK 4 and ILLI-BACK 7.

c. Comparison between NUS-BACK and the other algorithms

As explained in an earlier section, the better performance of NUS-BACK could be attributed to its flexibility in selecting the best pair of sensor deflections for a given pavement property. Another significant aspect on the performance of NUS-BACK is worth mentioning at this juncture. There has been reservation to the use of D_7 in backcalculation due to its very small value, because of the fact that a small error in the measured values may cause significant changes in the backcalculated results. Fortunately the NUS-BACK algorithm has the flexibility

to permit the user choices to overcome this problem: (a) As can be seen from Table 3.2, instead of using sensor deflections D_4 and D_7, the user could pair deflections among D_4, D_5, D_6 and D_7 without suffering much loss in the resulting *RMSPE*; (b) Alternatively, the concept of deflection-pair backcalculation sweep introduced earlier may be employed. The user may apply NUS-BACK to perform a backcalculation sweep using different pairs of sensor deflections to determine whether the sensor deflection pair D_4 and D_7 gives consistent results with the next few best pairs. This backcalculation sweep could identify faulty sensor readings and provide the necessary "quality" check of the backcalculated results. The closed-form NUS-BACK algorithm is highly efficient computationally. The backcalculation computation inclusive of the pair-wise sweep could be completed in less than a second.

Comments on Effect of Temperature on Backcalculation Results

It is noted that temperature differentials in concrete slabs have been known to have significant effects on the behavior of concrete slabs and their load-deflection characteristics. The measurement of the deflections generally would not be performed at mid day to avoid the concrete slabs curl up and cause the loss contact between concrete slab and subgrade or subbase. In this study, the selection of the deflections basins for 50 JCP sections and 76 CRCP sections did not consider the effect of temperature on the concrete slab. To take into account this issue, an examination was conducted on all selected pavement sections from LTPP database, and it was found that 25% and 20% of deflection basins in the JCP and CRCP sections, respectively, were measured at mid day (around 11 am – 2 pm). To evaluate the effect of temperature differentials in concrete slab, a comparison between *RMPSE* without

temperature consideration and *RMPSE* with temperature consideration is presented in Tables 3.6 (a) for *RMSPE* on E_c and 3.6 (b) for *RMSPE* on *k*. The *RMSPE* without temperature consideration was calculated after omitting the pavement sections whose layer properties based on deflections measured at mid day. From the table, it seems that there is a significant difference of *RMSPE* on E_c only for two ILLI-BACK programs. This may be contributed by the use of weighted cross-sectional area as deflection matching criteria in their algorithm. In addition, CRCP pavement sections were less affected by this issue as the presence of reinforced steel in the CRCP pavement could minimize the curling effect.

Table 3.6 (b) indicates that the *RMSPE* on *k* increases after the pavement sections whose layer properties based on deflection measured at mid day are dropped. It is proved that the temperature differentials have insignificant influence on subgrade. The high deviation between measured and computed *k* is more affected by the difference of times and location of measurements.

3.2.6 Summary

This section has presented an analysis to compare the relative performance of four backcalculation algorithms in estimating the pavement slab elastic modulus E_c and the modulus of subgrade reaction *k* of concrete pavements. The LTPP database of deflection test data and measured pavement properties were used as the basis for assessing the relative suitability of different backcalculation algorithms for specific practical applications. The relative performance of four backcalculation algorithms were evaluated by comparing the backcalculated E_c and *k* against the corresponding measured values.

The four algorithms examined in this section differ in the number of sensors and sensor configuration used in the backcalculation analysis, as well as their criteria for matching the calculated and measured deflections. ILLIBACK4 and ILLIBACK7 have the most stringent criteria in matching the weighted cross-sectional area of the measured deflection basin, followed by the LTTP best-fit method that matches the computed point deflections with the corresponding measured deflections. The NUSBACK has the most flexible requirement as it permits the selection of two most suitable deflection points for backcalculating each pavement property.

The analysis presented in this section illustrates that the choice of sensor configuration (i.e. the number of sensors included as well as the locations of the selected sensors) has significant effects on the performance of the backcalculation algorithms. Since the actual pavement system does not deform exactly in the manner described by the elastic theory, forced matching of the computed and measured deflection basins does not necessarily produce the best results in backcalculation analysis. This point has been illustrated by the analysis presented in this study. The stringent requirements imposed by the two ILLIBACK algorithms did not lead to better performance. The relatively superior performance of NUSBACK indicates that although the theoretical and measured deflection basins are not the same, it is possible to identify selected sensor deflections for backcalculation analysis and produce satisfactory results. A concept of deflection-pair backcalculation sweep using NUSBACK was also introduced. It serves to identify the most suitable deflection pair for backcalculation of a particular pavement property, and to provide a quality check on the presence of faulty sensor readings.

According to the results produced in this section, NUS-BACK backcalculation program was recommended to be used for the evaluation of the rigid pavement system.

3.3 Consideration of Finite Slab Size in Backcalculation Analysis of Rigid Pavements

3.3.1 Background

Practically all of the backcalculation algorithms developed so far for jointed concrete pavements are based on the assumption of a slab of infinite plane dimensions resting on dense-liquid foundation. The issue of finite slab size, and that of the associated load transfer across joints, are usually avoided by having the test load applied in an interior point of the slab concerned so that their effects can be minimized.

There have been studies that attempted to include the effect of slab size in backcalculation analysis with the intention to improve the accuracy of computed pavement properties. For instance, Crovetti developed a slab size correction for a square slab (Croveti, 1994; Hall et al., 1996; Khazanovich et al., 2001), while Korenev derived an alternative correction procedure by generalizing Westergaard's solution of an infinite slab to the case of a circular slab (Hall et al., 1996; Khazanovich et al., 2001; Korenev, 1954). However, the applications of such corrections are not commonly adopted in practice, possibly due to one or more of the following reasons:

a. A backcalculation procedure that considers the effect of slab size may require the load transfer efficiency (LTE) of the joints as input. In such a case, the actual LTE values (which are likely to be different between transverse and longitudinal joints) of all the joints have to be determined for each slab tested. This could present a practical problem as such information requires additional field tests and is not easily available;

b. Instead of LTE, some backcalculation procedures may require the joint dimensions, joint reinforcement details, and actual field conditions of the joints

as input. The same practical problem as mentioned under item (a) will be encountered.

c. The actual slab dimensions will have to be recorded. This is not an issue as critical as items (a) and (b), but could be a problem on a road section with variables joint spacing.

d. To obtain correct backcalculation answers in applying the corrections, the specific location of the applied test load, with respect to each of the four joints, will have to be recorded for every slab tested. Though not difficult to measure on site, this requirement may significantly slow down the field test operation, which is undesirable as the speed of testing is a critical issue of the nondestructive deflection test from the following standpoints: test efficiency, traffic delay, traffic safety, and safety of the field test personnel.

While the consideration of actual slab size and field conditions of load transfer at joints is desirable for theoretical exactness point of view, there are practical issues involved as highlighted above. This section assesses the practical need for considering finite slab size in backcalculation analysis by examining the improved accuracy achievable with the incorporation of the effect of slab size in the analysis.

3.3.2 Methods of Backcalculation

This section describes the following five backcalculation methods adopted in the present study:

a. A closed-form backcalculation algorithm for an infinite pavement slab based on the NUS-BACK program (Fwa et al., 2000);

b. A backcalculation algorithm for a single rectangular finite slab using a closed-form forward deflection calculation program ONE-SLAB (Li et al., 1996);

c. A backcalculation algorithm for the central slab of a nine-slab system using a closed-form forward deflection calculation program NINE-SLAB developed by Liu and Fwa (2007);

d. A backcalculation algorithm for a finite pavement slab using parameters corrected by Crovetti's method (Crovetti, 1994) as input to infinite slab backcalculation analysis; and

e. A backcalculation algorithm for a finite pavement slab using correction by Korenev's method (Korenev, 1954) based on an infinite slab backcalculation program.

The theoretical basis and backcalculation procedure adopted by infinite-slab algorithm have been described in detail in chapter 2.

3.3.2.1 Backcalculation Procedure for One-slab and Nine-slab Algorithm (ONE-BACK and NINE-BACK)

Formulation

In this research, both ONE-BACK and NINE-BACK backcalculation algorithms were developed using the Gauss-Newton method (Matsui et al., 1990). The Gauss-Newton method is an iterative method was used to solve nonlinear least squares problems, as stated in Eq. (2-22) as follows.

$$S(p) = \sum_{i=1}^{m} (f_i(p))^2 \qquad (2\text{-}22)$$

To solve the problem, the Gauss-Newton needs the user to provide an initial guess (seed) for the parameter vector *p*.

Given an estimate for a set of unknown parameters *{P}* and the adjustment vector *{ΔP}*, the subsequent guesses p^x for the parameter vector are then produced by the recurrence relation as follows.

$$\{P\}^x = \{P\}^{x-1} + \{\Delta P\} \tag{3-3}$$

where x is the number of iteration.

In this research, the unknown parameter represents layer moduli to be backcalculated. The adjustment vector *{ΔP}* is obtained by solving the following simultaneous equations (Almedia et al., 1994):

$$\{S\}\{\Delta P\} = \{R\} \tag{3-4}$$

where:

{S} = sensitivity matrix, with a generic term given by:

$$S_g = \sum_{i=1}^{n} w_i \frac{\partial^2 w_{ci}}{\partial p_g^2} \qquad g = 1,.., m \tag{3-5}$$

{R} = vector of residuals, with a generic term given by:

$$R_g = \sum_{i=1}^{n} w_i \left(w_{mi} - w_{ci}\right) \frac{\partial w_{ci}}{\partial p_g} \tag{3-6}$$

in which i is the sensor index; n is the number of measured deflection; w_i is a weighting coefficient; w_m and w_c are the measured and calculated deflections, respectively.

In this backcalculation algorithm, the forward calculation program ONE-SLAB and NINE-SLAB will be called to compute w_c as many as two times per iteration, that is, to calculate the adjustment vector using Eq. (3-5) and (3-6) and to examine the error function as to whether this function has fulfill the convergence or stopping criterion.

According to Eq. (3-5) and (3-6), the first and the second derivatives of w_{ci} with respect to p_g were performed using the numerical differential method (Zha and Xiao,

2003). According to the definition of derivatives and the given increment of p_g, named as h, where h equal to $0.001p_g$, the approximations of the first and second derivatives can be assumed as:

$$\frac{\partial w_{ci}}{\partial p_g} = \frac{w_{ci}(p_g + h) - w_{ci}(p_g - h)}{2h} \tag{3-7}$$

$$\frac{\partial^2 w_{ci}}{\partial p_g^2} = \frac{[w_{ci}(p_g + h) - 2w_{ci}(p_g) + w_{ci}(p_g - h)]}{h^2} \tag{3-8}$$

Hence, from Eq. (3-3) and by setting the weighting coefficient (w_k) equal to one, the adjustment vector $\{\Delta P\}$ for each layer modulus is as follows.

$$\{\Delta P\} = \frac{\sum_{i=1}^{n}(w_{mi} - w_{ci})\dfrac{w_{ci}(p_g + h) - w_{ci}(p_g - h)}{2h}}{\sum_{k=1}^{n}\dfrac{\{w_{ci}(p_g + h) - 2w_{ci}(p_g) + w_{ci}(p_g - h)\}}{h^2}} \tag{3-9}$$

This procedure is iterative. At step x of the computation, after Eq. (3-4) has been solved, the unknown parameters (layer moduli) are updated by using Eq. (3-3).

Error Function

In this research, the error function used is based on an output error criterion in the form of the sum of the square relative errors. This form of errors constitutes one of three common basic forms of output errors used in pavement back-analysis problem so far (Fwa, 1998). This error has a form as shown in Eq. (2-16).

$$F(\ell_k, k, E_c) = \sum_{i=0}^{n} \alpha_i \left(w_{ci} - w_{mi}\right)^2 \tag{2-16}$$

in which α_i are weighting factors; w_{ci} and w_{mi} are computed and measured deflections at point i, in which the computed deflection is a function of the radius of relative stiffness, the modulus of subgrade reaction and the elastic modulus of concrete slab. In

this research, each point is assumed to have same weight; therefore, α_i is set to be 1 for all points of measurements.

Iterative Search Algorithm

In this research, the backcalculation procedure will be conducted iteratively until one of the two following requirements is fulfilled: (i) the iteration has reached the maximum number specified, and (ii) the error function produces a value that is less than the pre-determined convergence criterion. Although the requirement to terminate the program could be selected from the two requirements above, the termination of the backcalculation program caused by the second criterion is preferred.

The selected terminating condition selected should be sufficient to ensure that the backcalculation layer moduli have converged. Sometimes a very small convergence criterion or a very high iteration number is not a good terminating criterion since it could increase the computation time, although this indicates that the backcalculation results are highly accurate.

Initially, the maximum error produced by ONE-BACK was set to maximum value at 10^{-24} mm^2 for the iterative backcalculation program to exit, or alternatively, the program may converge after performing 999 loops. As the set minimum error is highly conservative, it serves to ensure that the program searches the smallest possible error within the range of the number of loops. For practical applications, the maximum error at 10^{-10} mm^2 is sufficient to state that the program has converged. Since the unit of deflection used in the error function is millimeter and the error form used is square error, therefore, the deviation of computed and measured deflection of the order of 10^{-5} millimeter or 10^{-2} micrometer is assumed to be small enough.

Because of this reason and also to cut off the computation time, the maximum error of 10^{-10} mm^2 then was used by the NINE-BACK backcalculation program algorithm. The number of iteration in NINE-BACK is set to equal to 9999. The selection of this iteration number is just to assure that the program could reach the convergence criterion before the maximum iteration number is attained.

Seed Moduli

As mentioned previously, all programs based on the Gauss-Newton iterative method require seed values of layer moduli. The determination of the initial moduli is important because it can help to reduce the computational time and that the results would converge to the correct answer.

The backcalculated programs ONE-BACK and NINE-BACK in this research use initial layer moduli as their seed value. Both programs have the same seed moduli, but there are some slightly differences in their usage. ONE-BACK program determines seed moduli based on three ranges of average measured deflection as follows.

a. For average measured deflection < 0.045 mm, seed value of elastic modulus of concrete slab E_c = 40 GPa, and seed value of k = 200 MN/m^3

b. For average measured deflection ≥ 0.045 mm and < 0.1 mm, seed E_c = 30 GPa and seed k = 150 MN/m^3

c. For average measured deflection ≥ 0.1 mm, seed E_c = 20 GPa and seed k = 13 MN/m^3

   NINE-BACK only employs one pair of seed moduli, i.e. E_c = 20 GPa and k = 13 MN/m^3, in its initial iteration and they will be adjusted after evaluating the backcalculated moduli resulted after the program is terminated. The backcalculated moduli at the end of program run should be in the range of 20 to

42 GPa for E_c and 13 to 220 MN/m^3 for k value. If the backcalculated moduli fall beyond the range of moduli, the seed moduli have to be adjusted using another pair of seed values given, E_c = 30 GPa; k = 150 MN/m^3 or E_c = 40 GPa; k = 200 MN/m^3.

3.3.2.2 Backcalculation Using Crovetti's Corrections for Finite Slab Size

To take into account the effect of finite slab size, Crovetti developed a slab size correction for a square slab based on the results of finite element analysis (Crovetti, 1994). Crovetti and Crovetti (1994) applied the proposed correction in the backcalculation of E_c and k for concrete pavements of square slabs. This procedure was subsequently examined in a study conducted to backcalculate k by Hall et al. (1996) who also applied the procedure to rectangular slabs by taking the smaller slab dimension, length or width, in the correction factor calculation. Crovetti (2002) reported the use of the correction factors in backcalculation analysis of the quality of support beneath jointed concrete slabs.

The backcalculation procedure essentially applies corrections to selected parameters computed from a closed-form infinite-slab backcalculation algorithm to obtain revised estimations of E_c and k. The infinite-slab backcalculation algorithm used is that employed in the ILLI-BACK backcalculation program developed by Ioannides et al. (1989). The steps involved in the backcalculation procedure as described by Crovetti (2002) based on data of deflection tests using a 30-cm diameter loading plate are as follows:

a. Calculate deflection basin parameter *AREA* by Equation (3-10) using surface deflections at 0, 30.48, 60.96 and 91.44 cm from the center of loading plate.

$$AREA\,(cm) = \frac{15.24}{D_1}\left[D_1 + 2D_3 + 2D_5 + D_6\right] \qquad (3\text{-}10)$$

where D_1, D_3, D_5 and D_6 are measured deflections at 0, 305, 610 and 914 mm respectively from the center of loading plate.

b. Estimate the radius of relative stiffness ℓ_{est} from Equation (3-11) based on infinite-slab backcalculation analysis,

$$\ell_{est}\,(\text{cm}) = \left[\frac{\ln\left(\frac{91.44 - AREA}{4603.189}\right)}{-2.069416}\right]^{4.387009} \tag{3-11}$$

c. Calculate adjustment factors for deflection D_1 and ℓ_{est} from Equations (3-12a) and (3-12b),

$$C_d = 1 - 1.15085\, e^{-0.71878\left[\frac{L}{\ell_{est}}\right]^{0.80151}} \tag{3-12a}$$

$$C_\ell = 1 - 0.89434\, e^{-0.61662\left[\frac{L}{\ell_{est}}\right]^{1.04831}} \tag{3-12b}$$

d. Calculate adjusted D_1 as $(D_1)_{adj} = C_d$ (measured D_1)

e. Calculate adjusted ℓ as $\ell_{adj} = C_\ell\, \ell_{est}$

f. Calculate E_c and k by Equations (3-13a) and (3-13b),

$$k = \frac{P}{(D_1)_{adj}(\ell_{adj})^2}\left(0.1253 - 0.008\left[\frac{a}{\ell_{adj}}\right] - 0.028\left[\frac{a}{\ell_{est}}\right]^2\right) \tag{3-13a}$$

$$E_c = \frac{12(\ell_{adj})^4(1-\mu^2)k}{H^3} \tag{3-13b}$$

where P = applied test load

a = radius of applied load, expressed in the same unit as ℓ_{adj}

μ = Poisson's ratio of concrete

H = thickness of concrete slab

3.3.2.3 Backcalculation Using Korenev's Correction for Finite Slab Size

Hall et al. (1996) proposed some refinements to Crovetti's correction procedure to more closely represent the effect of rectangular pavement slabs. The refinements were based on the work of Korenev (1954) who developed an analytical solution for interior loading by generalizing Westergaard's solution for deflection of an infinite slab to the case of a circular slab.

Hall et al. (1996) adopted the following changes to the Crovetti's correction procedure described in the preceding section:

a. For slabs with its length less than or equal to twice the slab width, L in Equations (3-12a) and (3-12b) is computed as

$$L = \sqrt{(Slab\ Length)\,(\text{Slab Width})} \tag{3-14}$$

b. For slabs with its length more than twice the slab width, L in Equations (3-12a) and (3-12b) is computed as

$$L = \sqrt{2}\,(\text{Slab Width}) \tag{3-15}$$

c. The corrected k value is computed as

$$k = \frac{k_{est}}{C_d C_\ell^2} \tag{3-16}$$

The corrected E_c is computed from Equation (3-13b) using the corrected k value obtained from Equation (3-16).

3.3.3 LTTP Database and Input Parameter Used in Evaluation

The data for this study were extracted from the database of LTPP program (Elkins et al., 2003). These data included deflection test data and measured pavement properties for some pavement sections. Because the purpose of this study was to evaluate the effect of slab size on jointed concrete pavement (JCP), only JCP

pavement sections having measured E_c or k, or both were considered. The properties of JCP pavement sections evaluated are listed in Tables 3.1 and 3.3.

Seven deflection readings per deflection basin, D_1, D_2, D_3, D_4, D_5, D_6, and D_7 measured at 0, 203, 305, 457, 610, 914 and 1524 mm, respectively, from the center of a loading plate of 300-mm diameter and the load level 71.1 kN of the FWD tests, applied on an interior point of the slab, was considered in this study.

3.3.4 Analysis of Effects of Finite Slab Size

3.3.4.1 Results of Backcalculation Analysis

The results of backcalculation analysis are found in Figure 3.7 in which the backcalculated values of k or E_c are plotted against the corresponding measured values extracted from the LTPP database. It is noted more than one deflection basins are recorded for each pavement section in the LTPP database, although only one measured E_c and one k value are reported per pavement section. In other words, while only one value each of the measured E_c and k are available in one pavement section, more than one backcalculated E_c and one k values respectively are obtained for the same pavement section. Parts (a) and (b) of Figures 3.7 compare the measured k values with the corresponding pavement-section average backcalculated values, while parts (c) and (d) compare them with the backcalculated values obtained from individual deflection basins. The same arrangement of plots is presented in parts (e), (f), (g) and (h) of Figure 3.7 for E_c.

3.3.4.2 Basis of Evaluation

The assessment of the relative performance of the five backcalculation methods is made based on similar indicators as previous section, that is, $RMSPE_1$ (errors

computed using average backcalculated property values), $RMSPE_2$ (errors computed using individual backcalculated property values), frequency distribution of percent errors for both average and individual backcalculated property values; and statistical significance tests to determine if there are significant differences between the pavement-section average backcalculated values and the measured values for each of the five backcalculated methods.

3.3.4.3 Results of Evaluation Analysis

The data presented in Figure 3.7 were used to compute the $RMSPE_1$ and $RMSPE_2$ for the backcalculated E_c and k values by the five backcalculation methods. Table 3.7 summarizes the outcomes of the *RMSPE* analysis. The frequency plots and frequency distribution of the percent errors of the backcalculated E_c and k values are presented in Figures 3.8 and 3.9.

Comparison of Backcalculation Programs Based on *RMSPE*

The *RMSPE* values computed in Table 3.7 represent quantitatively the deviations of the backcalculated E_c or k values from their corresponding measured values. The following observations may be made:

a. Overall, NINE-BACK yielded the lowest *RMSPE* values, although the differences between the performance of NINE-BACK and NUS-BACK are relatively small. There are practically no differences in the *RMSPE* of backcalculated k values by the two backcalculated programs, although NINE-BACK appears to outperform NUS-BACK in the prediction of E_c.

   The basic difference between the NINE-BACK program (based on a nine-slab model of jointed pavement system) and the NUS-BACK program (based on an

infinite slab without joints) is the presence of joints in the model of the former program representing a discontinuity that allows only the transfer of load but not bending moments. The results suggest that the consideration of joints have produced some positive improvements in the prediction of E_c, but there are practically no effects on the backcalculated k values.

b. The ONE-BACK backcalculation program based on the theoretical solution of a single slab with free edges, and the two finite-slab backcalculation programs based on Crovetti's and Korenev's correction factors respectively, all produce much higher *RMSPE* values than those of either NINE-BACK or NUS-BACK. The finite-slab method with Korenev's correction factors gives the highest *RMSPE* values for backcalculated k, while the method with Crovetti's correction factors results in the highest *RMSPE* values for backcalculated E_c.

It is noted that an infinite-slab model and a single-slab model represents the two theoretical extreme conditions of a jointed rigid pavement system. An actual in-service concrete pavement under load is likely to produce responses in between the predicted responses by the two models. In the case of backcalculation analysis, with a set of given deflections of an actual in-service pavement, an infinite-slab model will tend to under-estimate the load bearing properties of the pavement whereas a single slab model will tend to over-estimate the same properties. In other words, the infinite-slab model gives the lower-bound solutions of the backcalculated properties, while the single-slab model gives the upper-bound solutions. The results of Table 3.7 indicate that, for the cases analyzed in this study, the infinite-slab and the nine-slab models provide better representations than the single-slab models.

Comparing the *RMSPE* values of the ONE-BACK program and the other two finite-slab programs, better results are obtained with the ONE-BACK backcalculation program. This suggests that the application of Crovetti's and Korenev's correction factors respectively, which may be considered to be partially empirical in nature, appear to have resulted in over correction and led to higher deviations than the upper bound represented by the theoretical ONE-BACK solutions.

c. The magnitudes of *RMSPE* of the backcalculated k are larger than the corresponding *RMSPE* of the backcalculated E_c, regardless of the backcalculation algorithm adopted. This could possibly be attributed to two reasons:

- The times of measurements of k and E_c were different from the times of deflection tests. k values are affected more because compared to E_c, they tend to vary more with the environmental factors which often change with the season and climate.
- The locations of k or E_c measurements were likely to be different from the points of deflection tests. This location effect would have a higher impact on k than E_c because k varies with the soil condition along the pavement section while E_c of the concrete slab, which is a manufactured and controlled material, does not vary significantly within a pavement section.

Comparison Based on Frequency Distribution of Percent Errors

Two types of frequency plots are prepared. The cumulative frequency distributions of absolute percent errors backcalculated k and E_c are presented in Figure 3.8. The frequency distributions of the algebraic percent errors are presented in the

bar-chart plots of Figure 3.9 for the backcalculated k and E_c values. The following observations may be made:

a. In terms of the absolute percent errors of backcalculated k, Figures 3.8(a) and 3.8(b) show that the infinite-slab model, the nine-slab model and the one-slab model exhibit more or less similar error trends, outperforming the two finite-slab solutions with Crovetti's and Korenev's corrections respectively.

b. In terms of the absolute percent errors of backcalculated E_c, Figures 3.8(c) and 3.8(d) show that the nine-slab model marginally outperforms the infinite-slab model, the one-slab model and the finite-slab model with Korenev's corrections. The finite-slab model with Crovetti's corrections produced much larger errors than the other four methods.

c. The bar-chart plots in Figure 3.9 offer a qualitative assessment of the biasness of the predicted values of the five backcalculation methods. Based on the percentage of cases of over- and under-estimation respectively as summarized in Table 3.8, it may infer that more cases of the infinite-slab and the nine-slab backcalculated solutions tend to under-estimate k and E_c, while more cases of the one-slab and the two finite-slab backcalculated solutions tend to over-estimate the same properties (with the only exception that the finite-slab model with Korenev's corrections has marginally more under-estimation cases for E_c).

Comparison Based on Statistical Characteristics of Errors

Since each pavement section studied has a measured k or E_c value and an average backcalculated k or E_c value by a given backcalculation method, a statistical test on the pair-wise differences of the measured and backcalculated values can be conducted to determine if the backcalculation method would provide a good estimation of measured

values. The Student's *t* test is a suitable statistical hypothesis test for this purpose (Montgomery and Runger, 2003). Table 3.9 summarizes the results of the hypothesis testing. The null hypothesis is that there is no difference between the backcalculated and measured values. The following observations may be made:

a. At a level of significance of 0.05 (i.e. 95% level of significance), the hypothesis that there is no difference between the backcalculated and measured *k* values is accepted for the following three solutions: infinite-slab solution by NUS-BACK, nine-slab solution by NINE-BACK, single-slab solution by ONE-BACK. The hypothesis is rejected for the two solutions using Crovetti's and Korenev's corrections respectively.

b. At a level of significance of 0.05 (i.e. 95% level of significance), the hypothesis that there is no difference between the backcalculated and measured E_c values is accepted for the following four solutions: infinite-slab solution by NUS-BACK, nine-slab solution by NINE-BACK, single-slab solution by ONE-BACK, and finite-slab solution with Korenev's corrections. The hypothesis is rejected for the solution using Crovetti's corrections.

c. A further statistical test can be conducted to check if any of the backcalculation methods had under- or over-estimated the *k* or E_c value. This involves an alternative hypothesis by means of a one-tailed *t* test. It was found that both the finite-slab methods with Crovetti's and Korenev's corrections over-estimated *k* at 95% confidence level, while the single-slab method based on ONE-SLAB over-estimated *k* at 90% confidence level. As for $E_{c,}$ only the finite-slab method with Crovetti's corrections was found to over-estimate the property at 95% confidence level.

Summary Remarks on Choice of Backcalculation Methods

The comparisons of the measured and backcalculated values of k and E_c by the five backcalculation methods highlight the following points regarding the issue of considering finite slab size in backcalculation analysis:

a. The results of backcalculation analysis confirm that the infinite-slab and one-slab solutions offer the lower and upper bound values, respectively, of the pavement properties. As indicated by the error analysis based on *RMSPE*, frequency plots and statistical hypothesis testing, the theoretical one-slab solutions tend to over-estimate k and E_c. On the other hand, although the infinite-slab solutions show some tendency to under-estimate the two properties, the differences between the measured and backcalculated values were found statistically not significant.

b. In comparison with the infinite-slab solutions, the theoretical nine-slab model provides some improvements in the prediction of E_c, and comparable quality of backcalculated k values. In general, the error analyses performed indicate that there were little differences in the relative performance of the two backcalculation solutions. However, the need for additional input information on slab dimensions and joint load transfer details presents a major practical hurdle for the use of nine-slab model in practice. Since the nine-slab model represents an interior slab without major joint defects, one may suggest that unless there are serious joint defects, it is practical and logical to apply the infinite-slab model to provide conservative estimations of k and E_c.

c. The results of the backcalculation analysis have shown that the finite-slab solutions based on either Crovetti's or Korenev's corrections produced the largest errors with respect to measured k and E_c values. Statistical tests also

indicate that the two solutions tend to over-estimate the pavement properties, which is undesirable in terms of pavement evaluation and rehabilitation analysis.

3.3.5 Summary

This section has presented an analysis to compare the relative performance of five backcalculation methods to study the effects of considering finite slab size in backcalculation analysis of the modulus of concrete slab (E_c) and modulus of subgrade reaction (k) of concrete pavements. The LTPP database of deflection test data and measured pavement properties were used as the basis for the analysis. The relative performance of the five backcalculation methods was evaluated by comparing the backcalculated k and E_c with the corresponding methods.

The analysis based on field measured data indicated that the theoretical solutions of the infinite-slab backcalculation model and the one-slab backcalculation model can be used to provide the lower and upper bound values, respectively, in the estimation of k and E_c. Comparisons of the results of the two models showed that the infinite-slab model produced superior solutions with much smaller errors as compared with the one-slab model.

The use of the nine-slab model, considering the exact slab size and load transfer across joints, did not create nay noticeable differences in backcalculating k as compared with the infinite-slab solutions, but did achieve some improvements in the estimation of E_c. However, the differences or improvements were marginal and found not significant statistically. It shows that for jointed concrete pavements with normal functioning joints, the infinite-slab model is adequate in providing sufficiently accurate backcalculated k and E_c for practical applications.

Since the detailed joint properties and joint reinforcement data required for an accurate nine-slab representation are not readily available, the findings of the study suggest that for normal nondestructive deflection testing and evaluation analysis of jointed concrete pavements with non-defective joints, it is practical to adopt the infinite-slab backcalculation model as it provides sufficiently accurate and yet conservative estimations of k and E_c. The use of backcalculation methods that consider the finite slab dimensions and incorporate the effect of joint load transfer, such as the nine-slab model, would be practically justified only in detailed field investigation of pavements with defective joints where the load transfer function of the joints has been affected.

The use of the two finite-slab models with Crovetti's and Korenev's corrections respectively, for backcalculation analysis is not recommended based on the findings of this study. Both models produced lager errors than the other three models considered, and tended to over-estimate k and E_c. The solutions with Crovetti's corrections were found to over-estimate k and E_c at 95% confidence level, and the solutions with Korenev's corrections over-estimate k at the same confidence level.

Table 3.1: Measured Properties of 26 JCP Sections for Analyzing *k*

Case	State/Province	Test Section Code	Number of Deflection Basins	Measured k-value (MN/m^3)	Measured E_c (GPa)	Lane Width (m)	Joint Spacing (m)
1	Colorado	0213	11	114.76	24.50	4.27	4.57
2	Colorado	0214	10	122.09	33.12	3.66	4.57
3	Colorado	0215	10	103.09	29.33	3.66	4.57
4	Colorado	0222	10	73.25	32.09	3.66	4.57
5	Delaware	0201	10	80.03	-	3.66	4.57
6	Delaware	0203	10	51.55	29.74	4.27	4.57
7	Delaware	0204	10	74.61	30.34	3.66	4.57
8	Delaware	0205	10	47.48	-	3.66	4.57
9	Delaware	0206	9	65.11	37.12	4.27	4.57
10	Delaware	0207	10	54.26	27.74	4.27	4.57
11	Delaware	0208	10	54.26	28.94	3.66	4.57
12	Delaware	0259	11	59.69	37.76	3.66	4.57
13	Iowa	0213	11	39.61	32.66	4.27	4.57
14	Iowa	0219	10	17.36	35.36	4.27	4.57
15	Iowa	0223	10	12.21	39.05	3.66	4.57
16	Michigan	0214	10	130.22	34.16	3.66	4.57
17	Michigan	0215	10	69.18	33.12	3.66	4.57
18	Michigan	0217	10	62.40	-	4.27	4.57
19	Michigan	0219	11	105.81	27.26	3.66	4.57
20	Michigan	0220	10	92.24	32.43	3.66	4.57
21	North Carolina	0203	20	92.24	30.71	4.27	4.57
22	North Carolina	0204	10	61.04	35.06	3.66	4.57
23	North Carolina	0205	10	50.19	29.33	3.66	4.57
24	North Carolina	0208	20	40.70	32.70	3.66	4.57
25	Texas	A807	10	86.82	34.50	3.35	4.57
26	Texas	A808	8	86.82	35.19	3.35	4.57

Remarks:
- : *data not available*

Table 3.2: Root-Mean-Square Percent Errors for *k* and E_c Backcalculated Using NUS-BACK (Load Level = 71.1 kN)

k		E_c (CRCP)		E_c (JCP)	
Sensor Configuration	$RMSPE_1$ Value	Sensor Configuration	$RMSPE_1$ Value	Sensor Configuration	$RMSPE_1$ Value
47	75.97	13	41.92	13	25.49
57	76.25	14	52.87	12	31.04
45	76.31	12	56.55	14	35.00
37	76.32	15	68.03	15	49.11
46	76.40	16	88.08	24	65.18
27	76.60	23	94.73	16	66.63
56	77.04	24	94.74	25	75.57
17	78.23	25	96.46	26	87.08
36	78.77	26	112.64	34	87.45
26	80.13	35	118.58	35	89.72
35	82.86	17	124.17	17	91.50
67	82.96	36	125.96	23	94.82
25	85.97	46	136.60	36	96.73
16	88.17	34	142.59	46	106.46
34	92.41	27	146.47	27	108.73
24	97.11	45	148.70	56	113.91
15	105.36	56	150.24	45	116.00
23	124.22	37	157.40	37	117.81
14	130.41	47	172.00	47	129.89
13	182.98	57	186.36	57	143.89
12	279.09	67	6142.79	67	2544.56

Table 3.3: Measured Properties of 50 JCP Sections for Analyzing E_c

Case	State/Province	Test Section Code	No of Deflection Basins	Measured Ec (GPa)	Lane Width (m)	Joint Spacing (m)	Case	State/Province	Test Section Code	No of Deflection Basins	Measured Ec (GPa)	Lane Width (m)	Joint Spacing (m)
1	Arizona	7614	19	30.71	3.658	4.572	26	Michigan	0220	9	32.43	3.658	4.572
2	Arkansas	3059	18	24.50	3.658	13.716	27	Minnesota	3013	20	37.61	4.267	4.572
3	Colorado	0213	10	24.50	4.267	4.572	28	Missouri	4069	20	24.15	3.658	18.745
4	Colorado	0214	10	33.12	3.658	4.572	29	Nebraska	3023	20	26.22	3.658	4.724
5	Colorado	0215	10	29.33	3.658	4.572	30	Nevada	3013	20	37.43	3.658	4.724
6	Colorado	0222	10	32.09	3.658	4.572	31	New Jersey	4042	11	36.05	3.658	23.835
7	Colorado	7776	20	27.60	3.658	3.962	32	New Mexico	3010	20	41.06	3.658	4.115
8	Connecticut	4008	11	34.16	3.658	12.192	33	New York	4017	16	25.01	3.658	19.355
9	Delaware	0203	10	29.74	4.267	4.572	34	New York	4018	10	27.08	3.658	19.355
10	Delaware	0204	9	30.34	3.658	4.572	35	North Carolina	0203	10	30.71	4.267	4.572
11	Delaware	0208	10	28.94	3.658	4.572	36	North Carolina	0204	10	35.06	3.658	4.572
12	Delaware	0259	11	37.76	3.658	4.572	37	Ohio	3801	19	25.88	3.658	6.096
13	Iowa	0213	10	32.66	4.267	4.572	38	Oklahoma	3018	20	30.71	3.658	4.572
14	Iowa	0219	10	35.36	4.267	4.572	39	Oklahoma	4162	20	40.54	3.658	4.572
15	Iowa	0223	10	39.05	3.658	4.572	40	Texas	A807	10	34.50	3.353	4.572
16	Iowa	3006	20	31.57	3.658	6.096	41	Texas	A808	8	35.19	3.353	4.572
17	Iowa	3009	25	31.22	3.658	6.096	42	Utah	3010	11	31.22	3.658	4.572
18	Iowa	3028	18	30.36	3.658	6.096	43	Vermont	1682	13	33.12	3.658	4.572
19	Iowa	3055	20	23.98	3.658	6.096	44	Washington	3011	20	36.40	3.658	3.505
20	Kansas	4054	10	28.98	3.658	9.144	45	Washington	3014	20	32.43	3.658	3.505
21	Louisiana	4001	14	37.78	3.658	17.831	46	Washington	3019	20	34.16	3.658	3.505
22	Maine	3014	20	23.29	3.658	6.096	47	Washington	3813	20	36.40	3.658	4.572
23	Michigan	0214	12	34.16	3.658	4.572	48	Washington	7409	21	23.63	3.658	3.505
24	Michigan	0215	10	33.12	3.658	4.572	49	Wisconsin	3008	20	46.92	3.658	4.724
25	Michigan	0219	11	27.26	3.658	4.572	50	Wisconsin	3009	20	43.30	3.658	4.663

Table 3.4: Measured Properties of 76 CRCP Sections for Analyzing E_c

Case	State/Province	Test Section Code	Number of Deflection Basins	Measured Ec (GPa)	Case	State/Province	Test Section Code	Number of Deflection Basins	Measured Ec (GPa)
1	Alabama	3998	19	47.61	39	Oklahoma	5021	20	34.16
2	Alabama	5008	20	37.95	40	Oregon	5006	21	27.60
3	Arizona	7079	21	27.60	41	Oregon	5008	21	31.40
4	Arkansas	5803	19	33.81	42	Oregon	5021	18	24.50
5	Arkansas	5805	19	27.60	43	Oregon	5022	21	22.43
6	California	7455	11	32.43	44	Oregon	7081	21	27.26
7	Connecticut	5001	15	41.40	45	Pennsylvania	1598	16	42.78
8	Delaware	5004	13	23.12	46	Pennsylvania	1617	19	40.37
9	Georgia	5023	17	36.57	47	Pennsylvania	5020	15	49.34
10	Idaho	5025	20	30.71	48	South Carolina	5017	20	20.01
11	Illinois	5020	20	24.15	49	South Carolina	5034	20	21.74
12	Illinois	5843	20	41.75	50	South Carolina	5035	20	19.67
13	Illinois	5849	20	26.91	51	South Dakota	5020	20	25.53
14	Illinois	5854	20	27.60	52	South Dakota	5025	20	27.95
15	Illinois	5869	20	45.20	53	South Dakota	5040	20	31.74
16	Illinois	5908	20	22.43	54	Texas	3719	17	44.85
17	Illinois	9267	20	43.82	55	Texas	3779	20	29.33
18	Indiana	5022	20	41.40	56	Texas	5024	20	31.74
19	Indiana	5043	20	36.92	57	Texas	5035	18	28.64
20	Iowa	5042	20	27.95	58	Texas	5154	20	33.47
21	Iowa	5046	20	32.09	59	Texas	5274	19	38.30
22	Iowa	9116	19	34.16	60	Texas	5283	18	32.43
23	Maryland	5807	17	33.19	61	Texas	5284	18	30.71
24	Michigan	5363	20	31.74	62	Texas	5287	20	22.43
25	Minnesota	5076	21	37.95	63	Texas	5301	20	37.26
26	Mississipi	5006	20	32.09	64	Texas	5310	20	34.85
27	Mississipi	5025	20	30.71	65	Texas	5317	17	35.54
28	Mississipi	5803	19	32.09	66	Texas	5323	20	30.71
29	Mississipi	5805	20	38.99	67	Texas	5328	20	26.57
30	Missouri	5047	20	37.26	68	Texas	5334	20	37.95
31	Nebraska	5052	20	24.50	69	Texas	5335	20	36.57
32	North Carolina	5037	19	19.32	70	Texas	5336	20	29.67
33	North Carolina	5826	16	32.43	71	Virginia	2564	18	24.84
34	North Carolina	5827	16	21.05	72	Virginia	5008	20	24.15
35	Ohio	5003	20	25.53	73	Virginia	5009	16	20.70
36	Oklahoma	4155	19	30.02	74	West Virginia	5007	15	20.36
37	Oklahoma	4158	18	33.12	75	Wisconsin	5037	20	36.23
38	Oklahoma	4166	11	34.50	76	Wisconsin	5040	20	43.82

Table 3.5: *RMSPE* of Backcalculated Pavement Properties and Coefficient of Correlation with Measured Values from Four Different Methods

(a) Root-Mean-Square Percent Error (*RMSPE*)

Backcalculation Program	k		E_c			
	$RMSPE_1$	$RMSPE_2$	$RMSPE_1$		$RMSPE_2$	
			CRCP	JCP	CRCP	JCP
Load = 40 kN						
NUSBACK	69.95	71.33	51.56	40.71	61.31	51.81
ILLIBACK4	99.49	107.72	67.59	51.93	74.67	61.26
ILLIBACK7	83.69	88.34	84.79	68.05	86.96	73.02
LTPP Best-Fit Method	77.83	82.23	55.29	48.93	57.99	53.48
Load = 53.3 kN						
NUSBACK	72.54	74.85	35.53	34.54	48.46	46.95
ILLIBACK4	102.13	107.53	55.11	49.43	63.55	56.88
ILLIBACK7	86.79	90.73	74.93	65.54	79.91	68.48
LTPP Best-Fit Method	81.73	85.88	49.59	46.41	54.15	49.92
Load = 71.1 kN						
NUSBACK	75.97	78.39	41.92	25.49	47.14	33.02
ILLIBACK4	107.70	111.15	66.63	43.26	66.02	49.56
ILLIBACK7	91.51	94.52	85.17	59.08	86.13	64.16
LTPP Best-Fit Method	81.38	82.91	49.59	43.89	52.59	42.83

Note : The number of pavement sections used in calculation is as follows:

(a) For k: 26 sections (NUS-BACK and ILLI-BACK) methods, 15 sections (LTTP Best-Fit Method)

(b) For E_c of CRCP: 76 sections (NUS-BACK and ILLI-BACK) methods, 75 sections (LTTP Best-Fit Method)

(c) For E_c of JCP: 50 sections (NUS-BACK and ILLI-BACK) methods, 43 sections (LTTP Best-Fit Method)

(b) Coefficient of Correlation

Backcalculation Program	Coefficient of correlation		
	k	Ec	
		CRCP	JCP
Load = 40 kN			
NUSBACK	0.353	0.429	0.173
ILLIBACK4	0.288	0.434	0.192
ILLIBACK7	0.313	0.406	0.139
LTPP Best-Fit Method	0.367	0.404	0.349
Load = 53.3 kN			
NUSBACK	0.377	0.276	0.088
ILLIBACK4	0.323	0.351	0.151
ILLIBACK7	0.343	0.338	0.117
LTPP Best-Fit Method	0.298	0.385	0.348
Load = 71.1 kN			
NUSBACK	0.367	0.399	0.362
ILLIBACK4	0.304	0.381	0.323
ILLIBACK7	0.327	0.373	0.232
LTPP Best-Fit Method	0.326	0.377	0.331

Table 3.6: *RMSPE* of Backcalculated Pavement Properties with Temperature Consideration

(a) *RMSPE* on E_c

Backcalculation program	RMSPE without temperature consideration				RMSPE with temperature consideration			
	$RMSPE_1$ (%)		$RMSPE_2$ (%)		$RMSPE_1$ (%)		$RMSPE_2$ (%)	
	CRCP	JCP	CRCP	JCP	CRCP	JCP	CRCP	JCP
NUS-BACK	41.92	25.49	47.14	33.02	40.56	25.34	47.90	33.02
ILLI-BACK4	66.63	43.26	66.02	49.56	69.80	37.96	67.01	44.98
ILLI-BACK7	85.17	59.08	86.13	64.16	89.37	50.52	88.50	55.97
LTTP Best Fit	49.59	43.89	52.59	42.83	49.78	44.48	52.33	43.55

Note : The number of pavement sections used in calculation is as follows:

(a) For E_c of CRCP without temperature consideration: 76 sections (NUS-BACK and ILLI-BACK) methods, 75 sections (LTTP Best-Fit Method)

(b) For E_c of CRCP with temperature consideration: 61 sections (NUS-BACK and ILLI-BACK) methods, 60 sections (LTTP Best-Fit Method)

(c) For E_c of JCP: 50 sections (NUS-BACK and ILLI-BACK) methods, 43 sections (LTTP Best-Fit Method)

(d) For E_c of JCP: 39 sections (NUS-BACK and ILLI-BACK) methods, 33 sections (LTTP Best-Fit Method)

(b) *RMSPE* on *k*

Backcalculation program	RMSPE without temperature consideration		RMSPE with temperature consideration	
	$RMSPE_1$ (%)	$RMSPE_2$ (%)	$RMSPE_1$ (%)	$RMSPE_2$ (%)
NUS-BACK	75.97	78.39	83.33	86.50
ILLI-BACK4	107.70	111.15	120.33	126.88
ILLI-BACK7	91.51	94.52	101.98	106.63
LTTP Best Fit	81.38	82.91	85.26	88.89

Note : The number of pavement sections used in calculation is as follows:

(a) For *k* without temperature consideration: 26 sections (NUS-BACK and ILLI-BACK) methods, 15 sections (LTTP Best-Fit Method)

(a) For *k* with temperature consideration: 20 sections (NUS-BACK and ILLI-BACK) methods, 13 sections (LTTP Best-Fit Method)

Table 3.7: *RMSPE* of Backcalculated Pavement Properties from Five Different Methods

Backcalculation Program	k		E_c	
	$RMSPE_1$ (%)	$RMSPE_2$ (%)	$RMSPE_1$ (%)	$RMSPE_2$ (%)
Infinite-slab model using NUS-BACK	75.975	78.391	25.485	32.988
Single-slab model using ONE-BACK	100.529	93.898	29.606	41.469
Nine-slab model using NINE-BACK	75.969	82.295	20.596	26.069
Finite-slab model with Crovetti's Correction	121.870	125.627	39.545	46.046
Finite-slab model with Korenev's Correction	146.088	148.584	31.500	35.232

Note : The number of pavement sections used in calculation is as follows: 26 sections for k and 50 sections E_c.

Table 3.8: Percentages of Over-Estimation and Under-Estimation Cases

(a) Results for Backcalculated *k* values

Backcalculation Method	Pavement-Section Average Backcalculated *k*		Individual Deflection-Basin Backcalculated *k*	
	% Under-Estimation Cases	% Over-Estimation Cases	% Under-Estimation Cases	% Over-Estimation Cases
Infinite-slab model using NUS-BACK	69%	31%	73%	27%
Nine-slab model using NINE-BACK	62%	38%	63%	37%
Single-slab model using ONE-BACK	42%	58%	46%	54%
Finite-slab model with Crovetti's corrections	39%	61%	39%	61%
Finite-slab model with Korenev's corrections	27%	73%	33%	67%

(b) Results for Backcalculated E_c values

Backcalculation Method	Pavement-Section Average Backcalculated E_c		Individual Deflection-Basin Backcalculated E_c	
	% Under-Estimation Cases	% Over-Estimation Cases	% Under-Estimation Cases	% Over-Estimation Cases
Infinite-slab model using NUS-BACK	56%	44%	57%	43%
Nine-slab model using NINE-BACK	54%	46%	56%	44%
Single-slab model using ONE-BACK	46%	54%	53%	47%
Finite-slab model with Crovetti's corrections	28%	72%	30%	70%
Finite-slab model with Korenev's corrections	54%	46%	51%	49%

Table 3.9: Statistical Tests on Pairwise Differences between Backcalculated and Measured Pavement Properties

(a) Test on hypothesis that there is no difference between backcalculated and measured *k*

Property	Infinite-Slab Solution	Nine-Slab Solution	One-Slab Solution	Solution with Crovetti's Correction	Solution with Korenev's Correction
Mean Difference	-5.06	5.26	28.16	52.28	73.99
Standard Deviation	75.81	75.59	96.50	110.09	125.97
t statistic	-0.34	0.35	1.49	2.42	3.00
Critical t at $\alpha = 0.05$ *	± 2.06	± 2.06	± 2.06	± 2.06	± 2.06
Conclusion	Accept	Accept	Accept	Reject	Reject

Note: (1) α is the level of significance. Test is conducted at confidence level of 95% for $\alpha = 0.05$.
(2) The degree of freedom is (26 – 1) = 25

(b) Test on hypothesis that there is no difference between backcalculated and measured E_c

Property	Infinite-Slab Solution	Nine-Slab Solution	One-Slab Solution	Solution with Crovetti's Correction	Solution with Korenev's Correction
Mean Difference	-0.94	-3.33	1.60	21.07	1.72
Standard Deviation	25.47	20.32	29.56	33.47	31.45
t statistic	-0.19	-0.84	0.28	3.21	0.28
Critical t at $\alpha = 0.05$	± 2.01	± 2.01	± 2.01	± 2.01	± 2.01
Conclusion	Accept	Accept	Accept	Reject	Accept

Note: (1) α is the level of significance. Test is conducted at confidence level of 95% for $\alpha = 0.05$.
(2) The degree of freedom is (50 – 1) = 49

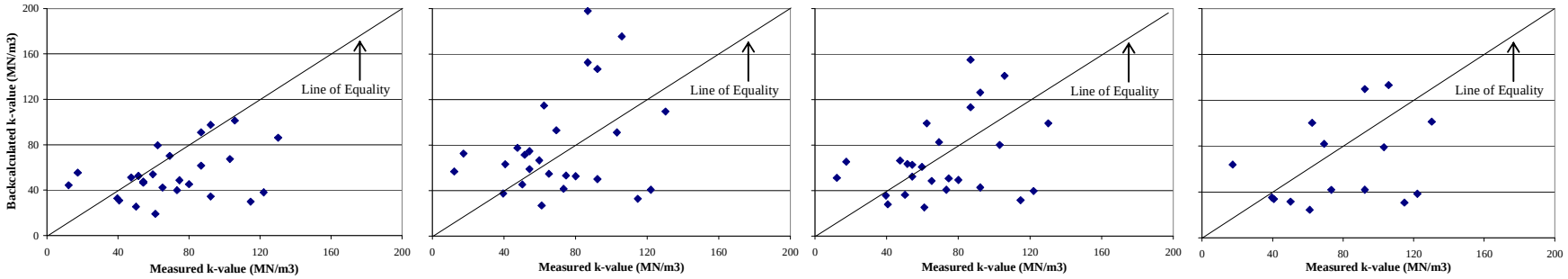

NUS-BACK ILLI-BACK4 ILLI-BACK7 LTPP Best-Fit Method

(a) Based on the mean backcalculated *k* values of each pavement section

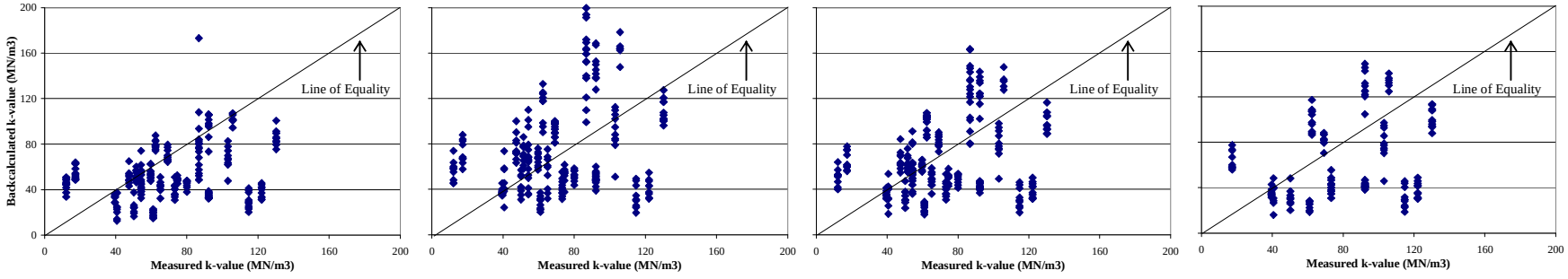

NUS-BACK ILLI-BACK4 ILLI-BACK7 LTPP Best-Fit Method

(b) Based on backcalculated *k* values of individual deflection basins

Figure 3.1: Comparison between Measured and Backcalculated *k* values of JCP (Load Level = 71.1 kN) from Four Different Methods

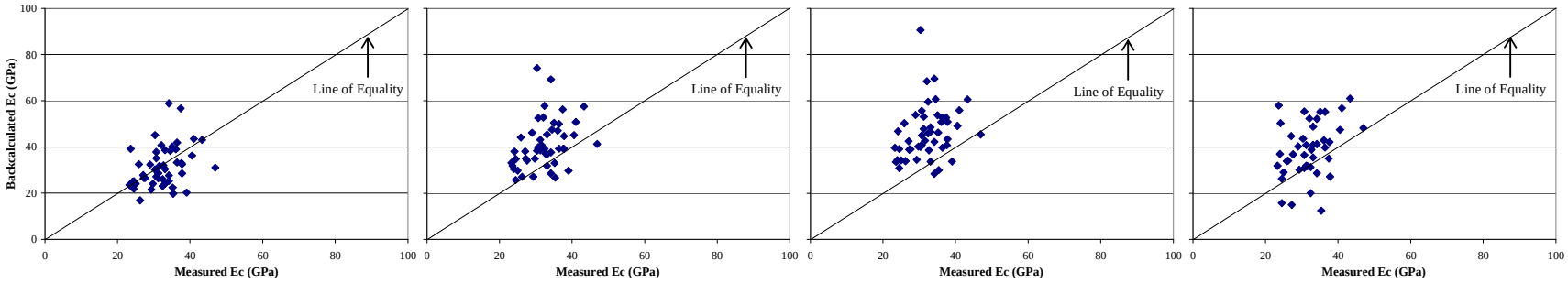

NUS-BACK ILLI-BACK4 ILLI-BACK7 LTPP Best-Fit Method

(a) Based on the mean backcalculated E_c values of each pavement section

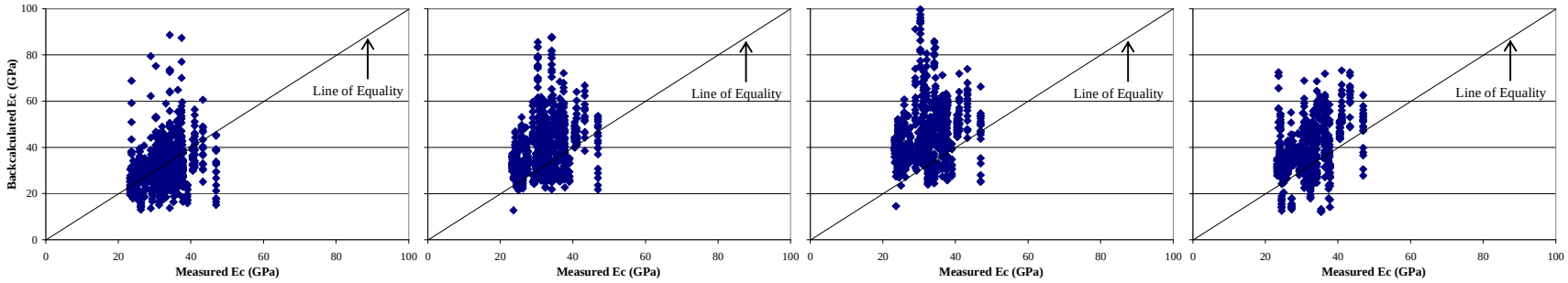

NUS-BACK ILLI-BACK4 ILLI-BACK7 LTPP Best-Fit Method

(b) Based on backcalculated E_c values of individual deflection basins

Figure 3.2: Comparison between Measured and Backcalculated E_c values of JCP (Load Level = 71.1 kN) from Four Different Methods

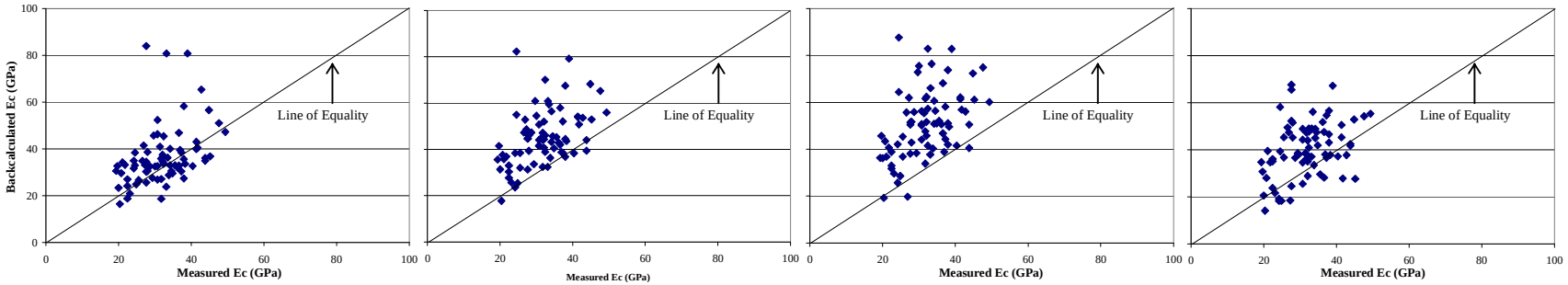

NUS-BACK ILLI-BACK4 ILLI-BACK7 LTPP Best-Fit Method

(a) Based on the mean backcalculated E_c values of each pavement section

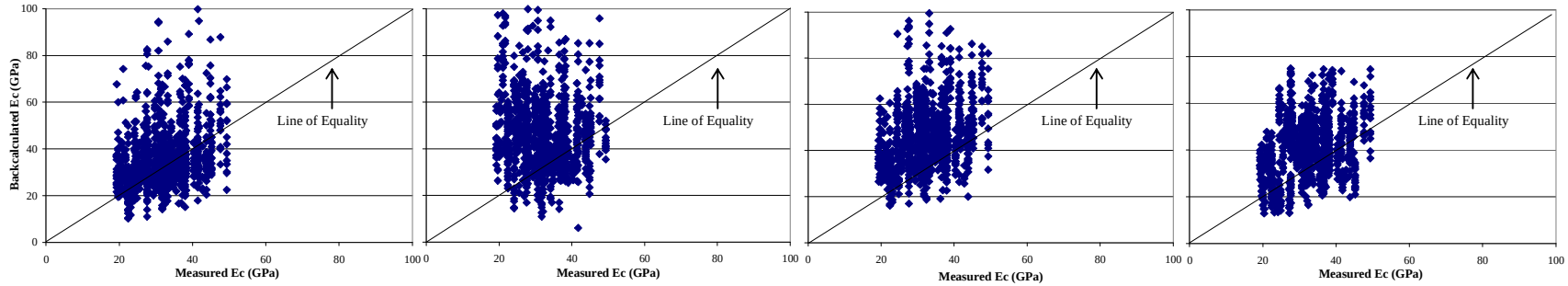

NUS-BACK ILLI-BACK4 ILLI-BACK7 LTPP Best-Fit Method

(b) Based on backcalculated E_c values of individual deflection basins

Figure 3.3: Comparison between Measured and Backcalculated E_c values of CRCP (Load Level = 71.1 kN) from Four Different Methods

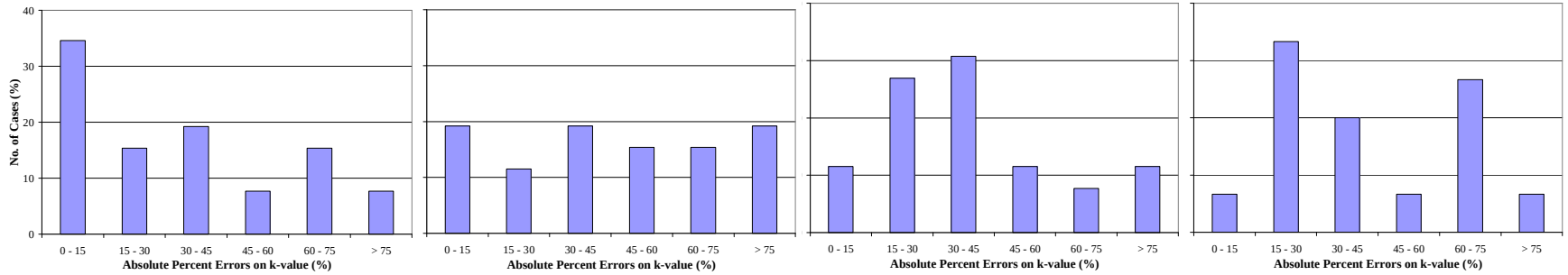

NUS-BACK ILLI-BACK4 ILLI-BACK7 LTPP Best-Fit Method

(a) Based on the mean backcalculated *k* values of each pavement section

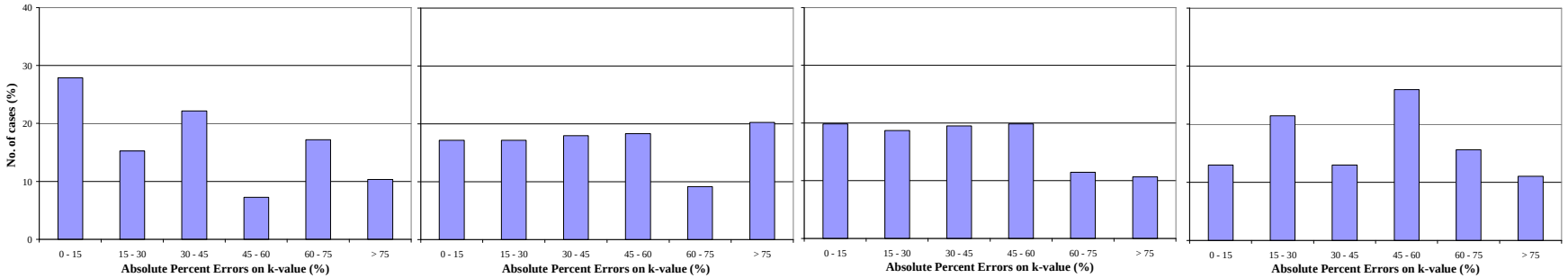

NUS-BACK ILLI-BACK4 ILLI-BACK7 LTPP Best-Fit Method

(b) Based on backcalculated *k* values of individual deflection basins

Figure 3.4: Absolute Percent Errors of Backcalculated *k* values (Load Level = 71.1 kN)

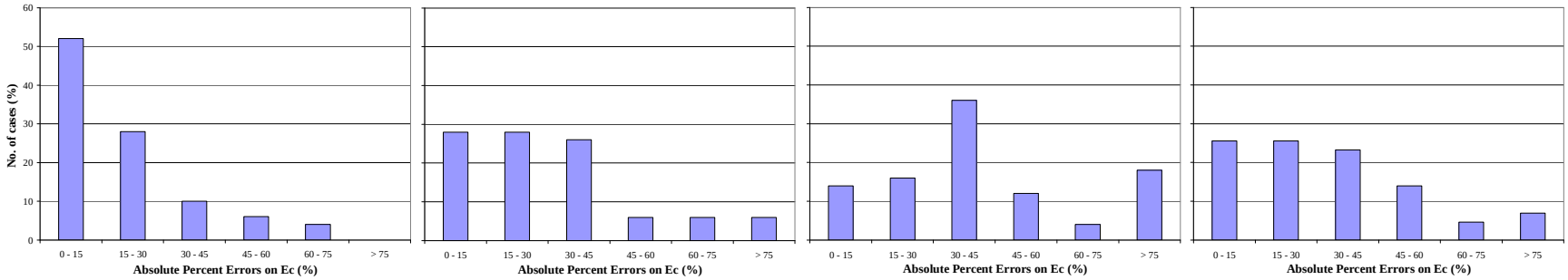

NUS-BACK ILLI-BACK4 ILLI-BACK7 LTPP Best-Fit Method

(a) Based on the mean backcalculated E_c values of each pavement section

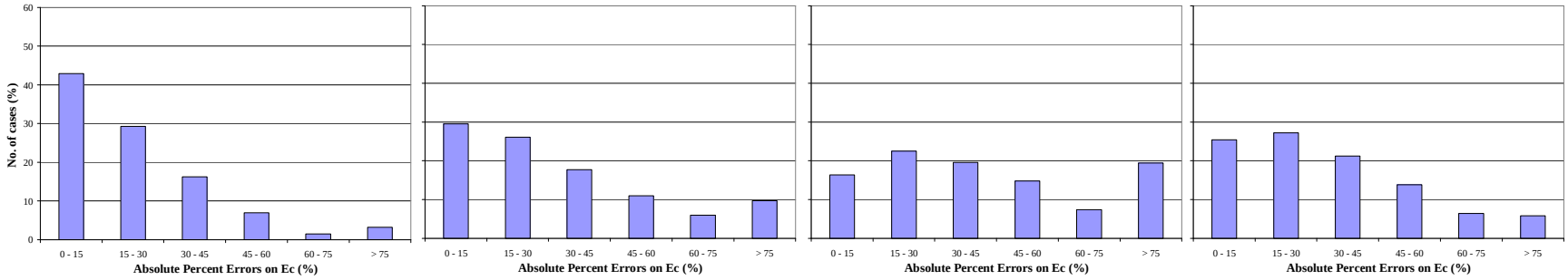

NUS-BACK ILLI-BACK4 ILLI-BACK7 LTPP Best-Fit Method

(b) Based on backcalculated E_c values of individual deflection basins

Figure 3.5: Absolute Percent Errors of Backcalculated E_c values of JCP (Load Level = 71.1 kN)

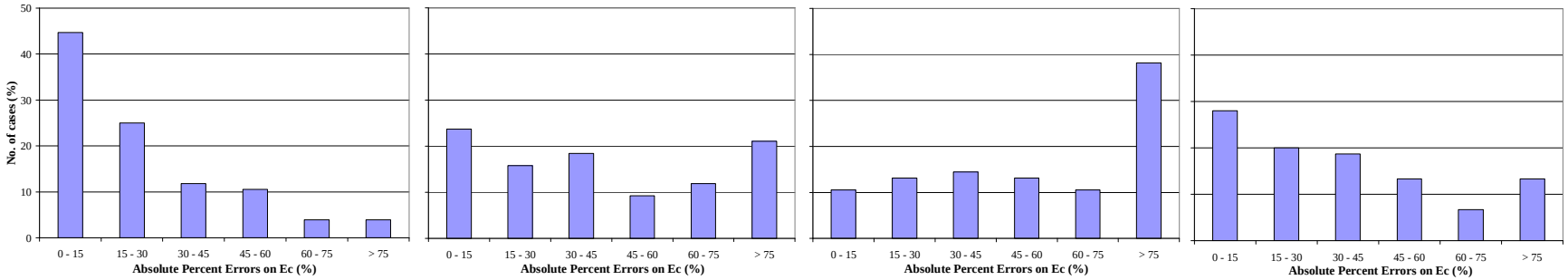

NUS-BACK ILLI-BACK4 ILLI-BACK7 LTPP Best-Fit Method

(a) Based on the mean backcalculated E_c values of each pavement section

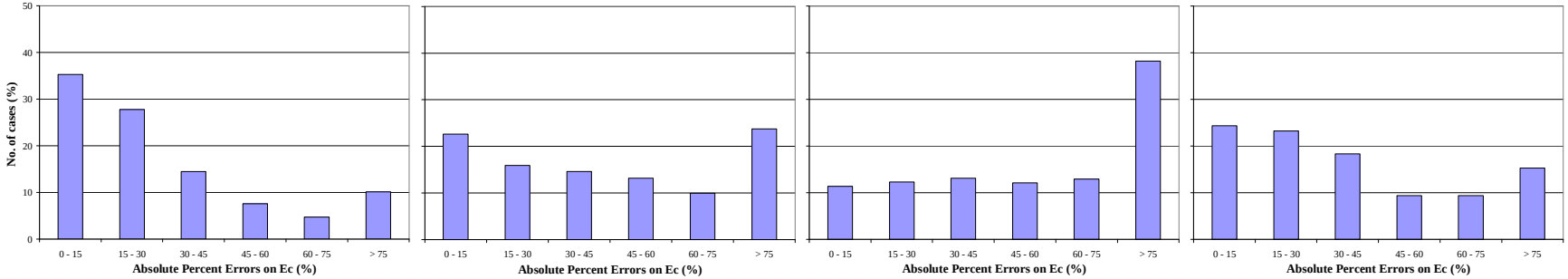

NUS-BACK ILLI-BACK4 ILLI-BACK7 LTPP Best-Fit Method

(b) Based on backcalculated E_c values of individual deflection basins

Figure 3.6: Absolute Percent Errors of Backcalculated E_c values of CRCP (Load Level = 71.1 kN)

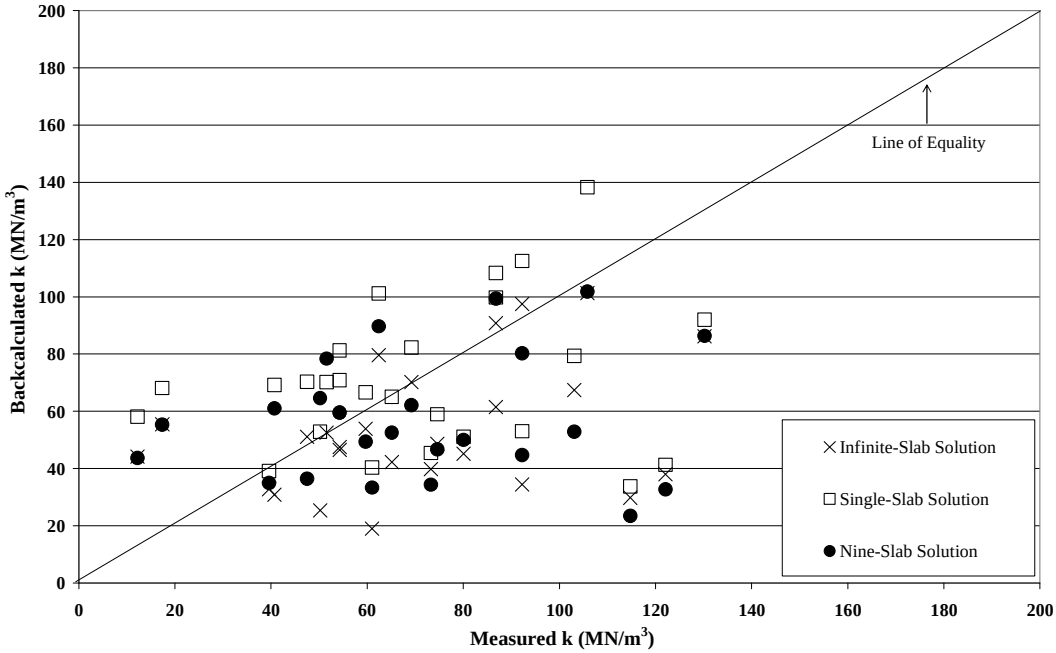

(a) Comparison of Theoretical Solutions Based on Pavement-Section Average Backcalculated *k*

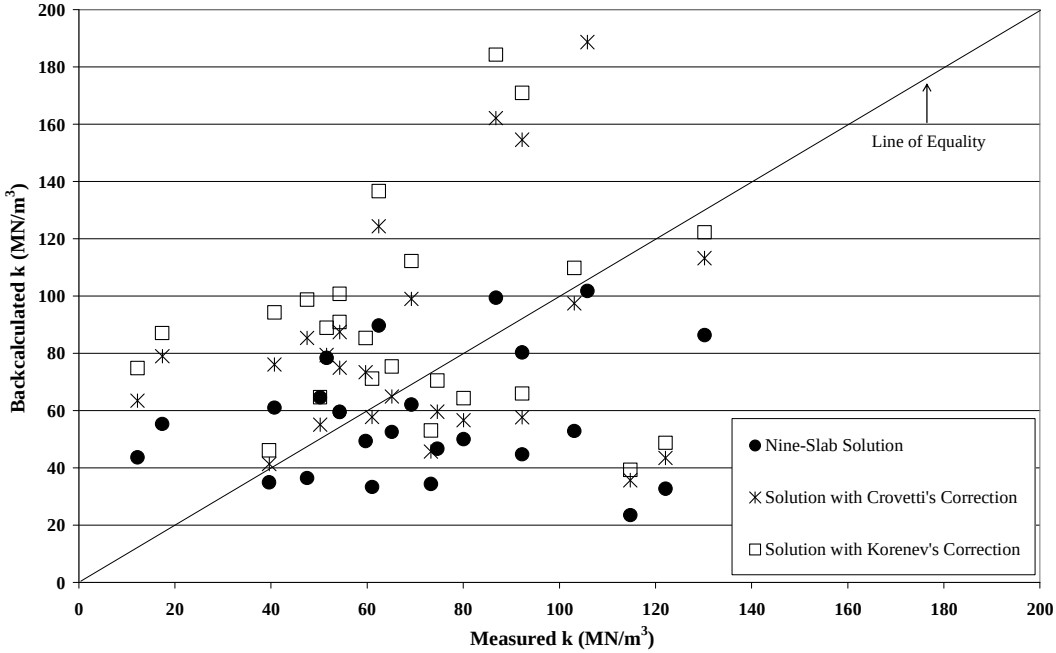

(b) Comparison of Solutions with Correction Factors Based on Pavement-Section Average Backcalculated *k*

Figure 3.7: Comparison between Backcalculated and Measured of *k* and E_c from Five Different Methods

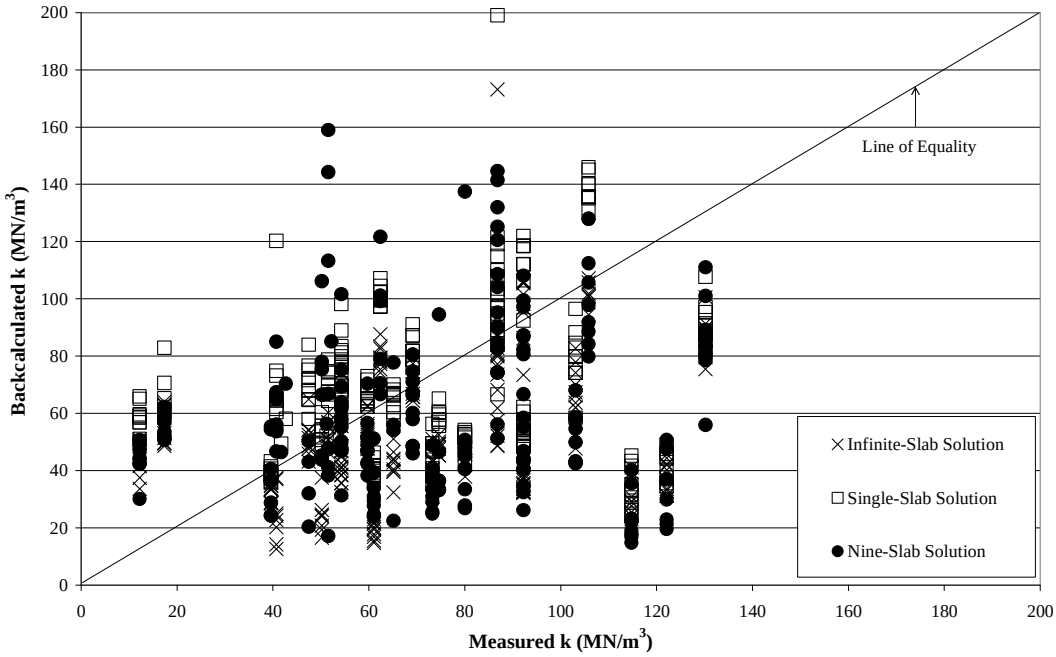

(c) Comparison of Theoretical Solutions Based on Individual Deflection-Basin Backcalculated *k*

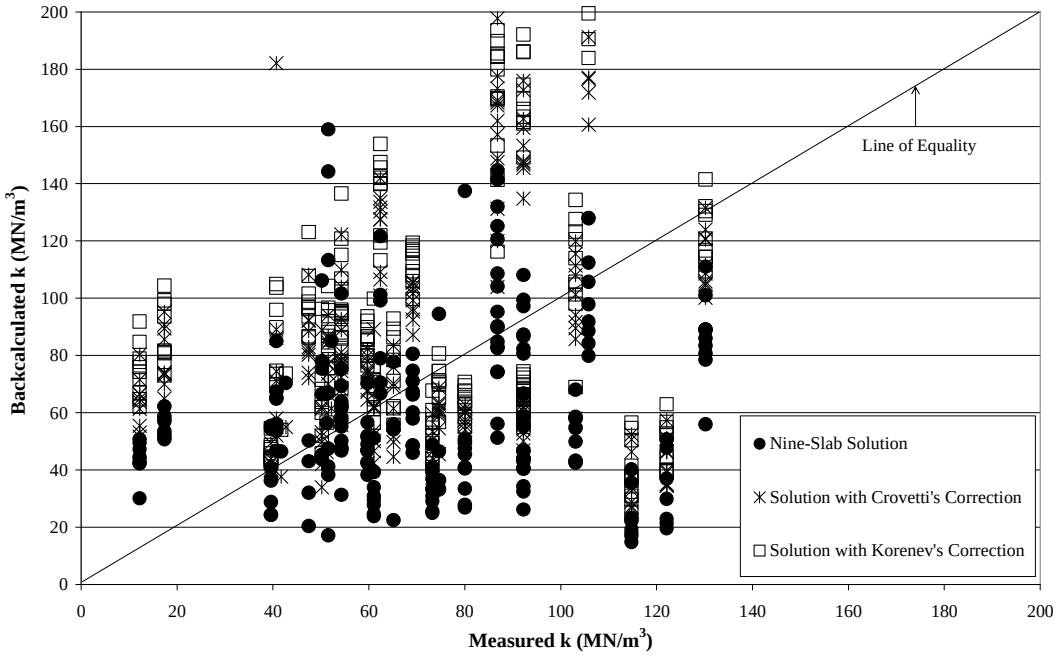

(d) Comparison of Solutions with Correction Factors Based on Individual Deflection-Basin Backcalculated *k*

Figure 3.7: Comparison between Backcalculated and Measured of *k* and E_c from Five Different Methods (continued)

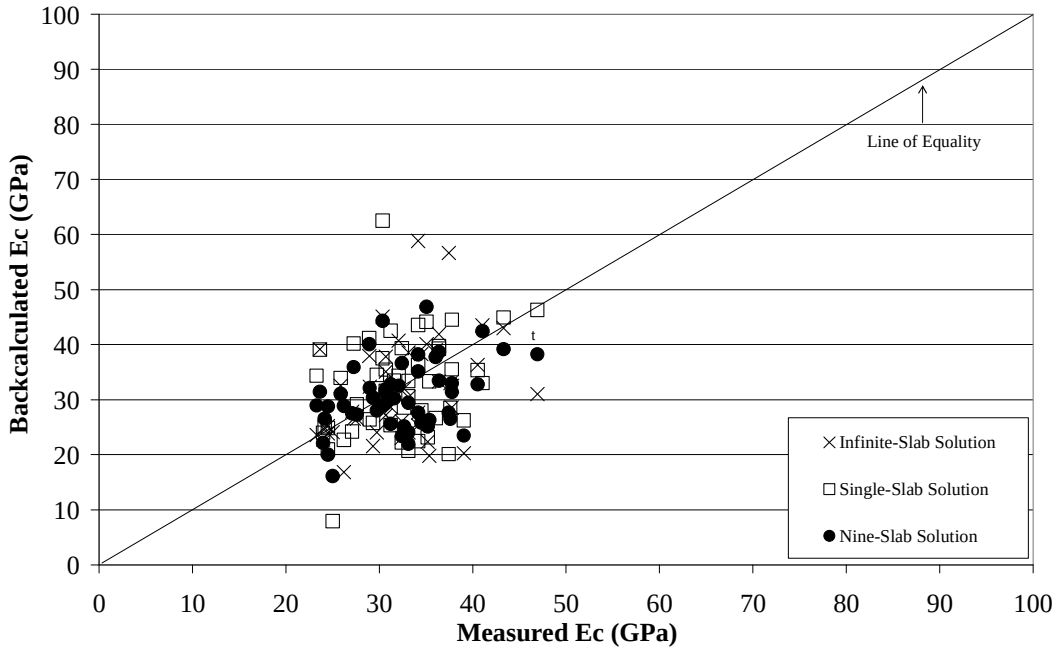

(e) Comparison of Theoretical Solution Based on Pavement-Section Average Backcalculated E_c

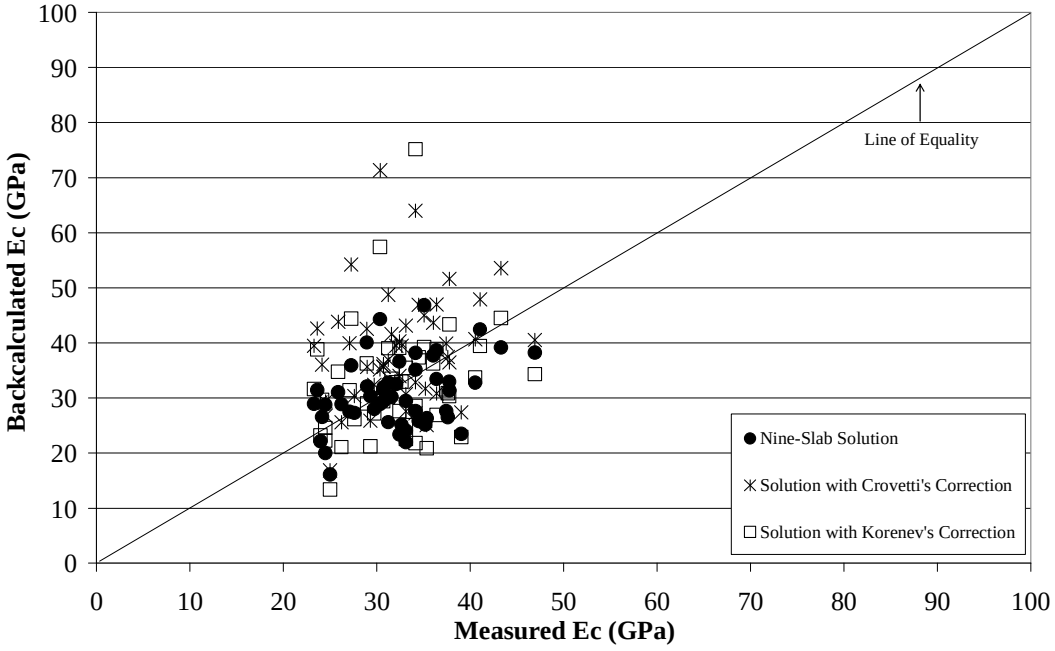

(f) Comparison of Solutions with Correction Factors Based on Pavement-Section Average Backcalculated E_c

Figure 3.7: Comparison between Backcalculated and Measured of k and E_c from Five Different Methods (continued)

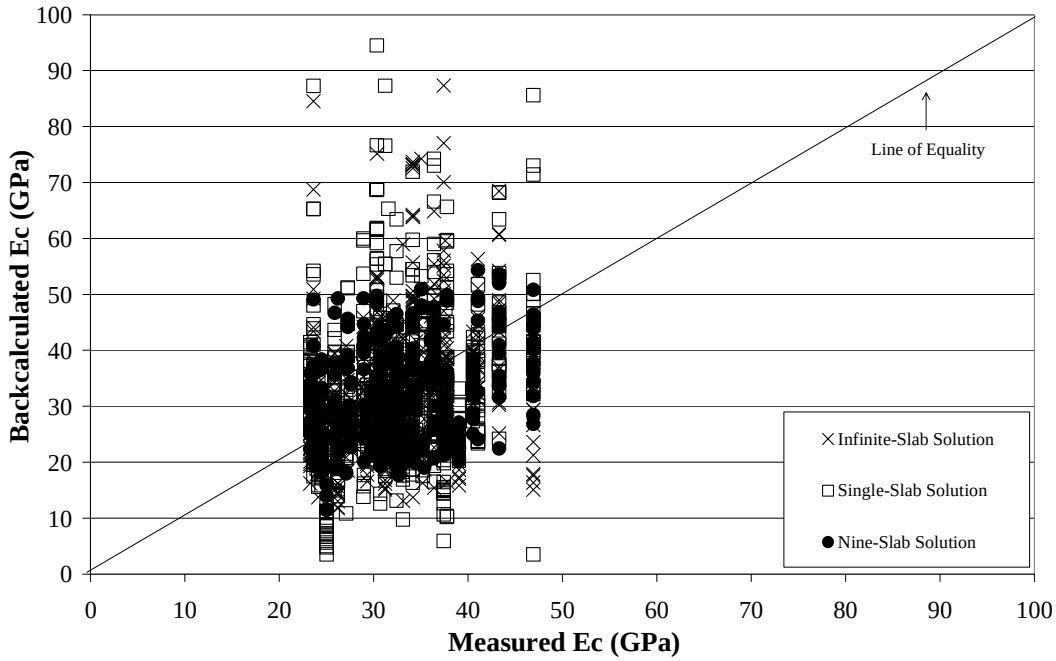

(g) Comparison of Theoretical Solution Based on Individual Deflection-Basin Backcalculated E_c

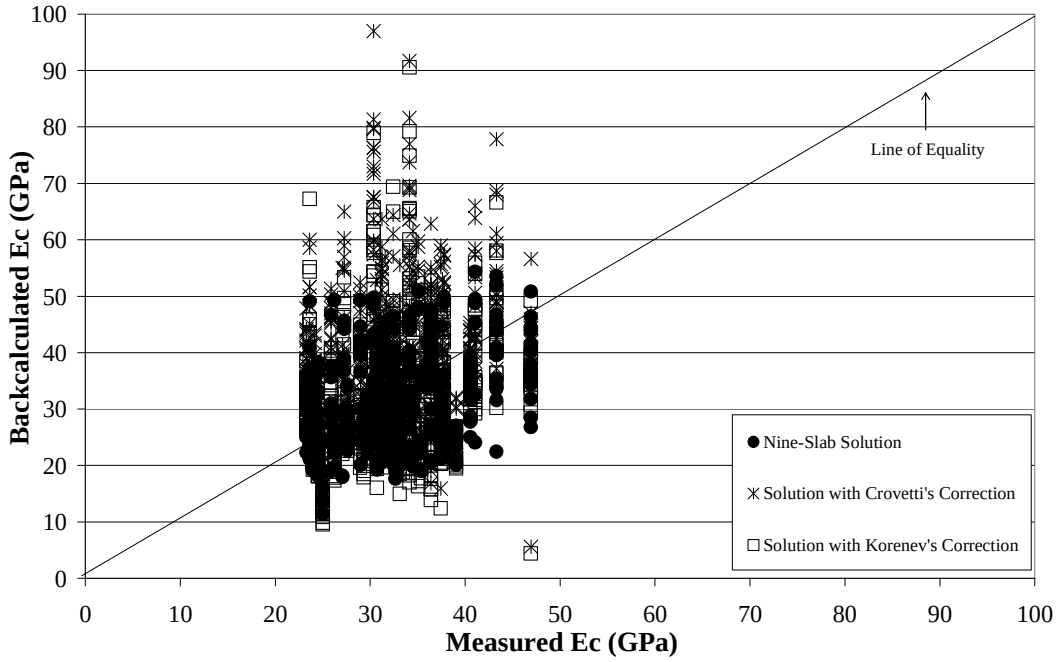

(h) Comparison of Solutions with Correction Factors Based on Individual Deflection-Basin Backcalculated E_c

Figure 3.7: Comparison between Backcalculated and Measured of k and E_c from Five Different Methods (continued)

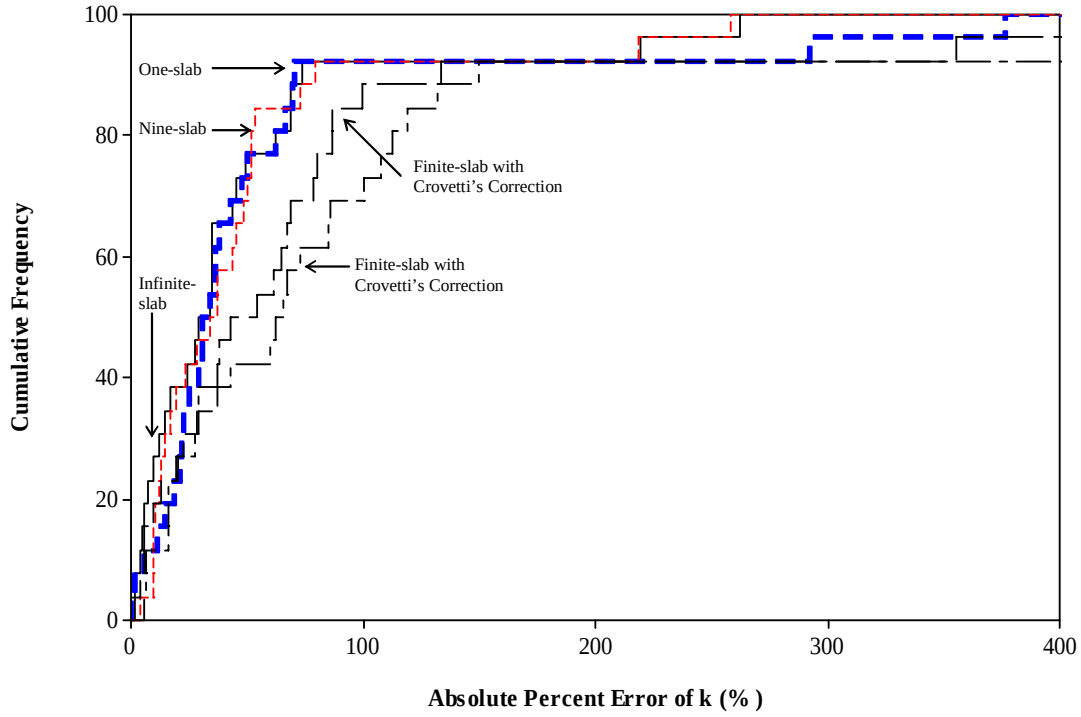

(a) Plot for Pavement-Section Average Backcalculated *k*

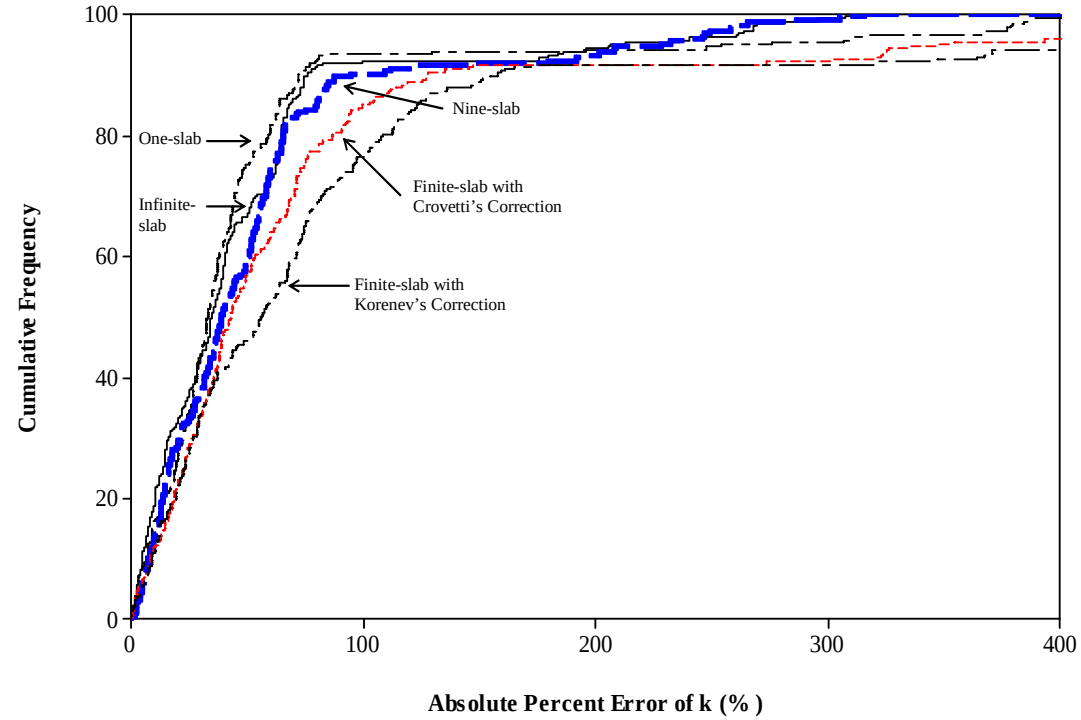

(b) Plot for Individual Deflection-Basin Backcalculated *k*

Figure 3.8: Cumulative Frequency Plots for Backcalculated *k* and E_c

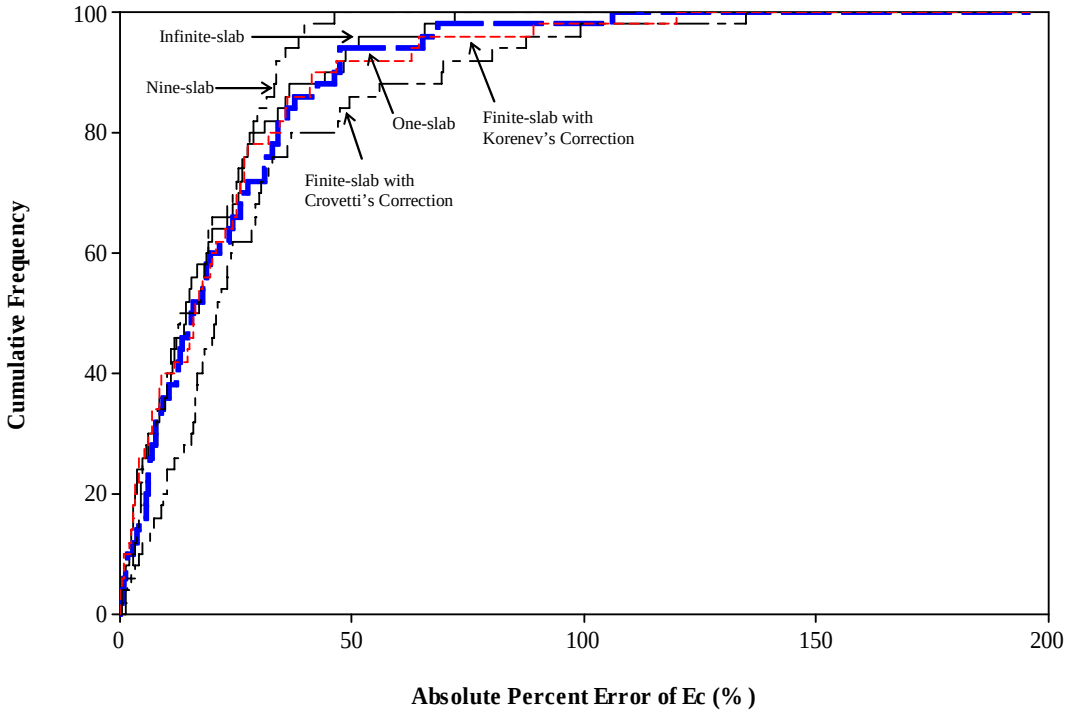

(c) Plot for Pavement-Section Average Backcalculated E_c

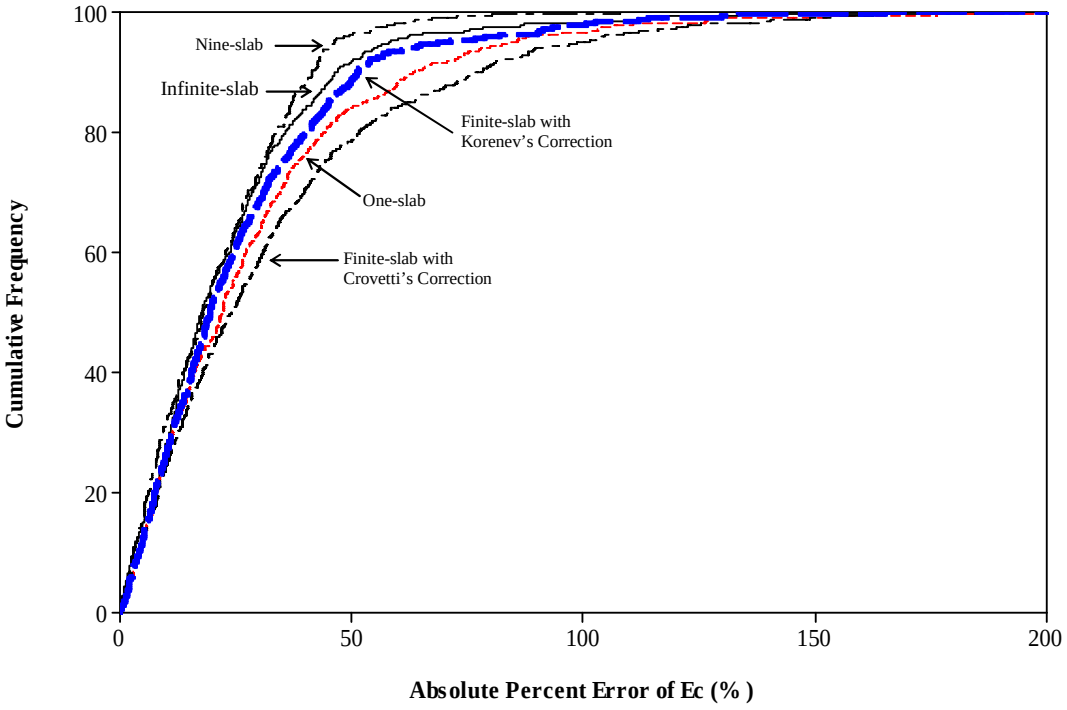

(d) Plot for Individual Deflection-Basin Backcalculated E_c

Figure 3.8: Cumulative Frequency Plots for Backcalculated k and E_c (continued)

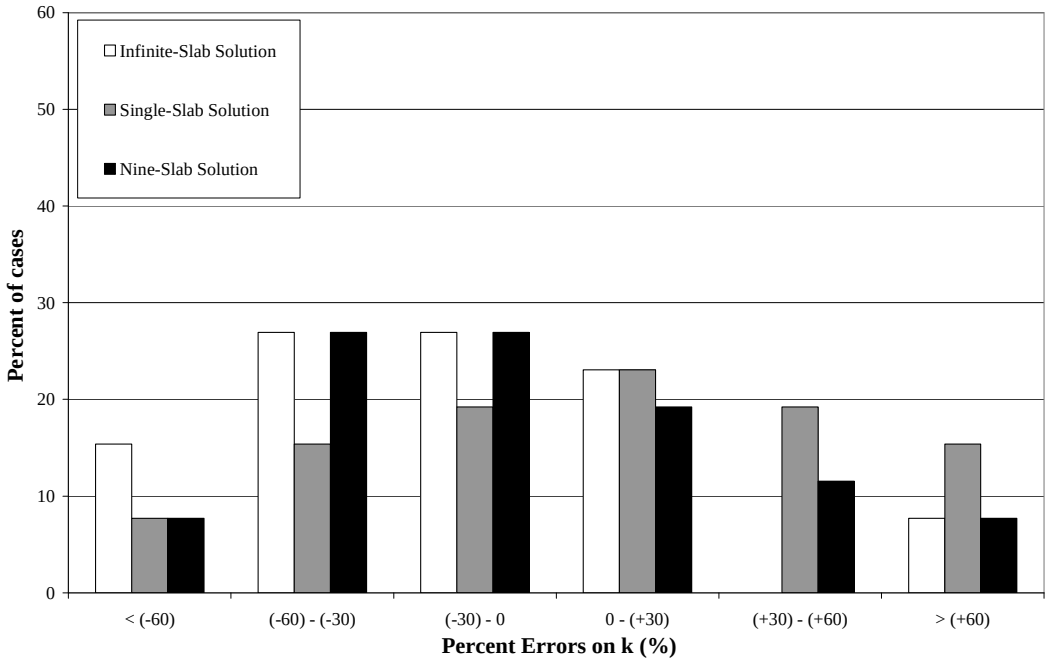

(a) Comparison of Theoretical Solutions Based on Pavement-Section Average Backcalculated *k*

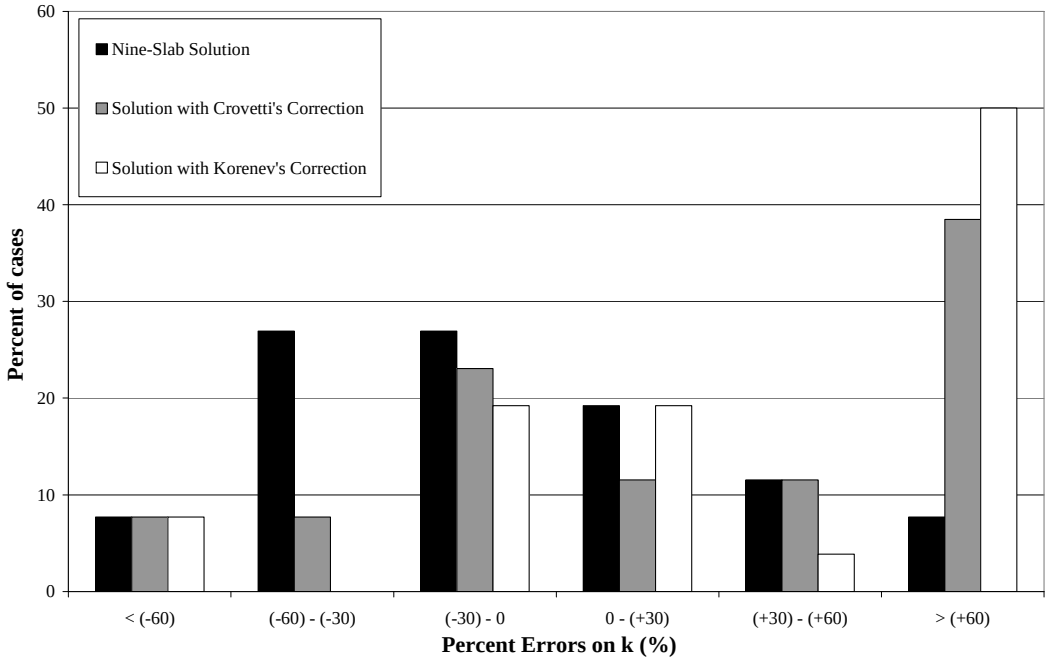

(b) Comparison of Solutions with Correction Factors Based on Pavement-Section Average Backcalculated *k*

Figure 3.9: Frequency Distributions of Percent Errors of Backcalculated Value of *k* and E_c

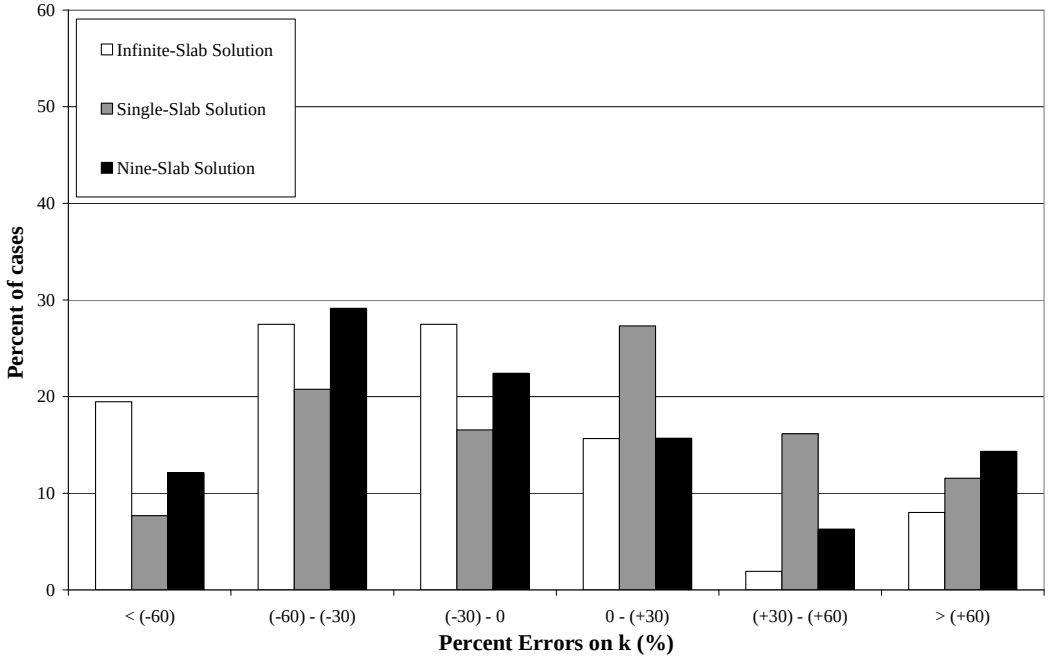

(c) Comparison of Theoretical Solutions Based on Individual Deflection-Basin Backcalculated *k*

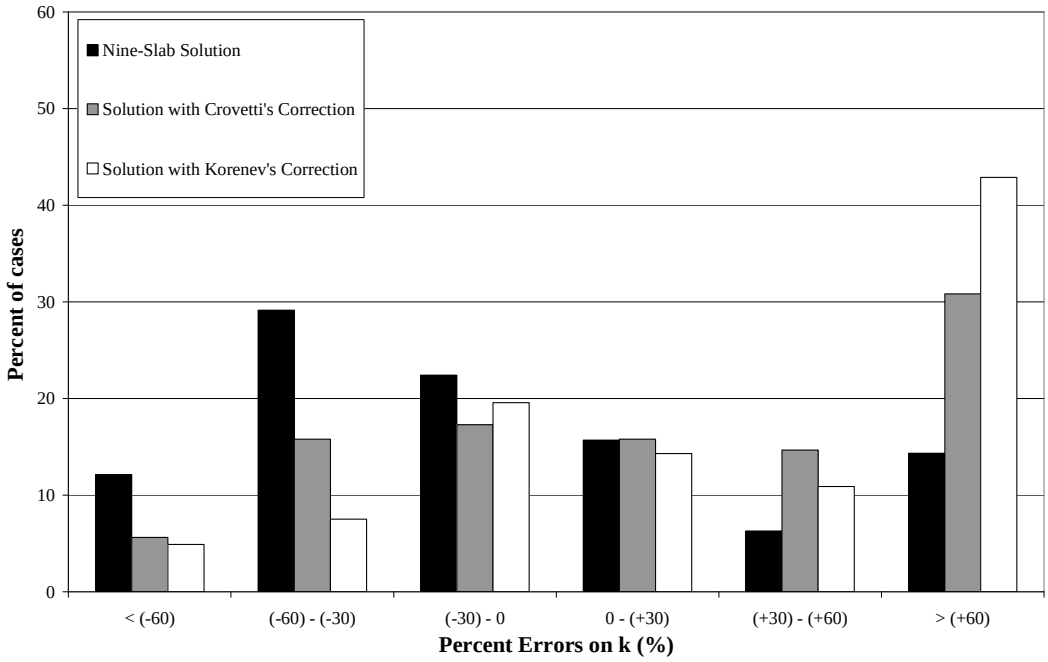

(d) Comparison of Solutions with Correction Factors Based on Individual Deflection-Basin Backcalculated *k*

Figure 3.9: Frequency Distributions of Percent Errors of Backcalculated Value of *k* and E_c (continued)

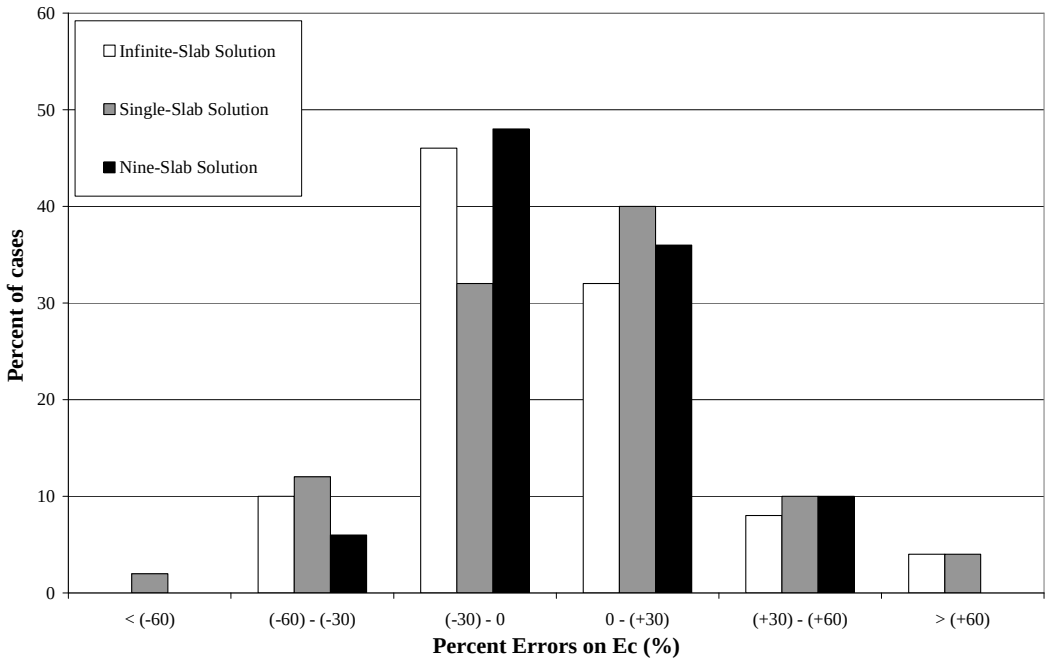

(e) Comparison of Theoretical Solution Based on Pavement-Section Average Backcalculated E_c

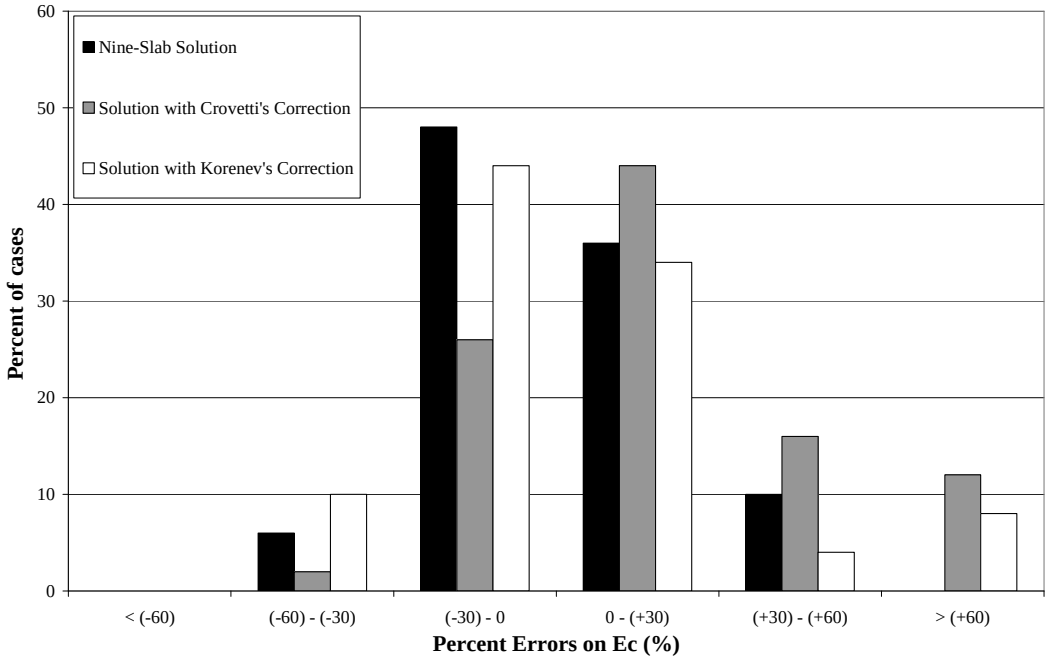

(f) Comparison of Solutions with Correction Factors Based on Pavement-Section Average Backcalculated E_c

Figure 3.9: Frequency Distributions of Percent Errors of Backcalculated Value of k and E_c (continued)

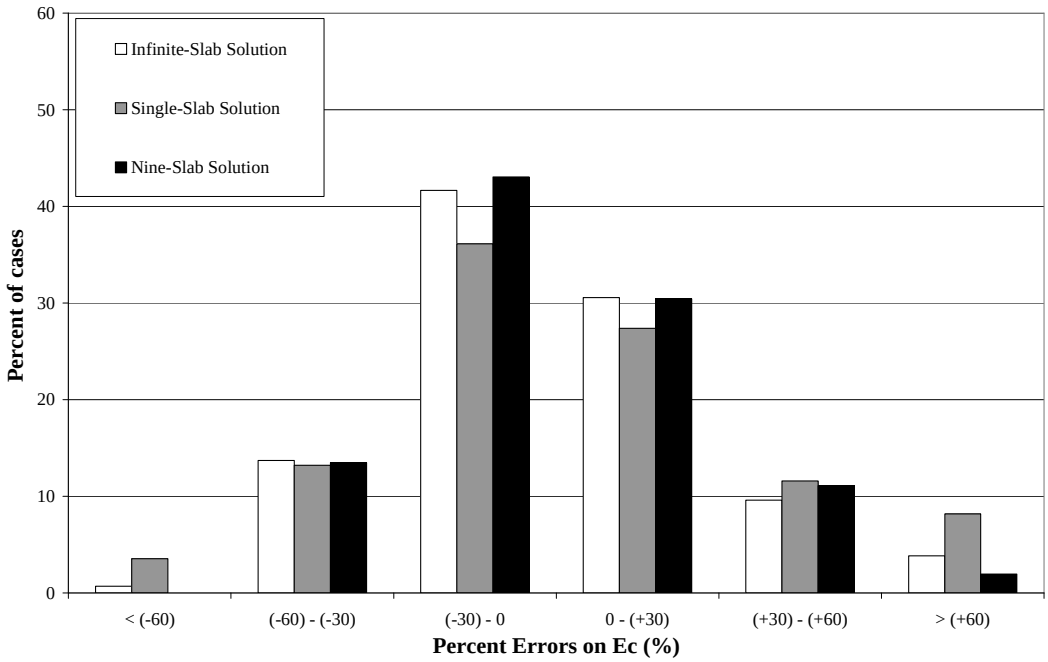

(g) Comparison of Theoretical Solution Based on Individual Deflection-Basin Backcalculated E_c

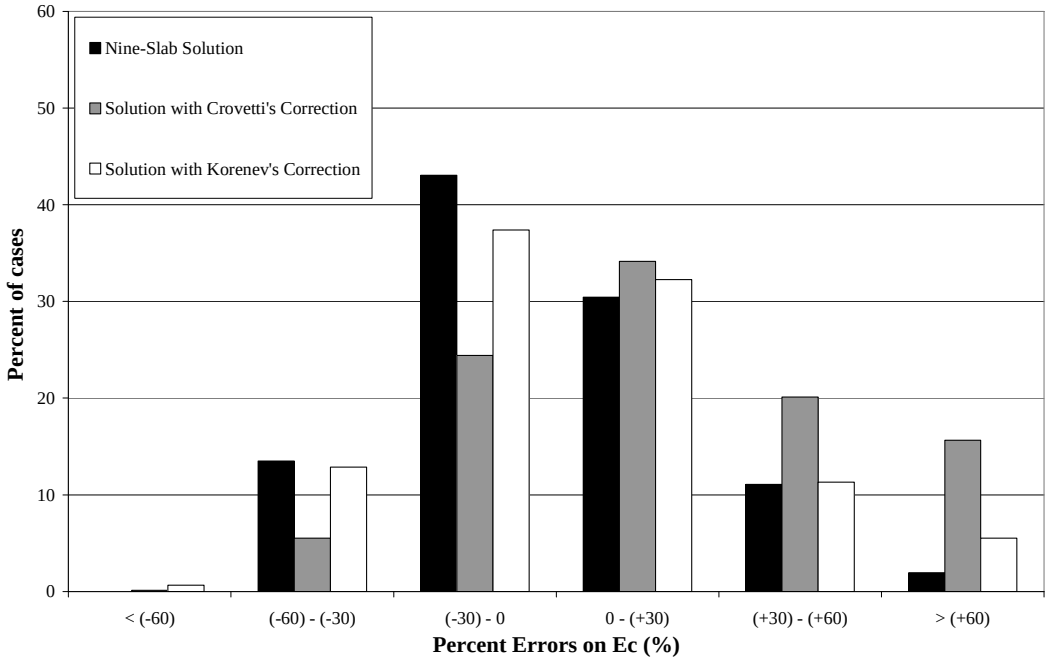

(h) Comparison of Solutions with Correction Factors Based on Individual Deflection-Basin Backcalculated E_c

Figure 3.9: Frequency Distributions of Percent Errors of Backcalculated Value of k and E_c (continued)

CHAPTER 4

DEVELOPING k-E_s RELATIONSHIP OF RIGID PAVEMENT SYSTEM USING BACKCALCULATION APPROACH

4.1 Introduction

The examination of a relationship between two subgrade soil models, i.e. dense liquid and elastic solid model (known as k-E_s relationship), on rigid pavement system was presented in two sections in this chapter. In Section 4.2, the examination of different k-E_s relationships on two-layer rigid pavement system was conducted, while the examination of the k-E_s relationships on rigid pavement system considering the presence of intermediate layer between concrete slab and subgrade was presented in Section 4.3.

4.2 Examining k-E_s Relationship of Pavement Subgrade Based on Load-Deflection Consideration

4.2.1 Background

Most rigid-pavement design methods in use today adopt the Westergaard's approach (1925) that considers the case of a pavement slab resting on a dense liquid foundation. In the theoretical model adopted by this approach, the pavement slab is characterized by its elastic modulus and Poisson's ratio, while the pavement subgrade is characterized by a single parameter k, the modulus of subgrade reaction. The commonly accepted method of measuring k is by means of a standard plate loading test conducted in the field (ASTM, 2006). However, the field plate loading test is elaborate and time consuming, and it is impractical to conduct this test on in-service

pavements in the case of structural rehabilitation or overlay designs. As a result, in practice the *k* value of a subgrade soil is usually estimated through its correlation with other soil properties.

Empirical correlations between *k* and soil properties such as the CBR (California bearing ratio), stabilometer resistance value, modulus of elasticity E_s, and soil classification type (PCA, 1966) have been used to estimate *k*. These correlations are approximate and it is not advisable to apply these correlations under conditions different from those they were first derived for. To overcome this problem, it has been of special interest to pavement engineers and researchers to establish a relationship between *k* and the modulus of elasticity E_s of the pavement subgrade. This is because E_s is a fundamental engineering property of pavement subgrade materials and that there exists various test methods for determining E_s either in the field or in the laboratory. For instance, the AASHTO Pavement Design Guide (1986, 1993), and the Mechanistic-Empirical Pavement Design Guide (MEPDG) (ARA Consulting Group Inc., 2004) all apply direct *k*-*E* relationships to convert the input value of subgrade E_s to a *k* value.

In this study, a review of several *k*-E_s relationships derived by past researchers is first performed by examining the theoretical basis adopted and assumptions made in each. Next, an attempt is made to study the relationship between *k* and E_s by means of an equivalency concept that identifies an equivalent *k*-model (a theoretical model of pavement slab supported by a dense liquid foundation) and an equivalent E_s-model (a theoretical model of pavement slab supported by an elastic solid foundation) for a given actual rigid pavement structure. The equivalency is established using backcalculation analysis based on load-deflection considerations. An illustration of the approach is made using the measured data of the LTPP (Long Term Pavement

Performance) database. A comparison is made with other existing k-E_s relationships to asses the reasonableness of the proposed approach.

4.2.2 Review of k-E_s Relationship by Past Researchers

Four k-E_s relationships derived by past researchers are presented in this section. They are: (a) the k-E_s relationship adopted by AASHTO (1986, 1993), (b) the k-E_s relationship derived by Khazanovich et al. (2001), (c) the k-E_s relationship derived by Vesic and Saxena (1974), and (d) the k-E_s relationship derived by Ullidtz (1987).

4.2.2.1 k-E_s Relationship by AASHTO (1986, 1993)

In the 1986 edition of the AASHTO Pavement Design Guide (AASHTO, 1986), and again in the 1993 edition (AASHTO, 1993), the value of k is calculated from a k-E_s relationship derived by matching the surface deflections calculated for the following two theoretical pavement systems:

(i) A uniformly distributed load is applied over the entire surface area of a circular perfectly-rigid plate of radius a supported on a dense liquid foundation. The maximum surface deflection $(w_{max})_k$ under this condition is given by

$$(w_{max})_k = \frac{q}{k} \tag{4-1}$$

where q = applied distributed load, and k = modulus of subgrade reaction.

(ii) A uniformly distributed load is applied on a circular surface area of radius a of an elastic solid foundation. The maximum surface deflection $(w_{max})_E$ under this condition is given by

$$(w_{\max})_E = \frac{\pi(1-\mu^2)qa}{2E_s} \tag{4-2}$$

where μ = Poisson's ratio of subgrade, a = radius of loaded area, and E_s = elastic modulus of subgrade.

Equating the above two maximum deflection expressions gives,

$$k = \frac{2E_s}{\pi\left(1-\mu^2\right)a} \tag{4-3}$$

For μ = 0.45 and a = 15 in. (0.381 m),

$$k\ (pci) = \frac{E_s\ (psi)}{18.8} \quad \text{or} \quad k\ (MN/m^3) = \frac{E_s\ (MPa)}{0.477} \tag{4-4}$$

Instead of matching the maximum surface deflections, AASHTO (1986, 1993) equated the volumes of soil displaced under the loading area for the theoretical pavement systems. This is equivalent to equating the deflection of the rigid plate (as given by Equation (4-1)) with the average surface deflection calculated for the case of uniform loading on an elastic solid foundation. This leads to the following relationship recommended by AASHTO (1986, 1993),

$$k\ (pci) = \frac{E_s\ (psi)}{19.4} \quad \text{or} \quad k\ (MN/m^3) = \frac{E_s\ (MPa)}{0.492} \tag{4-5}$$

A main issue that can be raised with the derivation of Equations (4-4) and (4-5) is the implicit assumption that a pavement slab can be represented by a finite circular plate, regardless of the actual dimensions of the real pavement slab. The validity of this assumption has been questioned by several researchers. Noting that the k value calculated from Equation (4-3) is dependent on the value of loading radius a, Huang (2003) commented that by setting a = 15 in. (0.381 m), both Equations (4-4) and (4-5) would "give a k value that is too large". This is because the actual equivalent a of an actual rigid pavement system would be larger than 15 in. (0.381 m). By analyzing actual pavement deflection test data, the equivalent a of actual pavements is obtained

varying from about 0.3 m to more than 2.0 m. This suggests that Equations (4-4) and (4-5) are likely to over-estimate the value of *k*.

4.2.2.2 k-E_s Relationship by Khazanovich et al. (2001)

Khazanovich et al. (2001) analyzed the deflection data of falling weight deflectometer tests from the LTPP (Long Term Pavement Performance) database. Backcalculation analyses were performed on these deflection data to estimate k and E_s by considering the following two theoretical rigid pavement systems (termed as the k-model and the E_s-model for easy reference):

(i) k-model: a theoretical pavement system of an infinite pavement slab supported on a dense-liquid foundation; and

(ii) E_s-model: a theoretical pavement system of an infinite pavement slab supported on an elastic solid foundation.

In the estimation of k and E_s values respectively, Khazanovich et al. (2001) adopted a best-fit approach based on the trial-and-error approach to match the theoretical and measured surface deflections. The following relationship was obtained:

$$k\ (MN/m^3) = 0.296\ E_s\ (MPa) \qquad (4\text{-}6)$$

with statistical coefficient of determination $R^2 = 0.872$ and standard error = 9.37 MN/m^3.

The Mechanistic-Empirical Pavement Design Guide (MEPDG) (ARA Consulting Group Inc. 2004) contains a software to perform an "E_s-to-k" conversion. An analysis of E_s and k generated by the software indicates that the k-E_s relationship can be closely represented Equation (4-6).

4.2.2.3 *k*-E_s Relationship by Vesic and Saxena (1974)

Vesic and Saxena (1974) derived an expression for the relationship between *k* and E_s of pavement subgrade by equating the radii of relative stiffness of the *k*-model and E_s-model. For the *k*-model, the radius of relative stiffness ℓ_k is given by,

$$\ell_k = \left(\frac{D}{k}\right)^{1/4} \tag{4-7}$$

where: $$D = \frac{E_c h_c^3}{12(1-\mu_c^2)} \tag{4-8}$$

D = flexural rigidity of pavement slab, E_c= elastic modulus of pavement slab, h_c = thickness of pavement slab, μ_c = Poisson's ratio of pavement slab.

The corresponding equation for the radius of relative stiffness ℓ_E of the *E*-model is,

$$\ell_E = \left(\frac{2D(1-\mu^2)}{E_s}\right)^{1/3} \tag{4-9}$$

where μ = Poisson's ratio of subgrade, E_s = elastic modulus of subgrade, and D is as defined in Equation (4-8).

By setting $\ell_k = \ell_E$, Vesic and Saxena (1974) arrived at the following *k*-*E* relationship,

$$k = \left(\frac{E_s}{E_c}\right)^{1/3}\left(\frac{E_s}{(1-\mu^2)h_c}\right) \tag{4-10}$$

The main basic assumption involved in the derivation of Equation (4-10) is the equating of the two radii of relative stiffness. This assumption apparently does not represent the actual conditions in the field exactly, as Vesic and Saxena (1974) suggested that to yield a good agreement with measured deflections, only 42% of the

value obtained from Equation (4-10) be used to estimate *k*. That is, the *k* value should be adjusted as follows,

$$Adjusted\ k = 0.42\left(\frac{E_s}{E_c}\right)^{1/3}\left(\frac{E_s}{(1-\mu^2)h_c}\right) \tag{4-11}$$

4.2.2.4 *k*-E_s Relationship by Ullidtz (1987)

Based on the equation for adjusted *k* given in Equation (4-11), Ullidtz (1987) made a further modification by introducing the concept of equivalent thickness of the concrete slab with respect to the subgrade. The equivalent thickness is defined as the thickness of subgrade material having the same flexural rigidity as that of the pavement slab (see Equation (4-8)). It is given in Equation (4-12) below,

$$h_e = h_c\left(\frac{E_c}{E_s}\frac{\left(1-\mu^2\right)}{\left(1-\mu_c^2\right)}\right)^{1/3} \tag{4-12}$$

The revised approximate relationship proposed by Ullidtz (1987) is given as Equation (4-13).

$$\text{Revised from Equation (4-11)}\quad Adjusted\ k = 0.54\left(\frac{E_s}{h_e}\right) \tag{4-13}$$

The incorporation of the equivalent thickness concept into the estimation of *k* from E_s is not likely to introduce any major changes in the calculation. The values of *k* computed from (4-13) are not expected to be much different from the corresponding *k* values calculated using Equation (4-11).

4.2.3 Proposed Procedure for Deriving k-E_s Relationship

4.2.3.1 Main Considerations

The following are the main considerations that form the basis of the proposed procedure:

(a) The k-model and the E_s-model are two theoretical rigid pavement systems having different load transmission mechanisms. Under an identical applied load, the two surface deflection basins produced by the models will have different deformed shapes and magnitudes of deflections. This means that the two deflection basins do not match, and artificially equate their deflections at selected points or the volumes of deflection basins produced by the two models is unlikely to correctly identify the equivalency of the k- and E_s-models.

(b) The k-model and the E_s-model are employed by researchers to simulate the structural responses of rigid pavements under loads, although neither of the two models could exactly represent the actual structural behaviors of the real-life rigid pavement. The common approach in pavement engineering is to apply backcalculation analysis of the deflection test data of the real pavement, for the purpose of identifying the k-model parameter values (or E_s-model parameter values if the E_s-model is used) that could best represent the structural behaviors of the real pavement. That is, by means of load-deflection backcalculation analysis, it is possible to identify an equivalent k-model and an equivalent E_s-model, respectively, with respect to a real pavement system. This equivalency concept is depicted in Figure 4.1.

Based on the above considerations, the proposed approach adopted in this research does not match the deflections or model parameters of the two theoretical models directly, but aims to derive a relationship between k and E_s of pavement

subgrade by examining the properties of the backcalculated equivalent *k*-model and equivalent E_s-model. Figure 4.2 depicts the main steps involved in this approach.

4.2.3.2 Backcalculation of Equivalent *k*-Model and E_s-Model

For the purpose of this study, closed-form backcalculation algorithms are adopted to derive the equivalent *k*-model and equivalent E_s-model respectively. The main reason for doing so is obvious because closed-form backcalculation algorithms provide unique solutions of the *k*-model and E_s-model, respectively, for a given set of deflection test data, thereby providing a unique pair of equivalent *k*- and E_s-models for each of the pavement sections analyzed. The closed-form backcalculation software NUSBACK and NUSBACK2 (Li et al., 1996, Fwa et al., 2000) for *k*-model and E_s-model, respectively, is ideal for this purpose.

For the *k*-model, NUSBACK backcalculates the modulus of subgrade reaction *k* and pavement slab elastic modulus E_c of a rigid pavement system represented by an infinite pavement slab resting on a dense liquid foundation. It considers any two deflection measurements, w_i and w_j, at horizontal distances r_i and r_j respectively from the center of loading area, and solve the following two equations,

$$w_i = \frac{P}{k\pi a^2} F_k(\ell_k, r_i) \tag{4-14a}$$

$$w_j = \frac{P}{k\pi a^2} F_k(\ell_k, r_j) \tag{4-14b}$$

where P = applied load, a = radius of loaded area, ℓ_k = radius of relative stiffness of *k*-model (see definition given in Equation (4-7)), F_k = deflection factor which is a function of ℓ_k and horizontal distance *r*.

For the E_s-model, NUSBACK2 backcalculates the subgrade elastic modulus E_s and pavement slab elastic modulus E_c of a rigid pavement system represented by an

infinite pavement slab resting on an elastic solid foundation. It considers any two deflection measurements, w_i and w_j, at horizontal distances r_i and r_j respectively from the center of loading area, and solve the following two equations,

$$w_i = \frac{P(1-\mu^2)}{E_s \ell_E} F_E(\ell_E, r_i) \quad (4\text{-}15a)$$

$$w_n = \frac{P(1-\mu^2)}{E_s \ell_E} F_E(\ell_E, r_j) \quad (4\text{-}15b)$$

where ℓ_E is the radius of relative stiffness of E_s-model (see definition given in Equation (4-9)), F_E is deflection factor which is a function of ℓ_E and horizontal distance r, all other variables are as defined in Equations (4-14a) and (4-14b).

Readers are referred to the references (Li et al., 1996, Fwa et al., 2000) for the detailed analytical solutions for both. NUSBACK provides closed-form solutions for k, ℓ_k and E_c by solving Equations (4-14a) and (4-14b), while NUSBACK2 provides closed-form solutions for E_s, ℓ_E and E_c by solving Equations (4-15a) and (4-15b). These parameter values are used in the comparison of the k-model and E_s-model for the purpose of examining the relationship between k and E_s.

4.2.4 Derivation of k-E_s Relationship Using LTPP Data

The proposed approach as described in the preceding section and depicted in Figure 4.2 requires the use of actual pavement test data to establish the relationship between k and E_s. For the present study, the falling weight deflectometer test data from the LTPP (Long Term Pavement Performance) (Elkin et al., 2003, LTPP DataPave Online, 2007) are used for this purpose. This section presents the derivation using the LTPP data.

4.2.4.1 LTPP Database

From the LTPP database, falling weight deflectometer deflection measurements of the General Pavement Study (GPS) and the Specific Pavement Study (SPS) were obtained for the analyses presented in this study. Deflection basins obtained for three applied load levels, i.e. 40, 53.3 and 71.1 kN, were included in the analysis. 50 JCP (jointed concrete pavement) sections were selected from the LTPP database for the purpose of this study. All the 50 sections contain measured E_c values, but only 26 of the road sections also contain measured k values. There are altogether 2,238 deflection basins (746 per load level) in the 50 JCP sections having measured E_c values, and 738 deflection basins (246 per load level) in the 26 JCP sections having measured k values. In addition, 75 CRCP (continuously reinforced concrete pavement) sections with measured E_c values were randomly selected from GPS road section database. There are 4,236 deflection basins (1,412 per load level) in the 75 CRCP sections. The deflection data were measurements of falling weight deflectometer tests performed at the center of each slab tested. Tables 4.1 and 4.2 list the selected details of the JCP and CRCP road sections.

4.2.4.2 Comparing of Equivalent *k*-Model and Equivalent E_s-Model

As explained earlier, given a real rigid pavement structure, it is meaningful to compare the theoretical equivalent k-model and the equivalent E_s-model because they each in their own way represents the same pavement structure based on load-deflection considerations. It is clear from Equations (4-14a) and (4-14b) that for the k-model, the surface of deflections and the shape of deflections basin under a given load are dependent on the parameters k and ℓ_k; while for the E_s-model, the governing parameters are E_s and ℓ_E as can be inferred from Equations (4-15a) and (4-15b).

Hence, the following two comparisons are made in this study to assess their respective suitability for use in deriving the relationship between k and E_s:

(i) Direct regression of k and E_s values to determine if a simple relationship involving these two properties can be established.

(ii) Comparison of the ℓ_k and ℓ_E values to examine how they are related, and whether there exists a ℓ_k-ℓ_E relationship that can be used as a basis to link k with E_s.

Direct Regression Equation for k and E

As presented earlier under the literature review section, this is the approach adopted by AASHTO (1986, 1993), Khazanovich et al. (2001), and MEPDG (ARA Consulting Group Inc., 2004) for the purpose of estimating k from E_s. In the present study based on the concept of equivalent k-model and E_s-model, the computed k and E_s values from the 2,238 JCP and 4,236 CRCP deflection basins are plotted in Figure 4.3. The following regression equation is obtained:

$$k\ (MN/m^3) = 0.259\ E_s\ (MPa) - 6.512 \qquad (4\text{-}16)$$

with statistical coefficient of determination $R^2 = 0.941$ and standard error = 8.317 MN/m^3. Equation (4-16) is slightly superior to Equation (4-6) obtained by Khazanovich et al. (2001) in terms of R^2 and standard error.

Relationship Between ℓ_k and ℓ_E

The backcalculated ℓ_k and ℓ_E values for the 2,238 JCP and 4,236 CRCP deflection basins are plotted in Figure 4.4. It is observed that there exists a well defined relationship between the 6,474 pairs of backcalculated values of ℓ_k and ℓ_E. The relationship is nonlinear. It can be closely described by the following second-

order polynomial regression equation with a statistical coefficient of multiple determination R^2 value close to unity,

$\ell_k = 0.183\ \ell_E^2 + 0.887\ \ell_E + 0.4008 \qquad R^2 = 0.998$, standard error = 7.344×10^{-3} m (4-17)

where both ℓ_k and ℓ_E are measured in m.

The well-defined relationship between ℓ_k and ℓ_E is of practical significance in establishing the relationship between k and E_s for the purpose of estimating k from the known subgrade E_s value of a rigid pavement structure.

It is of interest at this juncture to provide a further examination of assumption of $\ell_k = \ell_E$ set by Vesic and Saxena (1974) in deriving the k-E_s relationship. Vesic and Saxena's assumption of $\ell_k = \ell_E$ plus the introduction of adjustment factor 0.42 is equivalent to setting $\ell_E = (0.42)^{1/4}\ell_k$, i.e.

$\ell_E = (0.42)^{1/4}\ell_k = 0.805\ \ell_k$ (4-18)

Figure 4.5 shows that Vesic and Saxena's equivalent assumption of Equation (4-18) together with the ℓ_k-ℓ_E relationship derived in this study. It suggests that the equivalent linear ℓ_k-ℓ_E relationship assumed by Vesic and Saxena is a simplified approximation of the non-linear ℓ_k-ℓ_E relationship derived from field data.

4.2.4.3 Proposed Methods of Estimating k from E_s based on Equivalent k-Model and E_s-Model

The findings of the preceding sections suggest that, based on the concept of equivalent k-model and E_s-model, there are two possible methods of estimating k from E_s:

- Equivalent model k-E_s regression equation: Direct computation of k from the linear regression equation of k and E_s given by Equation (4-16).
- Equivalent model ℓ_k-ℓ_E relationship: Based on the ℓ_k-ℓ_E relationship of Equation (4-17), with known values of E_c, h_c, μ_c and μ (as defined in Equations (4-8) and (4-9)), compute k with the following steps:

  (i) Calculate ℓ_E from given values of E_c, h_c, μ_c and μ;

  (ii) Calculate ℓ_k from ℓ_k-ℓ_E relationship of Equation (4-17); and

  (iii) Calculate k from ℓ_k using Equation (4-7).

The applicable parameter ranges of the k-E regression relationship of Equation (4-16) and the ℓ_k-ℓ_E relationship of Equation (4-17) are identical and are as follows: 8.5 MN/m^3 ≤ k ≤ 280 MN/m^3, 72 MPa ≤ E_s ≤ 995 MPa, 16 GPa ≤ E_c ≤ 95 GPa, 0.185 m ≤ h_c ≤ 0.32 m, μ_c = 0.15 and 0.2 ≤ μ ≤ 0.45. The next section will compare these two k-E relationships with those existing k-E relationships reviewed earlier.

4.2.5 Comparison of Different k-E_s Relationships

4.2.5.1 Comparison with Measured k Values

In the JCP records of the LTPP database, 26 pavement sections contain measured k values. These measured k values are used as the basis for comparing the various k-E_s relationships. The k value reported for each of the 26 pavement sections is the average values measured by means of on-site plate bearing tests. Figure 4.6 shows the comparison of the measured k values with the estimated k values by various k-E_s relationships. The predicted k values in each plot of Figure 4.6 are obtained for the individual deflection basins in each pavement section, and plotted against the backcalculated E_s values.

The following observations may be made from Figure 4.6:

(a) Figure 4.6(a) indicates that the k-E_s relationship recommended by AASHTO (1986, 1993) over-estimates the k values by big margins, and the errors increase for higher E_s and k values.

(b) Figure 4.6(b) shows that the k-E_s relationship by Khazanovich et al (2001) derived from backcalculation analysis of actual pavements offers a much better matching with the measured k values than the AASHTO k-E relationship.

(c) Figure 4.6(c) plots the predicted k values by the non-adjusted k-E_s relationship derived by Vesic and Saxena (1974), which deviate significantly from the measured values for E_s values greater than about 200 MPa, and k values higher than about 150 MN/m^3.

(d) Figure 4.6(d) presents the case for the adjusted k-E_s relationship derived by Vesic and Saxena (1974). A markedly improved matching is achieved with the use of the adjustment factor 0.42. This result confirms the separate finding by Vesic and Saxena of the need to apply an adjustment factor in order to better match field measured data.

(e) Figure 4.6(e) indicates that the thickness equivalency concept introduced by Ullidtz (1987) to modify the adjusted k-E_s relationship did not bring about noticeable improvements to the predicted k vales. In fact, compared with the results of Figure 4.6(d), Ullidtz's adjustment produces somewhat higher deviations of k for E_s values higher than about 300 MPa.

(f) Figure 4.6(f) shows the k values predicted using the k-E_s regression equation derived by the present study based on the concept of equivalent k- and E_s-models. This method provides improved estimation of k, especially for values of E_s higher than about 350 MPa.

(g) Figure 4.6(g) presents the k values computed using the ℓ_k-ℓ_E relationship derived in this study. Compared with the other methods described, this method produces very good matching of measured and computed k values for E_s values higher than about 350 MPa.

Table 4.3 shows the root-mean-square errors (*RMSE*) of the predicted k values with respect to the measured values for the 7 methods presented in Figure 4.6. Overall, the statistics suggest that the AASHTO k-E_s relationship and the unadjusted k-E_s relationship derived by Vesic and Saxena should not be used because of the large errors involved. The magnitudes of errors of the other 5 methods are approximately of the same order, although the Ullidtz's method and the adjusted k-E_s relationship by Vesic and Saxena tend to produce relatively higher errors. In terms of the magnitude of *RMSE*, the following three methods have the best performance: the method of equivalent k- and E_s-models based on ℓ_k-ℓ_E relationship, the k-E_s relationship by Khazanovich et al. (2001), and the k-E_s regression equation derived from the method of equivalent k- and E_s-models.

4.2.5.2 Choice of Method to Estimate k from E_s

Based on the analysis presented in the preceding section, it appears that either of the following two approaches can be used to estimate k from E_s: (i) Direct estimation of k from E_s by the use of an appropriate k-E_s regression equation, or (ii) Estimation of k from E_s through an appropriate ℓ_k-ℓ_E relationship. There are, however, some basic differences between the two methods as highlighted below:

- The simple k-E_s regression equation gives a unique k value for each E_s value, regardless of the geometric and structural properties of the pavement slab. On the other hand, in the method based on ℓ_k-ℓ_E relationship, there is no unique one-

to-one correspondence of k and E_s values. Instead, besides the E_s value, the value of k is also dependent on the properties of the pavement slab, including E_c, h_c and μ_c.

- The k-E_s regression equation is a linear monotonously increasing function. The field measured data in Figure 4.6 suggest that this may not be the case. This could be the reason why the k-E_s regression methods shown in Figure 4.6 tend to over-estimate k values for large values of E_s. It is noted that the method based on ℓ_k-ℓ_E relationship does not suffer from this problem.
- Being derived from statistical regression analysis, the k-E_s regression equation in actual fact provides a form of mean estimate of k value for a given E_s value. As can be seen from Figure 4.3, it gives a mean response (i.e. predicted k value) for every E_s value, and is thus an approximate representation of the original actual response. In contrast, the method based on the well defined ℓ_k-ℓ_E relationship provides a better representation of the original pavement response. This difference between the two methods is not reflected in the *RMSE* comparison computed in Table 4.3 because the given measured k values are the mean values of the pavement sections. Table 4.4 computes the *RMSE* by the two methods for the backcalculated individual deflection basin data of Figure 4.3, and shows clearly that the method based on ℓ_k-ℓ_E relationship out-performs the method of k-E regression equation in estimating k values.
- A comparison of the two methods can also be made by examining their respective 95% confidence intervals for the estimated k. For the k-E_s regression equation (Equation 4-16), the 95% confidence interval is $k \pm 16.3$ (MN/m^3), which is about $k \pm (10.95\%)k$ for a mid-range k value of 150 MN/m^3. For the method based on ℓ_k-ℓ_E relationship, the corresponding 95% confidence interval is

about $k \pm (3.84\%)k$ for the same mid-range k value of 150 MN/m^3, which presents a good improvement over the k-E_s regression method.

In summary, it may be concluded that while the method of k-E_s regression equation and the method based on ℓ_k-ℓ_E relationship can both be applied to estimate k from E_s, the latter method provides better estimates of k from E_s, and is able to give a more representative estimated k value by taking into consideration the total load-deflection response of the entire pavement system.

4.2.6 Summary

This study has presented an approach to establish k-E_s relationship based on an equivalent model method. The equivalent model method establishes equivalency between two theoretical pavement models, a model of pavement slab supported by a elastic solid foundation (termed as E_s-model) and a model of pavement slab supported by a dense liquid foundation (termed as k-model). The equivalency is established based on load-deflection consideration by means of backcalculation analysis, with respect to the structural response of actual pavements. Closed-form backcalculation algorithms are employed to obtain a unique pair of k and E_s for each pavement section analyzed.

Applying the equivalent model method to the deflection test data of the LTPP (Long Term Pavement Performance) database, it is found that two procedures can be employed to estimate k from E_s. One is to develop a regression equation between k and E_s, and estimate k from E_s directly. It ignores the effects of pavement slab on load transmission in a rigid pavement system. Although simple and easy to apply, this regression equation is a simplified representation of the actual pavement response and could only provide a "mean" estimate of k for a given E_s value.

The second procedure, which is the recommended procedure of this study, relies on a well defined relationship between the radii of relative stiffness of the two theoretical rigid pavement systems, i.e. ℓ_k and ℓ_E. The ℓ_k-ℓ_E relationship is found valid for both JCP and CRCP, and for different applied loads levels. This procedure computes k from a known E_s value by establishing equivalency between the k-model and E_s-model based on the ℓ_k-ℓ_E relationship. Analyses presented in the study have demonstrated that, compared with the method of direct k-E_s relationship, this procedure provides an improved estimation of k from E_s.

4.3 Examining k-E_s Relationship of Rigid Pavement System by Considering Presence of Subbase Layer

4.3.1 Background

In the early days of applications of rigid pavement systems, the design of the rigid pavement generally only consisted of two layers, i.e. concrete slab and subgrade soil. However, because of the joint pumping problem, this design became uncommon later. All rigid pavements today are practically constructed with a subbase layer to serve as a drainage layer and to protect the subgrade soil against pumping and other moisture-related distresses. Therefore, to take into account the contribution of the subbase layer in a rigid pavement system, the use of composite k value in pavement design, instead of using only the k value of the subgrade soil, becomes a necessity today. Several major design methods, such as the American Association of State Highway and Transportation Officials/AASHTO (1986, 1993), Portland Cement Association/PCA (1984), and Federal Aviation Association/FAA (1995, 1996), have used composite k values in their charts or tables for the purpose of either new

structural design or rehabilitation and overlay design. This indicates that the concept of composite *k* value is quite important in those types of design.

Because of the simplicity by means of its use and the input data required, the employment of the *k* value-based design methods is very popular. Generally, only two or three input parameters are required: the modulus of subgrade reaction, the thickness of subbase (AASHTO 1972; PCA 1984; FAA 1995, 1996) and the modulus of subbase (AASHTO 1986, 1993).

The first aforementioned design methods can only be employed for the purpose of new structural design since they require measured subgrade *k* value for their input data. Unfortunately, subgrade *k* value is not easy to obtain since the plate loading test is costly and time-consuming. On the other hand, unlike the *k* value, the elastic modulus of subgrade, i.e. the subgrade modulus used by 1993 AASTHO method, can be easier to obtain since it can be measured directly by means of laboratory tests using samples of the pavement materials. In this sense, 1993 AASHTO method is preferable because of the ease to obtain the input data rather than the other methods.

However, some discrepancies are found in using those design methods: (i) the results of composite *k* value determination using the different design methods are not consistent since each method was developed based on specific experimental experience at a limited area and for certain material types, therefore, the use of the methods beyond the range of their specified parameter values is not possible, (ii) it is not advisable to interpolate parameter values in the tables and charts provided by the methods since they were developed based on empirical relationship among the parameters (subgrade and subbase moduli and subbase thickness), therefore, the interpolation results obtained are only approximation, and (iii) all the methods were developed based on empirical plate loading test with 30-in. (762-mm) plate diameter.

The small radius used in the test causes the result of the method is extremely high and not reasonable (Huang, 2003).

To overcome this problem, a proposed method was introduced in this study. This method extended the use of the equivalency concept of the two models of soil foundation, namely the *k*-model (a theoretical model of pavement slab supported by a one-layer dense liquid foundation) and the E_s-model (a theoretical model of pavement slab supported by a one-layer elastic solid foundation), as depicted in Figure 4-8, by adding subbase properties into the E_s-model. To obtain the subbase properties, the E_s-model with subbase (termed as $E_{s/sb}$-model) is introduced. Similar to the approach in Section 4.2, the equivalency is established using backcalculation analysis based on load-deflection considerations. In the following section, the approach is illustrated using the measured data of the LTPP (Long Term Pavement Performance) database, and a comparison is made with other design methods to asses the reasonableness of the proposed approach.

4.3.2 Determination of Composite *k* Value by Existing Method

4.3.2.1 Determination of Composite *k* by AASHTO (1972, 1986, 1993)

The AASHTO method is one of the most widely used methods in pavement design today because of the convenience and ease of use of the charts, including one for determining composite *k* value. The 1972 AASHTO Interim Guide specified a procedure to determine the composite *k* value on top of the subbase (AASHTO 1972). It provides nomographs developed using elastic layer theory, to determine composite *k* values from input values of subbase stiffness and modulus of subgrade reaction, which is based on a subgrade of infinite depth.

The later 1986 Design Guide and the subsequent 1993 Design Guide contain several modifications to the *k* value guidelines of the 1972 Interim Guide. They include an equation for *k* value for an unprotected subgrade, a depth adjustment to a rigid foundation, a seasonal adjustment procedure for *k* and a loss-of-support procedure (Hall et al. 1995; AASHTO 1986; AASHTO 1993).

The revised nomographs in the 1986 and 1993 Design Guide require the following input parameters to determine *k* value: subgrade resilient modulus (to replace *k* value in the previous guide), thickness and elastic modulus of the subbase layer. The laboratory determined resilient modulus of the subgrade was assumed equal to the in-situ elastic modulus. The computation of composite *k* values was applicable for values of parameter within the following range: subgrade resilient modulus 1,000 to 20,000 psi (6.9 to 137.9 MPa), elastic modulus of subbase 15,000 to 1,000,000 psi (103.43 to 6,895 MPa) and thickness of the subbase 4 to 20 inch (0.102 to 0.508 m).

Although the AASHTO method is one of the most widely accepted methods, there are several discrepancies involved in the procedure as indicated below:

a. Hall et al. (1995) stated that the composite *k* values produced by incorporating the effect of subbase layers sometimes are lower than those if the subbase layer does not exist in the pavement structure.

b. The resilient modulus (M_R) used to compute the composite *k* value is based on a plate load test using a base of 30-in (762 mm) diameter, applied on a two-layer system. Huang (2003) stated that this procedure is misleading and will result in stresses and deflections that are too small.

4.3.2.2 Determination of Composite *k* by PCA (1984)

The PCA procedure expresses the composite *k* value as a function of the subgrade soil *k* value, base thickness, and base type (granular or cement treated). The values obtained using PCA method were derived by applying the Burmister theory of two-layer systems to the results of plate load tests on subgrade and subbase of full-scale test slabs (PCA 1984). The ranges of parameter values used in the PCA method are as follows: modulus of subgrade reaction and base thickness 50 to 300 pci (13.57 to 81.42 MN/m^3) and 4 to 14 inch (0.102 to 0.356 m) respectively for untreated subbase; and 50 to 200 pci (13.57 to 54.28 MN/m^3) and 4 to 12 inch (0.102 to 0.305 m) respectively for cement-treated subbase.

The use of PCA method to determine the composite *k* value is straightforward as far as the data available are similar to those listed in PCA's field data. However, extrapolation beyond the range of the given values is questionable. Another disadvantage of this method is that the modulus of subbase is unknown for both types of subbase (untreated and cemented treated subbase). It means that the subbase used in this method is assumed to have passed the specification requirements for the road construction and its material has the same quality as that used by PCA in its full-scale tests.

4.3.2.3 Determination of Composite *k* by FAA (1995, 1996)

The FAA publishes advisory circulars to provide guidance on airport pavement design for pavement thickness determination with the subgrade *k* value as a main input parameter. For a pavement system having a subbase layer, FAA requires the determination of a composite *k* value termed as the effective *k* value.

For unstabilized granular subbase, the composite *k* values associated with various thicknesses of subbase of different materials, such as well graded crushed aggregate and bank-run sand and gravel. For stabilized subbase, the effective or composite *k* value is determined by multiplying a stabilized layer by a factor of 1.2 to 1.6 to determine the equivalent thickness of well-graded crushed aggregate in increasing the subgrade modulus. It is applicable to cement stabilized, Econocrete and bituminous stabilized layers. To determine the effective *k* value, the method specified the following range of values to be used: modulus of subgrade reaction 50 to 300 pci (13.57 to 81.42 MN/m^3) and base thickness 4 to 14 inch (0.102 to 0.356 m) and 4 to 12 inch (0.102 to 0.305 m) for unstabilized and stabilized subbase respectively.

The use of the FAA method is straightforward, since only two data are required to determine the composite *k* value: the subbase thickness and the subgrade *k* value. The main drawbacks of this method are:

a. There are only 4 levels of *k* values represented in the method, i.e. 50, 100, 200 and 300 pci (13.57, 27.14, 54.28 and 81.42 MN/m^3). The accuracy of the results is unknown if the user has to interpolate using two aforementioned *k* values.

b. The FAA method also does not mention the value of subbase modulus used in the method, although it is stated that the material used in subbase layer should fulfill the material specifications specified by the FAA method before it can be used.

4.3.3 Proposed Procedure to Determine Composite *k* Value

4.3.3.1 Main Consideration

The use of *k*-model and E_s-model in representing a rigid pavement with two-layer foundation (subbase layer overlaying subgrade soil) involves different

considerations. The addition of subbase layer in the pavement system is easier to be considered in E_s-model since the stiffness of subbase layer is commonly represented in term of elastic modulus. However, it is not possible to match directly the E_s-model with subbase (i.e. the $E_{s/sb}$-model) with *k*-model to obtain a composite *k* value, because of the difference in the way the two models represent the composite form of the two-layer foundation.

To derive the relationship between the composite *k* and the $E_{s/sb}$-model, a matching between *k*-model and $E_{s/sb}$-model must be made. To do so, it is necessary to first transform a two-layer solid foundation into an equivalent one-layer solid foundation. In this study, this is achieved by means of backcalculation analysis as shown in Figure 4.8. Three equivalent models now have to be considered as will be explained in the following two sub-sections.

Similar to the development of the k-E_s relationship presented in Section 4.2, the development of the k-$E_{s/sb}$ relationship also requires the use of actual data from LTPP (Long Term Pavement Performance) database (Elkin et al. 2003, LTPP DataPave Online 2007). The brief description about the actual data from LTPP database used in this study is presented in the LTPP Database section.

4.3.3.2 Backcalculation of Equivalent *k*-Model, E_s-Model and $E_{s/sb}$-Model

Two closed-form backcalculation algorithms and one forward-calculation algorithm were applied in this study to derive the new approach. The closed-form backcalculation programs NUSBACK and NUSBACK2 (Li et al. 1996, Fwa et al. 2000) for *k*-model and E_s-model, respectively, and the forward calculation program NUS-DEF3 (Li et al. 1997) for $E_{s/sb}$-model are selected for the purpose of this study.

The two closed-form backcalculation programs, NUSBACK and NUS-BACK2, backcalculate two unknowns of a rigid pavement system represented by an infinite pavement slab resting directly on a dense liquid and elastic solid foundation. The two unknowns backcalculated by NUS-BACK and NUS-BACK2 are the elastic modulus of concrete slab (E_c) and the modulus of subgrade reaction (k) for the case of dense liquid foundation, and elastic modulus of concrete slab (E_c) and elastic modulus of subgrade (E_s) for the case of solid foundation. Both programs consider any two deflection measurements, w_i and w_j, at horizontal distances r_i and r_j respectively from the center of loading area, and solve the following deflection equations (as derived by Panc (1975) and Losberg (1960)),

$$w_i = \frac{P}{k\pi a^2} F_k(\ell_k, r_i) \text{ and } w_j = \frac{P}{k\pi a^2} F_k(\ell_k, r_j) \qquad \text{for NUS-BACK} \tag{4-19}$$

$$w_i = \frac{P(1-\mu_s^2)}{E_{s_1}\ell_{E_{s_1}}} F_{E_{s_1}}(\ell_{E_{s_1}}, r_i) \text{ and } w_j = \frac{P(1-\mu_s^2)}{E_{s_1}\ell_{E_{s_1}}} F_{E_{s_1}}(\ell_{E_{s_1}}, r_j) \qquad \text{for NUS-BACK2} \tag{4-20}$$

where:

$$\ell_k = \left(\frac{E_c h_c^3}{12(1-\mu_c^2)k} \right)^{1/4} \tag{4-21}$$

$$\ell_{E_{s_1}} = h_c \left(\frac{E_c(1-\mu_s^2)}{6E_{s_1}(1-\mu_c^2)} \right)^{1/3} \tag{4-22}$$

P = applied load (kN) , a = radius of loaded area (m), F_k and $F_{E_{s_1}}$ = deflection factors of k-model and E_s-model respectively, μ_c and μ_s = Poisson ratio of concrete slab and subgrade respectively, h_c = thickness of concrete slab (m), and ℓ_k and $\ell_{E_{s_1}}$ = radius of relative stiffness of k-model and E_s-model respectively (m). The closed-form solutions for NUS-BACK and NUS-BACK2 can be obtained by solving Equations (4-19) and

(4-20). For rigid pavements with slab thickness varying within the common range of 150 to 600 mm, it is found that k was best estimated based on the measured deflections D_4 and D_7.

The forward calculation program NUS-DEF3 calculates surface deflections from three known moduli of a rigid pavement system, i.e. elastic modulus of concrete slab (E_c), subbase (E_{sb}) and subgrade (E_s). Based on the work of Burmister (1945) and Panc (1975), the deflection w_i at horizontal distances r_i from the center of loading area is given by the following equation:

$$w_i = \frac{2(1-\mu_{sb}^{\ 2})\,P}{\pi\, a\, E_{s_b}} F_{E_{sb}}(\ell_{E_{s/sb}}, c, r_i) \tag{4-23}$$

where:

$$c = \frac{(1+\mu_{sb})E_s}{(1+\mu_s)E_{sb}} \tag{4-24}$$

$$\ell_{E_{s/sb}} = h_c\left(\frac{E_c(1-\mu_{sb}^{\ 2})}{6E_{s_b}(1-\mu_c^{\ 2})}\right)^{(1/3)} \tag{4-25}$$

μ_{sb} = Poisson ratio of subbase, μ_s = Poisson ratio of subgrade, $\ell_{E_{s/sb}}$ = radius of relative stiffness of $E_{s/sb}$-model (m) and $F_{E_{s/sb}}$ = deflection factor of $E_{s/sb}$–model and all other variables are as previously defined.

4.3.3.3 Derivation of *k*- $E_{s/sb}$ relationship

As depicted in Figure 4.8, the *k*-model, E_s-model and $E_{s/sb}$-model are three different theoretical structural representations of the pavement foundation. Because each model has a different way to represent the same pavement structure, direct matching between the backcalculated *k* values and the backcalculated E_{s_1} values is not possible. Based on Equations (4-19) to (4-25), it is obvious that the properties of the

pavement system for the two foundation models can be represented by their radii of relative stiffness parameter, ℓ_k, $\ell_{E_{s_1}}$ and $\ell_{E_{s/sb}}$. The computation of composite *k* is made through establishing the relationship between $\ell_{E_{s_1}}$ and ℓ_k, as depicted in Figure 4.8.

ℓ_k is a function of E_c and *k*, $\ell_{E_{s_1}}$ is a function of E_c and E_{s_1}, and $\ell_{E_{s/sb}}$ is a function of E_c and E_{sb}. However, the relationship between ℓ_k and $\ell_{E_{s/sb}}$ is more difficult to be developed because while ℓ_k directly influences pavement deflections (see Equation (4-19) and *k*-model of Figure 4.8), $\ell_{E_{s/sb}}$ does not influence pavement deflections in the same way (see Equation (4-23) and $E_{s/sb}$-model of Figure 4.8). The parameter $\ell_{E_{s_1}}$ (see Equation (4-20) and E_s-model of Figure 4.8) has to be derived first from the $E_{s/sb}$-model, in order to derive a relationship between $\ell_{E_{s/sb}}$ and *k*. To link between $\ell_{E_{s/sb}}$, $\ell_{E_{s_1}}$ with ℓ_k, the following procedure was developed in this study. A forward calculation program NUS-DEF3 was applied in this study to calculate the deflection basins that corresponding with the known pavement properties, i.e. E_c, E_{sb} and E_s. Using the deflection basins, the radius of relative stiffness of E_s-model can be backcalculated by NUS-BACK2. In this case, the radius of relative stiffness $\ell_{E_{s_1}}$ is related to E_c and E_{s_1} which is a function of E_{sb}, E_s and the thickness of subbase. The final step is to develop a relationship between $\ell_{E_{s_1}}$ and ℓ_k, which can then be used to compute the composite *k*.

4.3.3.4 Relationship between ℓ_k and $\ell_{E_{s/sb}}$

The relationship between ℓ_k and $\ell_{E_{s/sb}}$ was derived in this study by using the 2,238 JCP and 4,236 CRCP deflection basins. After filtering the backcalculation results based on the acceptable range of slab modulus between 20 to 50 GPa, the total deflection basins used in this study was 4211. The new relationship obtained by applying the above procedure using 4211 deflection basins is given by the following second-order polynomial regression equation at 95% confidence level.

$$\ell_k\,(\text{m}) = 6.178*10^{-1}\ \ell_{E_{s/sb}}{}^2\,(\text{m}) + 3.644*10^{-1}\ \ell_{E_{s/sb}}\,(\text{m}) + 5.702*10^{-1} \qquad (4\text{-}26)$$

$R^2 = 0.675$, standard error = 8.7×10^{-2} m

Next, a more refined statistical relationship is explored by considering the properties of the two foundation models. The following equation was obtained.

$$\ell_k(\text{m}) = -1.99 + 2.16\ \ell_{E_{s/sb}}\,(\text{m}) - 5.75*10^{-3}\ E_c\,(\text{GPa}) + 8.46/E_{sb}\,(\text{MPa})$$

$$+ 5.97*10^{-1}\log E_s\,(\text{MPa}) + 1.01*10^{-1}/h_c\,(\text{m}) - 1.39*10^{-1}\ h_{sb}\,(\text{m}) \qquad (4\text{-}27)$$

$R^2 = 0.797$, standard error = 7.2×10^{-2} m

where h_c and h_{sb} are the thickness of the pavement slab and the subbase layer respectively (m), and all other variables are as defined earlier. The increase of the coefficient of multiple determination R^2 from 0.675 in Equation (4-26) to 0.797 in Equation (4-27), gives a more improved representation of the relationship between the two sets of backcalculated pavement foundation parameters. For easy reference in the subsequent sections, the Equations (4-26) and (4-27) are referred to models A and B, respectively.

4.3.3.5 Proposed Method of Estimating Composite *k* from E_{sb} *and* E_s Based on Equivalent *k*-model and E_s-model

Based on findings in the preceding sections, the proposed method to estimate composite *k* from E_{sb} and E_s is as follows:

- Calculate $\ell_{E_{s/sb}}$ from Equation (4-25) from given values of E_c, E_{sb}, h_c, μ_c and μ_{sb}.
- Calculate ℓ_k from ℓ_k - $\ell_{E_{s/sb}}$ relationship of Equation (4-26) or (4-27) (models A and B); and
- Calculate *k* from ℓ_k using Equation (4-21).

The applicable parameter ranges of the ℓ_k - $\ell_{E_{s/sb}}$ relationship of Equations (4-26) and (4-27) are identical and are as follows: 13.24 MN/m^3 ≤ *k* ≤ 417.63 MN/m^3, 120.67 MPa ≤ E_{sb} ≤ 28,299 MPa, 65.89 MPa ≤ E_s ≤ 1,417.81 MPa, 20 GPa ≤ E_c ≤ 50 GPa, 0 m ≤ h_{sb} ≤ 1.267 m and 0.183 m ≤ h_c ≤ 0.323 m.

4.3.4 Comparison of Composite *k* Values by Proposed Method and Existing Design Methods

In this section, a comparison of computed composite *k* values by the proposed method and the existing design methods is conducted. 26 JCP sections containing 270 test points with measured *k* value were selected for this purpose.

The proposed method and the existing design methods required pavement properties (E_c, E_{sb} and E_s) as input data. Backcalculation analysis of the 270 deflection basins of the JCP sections with measured *k* was conducted using NUS-BACK3, i.e. the backcalculation program for NUS-DEF3. Especially for PCA and FAA methods, the methods require the elastic modulus of subgrade (E_s) to be converted into modulus of subgrade reaction (*k*) before the modulus can be used in the chart or table provided by

the methods. To convert E_s to k, a well-define k-E_s relationship (Equation 4-17) was adopted.

4.3.4.1 Comparison Based on Under- and Over-estimation of Composite *k* Values

Figure 4.9 shows the comparison of the measured composite k values with the estimated composite k values by the proposed method and the existing design methods. The predicted composite k values in each plot of Figure 4.9 are obtained for the individual deflection basins in each pavement section. However, since each method has applicable ranges of parameter values (as mentioned earlier in the section of description of proposed method), not all of the pavement sections can be used in the comparison. Based on the applicable ranges of parameter values, the final number of pavement sections employed by each method is as follows: 267, 43, 63 and 24 pavement sections for the proposed method, PCA method, FAA method and AASHTO method respectively. Therefore, the numbers of pavement sections analyzed for the comparison study are 267 to 43, 63 and 24 for PCA, FAA and AASHTO methods, respectively.

Figure 4.10 depicts the number of cases of predicted k which under- and over-estimate the measured k from the 5 methods evaluated. The following observations may be made from Figures 4.9 and 4.10:

(i) Figure 4.9(a) plots the comparison between predicted k produced by the proposed method with models A and B with respect to measured k values and shows that most of the cases from both models under-estimate the k values. From Figure 4.10(a), it seems that both models produced similar number of under-estimation cases, i.e. 70.78% and 72.28% for models A and B respectively. It is

noted that the preferable method should produce more cases of under-estimation of measured *k*.

(ii) Figure 4.9(b) plots the comparison between the proposed method with models A and B and PCA method. Some cases produced by PCA method over-estimate the *k* values, as indicated by 23% of the total cases, as seen in Figure 4.10(b). Compared with the predicted *k* values by PCA method, all cases of the proposed method under-estimate *k* values.

(iii) Figure 4.9(c) shows the comparison between FAA method and the proposed method with models A and B. The relationship by FAA method offer a better matching with the measured *k* values than that of PCA method. Figure 4.10(c) indicates that only 6% of the total cases produced by FAA method over-estimate the measured *k* values, while all cases of the proposed method under-estimate the *k* values.

(iv) Figure 4.9(d) presents the comparison between AASHTO method and the proposed method with models A and B. From Figures 4.9(d) and 4.10(d), it is observed that AASHTO method over-estimate *k* values for all cases. On the other hand, all cases of the proposed method under-estimate the measured *k*.

4.3.4.2 Comparison based on *RMSE* and *RMSPE*

To evaluate the statistical significance of differences between the predicted and measured *k* values, two indicators were employed in this study, namely root-mean-square errors (*RMSE*) and root-mean-square percent errors (*RMSPE*). The *RMSE* and *RMSPE* of the predicted *k* values with respect to the measured values are tabulated in Table 4.6. Overall, PCA and AASHTO produce very large errors compared with other methods. If all 267 pavement sections were used in the comparison, the magnitude of

errors of the proposed method with models A and B are approximately of the same order. The errors produced by the proposed method also are better than that of PCA and AASHTO methods. It is noted that the errors produced by FAA method outperform the proposed method, but that is only applicable for the comparison of one-fourth of the total pavement sections used in this study. The comparison of the errors for the rest of the pavement sections is not possible since the limitation of the range of parameter values used by the charts developed by FAA.

4.3.4.3 Summary Remarks on Method to Estimate Composite *k* from E_s and E_{sb}

The comparison of the proposed method with two models, model A (simple quadratic ℓ_k - $\ell_{E_{s/sb}}$ relationship) and model B (multiple linear ℓ_k - $\ell_{E_{s/sb}}$ relationships with consideration of pavement properties) and the three existing design methods, PCA, FAA and AASHTO methods, highlights the following points regarding the issue of estimating composite *k* from E_s and E_{sb}:

- The two existing design methods, PCA and AASHTO methods were found to produce large errors in their estimation of composite *k* values. Another design method, FAA method, produces better results in terms of *RSME* and *RSMPE* than that of the proposed method. However, a main drawback of the design methods is the limited range of pavement properties required as input data. In this aspect, the proposed method is superior to the three design methods as it is applicable for a very wide range of input parameter values.
- The proposed model B is recommended to be used since some analysis results, such as analysis of under- and over-estimation, and analysis of *RMSE* and *RMSPE,* indicated that model B is better than model A.

4.3.5 Summary

This study presented a proposed method to estimate composite *k* from E_s and E_{sb} based on an equivalent model method. This relationship is developed to take into account the role of subbase layer in pavement system and adoption of the *k*-E_s relationship developed in Section 4.2. The equivalent concept establishes an equivalency of the three-layer pavement system into two theoretical pavement models: an equivalent model of pavement system constructed of concrete slab over a composite dense liquid foundation characterized by *k* value parameter, and an equivalent model of pavement system constructed of concrete slab over composite solid elastic foundation which each layer is characterized by its elastic modulus.

Two models of ℓ_k - $\ell_{E_{s/sb}}$ relationship to estimate composite *k* from E_s and E_{sb} are employed by the proposed method, namely model A (direct relationship between ℓ_k and $\ell_{E_{s/sb}}$) and model B (relationship among ℓ_k , $\ell_{E_{s/sb}}$ and parameters of pavement properties). Three existing design methods, i.e. PCA, FAA and AASHTO method, were employed for comparison with the two proposed models.

The results showed that the procedures for estimating composite *k* in the existing design methods have much limited applicable range compared with the proposed methods. The PCA and AASHTO methods of composite *k* calculation tend to over-estimate the measured values, while FAA method produced the best estimates compared with other methods although it is only applicable to about one-fourth of the cases analyzed.

A comparison was conducted between the composite *k* produced by model A and B and indicated that model B is preferable than model A in terms of analysis of under- and over-estimation, and analysis of *RMSE* and *RMSPE*.

Table 4.1: Properties of 50 JCP Sections

Case	Test Section Code	Measured Ec (GPa)	Measured k (MN/m^3)	Joint Spacing (m)	Slab Thickness (m)
1	4 - 7614	30.71	-	4.572	0.246
2	5 - 3059	24.50	-	13.716	0.239
3	8 - 213	24.50	114.76	4.572	0.221
4	8 - 214	33.12	122.09	4.572	0.213
5	8 - 215	29.33	103.09	4.572	0.290
6	8 - 222	32.09	73.25	4.572	0.221
7	8 - 7776	27.60	-	3.962	0.272
8	9 - 4008	34.16	-	12.192	0.264
9	10 - 203	29.74	51.55	4.572	0.297
10	10 - 204	30.34	74.61	4.572	0.279
11	10 - 208	28.94	54.26	4.572	0.307
12	10 - 259	37.76	59.69	4.572	0.259
13	19 - 213	32.66	39.61	4.572	0.216
14	19 - 219	35.36	17.36	4.572	0.284
15	19 - 223	39.05	12.21	4.572	0.297
16	19 - 3006	31.57	-	6.096	0.226
17	19 - 3009	31.22	-	6.096	0.269
18	19 - 3028	30.36	-	6.096	0.244
19	19 - 3055	23.98	-	6.096	0.254
20	20 - 4054	28.98	-	9.144	0.241
21	22 - 4001	37.78	-	17.831	0.249
22	23 - 3014	23.29	-	6.096	0.262
23	26 - 214	34.16	130.22	4.572	0.226
24	26 - 215	33.12	69.18	4.572	0.284
25	26 - 219	27.26	105.81	4.572	0.277
26	26 - 220	32.43	92.24	4.572	0.282
27	27 - 3013	37.61	-	4.572	0.203
28	29 - 4069	24.15	-	18.745	0.251
29	31 - 3023	26.22	-	4.724	0.305
30	32 - 3013	37.43	-	4.724	0.211
31	34 - 4042	36.05	-	23.835	0.226
32	35 - 3010	41.06	-	4.115	0.201
33	36 - 4017	25.01	-	19.355	0.224
34	36 - 4018	27.08	-	19.355	0.239
35	37 - 203	30.71	92.24	4.572	0.284
36	37 - 204	35.06	61.04	4.572	0.284
37	39 - 3801	25.88	-	6.096	0.234
38	40 - 3018	30.71	-	4.572	0.226
39	40 - 4162	40.54	-	4.572	0.234
40	48 - A807	34.50	86.82	4.572	0.211
41	48 - A808	35.19	86.82	4.572	0.312
42	49 - 3010	31.22	-	4.572	0.239
43	50 - 1682	33.12	-	4.572	0.206
44	53 - 3011	36.40	-	3.505	0.244
45	53 - 3014	32.43	-	3.505	0.264
46	53 - 3019	34.16	-	3.505	0.251
47	53 - 3813	36.40	-	4.572	0.203
48	53 - 7409	23.63	-	3.505	0.236
49	55 - 3008	46.92	-	4.724	0.272
50	55 - 3009	43.30	-	4.663	0.218

Table 4.2: Properties of 75 CRCP Sections

Case	Test Section Code	Measured E_c (GPa)	Slab Thickness (m)	Case	Test Section Code	Measured E_c (GPa)	Slab Thickness (m)
1	1 - 3998	47.61	0.208	39	41 - 5006	27.60	0.203
2	1 - 5008	37.95	0.234	40	41 - 5008	31.40	0.206
3	4 - 7079	27.60	0.229	41	41 - 5021	24.50	0.274
4	5 - 5803	33.81	0.203	42	41 - 5022	22.43	0.325
5	5 - 5805	27.60	0.203	43	41 - 7081	27.26	0.264
6	9 - 5001	41.40	0.208	44	42 - 1598	42.78	0.236
7	10 - 5004	23.12	0.229	45	42 - 1617	40.37	0.239
8	13 - 5023	36.57	0.213	46	42 - 5020	49.34	0.236
9	16 - 5025	30.71	0.211	47	45 - 5017	20.01	0.226
10	17 - 5020	24.15	0.218	48	45 - 5034	21.74	0.211
11	17 - 5843	41.75	0.264	49	45 - 5035	19.67	0.196
12	17 - 5849	26.91	0.183	50	46 - 5020	25.53	0.201
13	17 - 5854	27.60	0.254	51	46 - 5025	27.95	0.206
14	17 - 5869	45.20	0.226	52	46 - 5040	31.74	0.203
15	17 - 5908	22.43	0.224	53	48 - 3719	44.85	0.201
16	17 - 9267	43.82	0.216	54	48 - 3779	29.33	0.213
17	18 - 5022	41.40	0.249	55	48 - 5024	31.74	0.282
18	18 - 5043	36.92	0.191	56	48 - 5035	28.64	0.206
19	19 - 5042	27.95	0.203	57	48 - 5154	33.47	0.208
20	19 - 5046	32.09	0.211	58	48 - 5274	38.30	0.211
21	19 - 9116	34.16	0.198	59	48 - 5283	32.43	0.259
22	24 - 5807	33.19	0.229	60	48 - 5284	30.71	0.282
23	26 - 5363	31.74	0.254	61	48 - 5287	22.43	0.211
24	27 - 5076	37.95	0.231	62	48 - 5301	37.26	0.259
25	28 - 5006	32.09	0.208	63	48 - 5310	34.85	0.295
26	28 - 5025	30.71	0.211	64	48 - 5317	35.54	0.203
27	28 - 5803	32.09	0.201	65	48 - 5323	30.71	0.211
28	28 - 5805	38.99	0.208	66	48 - 5328	26.57	0.203
29	29 - 5047	37.26	0.211	67	48 - 5334	37.95	0.203
30	31 - 5052	24.50	0.193	68	48 - 5335	36.57	0.236
31	37 - 5037	19.32	0.198	69	48 - 5336	29.67	0.229
32	37 - 5826	32.43	0.203	70	51 - 2564	24.84	0.201
33	37 - 5827	21.05	0.206	71	51 - 5008	24.15	0.211
34	39 - 5003	25.53	0.246	72	51 - 5009	20.70	0.211
35	40 - 4155	30.02	0.246	73	54 - 5007	20.36	0.211
36	40 - 4158	33.12	0.262	74	55 - 5037	36.23	0.208
37	40 - 4166	34.50	0.257	75	55 - 5040	43.82	0.213
38	40 - 5021	34.16	0.241				

Table 4.3: *RSME* of Estimated *k* Values with Respect to Measured *k* Values

Methods	*RMSE* (MN/m^3)
AASHTO (1986, 1993)	462.89
Khazanovich et al. (2001)	34.77
Vesic and Saxena (1974)	
- without correction factor 0.42	162.05
- with correction factor 0.42	40.55
Ullidtz (1987)	49.64
Equivalent *k*- and *E*-models based on *k*-*E* correlation	35.81
Equivalent *k*- and *E*-models based on ℓ_k-ℓ_E relationship	34.23

Table 4.4: *RSME* of Estimated *k* Values with Respect to Backcalculated *k* Values

Methods	*RMSE* (MN/m^3)
Khazanovich et al. (2001)	39.32
Equivalent *k*- and *E*-models based on *k*-*E* correlation	24.77
Equivalent *k*- and *E*-models based on ℓ_k-ℓ_E relationship	6.76

Table 4.5: *RSME* and *RMSPE* of Estimated Composite *k* Values with Respect to Measured *k* Values from Different Methods

Test points	Methods	*RMSPE* (%)	*RMSE* (MN/m^3)
267	The proposed method – model A	0.765	39.04
	The proposed method – model B	0.798	37.89
43	PCA method (1984)	0.805	75.02
	The proposed method – model A	0.604	66.65
	The proposed method – model B	0.589	64.89
63	FAA method (1995, 1996)	0.411	47.39
	The proposed method – model A	0.631	63.97
	The proposed method – model B	0.631	63.42
24	AASHTO method (1986, 1993)	2.569	169.57
	The proposed method – model A	0.727	73.18
	The proposed method – model B	0.708	71.18

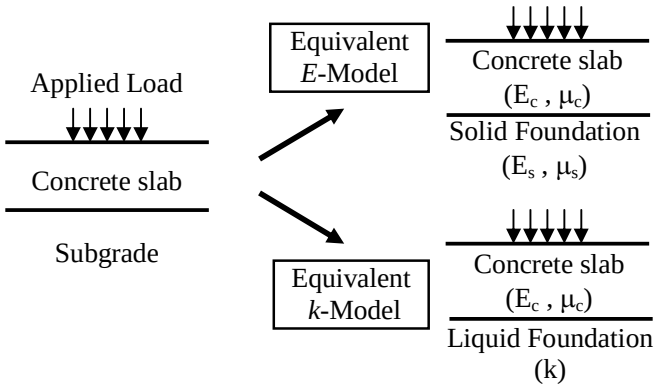

Figure 4.1: Equivalent *k*-model and Equivalent *E*-model

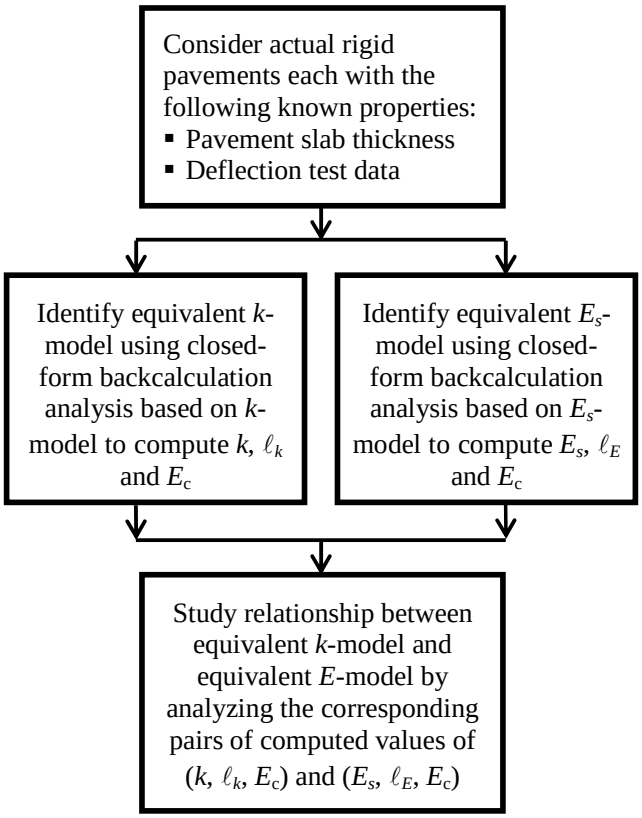

Figure 4.2: Proposed Approach for Deriving Relationship between k and E_s

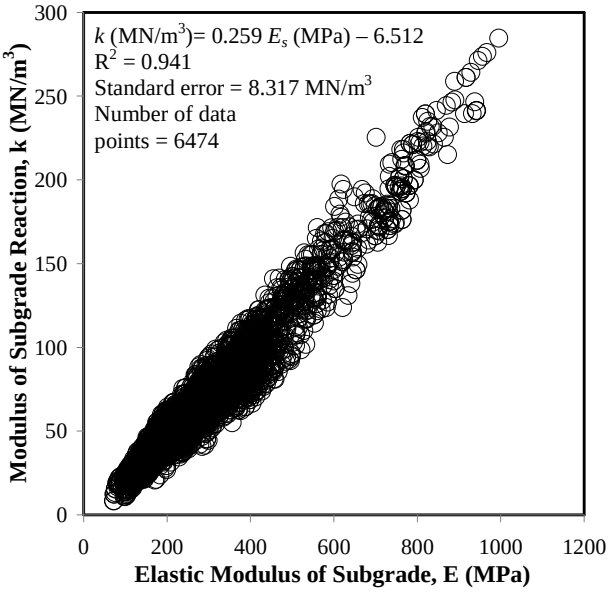

Figure 4.3: k-E_s Relationship Derived from Equivalent k-model and Equivalent E_s-model

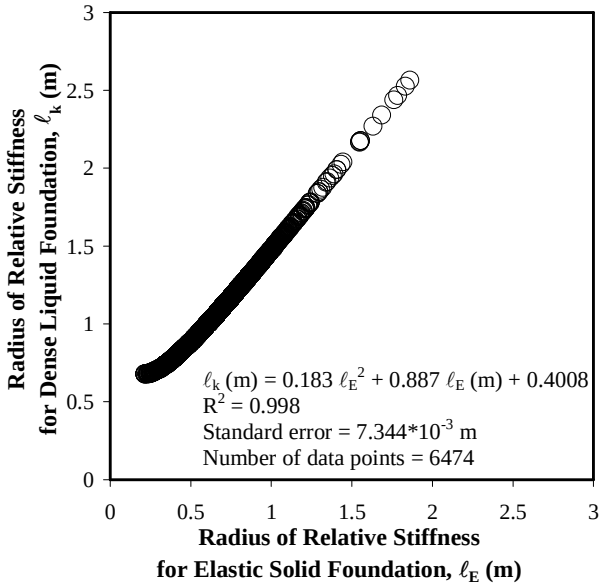

Figure 4.4: ℓ_k-ℓ_{Es} Relationship Derived from Equivalent *k*-model and Equivalent E_s-model

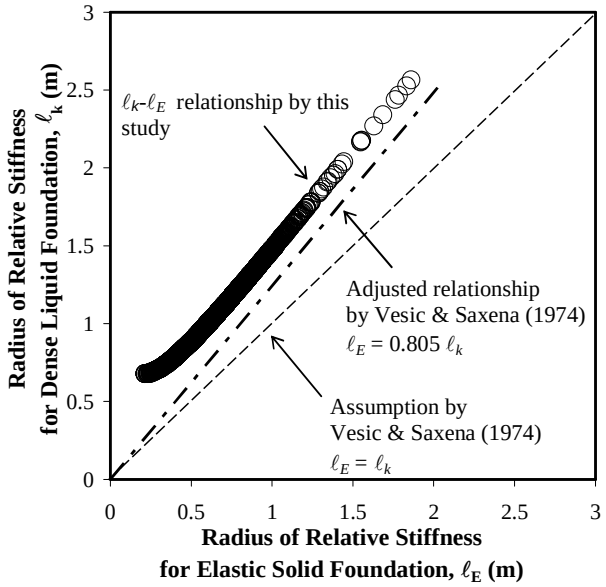

Figure 4.5: Comparison of Different ℓ_k-ℓ_{Es} Relationship

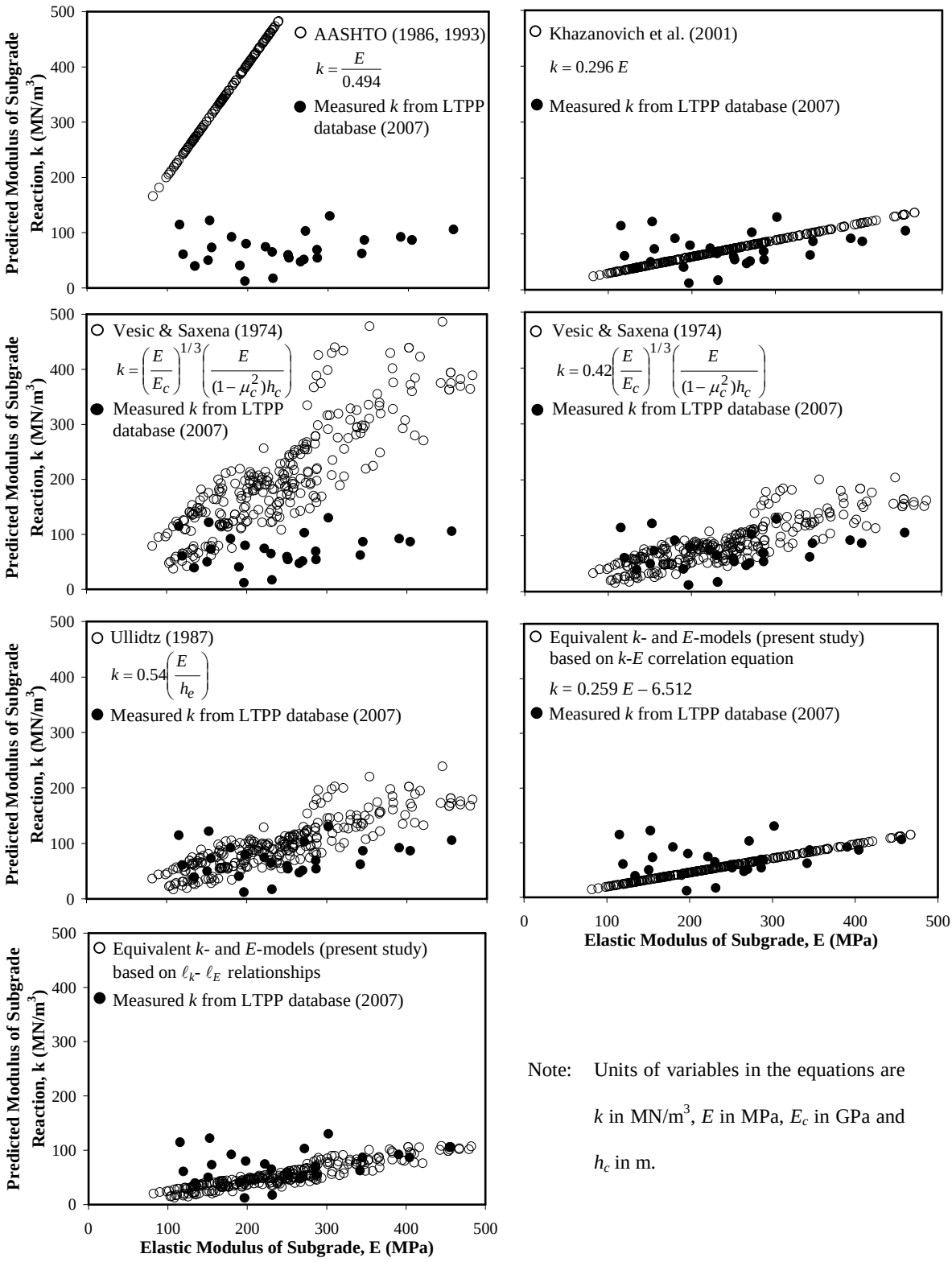

Note: Units of variables in the equations are k in MN/m^3, E in MPa, E_c in GPa and h_c in m.

Figure 4.6: Estimating k from E_s by Different Methods

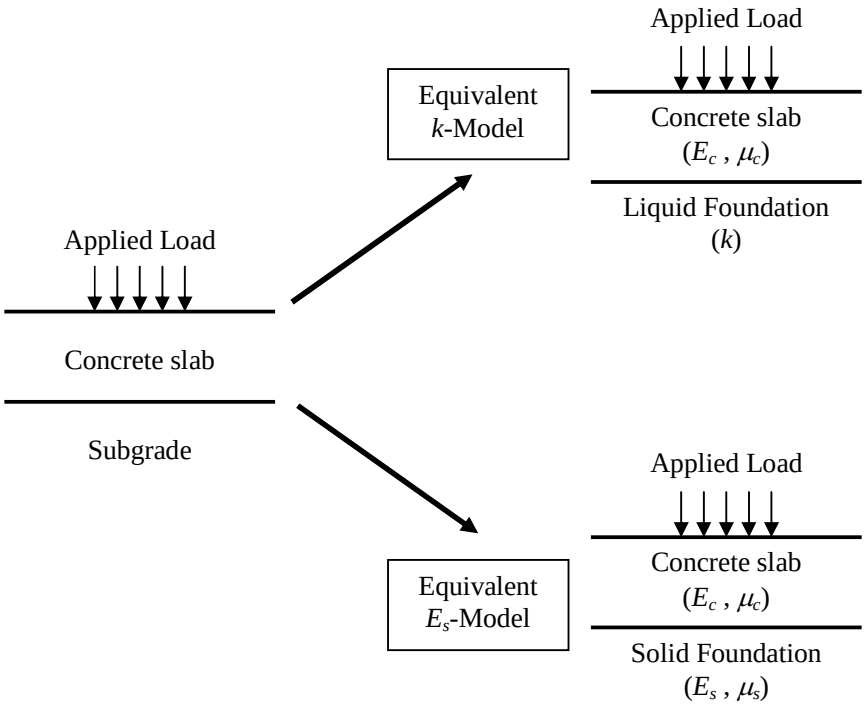

Figure 4.7: Equivalent *k*-model and Equivalent E_s-model

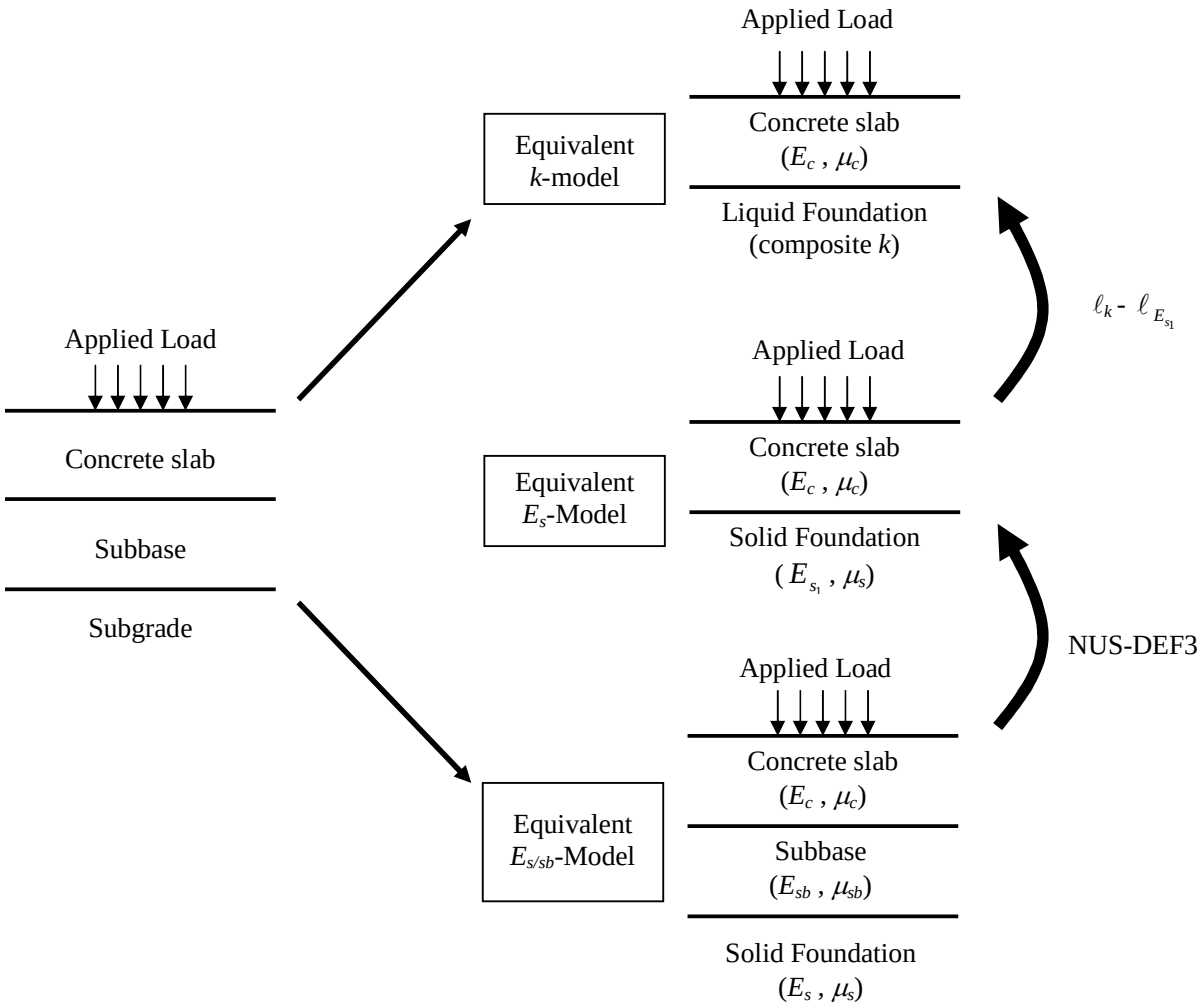

Figure 4.8: Equivalent *k*-model, E_s-model and $E_{s/sb}$-model

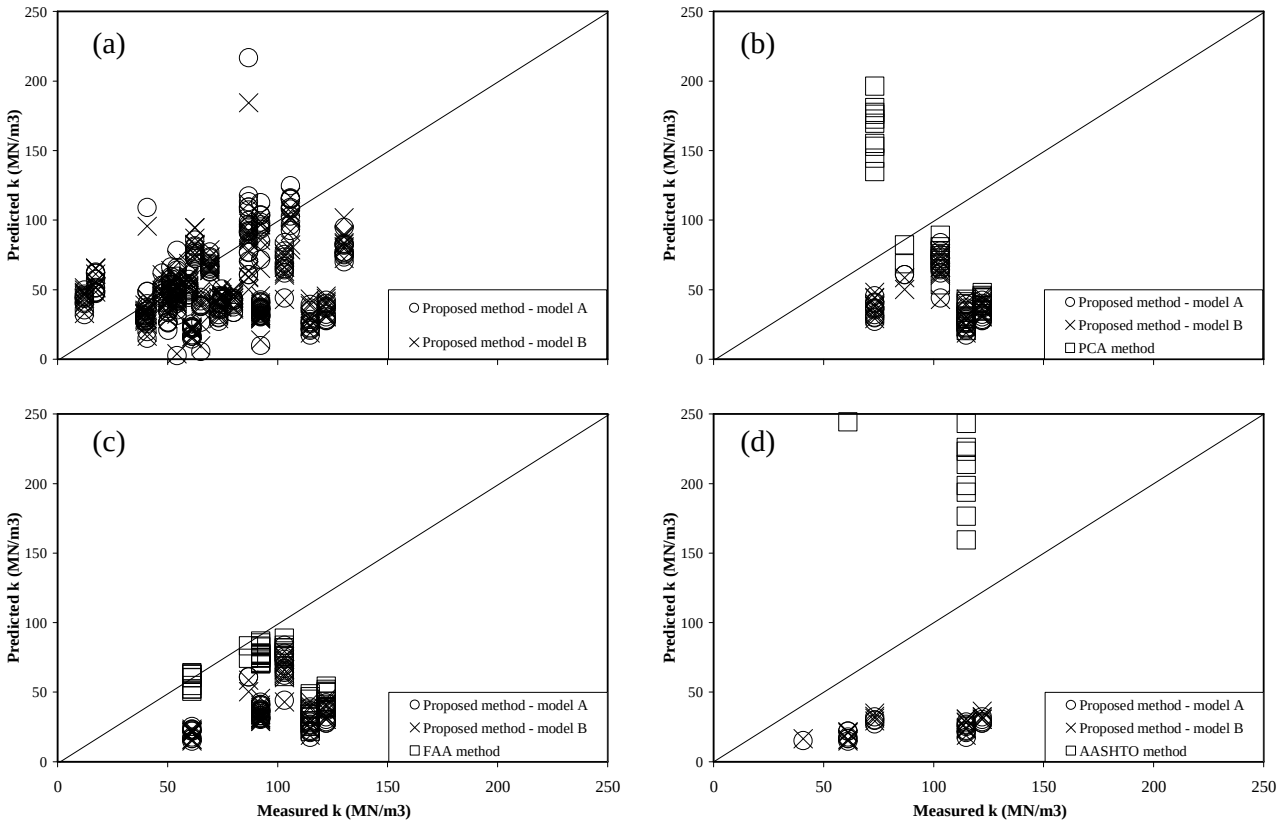

Figure 4.9: Comparison between Predicted and Measured *k* values

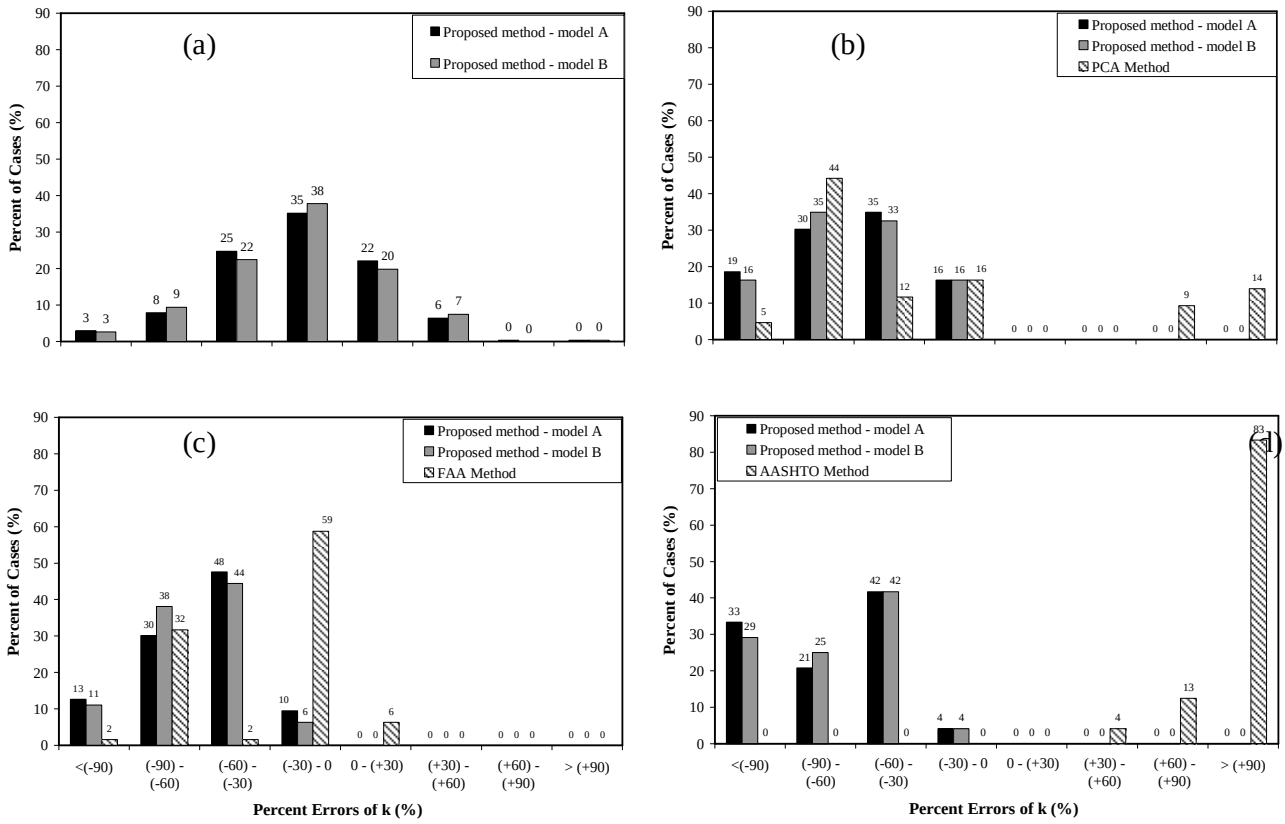

Figure 4.10: Frequency Distributions of Percent Errors of Predicted *k* Values

CHAPTER 5

DEVELOPMENT OF FORWARD CALCULATION SOLUTIONS FOR THREE- AND FOUR-LAYER FLEXIBLE PAVEMENT SYSTEMS

5.1 Introduction

The analytical solution of three-layer flexible pavement system was derived by Burmister in 1945. The solution is an extension of the solution for two-layer flexible pavement system developed earlier by Burmister (1943, 1945a). The intention was to overcome the practical problem in finding out an economical pavement with sufficient thickness over a weak subgrade to provide adequate support for heavy aircraft wheel loads. For this purpose, a granular layer is added between the surface layer and subgrade.

Today, an asphalt pavement system consisted of four layers is commonly encountered in practice. A four-layer pavement system generally has two different granular materials which form two different pavement courses between the surface layer and subgrade, namely as base and subbase courses.

The use of granular materials in the pavement system, either in a three- or four-layer system, usually has a purpose for economy, although they also may contribute to protect the subgrade by reducing the stress intensity through spreading the applied load over a larger area. In general, the use of granular material in the pavement system is to serve as a transition of two materials in the pavement system, i.e. surface layer and subgrade, which have a large difference in their structural capacity. In addition, the subbase also has a function as a filter to prevent the subgrade materials from infiltrating into the base course.

In this chapter, solutions for surface deflections of a three- and four-layer flexible pavement system are developed based on an extension of the theoretical solutions by Burmister for two- and three-layer pavement system (Burmister, 1945a; 1945b), respectively. The theoretical solutions are presented in this chapter, together with computer programs, 3L-DEF and 4L-DEF, developed in this study to compute surface deflections of a three- and four-layer pavement system under the action of a vertical load.

5.2 Solution for Surface Deflection

5.2.1 Determination of Surface Deflection Equation

Consider a flexible pavement system consisted of three layers, namely surface layer, subbase layer and subgrade (Figure 5.1) and another flexible pavement system consisted of four layers, i.e. surface layer, base layer, subbase layer and subgrade (Figure 5.2). Each of the layers is characterized by two engineering parameters: elastic modulus (E) and Poisson ratio (μ). A point load (P) is applied on the top of the surface layer. The first two layers for the three-layer flexible pavement system (i.e. surface and subbase layers) have thicknesses h_1 and h_2, respectively, and the first three layers for the four-layer flexible pavement system (i.e. surface, base and subbase layers) have thickness h_1, h_2 and h_3, respectively. The general solution of a three- and four-layer flexible pavement system should fulfill the assumptions and boundary conditions as stated in the preceding section (Section 2.1).

5.2.1.1 Boundary Conditions for Three-layer Flexible System

Based on the assumptions and general boundary conditions, Burmister (1943) set the boundary and continuity conditions for each interface, as given below.

Boundary conditions at the surface of the ground, $z = -h_1$

a. Distribution of surface loading, $\sigma_z = -mJ_0(mr)$

$$-mJ_0(mr)\{A_1m^2e^{-mh_1} + B_1m^2e^{mh_1} - C_1m(1-2\mu_1+mh_1)\,e^{-mh_1} + D_1m(1-2\mu_1-mh_1)\,e^{mh_1}\}$$

$$= -mJ_0(mr) \qquad (5\text{-}1)$$

b. Shearing stress at the surface, $\tau_{rz} = 0$

$$mJ_1(mr)\{A_1m^2e^{-mh_1} - B_1m^2e^{mh_1} + C_1m(2\mu_1-mh_1)\,e^{-mh_1} + D_1m(2\mu_1+mh_1)\,e^{mh_1}\} = 0 \qquad (5\text{-}2)$$

Continuity Conditions at the Interface between layer 1 and layer 2, $z = 0$

a. Normal Stress, $\sigma_{z1} = \sigma_{z2}$

$$\{A_1m+B_1m-C_1(1-2\mu_1)+D_1(1-2\mu_1)\} = \{A_2m+B_2m-C_2(1-2\mu_2)+D_2(1-2\mu_2)\} \qquad (5\text{-}3)$$

b. Shearing Stress, $\tau_{rz1} = \tau_{rz2}$

$$\{A_1m-B_1m+2C_1\mu_1+2D_1\mu_1\} = \{A_2m-B_2m+2C_2\mu_2+2D_2\mu_2\} \qquad (5\text{-}4)$$

c. Vertical settlement, $w_1 = w_2$

$$\{(1+\mu_1)/E_1\}\{A_1m-B_1m-2C_1(1-2\mu_1)-2D_1(1-2\mu_1)\}$$

$$= \{(1+\mu_2)/E_2\}\{A_2m-B_2m-2C_2(1-2\mu_2)-2D_2(1-2\mu_2)\} \qquad (5\text{-}5)$$

d. Horizontal displacement, $u_1 = u_2$

$$\{(1+\mu_1)/E_1\}\{A_1m+B_1m+C_1-D_1\} = \{(1+\mu_2)/E_2\}\{A_2m+B_2m+C_2-D_2\} \qquad (5\text{-}6)$$

Continuity conditions at the interface between layer and layer 3, $z = +h_2$

At infinite depth, stresses and displacement in layer 3 must be equal to zero. Therefore there are no coefficients A_3 and C_3 in the following equations.

a. Normal Stress, $\sigma_{z2} = \sigma_{z3}$

$$\{A_2 m e^{mh_2} + B_2 m e^{-mh_2} - C_2(1-2\mu_2-mh_2) e^{mh_2} + D_1(1-2\mu_1+mh_2) e^{-mh_2} \}$$

$$= \{B_3 m e^{-mh_2} + D_3(1-2\mu_2+mh_2) e^{-mh_2} \} \quad (5\text{-}7)$$

b. Shearing Stress, $\tau_{rz2} = \tau_{rz3}$

$$\{A_2 m e^{mh_2} - B_2 m e^{-mh_2} + C_2(2\mu_2+mh_2) e^{mh_2} + D_2(2\mu_2-mh_2) e^{-mh_2} \}$$

$$= \{ -B_3 m e^{-mh_2} + D_3(2\mu_2-mh_2) e^{-mh_2} \} \quad (5\text{-}8)$$

c. Vertical settlement, $w_2 = w_3$

$$\{(1+\mu_2)/E_2\} \{A_2 m e^{mh_2} - B_2 m e^{-mh_2} - C_2(2-4\mu_1-mh_2) e^{mh_2} - D_2(2-4\mu_2+mh_2) e^{-mh_2} \}$$

$$= \{(1+\mu_2)/E_2\} \{A_2 m - B_2 m - 2C_2(1-2\mu_2) - 2D_2(1-2\mu_2)\} \quad (5\text{-}9)$$

d. Horizontal displacement, $u_2 = u_3$

$$\{(1+\mu_2)/E_2\} \{A_2 m e^{mh_2} + B_2 m e^{-mh_2} + C_2(1+mh_2) e^{mh_2} - D_2(1-mh_2) e^{-mh_2} \}$$

$$= \{(1+\mu_3)/E_3\} \{B_3 m e^{-mh_2} - D_3(1-mh_2) e^{-mh_2} \} \quad (5\text{-}10)$$

5.2.1.2 Determination of Three-layer System Coefficients

All the coefficients of Equations (5-1) – (5-10) were determined to satisfy the boundary and continuity conditions, as follows.

Interface between layer 2 and layer 3, $z = +h$

The continuity conditions at this interface are satisfied by solving Equations (5-7) to (5-10) to obtain A_2 and C_2 represented by B_2 and D_2 as follows.

$$2A_2 m = 2B_2 mK(1-4\mu_2-2mh_2) e^{-2mh_2} - D_2 L e^{-2mh_2} + D_2 K(1-4\mu_2-2mh_2)(1-4\mu_2+2mh_2) e^{-2mh_2} \quad (5\text{-}11)$$

$$C_2 = 2B_2 mK e^{-2mh_2} + D_2 K(1-4\mu_2+2mh_2) e^{-2mh_2} \quad (5\text{-}12)$$

where:

$$K = \left\{ \frac{1-k}{1+(3-4\mu_2)k} \right\} \tag{5-13}$$

$$L = \left\{ \frac{(3-4\mu_3)-(3-4\mu_2)k}{(3-4\mu_3)+k} \right\} \tag{5-14}$$

$$k = \left\{ \frac{E_3(1+\mu_2)}{E_2(1+\mu_3)} \right\} \tag{5-15}$$

Interface between layer 1 and layer 2, $z = 0$

By solving Equations (5-3) to (5-6) simultaneously with Equations (5-11) and (5-12), the continuity conditions for the interface between layer 2 and layer 3 at $z = +h$ were satisfied.

$$4A_1m^2h_2KTe^{-2mh_2} + 2B_1mT + 2B_1m\left(\frac{1-\mu_2}{1-\mu_1}\right)Ke^{-2mh_2}$$

$$+2B_1m\left[\frac{(1-\mu_2)(3-4\mu_1)-(1-\mu_1)}{(1-\mu_1)}\right]KTe^{-2mh_2} - C_1 - C_1(1-4\mu_1)KT(1+2mh_2)e^{-2mh_2} -$$

$$2C_1KTe^{-2mh_2} - C_1\left(\frac{1-\mu_2}{1-\mu_1}\right)\left[1+(3-4\mu_1)T\right]Ke^{-2mh_2} + D_1(1-4\mu_1)T + 2D_1KTe^{-2mh_2} +$$

$$D_1(1+2mh_2)Ke^{-2mh_2} - \frac{(\mu_2+3\mu_1-4\mu_1\mu_2)}{(1-\mu_1)}\left[1+(3-4\mu_1)T\right]Ke^{-2mh_2} = 0 \tag{5-16}$$

$$2A_1mLTe^{-2mh_2} - 4A_1m^2h_2(1-4\mu_2-2mh_2)KTe^{-2mh_2} + 2A_1m\left(\frac{1-\mu_2}{1-\mu_1}\right)$$

$$+2A_1m\left[\frac{(1-\mu_2)(3-4\mu_1)-(1-\mu_1)}{(1-\mu_1)}\right]T - 2B_1m\left(\frac{1-\mu_2}{1-\mu_1}\right)(1-4\mu_2-2mh_2)Ke^{-2mh_2}$$

$$-2B_1m(1-4\mu_2)T - 2B_1m\left[\frac{(1-\mu_2)(3-4\mu_1)-(1-\mu_1)}{(1-\mu_1)}\right](1-4\mu_2-2mh_2)KTe^{-2mh_2}$$

$$-4C_1\mu_2-C_1(1-4\mu_1)LTe^{-2mh_2}+C_1(1-4\mu_1)(1+2mh_2)(1-4\mu_2-2mh_2)qKe^{-2mh_2}$$

$$+C_1\frac{(\mu_2+3\mu_1-4\mu_1\mu_2)}{(1-\mu_1)}+C_1\left[\frac{(\mu_2+3\mu_1-4\mu_1\mu_2)(3-4\mu_1)-2(1-\mu_1)}{(1-\mu_1)}\right]T$$

$$+C_1\left(\frac{1-\mu_2}{1-\mu_1}\right)Ke^{-2mh_2}+C_1\left[\frac{2(1-\mu_1)+(\mu_1-\mu_2)(3-4\mu_1)}{(1-\mu_1)}\right]KTe^{-2mh_2}$$

$$+4D_1\mu_2(1-4\mu_1)T+D_1Le^{-2mh_2}-D_1(1+2mh_2)(1-4\mu_2-2mh_2)Ke^{-2mh_2}$$

$$+D_1\left[\frac{(\mu_2+3\mu_1-4\mu_1\mu_2)}{(1-\mu_1)}\right](1-4\mu_2-2mh_2)Ke^{-2mh_2}+D_1\left[\frac{2(1-\mu_1)+(\mu_1-\mu_2)(3-4\mu_1)}{(1-\mu_1)}\right]T$$

$$+D_1\left(\frac{\mu_1-\mu_2}{1-\mu_1}\right)+D_1\left[\frac{(\mu_2+3\mu_1-4\mu_1\mu_2)(3-4\mu_1)-2(1-\mu_1)}{(1-\mu_1)}\right](1-4\mu_2-2mh_2)KTe^{-2mh_2}=0$$

(5-17)

where:

$$T=\left\{\frac{1-q}{1+(3-4\mu_1)q}\right\} \tag{5-18}$$

$$J=\left\{\frac{(3-4\mu_2)-(3-4\mu_1)q}{(3-4\mu_2)+q}\right\} \tag{5-19}$$

$$q=\left\{\frac{E_2(1+\mu_1)}{E_1(1+\mu_2)}\right\} \tag{5-20}$$

<u>Surface of layer 1, $z = -h_1$</u>

By solving boundary conditions in Equations (5-1) and (5-2), the coefficients A_1 and B_1 can be presented in C_1 and D_1 as given by:

$$2A_1m^2=e^{mh_1}+C_1m(1-4\mu_1+2mh_1)-D_1me^{2mh_1} \tag{5-21}$$

$$2B_1m^2=e^{-mh_1}+C_1me^{-2mh_1}-D_1m(1-4\mu_1-2mh_1) \tag{5-22}$$

Substitute Equations (5-21) and (5-22) into Equations (5-16) and (5-17) and solve them to obtain the coefficients C_1 and D_1 as follows:

$$C_1 m = \frac{-\left(\frac{1-T}{1-J}\right)}{\Delta}\begin{bmatrix} (1+2mh_1)Te^{mh_1} - JTe^{-mh_1} + (1+2mh_1)KLTe^{mh_1}e^{-4mh_2} \\ +\left\{(1+2mh_1)\left(\frac{1-J}{1-T}\right)LT^2 + 4m^2h_2^2(1+2mh_1)\left(\frac{1-J}{1-T}\right)KT^2 + 2mh_2K\right. \\ \left.+(1+2mh_1)\left(\frac{1-T}{1-J}\right)K - 2mh_2JKT\right\}e^{mh_1}e^{-2mh_2} \\ -\left\{\left(\frac{1-T}{1-J}\right)JK + \left(\frac{1-J}{1-K}\right)TL + 4m^2h_2^2\left(\frac{1-J}{1-T}\right)KT\right\}e^{-mh_1}e^{-2mh_2} \\ -LNe^{-mh_1}e^{-4mh_2} \end{bmatrix}$$

(5-23)

$$D_1 m = \frac{-\left(\frac{1-T}{1-J}\right)}{\Delta}\begin{bmatrix} e^{mh_1} - (1-2mh_1)Te^{-mh_1} - (1-2mh_1)KLTe^{-mh_1}e^{-4mh_2} \\ +\left\{\left(\frac{1-T}{1-J}\right)JK + \left(\frac{1-J}{1-T}\right)LT + 4m^2h_2^2\left(\frac{1-J}{1-T}\right)KT\right\}e^{mh_1}e^{-2mh_2} \\ -\left\{(1-2mh_1)\left(\frac{1-T}{1-J}\right)K + (1-2mh_1)\left(\frac{1-J}{1-T}\right)LT^2 - 2mh_2K\right. \\ \left.+4m^2h_2^2(1-2mh_1)\left(\frac{1-J}{1-T}\right)KT^2 + 2mh_2JNT\right\}e^{-mh_1}e^{-2mh_2} \\ +JKLTe^{mh_1}e^{-4mh_2} \end{bmatrix}$$

(5-24)

$$\Delta = -\left(\frac{1-T}{1-J}\right)\begin{bmatrix} e^{2mh_1} - \left\{J + \left(1+4m^2h_1^2\right)K\right\} + JTe^{-2mh_1} \\ -\left\{\left(\frac{1-T}{1-J}\right)K + \left(\frac{1-J}{1-T}\right)L + 4m^2h_2^2K\left(\frac{1-J}{1-T}\right)\right\}e^{-2mh_2} + KLe^{-2mh_1}e^{-4mh_2} \\ -\left\{\left(1+4m^2h_1^2\right)\left(\frac{1-J}{1-T}\right)LT^2 + 4m^2h_2^2\left(1+4m^2h_1^2\right)\left(\frac{1-J}{1-T}\right)KT^2\right. \\ +\left(\frac{1-T}{1-J}\right)J^2K + 8m^2h_1h_2(1-JT)K + 4m^2h_1^2\left(\frac{1-T}{1-J}\right)K\Big\}e^{-2mh_2} \\ +\left\{JK + \left(\frac{1-J}{1-T}\right)LT + 4m^2h_2^2\left(\frac{1-J}{1-T}\right)KT\right\}\left(e^{2mh_1}e^{-2mh_2} + e^{-2mh_1}e^{-2mh_2}\right) \\ -\left\{\left(1+4m^2h_1^2\right)KLT + JKL\right\}e^{-4mh_2} + JKLTe^{2mh_1}e^{-4mh_2} \end{bmatrix}$$

(5-25)

To obtain the deflection equation at surface ($z = -h_1$), substitute Equations (5-21) - (5-25) into the Equation (5-26) and solve them.

$$w = -\frac{1+\mu_1}{E_1} J_0(mr)\left\{A_1 m^2 e^{mz} - B_1 m^2 e^{-mz} - C_1 m(2-4\mu_1 - mz)e^{mz} - D_1 m(2-4\mu_1 + mz)e^{-mz}\right\} \tag{5-26}$$

$$w = J_0(mr)\frac{(1-\mu_1^2)}{E_1}\left\{\frac{Numerator}{Denominator}\right\} \tag{5-27}$$

in which:

$$Numerator = \begin{bmatrix} 1 + 4mh_1 Ke^{-2mh_1} - JKe^{-4mh_1} + 4mh_2 Ne^{-2mh_1}e^{-2mh_2} - LNe^{-4mh_1}e^{-4mh_2} \\ + \left\{4mh_1 K^2 L\left(\frac{1-J}{1-K}\right) + 16m^3 h_1 h_2^2 K^2 N\left(\frac{1-J}{1-K}\right)\right. \\ \left. + 4mh_1 N\left(\frac{1-K}{1-J}\right) - 4mh_2 JKN\right\}e^{-2mh_1}e^{-2mh_2} + \left\{JN\left(\frac{1-K}{1-J}\right) + KL\left(\frac{1-J}{1-K}\right)\right. \\ \left. 4m^2 h_2^2 KN\left(\frac{1-J}{1-K}\right)\right\}\left(e^{-2mh_2} - e^{-4mh_1}e^{-2mh_2}\right) + 4mh_1 KLNe^{-2mh_1}e^{-4mh_2} \\ + JKLNe^{-4mh_2} \end{bmatrix} \tag{5-28}$$

$$Denominator = \begin{bmatrix} 1 - \left(J + K + 4m^2 h_1^2 K\right)e^{-2mh_1} + JKe^{-4mh_1} - \left\{N\left(\frac{1-K}{1-J}\right) + L\left(\frac{1-J}{1-K}\right)\right. \\ \left. + 4m^2 h_2^2 N\left(\frac{1-J}{1-K}\right)\right\}e^{-2mh_1}e^{-2mh_2} + LNe^{-4mh_1}e^{-4mh_2} \\ - \left\{\left(1+4m^2 h_1^2\right)K^2 L\left(\frac{1-J}{1-K}\right) + 4m^2 h_2^2\left(1+4m^2 h_1^2\right)K^2 N\left(\frac{1-J}{1-K}\right)\right. \\ \left. + J^2 N\left(\frac{1-K}{1-J}\right) + 8m^2 h_1 h_2 N(1-JK) + 4m^2 h_1^2 N\left(\frac{1-K}{1-J}\right)\right\}e^{-2mh_1}e^{-2mh_2} \\ + \left\{JN\left(\frac{1-K}{1-J}\right) + KL\left(\frac{1-J}{1-K}\right) + 4m^2 h_2^2 KN\left(\frac{1-J}{1-K}\right)\right\}\left(e^{-2mh_2} + e^{-4mh_1}e^{-2mh_2}\right) \\ - \left\{KLN\left(1+4m^2 h_2^2\right) + JLN\right\}e^{-2mh_1}e^{-4mh_2} + JKLNe^{-4mh_2} \end{bmatrix} \tag{5-29}$$

It is known that Poisson's ratio has only a relatively small effect on the pavement response (Huang, 2003), therefore it could be assumed that the Poisson's ratio has the same value that equals to 0.5 for all material, or $\mu_1 = \mu_2 = \mu_3 = 0.5$, and Equations (5-13) – (5-15) and (5-18) – (5-20) could be simplified as follows:

$$K = \left[\frac{1-k}{1+(3-4\mu_2)k}\right] = \frac{1-E_3/E_2}{1+E_3/E_2} = \frac{E_2-E_3}{E_2+E_3} \tag{5-13}$$

$$L = \left[\frac{(3-4\mu_3)-(3-4\mu_2)k}{(3-4\mu_3)+k}\right] = \frac{1-E_3/E_2}{1+E_3/E_1} = \frac{E_2-E_3}{E_2+E_3} \tag{5-14}$$

$$k = \left[\frac{E_3(1+\mu_2)}{E_2(1+\mu_3)}\right] = \frac{E_3}{E_2} \tag{5-15}$$

Thus,

$$L = K = B = \frac{E_2-E_3}{E_2+E_3} \tag{5-30}$$

$$T = \left[\frac{1-q}{1+(3-4\mu_1)q}\right] = \frac{1-E_2/E_1}{1+E_2/E_1} = \frac{E_1-E_2}{E_1+E_2} \tag{5-18}$$

$$J = \left[\frac{(3-4\mu_2)-(3-4\mu_1)q}{(3-4\mu_2)+q}\right] = \frac{1-E_2/E_1}{1+E_2/E_1} = \frac{E_1-E_2}{E_1+E_2} \tag{5-19}$$

$$q = \left[\frac{E_2(1+\mu_1)}{E_1(1+\mu_2)}\right] = \frac{E_2}{E_1} \tag{5-20}$$

Thus,

$$J = T = A = \frac{E_1-E_2}{E_1+E_2} \tag{5-31}$$

For an arbitrary loading as a superposition of loadings having a distribution $\sigma_z = -pmJ_o(mr)$, which was equivalent to a concentrated load P at the

surface of layer 1 (Burmister, 1943), the deflection equation at the surface of the ground, Equation (5-27), could be simplified as follows:

$$w = \frac{3PJ_o(mr)}{4\pi E_1}\left[\frac{numerator}{denominator}\right] \tag{5-27}$$

In which:

$$Numerator = \begin{bmatrix} 1+\{4m\{Ah_1 + B(h_2 + h_1A^2 + 4m^2h_1h_2^2A^2 + h_1 - h_2A^2)e^{-2mh_2}\} \\ + AB^2h_1e^{-4mh_2}\}e^{-2mh_1} - \{A^2 + B^2e^{-4mh_2} \\ + (2AB + 4ABm^2h_2^2)e^{-2mh_2}\}e^{-4mh_1} \\ + \{2AB + 4ABm^2h_2^2\}e^{-2mh_2} + A^2B^2e^{-4mh_2} \end{bmatrix} \tag{5-28}$$

$$Denominator = \begin{bmatrix} 1-[A(2+4m^2h_1^2) - B\{(2+4m^2h_2^2) + (1+4m^2h_2^2)(1+4m^2h_1^2)A^2 \\ + A^2 + 8m^2h_1h_2(1-A^2) + 4m^2h_1^2\}e^{-2mh_2} \\ + AB^2(2+4m^2h_2^2)e^{-4mh_2}]e^{-2mh_1} \\ + [A^2 + B^2e^{-4mh_2} + AB(2+4m^2h_2^2)e^{-2mh_2}]e^{-4mh_1} \\ + AB(2+4m^2h_2^2)e^{-2mh_2} + A^2B^2e^{-4mh_2} \end{bmatrix} \tag{5-29}$$

To ensure that the derivation is correct, the following two checks were made:

a. If the thickness of layer 1 (H) equals to 0, then $E_2 = E_1$, $\mu_2 = \mu_1$ and $k = 1$, $A = 0$, so that the numerator and denominator of Equation (5-27) will reduce into the following form:

$$\text{Numerator} = 1 + 4mhBe^{-2mh} - B^2e^{-4mh} \tag{5-28}$$

$$\text{Denominator} = 1 - B(2+4m^2h^2)e^{-2mh} + B^2e^{-4mh} \tag{5-29}$$

b. If the thickness of layer 2 (h) becomes infinite, then $E_3 = E_2$, $\mu_3 = \mu_2$ and $n = 1$, $B = 0$, again, the numerator and denominator of Equation (5-27) will reduce into the following form:

$$\text{Numerator} = 1 + 4mHAe^{-2mH} - A^2e^{-4mH} \tag{5-28}$$

$$\text{Denominator} = 1 - A(2+4m^2H^2)e^{-2mH} + A^2e^{-4mH} \tag{5-29}$$

The numerator and denominator at point (a) and (b) are similar with the numerator and denominator of the deflection equation of two-layer pavement system at the surface of the ground as stated by Burmister (1945a).

5.2.1.3 Boundary Conditions for Four-layer Flexible System

Based on Burmister's assumption and general boundary condition in Section 2.1, the boundary and continuity conditions that are set for each interface are given below.

Boundary conditions at the surface of the ground, $z = -h_1$

a. Distribution of surface loading, $\sigma_z = -mJ_0(mr)$

$$-mJ_0(mr)\left\{A_1m^2e^{-mh_1} + B_1m^2e^{mh_1} - C_1m(1-2\mu_1+mh_1)e^{-mh_1} + D_1m(1-2\mu_1-mh_1)e^{mh_1}\right\} = -mJ_0(mr) \tag{5-32}$$

b. Shearing stress at the surface, $\tau_{rz} = 0$

$$mJ_1(mr)\left\{A_1m^2e^{-mh_1} - B_1m^2e^{mh_1} + C_1m(2\mu_1-mh_1)e^{-mh_1} + D_1m(2\mu_1+mh_1)e^{mh_1}\right\} = 0 \tag{5-33}$$

Continuity conditions at the interface between layer 1 and layer 2, $z = 0$

a. Normal stress, $\sigma_{z1} = \sigma_{z2}$

$$\{A_1m + B_1m - C_1(1-2\mu_1) + D_1(1-2\mu_1)\} = \{A_2m + B_2m - C_2(1-2\mu_2) + D_2(1-2\mu_2)\} \tag{5-34}$$

b. Shearing stress, $\tau_{rz1} = \tau_{rz2}$

$$\{A_1m - B_1m + C_1 2\mu_1 + D_1 2\mu_1\} = \{A_2m - B_2m + C_2 2\mu_2 + D_2 2\mu_2\} \tag{5-35}$$

c. Vertical settlement, $w_1 = w_2$

$$\frac{1+\mu_1}{E_1}\{A_1 m - B_1 m - C_1 2(1-2\mu_1) - D_1 2(1-2\mu_1)\} = \frac{1+\mu_2}{E_2}\{A_2 m - B_2 m - C_2 2(1-2\mu_2) - D_2 2(1-2\mu_2)\} \quad (5\text{-}36)$$

d. Horizontal displacement, $u_1 = u_2$

$$\frac{1+\mu_1}{E_1}\{A_1 m + B_1 m + C_1 - D_1\} = \frac{1+\mu_2}{E_2}\{A_2 m + B_2 m + C_2 - D_2\} \quad (5\text{-}37)$$

<u>Continuity conditions at the interface between layer 2 and layer 3, $z = h_2$</u>

a. Normal stress, $\sigma_{z2} = \sigma_{z3}$

$$\left\{A_2 m e^{mh_2} + B_2 m e^{-mh_2} - C_2(1-2\mu_2 - mh_2)e^{mh_2} + D_2(1-2\mu_2 + mh_2)e^{-mh_2}\right\} = \left\{A_3 m e^{mh_2} + B_3 m e^{-mh_2} - C_3(1-2\mu_3 - mh_2)e^{mh_2} + D_3(1-2\mu_3 + mh_2)e^{-mh_2}\right\} \quad (5\text{-}38)$$

b. Shearing stress, $\tau_{rz2} = \tau_{rz3}$

$$\left\{A_2 m e^{mh_2} - B_2 m e^{-mh_2} + C_2(2\mu_2 + mh_2)e^{mh_2} + D_2(2\mu_2 - mh_2)e^{-mh_2}\right\} = \left\{A_3 m e^{mh_2} - B_3 m e^{-mh_2} + C_3(2\mu_3 + mh_2)e^{mh_2} + D_3(2\mu_3 - mh_2)e^{-mh_2}\right\} \quad (5\text{-}39)$$

c. Vertical settlement, $w_2 = w_3$

$$\frac{1+\mu_2}{E_2}\left\{A_2 m e^{mh_2} - B_2 m e^{-mh_2} - C_2(2-4\mu_2 - mh_2)e^{mh_2} - D_2(2-4\mu_2 + mh_2)e^{-mh_2}\right\} = \frac{1+\mu_3}{E_3}\left\{A_3 m e^{mh_2} - B_3 m e^{-mh_2} - C_3(2-4\mu_3 - mh_2)e^{mh_2} - D_3(2-4\mu_3 + mh_2)e^{-mh_2}\right\} \quad (5\text{-}40)$$

d. Horizontal displacement, $u_2 = u_3$

$$\frac{1+\mu_2}{E_2}\left\{A_2 m e^{mh_2} + B_2 m e^{-mh_2} + C_2(1+mh_2)e^{mh_2} - D_2(1-mh_2)e^{-mh_2}\right\} = \frac{1+\mu_3}{E_3}\left\{A_3 m e^{mh_2} + B_3 m e^{-mh_2} + C_3(1+mh_2)e^{mh_2} - D_3(1-mh_2)e^{-mh_2}\right\} \quad (5\text{-}41)$$

Continuity conditions at the interface between layer 3 and layer 4, $z = h_2+h_3$

a. Normal stress, $\sigma_{z3} = \sigma_{z4}$

$$\begin{aligned}&\left\{A_3 me^{m(h_2+h_3)} + B_3 me^{-m(h_2+h_3)} - C_3\left(1-2\mu_2 - m(h_2+h_3)\right)e^{m(h_2+h_3)}\right.\\&\left.+ D_3\left(1-2\mu_2 + m(h_2+h_3)\right)e^{-m(h_2+h_3)}\right\} = \left\{B_4 me^{-m(h_2+h_3)} + D_4\left(1-2\mu_4 + m(h_2+h_3)\right)e^{-m(h_2+h_3)}\right\}\end{aligned} \tag{5-42}$$

b. Shearing stress, $\tau_{rz3} = \tau_{rz4}$

$$\begin{aligned}&\left\{A_3 me^{m(h_2+h_3)} - B_3 me^{-m(h_2+h_3)} + C_3\left(2\mu_3 + m(h_2+h_3)\right)e^{m(h_2+h_3)}\right.\\&\left.+ D_3\left(2\mu_3 - m(h_2+h_3)\right)e^{-m(h_2+h_3)}\right\} = \left\{- B_4 me^{-m(h_2+h_3)} + D_4\left(2\mu_4 - m(h_2+h_3)\right)e^{-m(h_2+h_3)}\right\}\end{aligned} \tag{5-43}$$

c. Vertical settlement, $w_3 = w_4$

$$\begin{aligned}&\frac{1+\mu_3}{E_3}\left\{A_3 me^{m(h_2+h_3)} - B_3 me^{-m(h_2+h_3)} - C_3\left(2-4\mu_3 - m(h_2+h_3)\right)e^{m(h_2+h_3)}\right.\\&\left.- D_3\left(2-4\mu_3 + m(h_2+h_3)\right)e^{-m(h_2+h_3)}\right\} = \frac{1+\mu_4}{E_4}\left\{- B_4 me^{-m(h_2+h_3)}\right.\\&\left.- D_4\left(2-4\mu_4 + m(h_2+h_3)\right)e^{-m(h_2+h_3)}\right\}\end{aligned} \tag{5-44}$$

d. Horizontal displacement, $u_3 = u_4$

$$\begin{aligned}&\frac{1+\mu_3}{E_3}\left\{A_3 me^{m(h_2+h_3)} + B_3 me^{-m(h_2+h_3)} + C_3\left(1+m(h_2+h_3)\right)e^{m(h_2+h_3)}\right.\\&\left.- D_3\left(1-m(h_2+h_3)\right)e^{-m(h_2+h_3)}\right\} = \frac{1+\mu_4}{E_4}\left\{B_4 me^{-m(h_2+h_3)}\right.\\&\left.- D_4\left(1-m(h_2+h_3)\right)e^{-m(h_2+h_3)}\right\}\end{aligned} \tag{5-45}$$

5.2.1.4 Determination of Four-layered System Coefficients

All the coefficients of Equations (5-32) – (5-45) were determined to satisfy the boundary and continuity conditions, as follows:

Interface between layer 3 and layer 4, $z = h_2+h_3$

The continuity conditions at this interface are satisfied by solving Equations (5-42) – (5-45) to obtain A_3 and C_3 represented by B_3 and D_3 as follows:

$$C_3 = 2B_3mNe^{-2mH} + D_3N(1\text{-}4\mu_3+2mH)e^{-2mH} \tag{5-46}$$

$$2A_3m = 2B_3mN(1\text{-}4\mu_3+2mH)e^{-2mH} + D_3N(1\text{-}4\mu_3+2mH)\,(1\text{-}4\mu_3\text{-}2mH)e^{-2mH}\text{-}D_3Le^{-2mH} \tag{5-47}$$

where:

$$N = \frac{1-n}{n(3-4\mu_3)+1} \tag{5-48}$$

$$L = \frac{(3-4\mu_4)-(3-4\mu_3)n}{(3-4\mu_4)+n} \tag{5-49}$$

$$n = \frac{E_4(1+\mu_3)}{E_3(1+\mu_4)} \tag{5-50}$$

$$H = h_2 + h_3 \tag{5-51}$$

Interface between layer 2 and layer 3, $z = h_2$

The continuity conditions for the interface between layer 2 and layer 3 at $z = h_2$ are satisfied by solving Equations (5-38) – (5-41) to constants A_3, B_3, C_3 and D_3 represented by A_2, B_2, C_2 and D_2 as given by:

$$\begin{aligned} &8A_3m(1-\mu_3)e^{mh_2} = 2A_2m\{(3-4\mu_3)+k\}e^{mh_2} + 2B_2m(k-1)(1-4\mu_3-2mh_2)e^{-mh_2} \\ &-C_2\left[\{(3-4\mu_3)+k\}(1-4\mu_2-2mh_2)-\{k(3-4\mu_2)+1\}(1-4\mu_3-2mh_2)\right]e^{mh_2} \\ &+D_2\left[\{(3-4\mu_3)-k(3-4\mu_2)\}+(k-1)(1-4\mu_2-2mh_2)(1-4\mu_3-2mh_2)\right]e^{-mh_2} \end{aligned} \tag{5-52}$$

$$\begin{aligned} &8B_3m(1-\mu_3)e^{-mh_2} = 2A_2m(k-1)(1-4\mu_3+2mh_2)e^{mh_2} + 2B_2m\{(3-4\mu_3)+k\}e^{-mh_2} \\ &-C_2\left[\{(3-4\mu_3)-k(3-4\mu_2)\}+(k-1)(1-4\mu_2-2mh_2)(1-4\mu_3+2mh_2)\right]e^{mh_2} \\ &+D_2\left[\{(3-4\mu_3)+k\}(1-4\mu_2+2mh_2)-\{k(3-4\mu_2)+1\}(1-4\mu_3+2mh_2)\right]e^{-mh_2} \end{aligned} \tag{5-53}$$

$$\begin{aligned} &4C_3(1-\mu_3)e^{mh_2} = 2B_2m(k-1)e^{-mh_2} + C_2\{k(3-4\mu_2)+1\}e^{mh_2} \\ &+D_2(k-1)(1-4\mu_2+2mh_2)e^{-mh_2} \end{aligned} \tag{5-54}$$

$$4D_3(1-\mu_3)e^{-mh_2} = -2A_2m(k-1)e^{mh_2} + C_2(k-1)(1-4\mu_2-2mh_2)e^{mh_2} + D_2\{k(3-4\mu_2)+1\}e^{-mh_2} \quad (5\text{-}55)$$

$$k = \frac{E_3(1+\mu_2)}{E_2(1+\mu_3)} \quad (5\text{-}56)$$

Interface between layer 1 and layer 2, *z = 0*

By solving Equations (5-34) to (5-37), the continuity conditions for the interface between layer 1 and layer 2 at *z = 0* were satisfied.

$$8A_2m(1-\mu_2) = 2A_1m\{(3-4\mu_2)+q\} - 2B_1m(1-q)(1-4\mu_2) - C_1[(1-4\mu_1)\{(3-4\mu_2)+q\} - (1-4\mu_2)\{q(3-4\mu_1)+1\}] + D_1[\{(3-4\mu_2)-q(3-4\mu_1)\} + (1-q)(1-4\mu_1)(1-4\mu_2)] \quad (5\text{-}57)$$

$$8B_2m(1-\mu_2) = -2A_1m(1-q)(1-4\mu_2) + 2B_1m\{(3-4\mu_2)+q\} - C_1[\{(3-4\mu_2)-q(3-4\mu_1)\} - (1-q)(1-4\mu_1)(1-4\mu_2)] + D_1[(1-4\mu_1)\{(3-4\mu_2)+q\} - (1-4\mu_2)\{q(3-4\mu_1)+1\}] \quad (5\text{-}58)$$

$$-4C_2(1-\mu_2) = 2B_1m(1-q) - C_1\{q(3-4\mu_1)+1\} + D_1(1-q)(1-4\mu_1) \quad (5\text{-}59)$$

$$4D_2(1-\mu_2) = 2A_1m(1-q) - C_1(1-q)(1-4\mu_1) + D_1\{q(3-4\mu_1)+1\} \quad (5\text{-}60)$$

$$q = \frac{E_2(1+\mu_1)}{E_1(1+\mu_2)} \quad (5\text{-}61)$$

Surface of layer 1, *z = -H*

By solving boundary conditions in Equations (5-32) and (5-33), the coefficient A_1 and B_1 can be presented in C_1 and D_1 as given by:

$$2A_1m^2 = e^{mh_1} + C_1m(1-4\mu_1+2mh_1) - D_1me^{2mh_1} \quad (5\text{-}62)$$

$$2B_1m^2 = e^{-mh_1} + C_1me^{-2mh_1} - D_1m(1-4\mu_1-2mh_1) \quad (5\text{-}63)$$

Burmister (1945a) stated that the deflection equation for layer 1 could be determined using the following equation.

$$w_1 = -\frac{1+\mu_1}{E_1} J_0(mr)\left\{A_1 m^2 e^{-mh_1} - B_1 m^2 e^{mh_1} - C_1 m(2-4\mu_1+mh_1)e^{-mh_1} - D_1 m(2-4\mu_1-mh_1)e^{mh_1}\right\} \quad (5\text{-}64)$$

Substitute Equations (5-62) and (5-63) into Equation (5-64), the deflection equation at the surface of the ground, for a surface loading with distribution σ_z = -*pmJ*$_0$*(mr)* (which was equivalent to a concentrated load *P* at the surface of layer 1), could be obtained as follows.

$$w_1 = \frac{2(1-\mu_1^2)P}{\pi E_1} \int_{mr=0}^{\infty} \left\{C_1 m e^{-mh_1} + D_1 m e^{mh_1}\right\} J_0(mr)\, dm \quad (5\text{-}65)$$

Two coefficients C_1 and D_1 were determined by substituting Equations (5-57) – (5-61) into Equations (5-51) – (5-56), and then substitute the results into Equations (5-46) and (5-47) to obtain two equalities, as given by:

$c_1 C_1\, m + d_1 D_1\, m + const_1 = 0$ (5-66a)

$c_2 C_1\, m + d_2 D_1\, m + const_2 = 0$ (5-66b)

Thus,

$$D_1 m = \frac{Numerator\ D_1}{Denominator\ D_1} = \frac{-\left\{(c_2 * const_1) - (c_1 * const_2)\right\}}{\left\{(c_2 * d_1) - (c_1 * d_2)\right\}} \quad (5\text{-}67)$$

$$C_1 m = \frac{Numerator\ C_1}{Denominator\ C_1} = \frac{-\left\{const_1 + D_1 m * d_1\right\}}{c_1} \quad (5\text{-}68)$$

where:

$$c_1 = \Big\langle \left[4NTXm^2 h_1 h_2 - 2NTZmh_1 - NSX\right]e^{-mH} - \left[2KNVZmh_1 + 2KNZmh_2 + NY\right]e^{2mh_2}e^{-mH} + \left[4KTm^2 h_1 h_2 - KS\right]e^{-2mh_2}e^{mH} - e^{mH} + \left[2KNTZmh_2 + NTY\right]e^{-2mh_1}e^{2mh_2}e^{-mH} + \left[NVX\right]e^{-2mh_1}e^{-mH} + \left[KV\right]e^{-2mh_1}e^{-2mh_2}e^{mH} + \left[T\right]e^{-2mh_1}e^{mH} \Big\rangle \quad (5\text{-}69a)$$

$$d_1 = \Big\langle \left[-KNSZ + 4KNTZm^2 h_1 h_2 + 2NTYmh_1\right]e^{2mh_2}e^{-mH} - \left[-2NVXmh_1 - 2NXmh_2 + NZ\right]e^{-mH} - \left[-2KVmh_1 - 2Kmh_2\right]e^{-2mh_2}e^{mH} - \left[-2Tmh_1\right]e^{mH} + \left[-2NTXmh_2 + NTZ\right]e^{2mh_1}e^{-mH} + \left[KNVZ\right]e^{2mh_1}e^{2mh_2}e^{-mH} - \left[2KTmh_2\right]e^{2mh_1}e^{-2mh_2}e^{mH} \Big\rangle \quad (5\text{-}69b)$$

$$const_1 = \langle [2NTXmh_2 - NTZ]e^{mh_1}e^{-mH} - [KNVZ]e^{mh_1}e^{2mh_2}e^{-mH} + [2KTmh_2]e^{mh_1}e^{-2mh_2}e^{mH}$$
$$+ [2KNTZmh_2 + NTY]e^{-mh_1}e^{2mh_2}e^{-mH} + [NVX]e^{-mh_1}e^{-mH} + [KV]e^{-mh_1}e^{-2mh_2}e^{mH}$$
$$+ [T]e^{-mh_1}e^{mH} \rangle$$

(5-69c)

$$c_2 = \langle [2VXmh_1 + 2Xmh_2 + (1-4\mu_3-2mh_2)]e^{mH} + [2KNVZmh_1(1-4\mu_3-2mH) + 2KLVmh_1$$
$$+ 2KNZmh_2(1-4\mu_3-2mH) + 2KLmh_2 + NY(1-4\mu_3-2mH)]e^{2mh_2}e^{-mH}$$
$$+ [-4NTXm^2h_1h_2(1-4\mu_3-2mH) + 2KTmh_1\{NZ(1-4\mu_3-2mH)+L\}$$
$$+ NSX(1-4\mu_3-2mH)]e^{-mH} + [KS(1-4\mu_3-2mh_2) - 4KTm^2h_1h_2(1-4\mu_3-2mh_2)$$
$$+ 2TYmh_1]e^{-2mh_2}e^{mH} - [2TXmh_2 + T(1-4\mu_3-2mh_2)]e^{-2mh_1}e^{mH} - [2KNTZmh_2(1-4\mu_3-2mH)$$
$$+ 2KLTmh_2 + NTY(1-4\mu_3-2mH)]e^{-2mh_1}e^{2mh_2}e^{-mH} - [KV(1-4\mu_3-2mh_2)]e^{-2mh_1}e^{-2mh_2}e^{mH}$$
$$- [NVX(1-4\mu_3-2mH)]e^{-2mh_1}e^{-mH} \rangle$$

(5-70a)

$$d_2 = \langle [SX - 4TXm^2h_1h_2 - 2Tmh_1(1-4\mu_3-2mh_2)]e^{mH} + [-4KNTZm^2h_1h_2(1-4\mu_3-2mH)$$
$$- 4KLTm^2h_1h_2 - 2NTYmh_1(1-4\mu_3-2mH) + KNSZ(1-4\mu_3-2mH) + KLS]e^{2mh_2}e^{-mH}$$
$$+ [-2KVmh_1(1-4\mu_3-2mh_2) - 2Kmh_2(1-4\mu_3-2mh_2) + Y]e^{-2mh_2}e^{mH}$$
$$+ [-2NXmh_2(1-4\mu_3-2mH) + \{NZ(1-4\mu_3-2mH)+L\}]e^{-mH}$$
$$- [VX]e^{2mh_1}e^{mH} - [KV\{NZ(1-4\mu_3-2mh_2)+L\}]e^{2mh_1}e^{2mh_2}e^{-mH} - [-2KTmh_2(1-4\mu_3-2mh_2)$$
$$+ TY]e^{2mh_1}e^{-2mh_2}e^{mH} - [-2NTXmh_2(1-4\mu_3-2mH) + T\{NZ(1-4\mu_3-2mh_2)+L\}]e^{2mh_1}e^{-mH} \rangle$$

(5-70b)

$$const_2 = \langle [VX]e^{mh_1}e^{mH} + [KV\{NZ(1-4\mu_3-2mH)+L\}]e^{mh_1}e^{2mh_2}e^{-mH} + [-2KTmh_2(1-4\mu_3-2mh_2)$$
$$+ TY]e^{mh_1}e^{-2mh_2}e^{mH} + [-2NTXmh_2(1-4\mu_3-2mH) + T\{NZ(1-4\mu_3-2mH)+L\}]e^{mh_1}e^{-mH}$$
$$- [2TXmh_2 + T(1-4\mu_3-2mh_2)]e^{-mh_1}e^{mH} - [2KNTZmh_2(1-4\mu_3-2mH) + 2KLTmh_2$$
$$+ NTY(1-4\mu_3-2mH)]e^{-mh_1}e^{2mh_2}e^{-mH} - [KV(1-4\mu_3-2mh_2)]e^{-mh_1}e^{-2mh_2}e^{mH}$$
$$- [NVX(1-4\mu_3-2mH)]e^{-mh_1}e^{-mH} \rangle = 0$$

(5-70c)

$$S = \frac{(1-\mu_2)}{(1-\mu_1)} + \frac{(1-\mu_2)(3-4\mu_1)T}{(1-\mu_1)} - 1 \tag{5-71}$$

$$V = \frac{(1-\mu_2)}{(1-\mu_1)} + \frac{(1-\mu_2)(3-4\mu_1)T}{(1-\mu_1)} - T \tag{5-72}$$

$$X = \frac{(1-\mu_3)}{(1-\mu_2)} + \frac{(1-\mu_3)(3-4\mu_2)K}{(1-\mu_2)} - K \tag{5-73}$$

$$Y = \frac{(1-\mu_3)}{(1-\mu_2)} + \frac{(1-\mu_3)(3-4\mu_2)K}{(1-\mu_2)} - 1 \quad (5\text{-}74)$$

$$T = \frac{1-q}{1+(3-4\mu_1)q} \quad (5\text{-}75)$$

$$K = \frac{1-k}{1+(3-4\mu_2)k} \quad (5\text{-}76)$$

$$Z = (2mh_2\text{-}2mH) \quad (5\text{-}77)$$

where m is a dummy variables; E_1, E_2, E_3, and E_4 are elastic moduli of layers 1, 2, 3, and 4; μ_1, μ_2, μ_3, and μ_4 are Poisson ratio of layers 1, 2, 3, and 4; J_0 is Bessel function of the first kind of zero order, and the rest is as described previously. The final terms of two constants C_1 and D_1 can be seen in Appendix A.

The infinite integral in Equation (5-65) was evaluated by means of numerical integration using composite Simpson rule (Matthews and Fink, 2004). A computer program called 4L-DEF was written to conduct the calculation of the deflections.

5.2.2 Comparison of Solutions with Other Methods

A forward-calculation program, CHEVRONX, developed by Michigan State University (Harichandran et al., 2001), was evaluated for purpose of comparison with 3L-DEF and 4L-DEF. Table 5.1 presents four cases to compare the deflections produced by 3L-DEF and CHEVRONX. The details of the four cases are as follows:

a. Case 1 (the original state): E_1 = 1,379.3 MPa (200 ksi), E_2 = 758.6 MPa (110 ksi), E_3 = 206.9 MPa (30 ksi), h_1 = 0.127 m (5 in.), h_2 = 0.254 m (10 in.), P = 71.1 kN (15,985 psi)

b. Case 2 (change the moduli of subbase and subgrade): E_2 = 206.9 MPa (30 ksi), and E_3 = 103.4 MPa (15 ksi), the rest of the data is same with case 1.

c. Case 3 (change the layer thicknesses): h_1 = 0.254 m (10 in.), h_2 = 0.635 m (25 in.), the rest of the data is same with case 1.

d. Case 4 (change the magnitude of the load): P = 44.5 kN (10 ksi), the rest of the data is same with case 1

Table 5.2 presents three cases used to compare the surface deflections produced by the 4L-DEF and CHEVRONX. The details of the three cases are as follows.

a. Case 1 (the original state): E_1 = 2,758 MPa (400 ksi), E_2 = 827.4 MPa (120 ksi), E_3 = 517.1 MPa (75 ksi), E_4 = 206.9 MPa (30 ksi), h_1 = 0.127 m (5 in.), h_2 = 0.254 m (10 in.), h_3 = 0.381 m (150 in.), and P = 71.1 kN (15985 lbs).

b. Case 2 (change the moduli of surface and subbase) : E_1 = 2,413.3 MPa (350 ksi), E_3 = 344.8 MPa (50 ksi), the rest of the data is same with case 1.

c. Case 3 (change the layer thicknesses): h_1 = 0.305 m (12 in.), h_2 = 0.432 m (17 in.), h_2 = 0.559 m (22 in.), the rest of the data is same with case 1.

Five sensors with distance r_1, r_2, r_3, r_4 and r_5 equal to 0.203, 0.305, 0.457, 0.61 and 0.914 m (or 8, 12, 18, 24 and 36 in.), respectively, from the load are adopted. The surface deflections listed in Table 5.1 and 5.2 are computed with assuming a non-slip interface between layers.

It is observed from Tables 5.1 and Table 5.2 that the deflections produced by 3L-DEF and 4L-DEF, respectively, developed based on a theoretical deflection by Burmister (1945), deviate slightly from that of the CHEVRONX program. The largest deviation between 3L-DEF and CHEVRONX programs is around 3.5% and the largest deviation between 4L-DEF and CHEVRONX programs is less than 2%, both at sensor 1 of case 3. It summarizes that 3L-DEF and 4L-DEF are sufficiently accurate to calculate the surface deflections of a three- and four-layer flexible pavement, respectively.

5.3 Comment on the Effect of Temperature on Asphalt Layer

It is known that asphalt layer has been recognized as an anisotropic material, but the degree of anisotropy and its implications for pavement design and analysis have not been well understood. In the development of forward solution based on Burmister's theory, the characteristics of the asphalt layer was simplified by assuming that the asphalt layer has uniform material characteristic in all directions (isotropic) and is not temperature-dependent. This assumption is not fully correct, but it is still partially applicable in the horizontal direction. The simplification on the derivation of forward solution in this study is necessary to be performed in order to ease in developing the closed-form backcalculation algorithm, as describe in Chapter 6.

5.4 Summary

A forward solution for a three-layer flexible pavement system, consisted of surface layer, granular subbase layer and subgrade, was developed by Burmister in 1943. In this study, a forward solution for a four-layer flexible pavement system was developed by extending the theoretical solutions by Burmister for three-layer pavement system. The development of these solutions could give a closer approximation to the actual multi-layer flexible pavement system constructed in practice. Computer programs 3L-DEF and 4L-DEF were developed using the respective forward solutions.

The verification of 3L-DEF and 4L-DEF programs were conducted by comparing the programs with a forward solution, namely CHEVRONX. The results of comparison show that they compare well with discrepancies within 4%. It is concluded that 3L-DEF and 4L-DEF could estimate accurately the surface deflections of three- and four-layer flexible pavements.

Table 5.1: Comparison of Computed Surface Deflections on Three-layer Flexible System

Methods	d_1 (mm)	d_2 (mm)	d_3 (mm)	d_4 (mm)	d_5 (mm)
Case 1: original state (E_1=1,379.3 MPa, E_2 =758.6 MPa, E_3 =206.9 MPa, h_1=0.127 m, h_2=0.254 m, P=71.1 kN)					
3L-DEF	0.2844	0.2330	0.1824	0.1475	0.1014
CHEVRONX	0.2896	0.2339	0.1826	0.1471	0.1011
Case 2: change the subbase and subgrade moduli (E_2 =206.9 MPa, E_3 =103.4 MPa), all other data are the same as case 1					
3L-DEF	0.6720	0.5319	0.3899	0.2994	0.1963
CHEVRONX	0.6680	0.5309	0.3912	0.2997	0.1963
Case 3: change the thicknesses (h_1=0.254 m, h_2=0.635 m), all other data are the same as case 1					
3L-DEF	0.1796	0.1520	0.1259	0.1092	0.0868
CHEVRONX	0.1862	0.1532	0.1260	0.1087	0.0861
Case 4: change the load (P =44.5 kN), all other data are the same as case 1					
3L-DEF	0.1779	0.1458	0.1141	0.0923	0.0634
CHEVRONX	0.1811	0.1463	0.1143	0.0919	0.0632
Note: d_1, d_2, d_3, d_4, d_5 and d_6 are deflections at radial distance 0.203, 0.305, 0.457, 0.61, and 0.914 respectively from the load					

Table 5.2: Comparison of Computed Surface Deflections on Four-layer Flexible System

Methods	d_1 (mm)	d_2 (mm)	d_3 (mm)	d_4 (mm)	d_5 (mm)
Case 1: original state (E_1=2,758 MPa, E_2=827.4 MPa, E_3=517.1 MPa, E_4=206.9 MPa, h_1=0.127 m, h_2=0.254 m, h_3=0.381 m, P=71.1 kN)					
4L-DEF	0.2243	0.1843	0.1472	0.1238	0.0936
CHEVRONX	0.2258	0.1852	0.1476	0.1237	0.0935
Case 2: change the surface and subbase layer moduli (E_1=2,413.3 MPa, and E_3=344.8 MPa), all other data are the same as case 1					
4L-DEF	0.2472	0.2037	0.1617	0.1338	0.0973
CHEVRONX	0.2489	0.2045	0.1621	0.1336	0.0970
Case 3: change the thicknesses (h_1=0.305 m, h_2=0.432 m, h_3=0.559 m), all other data are the same as case 1					
4L-DEF	0.1446	0.1284	0.1106	0.0974	0.0786
CHEVRONX	0.1473	0.1285	0.1105	0.0973	0.0782
Note: d_1, d_2, d_3, d_4 and d_5 are deflections at radial distance 0.203, 0.305, 0.457, 0.61 and 0.914 m respectively from the load					

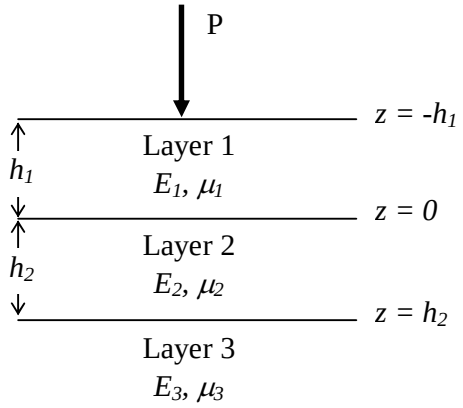

Figure 5.1: Schematic of Three-layer Flexible Pavement under Concentrated Load

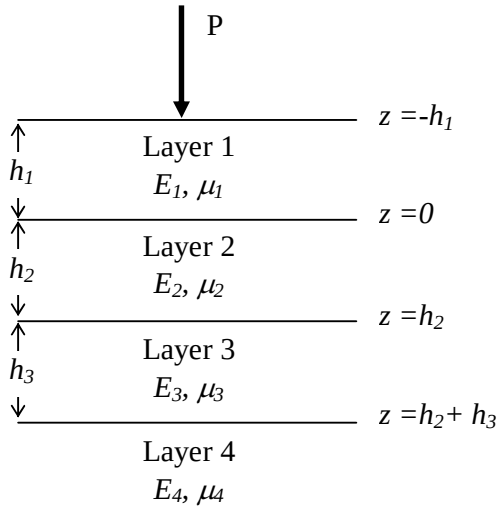

Figure 5.2: Schematic of Four-layer Flexible Pavement under Concentrated Load

CHAPTER 6

DEVELOPMENT OF CLOSED-FORM BACKCALCULATION ALGORITHM FOR MULTI-LAYER FLEXIBLE PAVEMENT SYSTEM

6.1 Introduction

Currently, no closed-form backcalculation algorithms are available for multi-layer flexible pavement systems with more than two pavement layers, including the subgrade. As highlighted in the previous chapter, all flexible pavements constructed today consist of three or more pavement layers, with four-layer pavement system being the most common.

In this chapter, two closed-form backcalculation algorithms are developed. The first close-form backcalculation algorithm, called 3L-BACK, is developed for a three layer flexible pavement system using the forward solution 3L-DEF. Another closed-form backcalculation algorithm, known as 4L-BACK, is developed for a four-layer flexible pavement system, using the forward solution 4L-DEF.

This chapter presents the theoretical basis, formulation and the development of the computer programs 3L-BACK and 4L-BACK.

6.2 Development of Backcalculation Procedure

6.2.1 Proposed Procedure

In the backcalculation analysis of layer moduli of a three- and a four-layer flexible pavement system, there are two known parameters (thickness layer and Poisson ratio) for each pavement layer. There are three unknowns (E_1, E_2 and E_3) for a three-layer system and four unknowns (E_1, E_2, E_3 and E_4) for a four-layer system. To

solve for the unknowns, the number of measured deflections required from different locations should be at least equal to the number of unknowns. For a three-layer system, at least three measured deflections from three different locations are required. The three measured deflection required to solve the three unknowns are given by

$$w_{31} = \frac{(1-\mu_1^2)P}{\pi E_1} F_{31}(q,k) \tag{6-1a}$$

$$w_{32} = \frac{(1-\mu_1^2)P}{\pi E_1} F_{32}(q,k) \tag{6-1b}$$

$$w_{33} = \frac{(1-\mu_1^2)P}{\pi E_1} F_{33}(q,k) \tag{6-1c}$$

where w_{31}, w_{32} and w_{33} are the measured deflections of a three-layer pavement system at distance r_1, r_2, and r_3 respectively from the load P; k and q are the moduli ratios as stated by Equations (5-15) and (5-20), and F_{31}, F_{32}, and F_{33} are deflection factors each is a function of k and q.

The same assumption is also valid for solving for the four unknown layer moduli of a four-layer system. Four measured deflections are required, as given by

$$w_{41} = \frac{(1-\mu_1^2)P}{\pi E_1} F_{41}(q,k,n) \tag{6-2a}$$

$$w_{42} = \frac{(1-\mu_1^2)P}{\pi E_1} F_{42}(q,k,n) \tag{6-2b}$$

$$w_{43} = \frac{(1-\mu_1^2)P}{\pi E_1} F_{43}(q,k,n) \tag{6-2c}$$

$$w_{44} = \frac{(1-\mu_1^2)P}{\pi E_1} F_{44}(q,k,n) \tag{6-2d}$$

where w_{41}, w_{42}, w_{43} and w_{44} are the measured deflections of a four-layer pavement system at distance r_1, r_2, r_3, and r_4 respectively from the load P; n, k, and q are the

moduli ratios as stated by Equations (5-50), (5-56) and (5-61), and F_{41}, F_{42}, F_{43}, and F_{44} are deflection factors each is a function of n, k and q.

All the equations above are composed of infinite integrals of product of Bessel functions. It is difficult to solve them directly. To overcome this problem, this study simplified the equations by dividing the two of them by the third one (for a three-layer system) or the three of them by the fourth one (for a four-layer system) to obtain two nonlinear equations with two unknowns k and q (for a three-layer system) or three non-linear equations with three unknowns n, k and q (for a four-layer system). For a three-layer system, the simplification of the equations can be performed by dividing Equations (6-1b) and (6-1c) by (6-1a) and this results in,

$$Y_{31} = w_{31}F_{32}(q,k) - w_{32}F_{31}(q,k) \quad (6\text{-}3a)$$

$$Y_{32} = w_{31}F_{33}(q,k) - w_{33}F_{31}(q,k) \quad (6\text{-}3b)$$

The similar simplification could also be performed for four-layer system, by dividing Equations (6-2b), (6-2c), and (6-2d) by (6-2a) and the following equations are obtained.

$$Y_{41} = w_{41}F_{42}(q,k,n) - w_{42}F_{41}(q,k,n) \quad (6\text{-}4a)$$

$$Y_{42} = w_{41}F_{43}(q,k,n) - w_{43}F_{41}(q,k,n) \quad (6\text{-}4b)$$

$$Y_{43} = w_{41}F_{44}(q,k,n) - w_{44}F_{41}(q,k,n) \quad (6\text{-}4c)$$

To obtain the roots (n, k, and q) from the nonlinear equations above, the Nelder-Mead optimization method was used. A brief introduction of this method is given in the subsequent section.

6.2.2 Nelder-Mead Optimization Method

The Nelder-Mead algorithm or simplex search algorithm, originally published in 1965 (Nelder and Mead, 1965), is one of the best known algorithms for

multidimensional unconstrained optimization without derivatives. The method is robust and only needs a relatively small number of function evaluations in obtaining a good reduction in the function value.

To enable minimizing a function with several variables, Nelder and Mead (1965) devised a simplex method for finding a local minimum of such function. A simplex S in R^n is defined as the convex hull of $(n+1)$ vertices. For example, a simplex in R^2 is a triangle, and a simplex in R^3 is a tetrahedron, as seen in Figure 6.1. For a case of two variables, the simplex S in R^2 is consisted of 3 vertices $x_0, \ldots, x_n \in R_x^2$ and $y_0, \ldots, y_n \in R_y^2$. If three variables are involved in the analysis, each vertex contains three coordinates, $x_0, \ldots, x_n \in R_x^3$; $y_0, \ldots, y_n \in R_y^3$ and $z_0, \ldots, z_n \in R_z^3$.

The Nelder-Mead method begins with a set of $(n+1)$ vertices that are considered as the vertices of a working simplex S, and the corresponding set of function values at the vertices f_j for $j = 0,\ldots, n$, where n is the number of variables considered. For the case of two variables, the function values at the vertices $x_0, \ldots, x_n \in R_x^2$ and $y_0, \ldots, y_n \in R_y^2$ are $f_j = f(x_j,y_j)$ *for* $j = 0,.., 2$; while for three variables, the function values at the vertices is $f_j = f(x_j,y_j,z_j)$ *for* $j = 0,.., 3$.

The method then performs a sequence of transformations of the working simplex S with the aim to decrease the function values f_j at its vertices. At each step, the transformation is determined by computing one or more test points together with their function values, and by comparison of these functions values with those at the vertices. This process is terminated when the working simplex S becomes sufficiently small, or when the function values f_j are close enough.

One iteration of the Nelder-Mead method consists of the following three steps.

1. Ordering. To start, it is necessary to evaluate the function values of the three vertices and the subscripts are then reordered to fulfill the following sequences: $f_1<f_2<f_3$. The f_1, f_2 and f_3 are function values of the vertices notated as *B* (for best vertex) = (x_1, y_1), *G* (for good vertex) = (x_2, y_2) and *W* (for worst vertex) = (x_3, y_3), respectively.

2. Calculate the midpoint *M* of the best side, that is, the midpoint of the line segment between B and G, given by following equation:

$$M = \frac{(B+G)}{2} = \left(\frac{x_1 + x_2}{2}, \frac{y_1 + y_2}{2} \right) \quad (6\text{-}5)$$

3. Transformation. Compute the new working simplex from the current one. There are three possible transformations used in the method, reflection, expansion or contraction (see Figure 6.2). First, try to replace only the worst vertex *W* with a better point by using one of the transformations with respect to the best side. All test points lie on the line defined by worst vertex *W* and midpoint *M*, and at most two of them are computed in one iteration. If this succeeds, the accepted point becomes the new vertex of the working simplex. If this transformation fails, shrink the simplex towards the best vertex *B*. The new point *R* (reflection) and *E* (expansion) is determined using the following equation.

$$R = M + (M - W) = 2M - W \quad (6\text{-}6)$$

$$E = R + (R - M) = 2R - M \quad (6\text{-}7)$$

While the contraction point *C* and shrink point are computed using the following equations (see Figure 6.2)

$$C_1 = 0.5\,(W + M) \quad \text{or} \quad C_2 = 0.5\,(M + R) \quad (6\text{-}8)$$

$$S = 0.5\,(B + W) \quad (6\text{-}9)$$

The logical decision of each step in the Nelder-Mead method could be summarized as follows.

(1) If $f_R < f_G$, then perform case (i), otherwise perform case (ii)

Case (i)

(2a) If $f_B < f_R$, then replace W with R, otherwise perform (3a).

(3a) Compute E and f_E.

If $f_E < f_B$, then replace W with E, otherwise replace W with R.

Case (ii)

(2b) If $f_R < f_W$, then replace W with R, otherwise perform (3b).

Compute C_1 and C_2; and perform $C = \min(C_1, C_2)$

If $f_C < f_W$, then replace W with C, otherwise compute S and f_S; and replace W with S and G with M.

(3b) Compute C_1 and C_2; and perform $C = \min(C_1, C_2)$

If $f_C < f_W$, then replace W with C, otherwise compute S and f_S; and replace W with S and G with M.

If there are three variables in the analysis, the first two step of Nelder-Mead iteration should be adjusted as follows (see Figure 6.2).

1. Ordering. The function values of the four vertices of tetrahedron are evaluated and the subscripts are then reordered to fulfill the following sequences: $f_1 < f_2 < f_3 < f_4$. The f_1, f_2, f_3 and f_4 are function values of the vertices notated as B (for best vertex) = (x_1, y_1, z_1), G (for good vertex) = (x_2, y_2, z_2), P *(for poor vertex)* = (x_3, y_3, z_3) and W (for worst vertex) = (x_4, y_4, z_4), respectively.

2. Calculate the midpoint *M* of the best side, that is, the midpoint of the three vertices B, G, and P given by following equation:

$$M = \frac{(B+G+P)}{3} = \left(\frac{x_1 + x_2 + x_3}{3}, \frac{y_1 + y_2 + y_3}{3}, \frac{z_1 + z_2 + z_3}{3} \right) \quad (6\text{-}5)$$

The last step of the procedure and also the logical decision of each step of Nelder-Mead method for three variables is the same as those for two variables.

6.2.3 Determination of Unique Solution

In this study, the Nelder-Mead method will minimize the absolute value of the functions Y_{31} and Y_{32}; and Y_{41}, Y_{42}, and Y_{43} stated in Equations (6-3) and (6-4), respectively, from a specified range of moduli ratios. It forms two curves of minimum value in a two-dimensional space and three curves of minimum value in a three-dimensional space, as shown in Figures 6.3 and 6.4, for three- and four-layer systems, respectively. For the three-layer system, a range of moduli ratios between 0 and 0.8 with increments of 0.05 for both moduli ratio *k* and *q* is selected as seed moduli ratio to be used in the Nelder-Mead optimization. A different range of moduli ratios, that is, between 0 and 0.6 with increments of 0.05 (for modulus ratio *q*) and between 0.2 and 0.6 with increments of 0.1 (for moduli ratio *n* and *k*) were selected for the four-layer system. The selection of a different range of moduli ratio and its increment in the four-layer backcalculation algorithm is caused by the different sensitivity among the three modulus ratios. The modulus ratio *q* is more sensitive than the other two ratios.

A moduli-ratio deviation value of 10^{-8} is selected as the minimum value at which the Nelder-Mead algorithm stops. The two curves Y_{31} and Y_{32} intersect in one point in the space at which the roots *k* and *q* are obtained. After the values of *k* and *q* are determined, the modulus of the surface layer is calculated by using Equation (6-1) and

the moduli of subbase and subgrade are obtained by using Equations (5-20) and (5-15), respectively.

With a similar procedure using the Nelder-Mead algorithm, for a four-layer system, the three curves of minimum deviation value of moduli-ratio, $Y_{41,}$ $Y_{42,}$ and Y_{43} may intersect in one point in the space at which the roots *q*, *k*, and *n* are obtained. However, it is difficult to obtain an intersection point of three curves in a three-dimensional space. Therefore, the algorithm will minimize the distances among three points which is located in the three curves $Y_{41,}$ $Y_{42,}$ and Y_{43}. The three points in the three curves having the minimum distance will be averaged and considered as roots of the three curves, that are, *q*, *k*, and *n*. After the values of *q*, *k*, and *n* are determined, the modulus of the surface layer is calculated from Equation (6-2) and the moduli of base, subbase and subgrade were determined from Equations (5-61), (5-56) and (5-50), respectively.

6.3 Comparison of the Backcalculated Moduli with Other Backcalculation Programs

For comparison with the closed-form backcalculation algorithms developed in this study, two other backcalculation programs were evaluated. They are EVERCALC (Sivaneswaran et al., 1991) and MICHBACK (Harichandran et al., 2001). Both programs use CHEVRONX as their forward calculation program. As previously mentioned in Chapter 2, EVERCALC and MICHBACK programs are backcalculation methods that use iterative methods to find the best result by matching the computed deflections with measured deflections. Both programs require seed moduli to initiate the backcalculation process. For MICHBACK, there are two options for selecting the seed moduli. The seed moduli may be determined by an internal program or by user-

input. The selection of the option of the seed moduli generation does not depend on the number of layers evaluated. Therefore, the seed moduli generated by the internal program were selected for MICHBACK program for both three- and four-layer backcalculation analyses. On the other hand, EVERCALC only permits user to generate the seed moduli using the internal program if the number of pavement layers in the backcalculation process equals or less than three layers. Therefore, for three-layer backcalculation analysis, the seed moduli generated by the internal program were selected, while for four-layer backcalculation analysis, a set of user-input seed moduli was employed.

As stated by several researchers (Mahoney et al., 1989; Uddin and McCullough, 1989), the determination of seed moduli could affect the results of the backcalculation. In this study, the seed moduli for EVERCALC program used by Watson and Rajapakse (2000) were adopted. The error obtained by using the seed moduli by Watson and Rajapakse (2000) were around 1 – 2%. The seed moduli recommended by Watson and Rajapakse (2000) are as follows: 10,000 MPa, 300 MPa, and 100 MPa for asphalt concrete, base and subgrade, respectively. In this study, a seed modulus of 200 MPa for subbase layer was added.

The backcalculation process in the two backcalculation programs, EVERCALC and MICHBACK, will run iteratively and it will stop if the predetermined error is satisfied or if the specified number of iteration is exceeded. In this study, an error of 0.1% and a number of maximum iteration of 1,000 were set as the termination criteria.

MICHBACK backcalculation program requires a minimum of five deflections for backcalculation process; while the number of deflections required by EVERCALC is depended on the number of layer properties to be determined. As mentioned previously, 3L-BACK and 4L-BACK need three and four deflections, respectively.

For the sake of comparison, five deflections were used in verification. To do so, EVERCALC and MICHBACK performed directly the backcalculation process using five deflections; while 3L-BACK and 4L-BACK require a multiple backcalculation runs of three- and four-combinations from 5 deflections, respectively. This results in 10 and 5 backcalculation runs, for 3L-BACK and 4L-BACK respectively, each case with 5 deflections. The comparison of the backcalculated moduli was performed between the backcalculation moduli produced by EVERCALC and MICHBACK and the average value of the backcalculation moduli from the 10 and 5 backcalculation runs of 3L-BACK and 4L-BACK programs respectively.

Two comparisons of backcalculation results were conducted in this study: (a) comparison using exact deflections from the respective forward-calculation algorithms of the backcalculation programs; and (b) comparison using deflections with measurement errors.

6.3.1 Comparison Using Exact Deflections

The comparison of the methods evaluated was conducted by using the exact deflections produced by the respective forward-calculation algorithms of the backcalculation programs.

Table 6.1 presented the backcalculated moduli of three-layer flexible pavement systems using the exact forward computed deflections. The comparison among three backcalculation programs in Table 6.1 indicates that the backcalculated modulus values deviate from the actual values by not more than 5% for all cases. It can be concluded that all three backcalculation programs perform equally well when the input deflections are exact as computed from their respective forward calculation algorithms.

The backcalculated moduli of four-layer flexible pavement system using the exact deflections are presented in Table 6.2. The results showed that the three backcalculation programs evaluated compared well in Case 1 where the backcalculated modulus values deviated by not more than 2%. In Case 2, EVERCALC produced larger deviations than the other two programs. In Case 3, 4L-BACK program could produce closer results to the true moduli than EVERCALC and MICHBACK. Overall, it may be concluded that 4L-BACK outperforms EVERCALC and MICHBACK in backcalculation analysis of four-layer flexible pavements when the input deflections are exact.

6.3.2 Comparison Using Deflections with Random Measurement Errors

In this section, surface deflections with measurement errors are considered to examine how the performances of the three backcalculation programs are affected by the presence of imperfect deflection measurements. For this purpose, thirty random deflections were generated using Pronk formula (1988) as follows.

$$d_m = d_t + 0.02 d_t \frac{(r_1 - 0.5) r_2}{|r_1 - 0.5|} + 2 \frac{(r_3 - 0.5) r_4}{|r_3 - 0.5|} \qquad (6\text{-}10)$$

in which d_m is the measured deflections (micrometers), d_t is the true deflections (micrometers); and $r_1 - r_4$ are random numbers between 0 and 1. The errors generated by Equation (6-10) were limited to within the range of around ± 2% to simulate the common deflection measurement errors produced by FWD (Irwin et al., 1989). The thirty sets of generated measured deflections for each backcalculation method are listed in Tables 6.3 and 6.4 for three- and four-layer flexible pavement systems, respectively.

Tables 6.5 and 6.6 present the results of the 30 sets of backcalculated layer moduli by the three backcalculation methods for the three- and four-layer flexible pavement systems, respectively. The statistics presented in the table measure the level of dispersion from the true elastic moduli. They consist of the maximum value, minimum value, mean value, standard deviation, coefficient of variation and root mean square error (*RMSE*). The root mean square error is defined as follows.

$$RMSE = \sqrt{\frac{1}{N}\sum_{i=1}^{N}\left[X_i - x_i\right]^2} \qquad (6\text{-}11)$$

where X_i is the computed moduli, x_i is the true moduli, and N is the number of cases. Figure 6.5 plots the deviations of backcalculated moduli from their corresponding true moduli for the case of three-layer flexible pavement system. The corresponding plot for the case of four-layer flexible pavement system is shown in Figure 6.6. The following observations can be made:

a. 3L-BACK outperformed EVERCALC and MICHBACK in all the measures of dispersion shown in Table 6.5, including the range of backcalculated moduli, standard deviation, coefficient of variations, and *RMSE*. The 3L-BACK backcalculated solutions have a narrower range, lower standard deviation, lower coefficient of variation, and smaller *RMSE*. The differences are most obvious for elastic modulus E_1 of the surface layer.

b. 4L-BACK also outperformed EVERCALC and MICHBACK. It was the method with the least dispersion in terms of the range of backcalculated moduli values, standard deviation, coefficient of variation (*CV*) and *RMSE*, as seen in Table 6.6. There were relatively little differences between the backcalculated results by MICHBACK and EVERCALC as indicated by the statistical dispersion measures. 4L-BACK was also more accurate in estimating the true values of

pavement layer moduli than the other two methods as shown by the values of *RMSE*. The *RMSE* of the backcalculated moduli by 4L-BACK is less than half of the corresponding errors produced by EVERCALC and MICHBACK respectively.

c. Figures 6.5 and 6.6 present clearly the dispersion of the elastic moduli computed by the three backcalculation programs for each set of deflections consisting measurement errors. These figures also presented qualitatively the accuracy of each backcalculation method in estimating the corresponding true value of the moduli (as represented by the horizontal line in each chart). Figures 6.5 and 6.6 show that the layer moduli calculated by EVERCALC and MICHBACK vary over larger ranges than those by 3L-BACK and 4L-BACK.

d. It is interesting that the modulus of the subgrade was not affected much by the measurement errors in the deflections. This is because the determination of subgrade modulus only depends on deflection produced by sensors further from the load, while the determination of the modulus of the overlying pavement layers depends on the inner deflections and also modulus of underlying pavement layers. In other words, the variation in determining the subgrade modulus is only affected by the errors in the outer measured deflections, while the variation in determining the overlying pavement layers is affected by the accumulation of errors involved in the several deflections used in backcalculation process.

6.4 Summary

Two closed-form backcalculation algorithms for three- and four-layer flexible pavement were developed based on Burmister's theoretical model for multi-layer

flexible pavement systems. The two backcalculation programs, 3L-BACK and 4L-BACK, were solved using the Nelder-Mead optimization method. This method was used to minimize the absolute value of the functions Y_{31} and Y_{32} for the three-layer flexible pavement system; and Y_{41}, $Y_{42,}$ and Y_{43} for the four-layer flexible pavement system. A specified range of moduli ratios was considered in defining two curves of minimum value in a two-dimensional space for the case of three-layer flexible pavement system, and three curves of minimum value in a three-dimensional space for the case of four-layer flexible pavement system. The two curves Y_{31} and Y_{32} intersect in one point in the space at which the moduli ratios k and q are obtained. In a similar manner, the three curves $Y_{41,}$ $Y_{42,}$ and Y_{43} intersect in one point in the space at which the moduli ratios q, k, and n are obtained. Since it is more difficult to obtain the intersection point of three curves in a three-dimensional space, the algorithm minimizes the distances among three points which is located in the three curves $Y_{41,}$ $Y_{42,}$ and Y_{43}. Three points in the three curves having the minimum distance will be averaged and considered as the roots of the three curves, that is, q, k, and n.

The proposed algorithms were verified using two types of deflections, that is, exact deflection and deflections with measurement errors. A comparison between the proposed algorithms and two other backcalculation algorithms was performed. Two backcalculated programs based on the iterative optimization approach, EVERCALC and MICHBACK, were selected for this purpose.

The results of verification using exact deflections showed that both closed-form programs could produce slightly more accurate backcalculated moduli than those the other two programs. Similar results were also obtained when the deflections with random measurement errors were used in the backcalculation analysis, where the two closed-form programs could estimate the true values of the layer moduli better than the

other two programs. This indicates that the two closed-form backcalculation programs are more reliable in backcalculating layer moduli than EVERCALC and MICHBACK.

Table 6.1: Comparison of Backcalculated Layer Moduli for Three-layer Flexible Pavement System by Different Methods

Methods	Backcalculated moduli (MPa)			Deviation with the true moduli (%)		
	E_1	E_2	E_3	E_1	E_2	E_3
Case 1: original state (E_1=1,379.3 MPa, E_2 =758.6 MPa, E_3 =206.9 MPa, h_1=0.127 m, h_2=0.254 m, P=71.1 kN)						
3L-BACK	1,381.6	758.5	206.8	0.19	0.01	0.00
EVERCALC	1,395.4	760.9	206.8	1.19	0.33	-0.03
MICHBACK	1,344.8	758.9	206.9	-2.48	0.06	0.01
Case 2: change the subbase and subgrade moduli (E_2 =206.9 MPa, E_3 =103.4 MPa), all other data are the same as case 1						
3L-BACK	1,373.0	208.3	103.3	-0.44	0.69	-0.09
EVERCALC	1,379.1	206.9	103.4	0.01	0.00	0.00
MICHBACK	1,325.7	208.6	103.5	-3.87	0.84	0.03
Case 3: change the thicknesses (h_1=0.254 m, h_2=0.635 m), all other data are the same as case 1						
3L-BACK	1,379.8	758.4	206.9	0.06	0.00	0.00
EVERCALC	1,382.0	758.2	206.9	0.22	-0.03	0.00
MICHBACK	1,375.1	756.8	207.2	-0.28	-0.22	0.15
Case 4: change the load (P =44.5 kN), all other data are the same as case 1						
3L-BACK	1,380.6	758.5	206.8	0.11	0.00	0.00
EVERCALC	1,445.7	755.6	206.9	4.84	-0.38	0.03
MICHBACK	1,320.9	758.9	206.9	-4.21	0.06	0.02

Table 6.2: Comparison of Backcalculated Layer Moduli for Four-layer Flexible Pavement System by Different Methods

Methods	Backcalculated moduli (MPa)				Deviation with the true moduli (%)			
	E_1	E_2	E_3	E_4	E_1	E_2	E_3	E_4
Case 1: original state (E_1=2,758 MPa, E_2=827.4 MPa, E_3=517.1 MPa, E_4=206.9 MPa, h_1=0.127 m, h_2=0.254 m, h_3=0.381 m, P=71.1 kN)								
4L-BACK	2,761.6	828.3	516.5	206.9	0.13	0.11	-0.12	0.05
EVERCALC	2,790.8	819.4	523.8	206.4	1.19	-0.97	1.29	-0.23
MICHBACK	2,799.7	819.4	523.9	206.3	1.51	-0.96	1.32	-0.26
Case 2: change the surface and subbase layer moduli (E_1=2,413.3 MPa, and E_3=344.8 MPa), all other data are the same as case 1								
4L-BACK	2,473.1	826.7	345.3	206.7	2.48	-0.09	0.16	-0.06
EVERCALC	2,533.9	841.7	335.6	207.7	5.00	1.73	-2.64	0.40
MICHBACK	2,464.0	827.7	342.2	207.2	2.10	0.04	-0.75	0.19
Case 3: change the thicknesses (h_1=0.305 m, h_2=0.432 m, h_3=0.559 m), all other data are the same as case 1								
4L-BACK	2,731.8	844.4	491.1	209.7	-0.95	2.06	-5.04	1.40
EVERCALC	2,893.7	759.4	607.0	200.7	4.92	-8.22	17.39	-2.97
MICHBACK	2,720.4	880.4	440.0	214.0	-1.36	6.40	-14.91	3.44

Notes: Seed moduli used in the backcalculation programs: 4L-BACK (not required), EVERCALC (E_1 = 10,000 MPa, E_2 = 300 MPa, E_3 = 200 MPa, E_4 = 100 MPa) (Watson and Rajapakse, 2000), and MICHBACK (provided by internal program)

Table 6.3: Deflections with Random Measurement Errors for Three-layer Flexible Pavement System

Set	Random deflections for each backcalculation program (mm)									
	3L-BACK					EVERCALC and MICHBACK				
	d1	d2	d3	d4	d5	d1	d2	d3	d4	d5
1	0.2882	0.2342	0.1853	0.1440	0.1038	0.2935	0.2351	0.1855	0.1436	0.1035
2	0.2847	0.2361	0.1816	0.1490	0.1007	0.2899	0.2370	0.1818	0.1486	0.1004
3	0.2833	0.2353	0.1820	0.1513	0.1036	0.2884	0.2362	0.1823	0.1508	0.1033
4	0.2818	0.2320	0.1829	0.1461	0.1029	0.2870	0.2329	0.1831	0.1457	0.1026
5	0.2802	0.2321	0.1808	0.1446	0.0988	0.2852	0.2330	0.1810	0.1442	0.0985
6	0.2820	0.2308	0.1802	0.1478	0.1052	0.2871	0.2317	0.1804	0.1474	0.1049
7	0.2865	0.2356	0.1822	0.1429	0.0980	0.2917	0.2365	0.1824	0.1425	0.0978
8	0.2818	0.2355	0.1824	0.1461	0.1027	0.2869	0.2365	0.1826	0.1457	0.1024
9	0.2846	0.2344	0.1836	0.1487	0.0986	0.2898	0.2354	0.1839	0.1482	0.0983
10	0.2809	0.2328	0.1836	0.1463	0.0986	0.2860	0.2337	0.1838	0.1458	0.0983
11	0.2857	0.2317	0.1810	0.1485	0.1019	0.2909	0.2326	0.1812	0.1481	0.1016
12	0.2876	0.2352	0.1840	0.1447	0.0998	0.2928	0.2361	0.1842	0.1443	0.0995
13	0.2837	0.2362	0.1828	0.1476	0.1009	0.2889	0.2372	0.1831	0.1472	0.1006
14	0.2805	0.2336	0.1820	0.1480	0.1009	0.2856	0.2345	0.1822	0.1475	0.1006
15	0.2856	0.2359	0.1824	0.1485	0.1005	0.2908	0.2368	0.1826	0.1480	0.1002
16	0.2844	0.2354	0.1834	0.1447	0.0989	0.2896	0.2363	0.1836	0.1443	0.0986
17	0.2860	0.2317	0.1851	0.1481	0.1012	0.2912	0.2326	0.1853	0.1476	0.1009
18	0.2806	0.2313	0.1841	0.1458	0.0985	0.2857	0.2322	0.1843	0.1453	0.0982
19	0.2858	0.2348	0.1839	0.1459	0.1014	0.2910	0.2358	0.1841	0.1454	0.1011
20	0.2829	0.2339	0.1798	0.1497	0.1042	0.2881	0.2348	0.1800	0.1493	0.1039
21	0.2823	0.2319	0.1828	0.1491	0.1024	0.2875	0.2328	0.1830	0.1486	0.1021
22	0.2852	0.2315	0.1828	0.1481	0.1012	0.2904	0.2324	0.1830	0.1476	0.1009
23	0.2804	0.2325	0.1818	0.1480	0.1028	0.2855	0.2334	0.1820	0.1476	0.1025
24	0.2828	0.2328	0.1814	0.1490	0.1024	0.2880	0.2337	0.1816	0.1486	0.1021
25	0.2883	0.2362	0.1848	0.1494	0.1025	0.2936	0.2371	0.1850	0.1489	0.1022
26	0.2872	0.2355	0.1846	0.1495	0.1030	0.2924	0.2364	0.1848	0.1490	0.1027
27	0.2842	0.2347	0.1829	0.1475	0.1022	0.2894	0.2356	0.1831	0.1470	0.1019
28	0.2858	0.2307	0.1829	0.1467	0.1001	0.2911	0.2316	0.1831	0.1462	0.0998
29	0.2843	0.2326	0.1841	0.1511	0.1021	0.2895	0.2336	0.1843	0.1506	0.1018
30	0.2818	0.2314	0.1805	0.1496	0.1036	0.2870	0.2323	0.1807	0.1492	0.1033

Note: The true deflections for d_1, d_2, d_3, d_4, and d_5 are 0.2844, 0.2330, 0.1824, 0.1475, and 0.1014 mm for 3L-BACK; 0.2896, 0.2339, 0.1826, 0.1471, and 0.1011 mm for EVERCALC and MICHBACK

Table 6.4: Deflections with Random Measurement Errors for Four-layer Flexible Pavement System

Set	Random deflections for each backcalculation program (mm)									
	4L-BACK					EVERCALC and MICHBACK				
	d1	d2	d3	d4	d5	d1	d2	d3	d4	d5
1	0.2271	0.1851	0.1497	0.1206	0.0959	0.2287	0.1861	0.1501	0.1206	0.0957
2	0.2247	0.1869	0.1466	0.1251	0.0930	0.2262	0.1878	0.1470	0.1251	0.0928
3	0.2234	0.1861	0.1468	0.1272	0.0958	0.2250	0.1870	0.1472	0.1272	0.0956
4	0.2220	0.1837	0.1477	0.1227	0.0951	0.2235	0.1846	0.1481	0.1226	0.0949
5	0.2212	0.1838	0.1459	0.1214	0.0911	0.2227	0.1847	0.1464	0.1213	0.0909
6	0.2223	0.1823	0.1455	0.1241	0.0972	0.2238	0.1832	0.1460	0.1241	0.0970
7	0.2263	0.1865	0.1470	0.1197	0.0904	0.2278	0.1874	0.1475	0.1196	0.0902
8	0.2224	0.1864	0.1474	0.1228	0.0948	0.2239	0.1874	0.1479	0.1227	0.0947
9	0.2242	0.1854	0.1479	0.1249	0.0910	0.2257	0.1863	0.1484	0.1248	0.0908
10	0.2217	0.1839	0.1480	0.1228	0.0909	0.2232	0.1848	0.1485	0.1228	0.0907
11	0.2255	0.1829	0.1462	0.1250	0.0941	0.2270	0.1838	0.1466	0.1249	0.0940
12	0.2268	0.1857	0.1483	0.1213	0.0921	0.2284	0.1867	0.1488	0.1213	0.0919
13	0.2236	0.1870	0.1477	0.1239	0.0930	0.2251	0.1879	0.1482	0.1238	0.0928
14	0.2208	0.1848	0.1465	0.1240	0.0932	0.2223	0.1858	0.1469	0.1239	0.0930
15	0.2256	0.1864	0.1472	0.1245	0.0929	0.2271	0.1873	0.1477	0.1244	0.0927
16	0.2240	0.1860	0.1483	0.1215	0.0912	0.2256	0.1869	0.1487	0.1214	0.0911
17	0.2259	0.1833	0.1496	0.1241	0.0933	0.2274	0.1843	0.1501	0.1241	0.0931
18	0.2212	0.1826	0.1484	0.1224	0.0908	0.2227	0.1835	0.1488	0.1224	0.0906
19	0.2257	0.1859	0.1486	0.1222	0.0935	0.2272	0.1868	0.1490	0.1221	0.0933
20	0.2230	0.1852	0.1452	0.1259	0.0964	0.2245	0.1861	0.1456	0.1258	0.0962
21	0.2223	0.1837	0.1474	0.1253	0.0945	0.2238	0.1847	0.1478	0.1252	0.0943
22	0.2249	0.1830	0.1473	0.1241	0.0933	0.2265	0.1840	0.1477	0.1240	0.0931
23	0.2211	0.1840	0.1464	0.1244	0.0951	0.2226	0.1849	0.1469	0.1244	0.0949
24	0.2232	0.1840	0.1465	0.1251	0.0945	0.2248	0.1849	0.1469	0.1250	0.0944
25	0.2215	0.1867	0.1470	0.1258	0.0968	0.2230	0.1876	0.1474	0.1257	0.0967
26	0.2252	0.1865	0.1464	0.1201	0.0933	0.2267	0.1874	0.1469	0.1200	0.0931
27	0.2242	0.1857	0.1478	0.1237	0.0945	0.2257	0.1866	0.1482	0.1236	0.0943
28	0.2253	0.1826	0.1477	0.1232	0.0923	0.2268	0.1835	0.1482	0.1231	0.0922
29	0.2240	0.1838	0.1483	0.1271	0.0942	0.2255	0.1847	0.1488	0.1270	0.0940
30	0.2224	0.1824	0.1454	0.1257	0.0957	0.2240	0.1833	0.1458	0.1257	0.0956

Note: The true deflections for d_1, d_2, d_3, d_4, and d_5 are 0.2243, 0.1843, 0.1472, 0.1238, and 0.0936 mm for 4L-BACK; 0.2258, 0.1852, 0.1476, 0.1237, and 0.0935 mm for EVERCALC and MICHBACK

Table 6.5: Summary of Statistics of Backcalculated Layer Moduli from Different Methods for Three-layer Flexible Pavement System

Properties	3L-BACK			EVERCALC			MICHBACK		
	E_1	E_2	E_3	E_1	E_2	E_3	E_1	E_2	E_3
Maximum value (MPa)	3,680.1	827.6	212.0	3,953.4	829.1	213.3	3,987.8	820.8	213.3
Minimum value (MPa)	1,548.8	629.5	201.8	472.4	630.3	203.1	472.3	628.9	201.8
Mean (MPa)	2,344.4	747.0	208.7	1,887.8	732.6	207.2	2,026.0	731.6	207.0
Standard Deviation (MPa)	555.57	50.68	2.59	962.90	59.90	2.84	1,042.74	58.56	3.00
Coefficient of Variation (%)	23.70	6.79	1.24	51.01	8.18	1.37	51.47	8.00	1.45
RMSE (MPa)	1,109.3	51.1	3.1	1,056.4	58.2	2.9	1,211.8	63.5	3.0

Notes: The true moduli values, E_1 = 1,379.3 MPa, E_2 = 758.6 MPa, and E_3 = 206.9 MPa

Table 6.6: Summary of Statistics of Backcalculated Layer Moduli from Different Methods for Four-layer Flexible Pavement System

Properties	4L-BACK				EVERCALC				MICHBACK			
	E_1	E_2	E_3	E_4	E_1	E_2	E_3	E_4	E_1	E_2	E_3	E_4
Maximum value (MPa)	4,760.7	973.1	582.9	225.1	7,683.4	1,014.9	1,181.2	223.6	7,734.2	995.0	1,212.8	221.3
Minimum value (MPa)	1,493.0	768.1	398.2	196.6	803.3	274.4	374.8	188.9	1,285.1	267.2	379.0	188.4
Mean (MPa)	2,795.2	844.1	482.5	212.7	3,497.7	766.9	578.1	205.3	3,701.4	748.3	590.6	204.5
Standard Deviation (MPa)	869.1	47.9	47.6	6.3	1,811.8	187.5	172.0	9.8	1,781.8	182.6	172.0	9.0
Coefficient of Variation (%)	31.09	5.68	9.87	2.97	51.80	24.45	29.75	4.78	48.14	24.41	29.12	4.41
RMSE (MPa)	855.3	50.0	58.3	8.5	1,927.8	193.9	179.7	9.8	1,988.8	196.1	184.3	9.2

Notes: The true moduli values, E_1 = 2,758 MPa, E_2 = 827.4 MPa, E_3 = 517.1 MPa, and E_4 = 206.9 MPa.

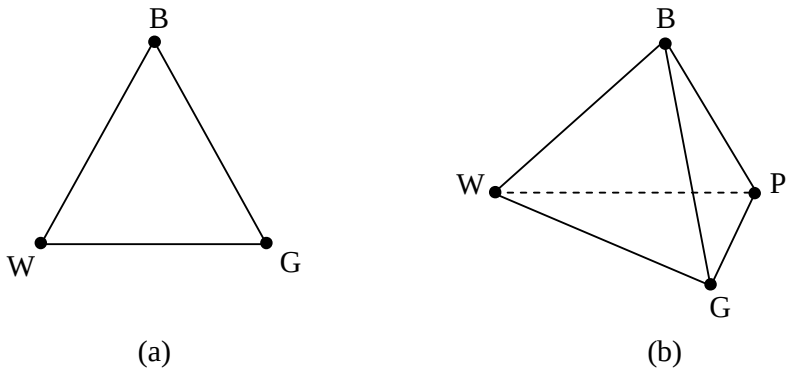

Figure 6.1: Geometries of Nelder-Mead Method: (a) 2-simplex (R^2), and (b) 3-simplex (R^3)

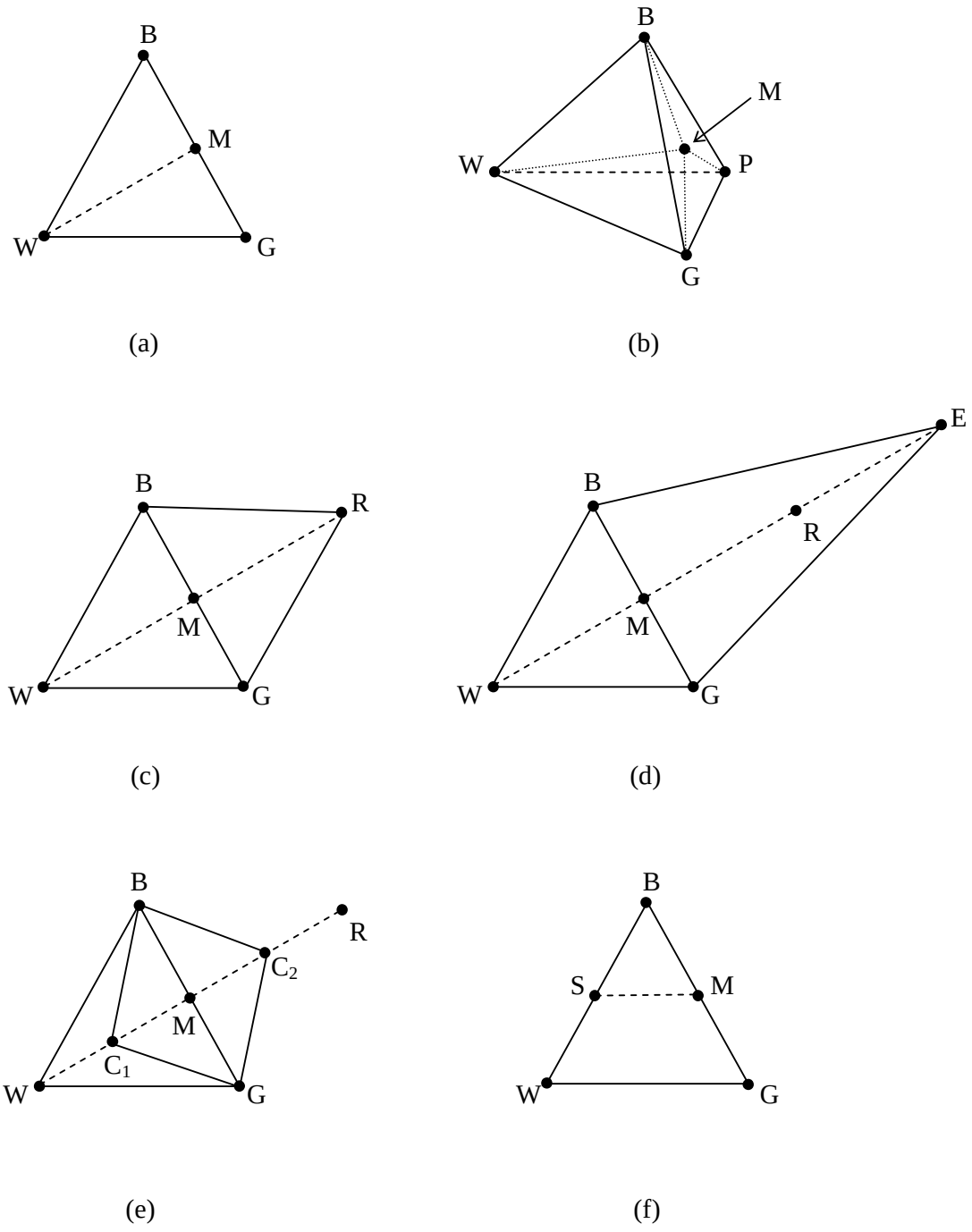

Figure 6.2: Procedures of Nelder-Mead Algorithm:
(a) and (b) determination of midpoint for R^2 and R^3, (c) reflection,
(d) expansion, (e) contraction, and (f) shrink

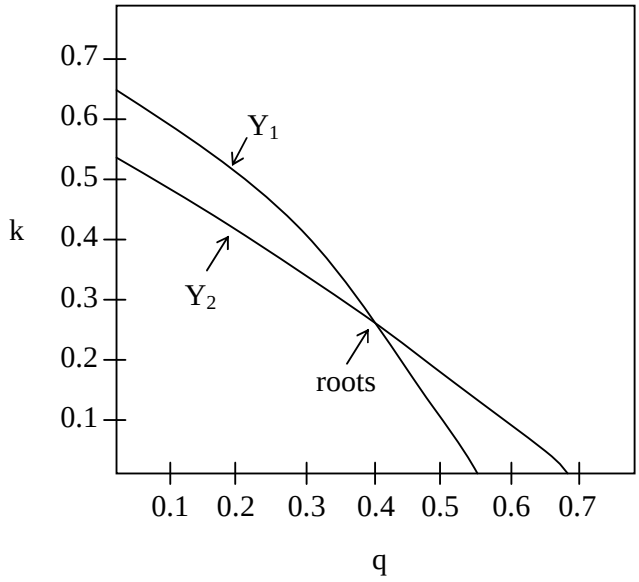

Figure 6.3 Illustration of Root Searching of Two Curves in Two Dimensional Spaces in the Proposed Procedure

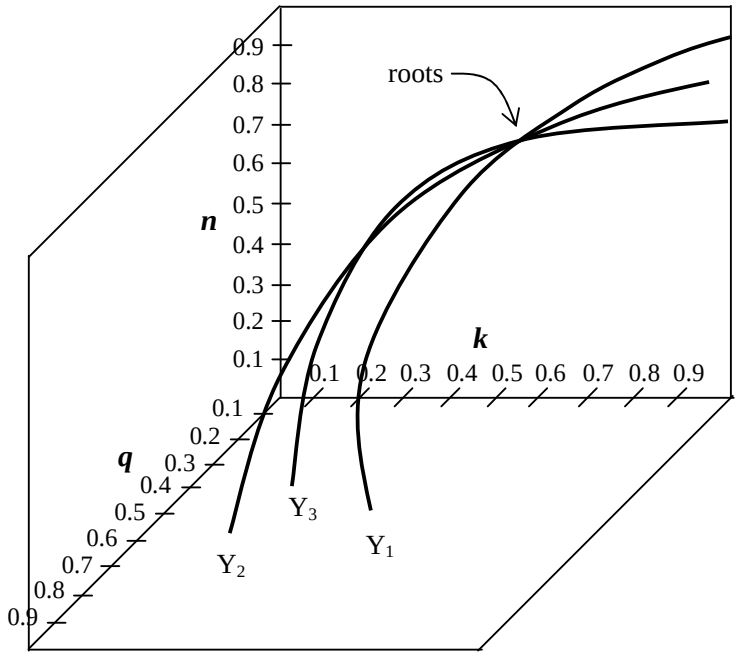

Figure 6.4: Illustration of Root Searching of Three Curves in Three Dimensional Spaces in the Proposed Procedure

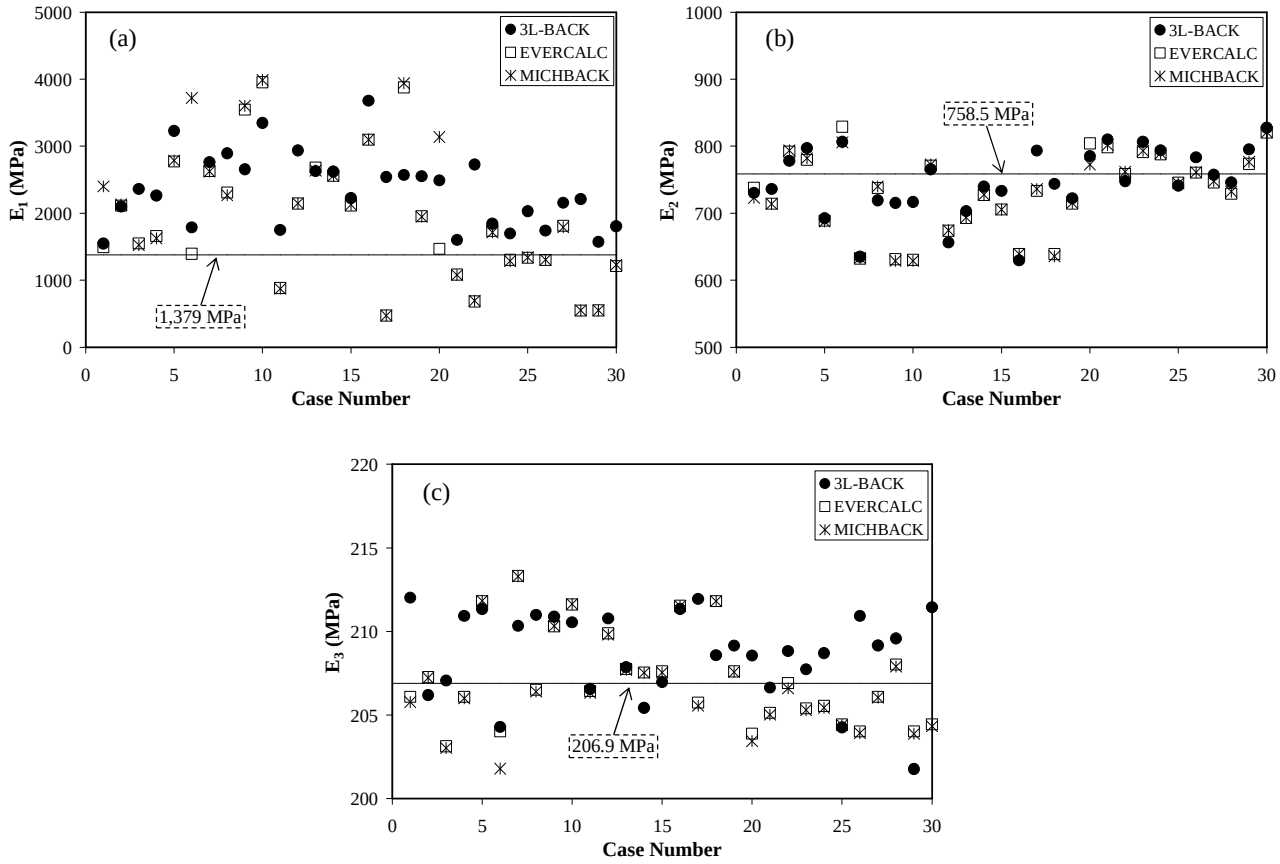

Figure 6.5: Comparisons between true and computed moduli of three-layer pavement system from different methods (The true value of the moduli: (a) E_1 = 1,379 MPa, (b) E_2 = 758.5 MPa, and (c) E_3 = 206.9 MPa)

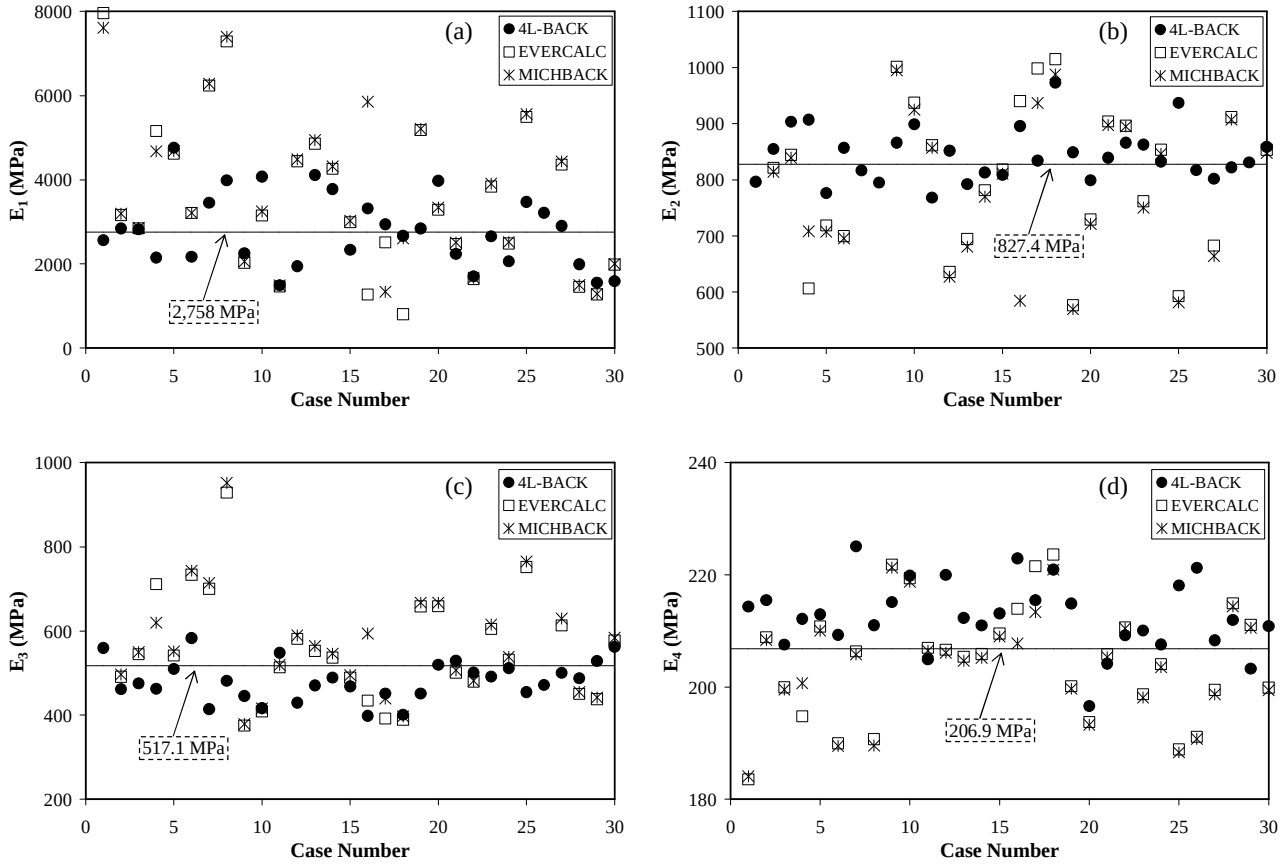

Figure 6.6: Comparisons between true and computed moduli of four-layer pavement system from different methods (The true value of the moduli: (a) E_1 = 2,758 MPa, (b) E_2 = 827.4 MPa, (c) E_3 = 517.1 MPa, and (d) E_4 = 206.9 MPa)

CHAPTER 7

CONCLUSIONS AND RECOMMENDATIONS

7.1 Introduction

In this chapter, several conclusions are highlighted to address the objectives of the study, i.e., to evaluate the existing backcalculation algorithms in determining k value and to develop a backcalculation-based procedure to determine the composite k value for a rigid pavement with a subbase layer (summarized in Section 7.2 and 7.3); and to develop closed-form backcalculation algorithms for a three- and four-layer flexible pavement system (summarized in Section 7.4). At the end of this chapter, several recommendations are also presented.

7.2 Backcalculation of Layer Moduli of Rigid Pavement

7.2.1 The Use of Infinite-Slab Backcalculation Algorithm to Evaluate Layer Moduli

In this study, several existing backcalculation programs were evaluated to examine their suitability to be used in practice. They are ILLI-BACK4, ILLI-BACK7, NUSBACK (closed-form backcalculation algorithm), and LTPP Best Fit (iterative-based backcalculation algorithm). For this purpose, actual data extracted from LTPP database were employed. Several aspects can be highlighted as follows.

a. Although all of the programs were developed based on plate theory and modeled using similar assumptions, the comparison between computed layer moduli produced by the programs and measured layer moduli yielded different results. This may be attributed by three factors: (i) deflection matching criterion used by

the program, (ii) the number of sensor used in the corresponding forward calculation, and (iii) the selection of sensor location.

b. Since the measured deflections lie in between the range of deflections of rigid slab resting on liquid foundation and on solid foundation, and the deflection basin itself could contain measurement errors, the application of a strict matching deflection criterion between the computed and measured deflection and the use of many sensors could give a worse solution.

c. Among the four programs, NUS-BACK is the backcalculation program that has the least conformance control of deflection matching criterion by offering the flexibility to choose the best pair of sensor deflections. As a result, NUS-BACK could produce the least errors among the other backcalculation programs. Therefore, it is recommended to use NUS-BACK as the infinite-slab model for backcalculation.

7.2.2 The Use of Finite-Slab Backcalculation Algorithm to Evaluate Layer Moduli

Two finite-slab models, i.e. one-slab and nine-slab model, together with two adjusted infinite-slab model using Crovetti's correction factor (Crovetti, 2002) and Korenev's correction factor (Korenev, 1954), respectively, were compared with the results of the infinite-slab model, NUS-BACK, to evaluate the use of finite-slab backcalculation algorithm in practice. The following aspects may be highlighted.

a. The use of nine-slab model was expected to be able to simulate better the real rigid pavement system. However, since the detailed data of joint properties and joint reinforcements are not readily available, the use of the nine-slab model could face difficulty in practice.

b. The results of the evaluation proved that since there was no significant differences in the backcalculated layer properties between the infinite-slab and the nine-slab backcalculated programs, it was recommended that the infinite-slab model is adequate in providing sufficiently accurate backcalculated k and E_c for practical applications.

c. Another finding from the study is that the use of Crovetti's and Korenev's correction factors could produce larger errors than the other models considered (infinite-slab, one-slab and nine-slab) and are prone to over-estimate k and E_c. Therefore, those correction factors were not recommended to be employed in practice.

d. In summary, the NUS-BACK program was used for this research based on the findings in this evaluation that the infinite-slab model is adequate to provide accurate backcalculated layer moduli and the NUS-BACK program is the preferable infinite-slab backcalculation program.

7.3 Development of k-E_s Relationship on Rigid Pavement System

7.3.1 k-E_s Relationship on Two-layer Rigid Pavement System

This section summarizes the results of the development of k-E_s relationship for two-layer rigid pavement system based on backcalculation approach by establishing equivalency between a model of pavement slab supported by a dense liquid foundation (k-model) and one supported by an elastic solid foundation (E_s-model). The following observations may be made.

a. Two equivalent models were considered. The first model is a regression equation between k and E_s, which allows k to be estimated from E_s directly. It ignores the effects of pavement slab on load transmission in a rigid pavement system.

Although simple and easy to apply, this regression equation is a simplified representation of the actual pavement response and could only provide a "mean" estimate of k for a given E_s value.

b. The second model is a relationship between the radii of relative stiffness of the two equivalent theoretical rigid pavement systems, i.e. ℓ_k and ℓ_E. This procedure computes k from a known E_s value by establishing equivalency between the k-model and E_s-model based on the ℓ_k-ℓ_E relationship. Analyses presented in the study have demonstrated that, compared with the method of direct k-E_s relationship, this procedure provides an improved estimation of k from E_s.

7.3.2 k-E_s Relationship on Three-layer Rigid Pavement System with Consideration of Subbase Layer

A further development of k-E_s relationship for three-layer rigid pavement system based on equivalency concepts was conducted using backcalculation approach to take into account the role of subbase layer (E_{sb}) and subgrade (E_s) in estimating composite k. A comparison between the proposed relationship and three existing design methods (PCA, FAA and AASHTO methods) was also presented. The following aspects may be highlighted.

a. Two models of ℓ_k - $\ell_{E_{s/sb}}$ relationship were proposed, i.e. a direct relationship between ℓ_k and $\ell_{E_{s/sb}}$ (model A) and a relationship among ℓ_k, $\ell_{E_{s/sb}}$ and pavement properties (layer moduli and thicknesses) (model B).

b. A comparison between both models indicated that model B is preferable to model A in terms of *RMSE*, and by the results of over- and under-estimation

analysis. In addition, model B showed a more comprehensive representation of all the parameters used in the analysis.

c. Another comparison between the proposed relationship and the existing k-E_s relationships in the design methods revealed that the k-E_s relationships used by FAA, PCA and AASHTO were not comparable with the new proposed k-E_s relationships, in terms of accuracy and the range of input data specified. The performance of k-E_s relationships of PCA and AASHTO were less satisfied than that of the proposed k-E_s relationship, although the FAA relationship performed better for its applicable range of data.

7.4 Closed-form Backcalculation of Layer Moduli of Flexible Pavement

In this study, two forward solutions based on Burmister theory for three- and four-layer flexible pavement systems, namely 3L-DEF and 4L-DEF respectively, were proposed. Both solutions were verified using another forward calculation program, CHEVRONX, developed by Michigan State University. Two closed-form backcalculation programs, 3L-BACK and 4L-BACK, were developed using the respective forward solutions 3L-DEF and 4L-DEF. The verification of the proposed backcalculation programs was conducted by using two iterative backcalculation programs, EVERCALC and MICHBACK, which use CHEVRONX as their forward solution program. The verification results are summarized as follows.

a. A comparison between 3L-DEF and 4L-DEF, and CHEVRONX showed that the deflections produced based on Burmister theory compared well with those by CHEVRONX program. The largest discrepancies were around 3.5%.

b. Two comparisons were performed between each of the two closed-form backcalculation programs (3L-BACK and 4L-BACK) and the iterative

optimization programs (EVERCALC and MICHBACK), using exact deflections and deflections with measurement errors. The first comparison resulted that 3L-BACK and 4L-BACK can produce relatively better solutions with much smaller errors as compared with EVERCALC and MICHBACK. The second comparison using deflection with measurement errors revealed that the closed-form backcalculation programs were less sensitive to errors as indicated by smaller values of measures of dispersion such as range, mean, standard deviation, coefficient of variation and *RMSE* values, as compared with those of EVERCALC and MICHBACK programs.

c. Between the two closed-form backcalculation programs, 3L-BACK could produce better results than those of 4L-BACK in determining the layer moduli. This is because it is easier to locate the global minima in two-dimensional space than the three-dimensional space in the case of 4L-BACK. For complex systems having many equations and constraints to be solved, the use of closed-form method is more difficult to be implemented.

7.5 Recommendation for Further Research

This section identifies some areas for further research to enhance the efficiency and accuracy of backcalculation algorithms for estimating pavement layer properties of rigid and flexible pavement systems.

a. The assumption of the subgrade used in this research is that the subgrade has an infinite thickness. The backcalculation algorithms developed are unable to handle a case where a stiff layer is present within the pavement system. This applies for both rigid and flexible pavements.

b. This research has developed a solution of a four-layer flexible pavement system. Today, the actual pavement can consist of more than four layers, especially in developing countries where the technology of recycled pavement is still not available. Therefore, a solution of a pavement system consisted of more than four layers might be necessary to be developed. However, the development of a closed-form backcalculation algorithm would be extremely complex. One alternative is the use of genetic-algorithm approach to solve for more than four unknowns of the layer moduli.

c. The research so far separated the development of backcalculation algorithm into two parts, that is, the development of backcalculation algorithm on rigid pavement as one part, and the development of backcalculation algorithm on flexible pavement as another part. In the future, it may be necessary to develop a backcalculation algorithm for a composite structure (e.g. a flexible layer on top of a rigid pavement).

d. To take into account the effect of temperature on asphalt layer, the application of three- and four-layer backcalculation algorithm at different temperature-load conditions is recommended to be performed.

LIST OF REFERENCES

AASHTO (1972). “Interim Guide for Design of Pavement Structures”, American Association of State Highway Officials, Washington DC.

AASHTO (1986). “AASHTO Guide for Design of Pavement Structures 1986”, American Association of State Highway and Transportation Officials, Washington, DC.

AASHTO (1993). “AASHTO Guide for Design of Pavement Structures 1993”, American Association of State Highway and Transportation Officials, Washington, DC.

AASHTO (1994). “Standard Method of Test for Resilient Modulus of Unbound Granular Base/Subbase Materials and Subgrade Soils - SHRP Protocol P46”, AASHTO T294-92, American Association of State Highway and Transportation Officials, Washington, DC.

AASHTO (2004a). “Repetitive Static Plate Load Test of Soils and Flexible Pavement Components for Use in Evaluation and Design of Airport and Highway Pavements” Nonrepetitive Static Load Test“, AASHTO T221-90, Standard Specifications for Transportation Materials and Methods of Sampling and Testing 13rd edition. American Association of State Highway and Transportation Officials, Washington, DC.

AASHTO (2004b). “Nonrepetitive Static Plate Load Test of Soils and Flexible Pavement Components for Use in Evaluation and Design of Airport and Highway Pavements” Nonrepetitive Static Load Test“, AASHTO T222-81, Standard Specifications for Transportation Materials and Methods of Sampling

and Testing 13rd edition. American Association of State Highway and Transportation Officials, Washington, DC.

Almedia, J.R.de, Brown, S.F., and Thom, N.H. (1994). "A Pavement Evaluation Procedure Incorporating Material Non-Linearity", Nondestructive Testing of Pavements and Backcalculation of Moduli: Second Volume, ASTM STP 1198, American Society for Testing and Materials, West Conshohocken, PA. pp. 218-232.

ARA Consulting Group Inc. (2004). *Guide for Mechanistic-Empirical Design of New and Rehabilitated Pavement Structures*, Final Report, National Cooperative Highway Research Program, Transportation Research Board, Washington D.C.

ASTM (1995). "Standard Test Method for Indirect Tension Test for Resilient Modulus of Bituminous Mixtures", ASTM D4123-82, American Society for Testing and Materials, Conshohocken, PA.

ASTM (2003a). "Repetitive Static Plate Load Test of Soils and Flexible Pavement Components, for Use in Evaluation and Design of Airport and Highway Pavements", ASTM D1195-93, American Society for Testing and Materials, Conshohocken, PA.

ASTM (2003b). "Nonrepetitive Static Plate Load Test of Soils and Flexible Pavement Components, for Use in Evaluation and Design of Airport and Highway Pavements", ASTM D1196-93, American Society for Testing and Materials, Conshohocken, PA.

ASTM (2004). "Revision of D4123-82 (1995) Standard Test Method for Indirect Tension Test for Resilient Modulus of Bituminous Mixtures", ASTM WK3751 (Work Item), American Society for Testing and Materials, Conshohocken, PA.

ASTM (2006). *Nonrepetitive Static Plate Load Test of Soils and Flexible Pavement Components, for Use in Evaluation and Design of Airport and Highway Pavements*, ASTM D1196-93, American Society for Testing and Materials, Conshohocken, PA.

Boussinesq, J. (1885). Application des Potentiels a l'etude de l'equilibre et du Mouvementdes Solids Elastiqus, Guthier-Villars, Paris, France.

Burmister, D.M. (1943). "The Theory of Stresses and Displacements in Layered Systems and Applicationsto Design of Airport Runways", Highway Research Board Proceedings, Vol. 23, pp. 126-148.

Burmister, D.M (1945a), The General Theory of Stresses and Displacements in Layered Soil Systems. I, Journal of Applied Physics, Vol. 16, pp. 89-94.

Burmister, D.M (1945b), The General Theory of Stresses and Displacements in Layered Soil Systems. III, Journal of Applied Physics, Vol. 16, pp. 296-302.

Childs, L.D. (1967). "Cement-treated Subbases for Concrete Pavements", Highway Research Record 189, Highway Research Board, pp. 19-43.

Crovetti, J.A. (1994). Evaluation of Jointed Concrete Pavement Systems Incorporating Open-Graded Permeable Bases, Ph.D. dissertation, University of Illinois at Urbana-Champaign.

Crovetti, J. A. (2002). "Deflection-Based Analysis Techniques for Jointed Concrete Pavement Systems", CD-ROM Proceedings of 81st Annual Meeting of Transportation Research Board, Washington D. C.

Crovetti, J.A. and Crovetti, M.R.T. (1994). "Evaluation of Support Conditions under Jointed Concrete Pavement Slabs", Nondestructive Testing of Pavements and Backcalculation of Moduli, 2nd Volume, ASTM STP 1198, American Society for Testing and Materials, Philadelphia, pp. 455-472.

Crovetti, J.A. and Darter, M.I. (1985). " Void Detection for Jointed Concrete Pavement", Transportation Research Record 1041, Transportation Research Board, Washington, DC.

Darter, M.I., Hall, K.T., and Kuo, C.M. (1995). "Support under Portland Cement Concrete Pavements", NCHRC Report 372, Transportation Research Board.

Elkins, G.E., Schmalzer, P., Thompson, T., and Simpson, A. (2003). Long-Term Pavement Performance Information Management System Pavement Performance Database Users Guide, FHWA Report No. FHWA-RD-03-088, Federal Highway Administration, Washington, DC, USA.

FAA (1995). "Airport Pavement Design and Evaluation", Advisory Circular No. 150/5320-6D, Federal Aviation Administration.

FAA (1996). "Change 1 to Airport Pavement Design and Evaluation", Advisory Circular No. 150/5320-6D Change-1, Federal Aviation Administration.

Fwa, T.F. (1998). "Nondestructive Evaluation of Pavement Properties", Proceeding of 3rd International Conference on Road and Airport Pavement Technology (ICPT), Beijing, China, pp. 25-48.

Fwa, T.F., Tan, K.H. and Li, S. (2000). "Closed-Form and Semi-Closed-Form Algorithm for Backcalculation of Concrete Pavement Parameters", Nondestructive Testing of Pavement and Backcalculation of Moduli : Third Volume, ASTM STP 1375, pp. 267-280.

Fwa, T.F. and Chandrasegaran, S. (2001). "Regression Model for Backcalculation of Rigid-Pavement Properties", Journal of Transportation Engineering, Vol. 127, ASCE, pp. 353-355.

Fwa, T.F. and Rani, T.S. (2005). “Seed Moduli Generation Algorithm for Backcalculation of Flexible Pavement Moduli”, Transportation Research Record 1905, pp. 117 -127.

Fwa, T.F. (2006). “Structural Evaluation of Highway Pavements”. CRC Press, Florida, Chapter 20 in The Handbook of Highway Engineering edited by T.F. Fwa.

Goktepe, A.B., Agar, E. and Lav, A.H. (2006), Advances in Backcalculating the Mechanical Properties of Flexible Pavements, Advances in Engineering Software 37, Elsevier, pp. 421-431.

Grogan, W.P., Freeman, R.B., and Alexander, D.R. (1998). “Impact of FWD Testing Variability on Pavement Evaluations”, Journal of Transportation Engineering, Vol. 124, No. 5, ASCE, pp. 437-442.

Hall, J.W., Jr. and McCaffrey, P.S, Jr. (1994). “Misleading Results from Nondestructive Testing – A Case Study”, Nondestructive Testing of Pavements and Backcalculation of Moduli: Second Volume, ASTM STP 1198, American Society for Testing and Materials, West Conshohocken, PA. pp. 251-260.

Hall, K.T., Darter, M.I. and Kuo, C.M. (1995). “Improved Methods for Selection of k Value for Concrete Pavement Design”, Transportation Research Record 1505, pp. 128 -136.

Hall, K.T., Darter, M.I., Hoerner, T.E., and Khazanovich, L. (1996). “LTPP Data Analysis – Phase I: Validation of Guidelines for k-Value Selection and Concrete Pavement Performance Prediction”, Technical Report No. FHWA-RD-96-198, Federal Highway Administration.

Harichandran, R.S, Mahmood, T., Raab, A.R., and Baladi, G.Y. (1994). “Backcalculation of Pavement Layer Moduli, Thicknesses and Stiff Layer Depth Using a Modified Newton Method”, Nondestructive Testing of Pavements and

Backcalculation of Moduli: Second Volume, ASTM STP 1198, American Society for Testing and Materials, West Conshohocken, PA. pp. 68-82.

Hoffman, M.S. and M.R. Thompson (1981). "Mechanistic Interpretation of Non-destructive Testing Deflections", Civil Engineering Studies, Transportation Engineering Series No. 32, Illinois Cooperative Highway and Transportation Research Program Series No. 190, University of Illinois, Urbana, Illinois, USA.

Huang, Y.H. (2003). Pavement Analysis Design 2nd Edition, Prentice-Hall, New Jersey, USA.

Huang, Y.H. and G.W. Sharpe (1989). "Thickness Design of Concrete Pavements by Probabilistic Method", Proceedings of 4th International Conference on Concrete Pavement Design and Rehabilitation, Purdue University, pp. 251-265.

ICAO (1983). "Aerodrome Design Manual – Part 3: Pavements", 2nd edition, International Civil Aviation Organization.

Ioannides, A.M., E.J. Barenberg and J.A. Lary. (1989). "Interpretation of Falling Weight Deflectometer Results Using Principles of Dimensional Analysis", Proceedings, 4th International Conference on Concrete Pavement Design and Rehabilitation, pp. 231 – 247.

Irwin, L.H., Yang, W.S., and Stubstad, R.N. (1989). "Deflection Reading Accuracy and Layer Thickness Accuracy in Backcalculation of Pavement Layer Moduli", Nondestructive Testing of Pavements and Backcalculation of Moduli, ASTM STP 1026, American Society for Testing and Materials, West Conshohocken, PA. pp. 229-244.

Jackson, D.J., Murphy, M.R., and Wimsatt, A. (1994). "Strategies for the Application of the Falling Weight Deflectometer to Evaluate Load Transfer Efficiency at Joints in Jointed Concrete Pavement", Nondestructive Testing of Pavements and

Backcalculation of Moduli: Second Volume, ASTM STP 1198, American Society for Testing and Materials, West Conshohocken, PA. pp. 395-402.

Jiang, Y.J. and Tayabji, S.D. (1998). "Mechanistic Evaluation of Test Data from LTPP Jointed Concrete Pavement Test Sections", Proceedings of 77th Annual Meeting Transportation Research Board (TRB), Washington, DC, USA.

Jiang, Y.J. and Tayabji, S.D. (2000). "Evaluation of Concrete Pavement Conditions and Design Features using LTPP FWD Deflection Data", Nondestructive Testing of Pavements and Backcalculation of Moduli: Third Volume, ASTM STP 1375, American Society for Testing and Materials, West Conshohocken, PA. pp. 281-294.

Khazanovich, L. and Ioannides, A. M. (1993). "Finite Element Analysis of Slabs-on-Grade Using Higher Order Subgrade Soil Models", Proceedings, ASCE Specialty Conference on Airport Pavement Innovation – Theory to Practice, Waterways Experiment Station, Vicksburg, MS, pp. 16 – 30.

Khazanovich, L., McPeak, T. J., and Tayabji, S. D. (2000). "LTPP Rigid Pavement FWD Deflection Analysis and Backcalculation Procedure", Nondestructive Testing of Pavements and Backcalculation of Moduli: Third Volume, ASTM STP 1375, American Society for Testing and Materials, West Conshohocken, PA. pp. 246-266.

Khazanovich, L., Tayabji, S.D., and Darter, M.I. (2001). "Backcalculation of Layer Parameters for LTPP Test Sections", Volume I: Slab on Elastic Solid and Slab on Dense-Liquid Foundation Analysis of Rigid Pavements, Report No. FHWA-RD-00-86, Federal Highway Administration.

Kim, Y.R., and Park, H. (2002). “Use of Falling Weight Deflectometer Multi-Load Data for Pavement Strength Estimation”, Final Report No. FHWA/NC/2002-006, FHWA, North Carolina Department of Transportation.

Korenev, B. G. (1954). Problems of Analysis of Beams and Plates on Elastic Foundation. Gosudarstvennoe Izdatel’stvo Literatury po Stroitel’stvu I Arkhitekture, Moscow, USSR (in Russian), 1954.

Lavenberg, K. (1944). “A Method for the Solution of Certain Nonlinear Problems in Least Squares”, Quarterly of Applied Mathematics, Volume 2, pp. 164-168.

Li, S., Fwa, T.F., and Tan, K.H. (1996). “Closed-Form Back-Calculation of Rigid-Pavement Parameters”, Journal of Transportation Engineering, Vol. 122, No. 1, ASCE, pp. 5-11.

Liu W. and Fwa, T.F. (2007). “Nine-slab Model for jointed Concrete Pavements”. International Journal of Pavement Engineering, Volume 8, Issue 4, pp. 277-306.

Losberg, A. (1960). *Structurally Reinforced Concrete Pavements*. Doktorsavhandlingar Vid Chalmers Tekniska Hogskola, Goteborg, Sweden.

“LTPP DataPave Online.” *LTPP Products Online* <http://www.ltpp-products.com/DataPave/index.asp>.

Lytton, R.L. (1989). “Backcalculation of Pavement Layer Properties”, Nondestructive Testing of Pavements and Backcalculation of Moduli, ASTM STP 1026, American Society for Testing and Materials, West Conshohocken, PA, pp. 7–38.

Mahoney, J.P., Coetzee, N.F., Stubstad, R.N., and Lee, S.W. (1989). “A Performance Comparison of Selected Backcalculation Computer Programs”, ASTM STP 1026, American Society for Testing and Materials, West Conshohocken, PA, pp. 452–467.

Marquardt, D.W. (1963). “An Algorithm for Least Squares Estimation of Nonlinear Parameters”, SIAM Journal, Volume 11, pp. 431-441.

Matsui, K., Uchida, S. Tukano, H. and Inoue, T. (1990). “Pavement Rehabilitation Design Prognosis of Elastic Layered Properties”, Proceedings of 6th Conference Road Engineering Association of Asia and Australia, Vol. 1.

Matsui, K., Kikuta, Y., Nishizawa, T., and Kasahara, A. (2000). “Comparative Studies of Backcalculated Result from FWDs with Different Loading Duration”, Nondestructive Testing of Pavements and Backcalculation of Moduli: Third Volume, ASTM STP 1375, American Society for Testing and Materials, West Conshohocken, PA. pp. 470-483.

Matthews, J.H. and Fink, K.D. (2004), Numerical Methods Using Matlab, 4th edition, Pearson Education Inc., Upper Saddle River, NJ.

McCullough, B.F. and Taute, A. (1982). “Use of Deflection Measurement for Determining Pavement Material Properties”, Tranportation Research Record 852, pp. 8-14.

Middlebrooks, T.A. and Bertram, G.E. (1942). “Soil Tests for Design of Runways Pavements”, Proceedings, Highway Research Board.

Montgomery, D.C. and Runger, G.C. (2003). “Applied Statistics and Probability for Engineers”, John Wiley and Sons, Inc., New York.

Nelder, J.A. and Mead, R. (1965). “A Simplex Method for Function Minimization”, The Computer Journal, Vol. 7, pp. 308-313.

Panc, V. (1975). *Theories of Elastic Plates*, Noordhoff International Publishing, Leyden.

PCA (1966). Thickness Design for Concrete Pavements, Portland Cement Association.

PCA (1984). Thickness Design for Concrete Highway and Street Pavements, Portland Cement Association.

Pradhan, M.M. (1999). "Selection of the Methods of Evaluation of Utah's Rigid Pavement Conditions", Proceedings of 78th Annual Meeting of Transportation Research Board (TRB), Washington, DC, USA.

Pronk, A.C. (1988). "Interpretation Problems and Reliability of Falling Weight Deflectometer (FWD) Measurements on Three Layer Systems", Proceeding of Association of Asphalt Paving Technologist, Williamsburg, VA., Vol. 57, pp. 502-518.

Roesset, J.M. and Shao, K.Y. (1985). "Dynamic Interpretation of Dynaflect and FWD Test", Tranportation Research Record 1022, pp. 7-16.

Rufino, D., Roesler, J. and Barenberg, E.J. (2002). "Evaluation of Different Methods and Models for Backcalculating Pavement Properties Based on Denver International Airport Data", Federal Aviation Administration Technology Transfer Conference, Atlanta, NJ.

Scullion, T., Uzan, J., and Paredes, M. (1990). "MODULUS: A Microcomputer-Based Backcalculation System, Transportation Research Record 1260, pp.180-191.

Sivaneswaran, N., S.L. Kramer, and J.P. Mahoney, 1991, Advanced Backcalculation using a Nonlinear Least Square Optimization Technique, Presented at the 70th Annual Meeting of the Transportation Research Board, Washington, D.C.

Stubstad, R.N., Mahoney, J.P., and Coetzee, N.F. (1994). "Effect of Material Stress Sensitivity on Backcalculated Moduli and Pavement Evaluation", Nondestructive Testing of Pavements and Backcalculation of Moduli: Second Volume, ASTM STP 1198, pp. 233-247.

Teller, L.W. and Sutherland, E.C. (1943), "The Structural Design of Concrete Pavements", Public Roads, Vol. 23, pp. 167 – 212.

Tia, M., Eom, K.S., and Ruth, B.E. (1989). "Development of the DBCONPAS Computer Program for Estimation of Concrete Pavement Parameters from FWD Data", Nondestructive Testing of Pavements and Backcalculation of Moduli, ASTM STP 1026, American Society for Testing and Materials, West Conshohocken, PA. pp. 291-312.

Uddin, W., and McCullough, B.F. (1989). "In Situ Material Properties from Dynamic Deflection Equipment", ASTM STP 1026, American Society for Testing and Materials, West Conshohocken, PA, pp. 278– 290.

Ullidtz, P. (1987). *Pavement Analysis*, Elsevier, Amsterdam, the Netherlands.

Uzan, J. and Witczak, M. W. (1985). "Composite Subgrade Modulus for Rigid Airfield Pavement Design upon Multilayer Theory", Proceedings 3rd International Conference on Concrete Pavement Design and Rehabilitation, Purdue University.

Uzan, J. (1994). "Advanced Backcalculation Techniques", Nondestructive Testing of Pavements and Backcalculation of Moduli: Second Volume, ASTM STP 1198, pp. 3-37.

Van Til, C.J., B.F. McCullough, B.A. Vallerga, and R.G. Hicks. (1972). "Evaluation of AASHO Interim Guides for Design of Pavement Structures", NCHRP 128, Highway Research Board.

Vesic, A.S. and K. Saxena (1974). "Analysis of Structural Behavior of AASHO Road Test Rigid Pavements", NCHRP Report No. 97, Highway Research Board.

Watson, D.K., and Rajapakse, R.K.N.D. (2000). “Seasonal Variation in Material Properties of a Flexible Pavement”, Canadian Journal of Civil Engineering, Volume 27, National Research Council Canada, pp. 44-54.

Westergaard, H.M. (1925), “Theory of Stresses in Road Slabs”, Proceedings, Fourth Annual Meeting of the Highway Research Board.

Winkler, E. (1867), Die Lehre von der Elasticitaet und Festigkeit. Prag, Dominicus.

Zha, X. and Xiao, Q. (2003). “Homotopy Method for Backcalculation of Pavement Layer Moduli”, Proceedings of International Symposium Non-Destructive Testing in Civil Engineering 2003, Berlin, Germany.

APPENDIX A

FINAL TERMS OF CONSTANTS C_1 AND D_1

According to Equations (5-67) and (5-68), the final terms of constants C_1 and D_1 are as follows.

A.1Final terms of constant C_1

$$C_1 m = \frac{Numerator\ C_1}{Denominator\ C_1} = -\left\{\sum_{i=1}^{64} \frac{(Num\ C_1)_i}{(Denom\ C_1)_i}\right\}$$

A.1.2 The list of Numerator C_1

$$(Num\ C_1)_1 = \langle 2NTVXY(1+2mh_1) + KTV\{NZ^2+L\}(1+2mh_1) + 2KNTVXZmh_2(1+2mh_1) + 2KNTV^2XZmh_1(1+2mh_1)\rangle e^{mh_1} e^{2mh_2} e^{mH}$$

$$\begin{aligned}(Num\ C_1)_2 = \langle & 2K^3LNV^2Zmh_2(1+4mh_1) - 2K^3NSTVZ\{NZ^2+L\}mh_2(1+4mh_1) \\ & + 8K^3NT^2Z\{NZ^2+L\}m^3h_2^3(1+2mh_1) + 8K^2N^2T^2YZ^2m^2h_2^2(1+2mh_1) \\ & + 2K^3NSTVZ\{NZ^2+L\}mh_2(1+2mh_1) - 8KN^2T^2XZ^2m^2h_2^2(1+2mh_1) + 4KLNT^2Xm^2h_2^2(1+2mh_1) \\ & + 2KNT^2Z\{NZ^2+L\}mh_2(1+2mh_1) + 2KN^2STVX^2Zmh_2(1+2mh_1) + 4KN^2T^2Y^2Zmh_2(1+2mh_1) \\ & + 2KN^2T^2Y^2Zmh_2 + 4K^2NT^2Y\{NZ^2+L\}m^2h_2^2(1+2mh_1) + K^2NSTVY\{NZ^2+L\}(1+2mh_1) \\ & - 4N^2T^2XYZmh_2(1+2mh_1) + NT^2Y\{NZ^2+L\}(1+2mh_1) + N^2STVX^2Y(1+2mh_1) \\ & + N^2T^2Y^3(1+2mh_1) + KNV^2X\{NZ^2+L\}(1+2mh_1) + N^2V^2X^2Y(1+2mh_1) \\ & + KLNSTVX(1+2mh_1) - KN^2STVXZ^2(1+4mh_1) + LNT^2Y(1+2mh_1) + K^2N^2V^2YZ^2(1+4mh_1) \\ & + K^2LNV^2Y(1+2mh_1) - 4N^2T^2VX^2Ym^2h_1h_2(1+2mh_1) - 4KNT^2VX\{NZ^2+L\}m^2h_1h_2(1+2mh_1) \\ & + 8KN^2T^2XZ^2m^3h_1h_2^2 + 2N^2T^2VXYZmh_1(1+2mh_1) + 2KNT^2VZ\{NZ^2+L\}mh_1(1+2mh_1) \\ & - 4KN^2T^2Z^3m^2h_1h_2 + 8K^2N^2T^2VYZ^2m^2h_1h_2(1+2mh_1) - 2K^2LNT^2VYmh_2 \\ & + 2KN^2V^3X^2Zmh_1(1+2mh_1) + 2K^3N^2V^2Z^3mh_2(1+4mh_1) + 2K^3NV^3Z\{NZ^2+L\}mh_1(1+2mh_1) \\ & + 8K^3NT^2VZ\{NZ^2+L\}mh_1(1+2mh_1) - 8KN^2T^2VXZ^2m^2h_1h_2(1+2mh_1) \\ & + 2KN^2T^2VY^2Zmh_1(1+2mh_1) + 8KN^2T^2VX^2Zm^3h_1h_2^2(1+2mh_1) \\ & + 2KNT^2VZ\{NZ^2+L\}mh_1(1+2mh_1) - K^2N^2STVYZ^2(1+4mh_1) + 2KNVX\{NZ^2+L\}mh_2 \\ & - 4KN^2VXZ^2mh_2 + 2KN^2V^2X^2Zmh_2(1+4mh_1) - KN^2V^2XZ^2(1+2mh_1) \\ & - 2KN^2STVX^2Zmh_2(1+4mh_1) + 8KN^2T^2X^2Zm^3h_2^3 + 4N^2T^2X^2Ym^2h_2^2 - 2KNSTX\{NZ^2+L\}mh_2 \\ & - 2N^2STX^2Ymh_2 + N^2STXYZ - 2K^2LNSTYmh_2 + 4K^3NVZm^2h_2^2\{NZ^2+L\} + 4KN^2VX^2Zm^2h_2^2 \\ & + KN^2VY^2Z - 4K^2N^2STYZ^2mh_2 - 4K^3NSTZm^2h_2^2\{NZ^2+L\} - KN^2ST^2Z + 2N^2VX^2Ymh_2 \\ & - N^2VXYZ + 2K^2LNVYmh_2 + 2K^2LNT^2VYmh_2(1-2mh_1)\rangle e^{mh_1} e^{2mh_2} e^{-mH}\end{aligned}$$

$$(Num\,C_1)_3 = \langle LN^2TVXY(1+2mh_1) + KLN^2SV^2X^2(1+2mh_1) + 4KLN^2TV^2m^2h_2^2(1+2mh_1)$$
$$+ LN^2ST^2XY(1+2mh_1) - 16KLN^2T^3X^2m^4h_1h_2^3(1+2mh_1) - 4KLN^2TV^2X^2m^2h_1h_2(1+2mh_1)$$
$$- 4LN^2T^3XYm^2h_1h_2(1+2mh_1) - 4KLN^2TVX^2m^2h_2^2(1+4mh_1) + 8KLN^2T^3XZm^3h_1h_2^2(1+2mh_1)$$
$$+ 4KLN^2TV^2XZmh_1(1+2mh_1) + 2LN^2T^3YZmh_1(1+2mh_1) + 2KLN^2ST^2XZmh_2(1+4mh_1)$$
$$+ 4KLN^2ST^2X^2m^2h_2^2(1+4mh_1) + 8KN^3TV^2XZ^3m^2h_1^2 - 8KN^3TV^2X^2Z^2m^3h_1^2h_2$$
$$- 4N^3TVX^2YZmh_1 - 8KN^3TVX^2Z^2m^3h_1h_2^2 - 2KLN^2S^2TXmh_2 - 8KLN^2TX^2m^3h_2^3$$
$$+ 2N^3TVXYZ^2mh_1 + 4KN^3TVXZ^3m^2h_1h_2 + 8KLN^2TVXZm^2h_1h_2 + 2KN^3SV^2X^2Z^2mh_1$$
$$+ 2KLN^2SVX^2mh_2 + 2LN^2TXYmh_2 + 8KLN^2TX^2m^3h_2^3 - LN^2TYZ + 4KLN^2STXZm^2h_1h_2$$
$$- 2KLN^2STXZmh_2 + 2KLN^2TVXmh_2\rangle e^{mh_1}e^{2mh_2}e^{-3mH}$$

$$(Num\,C_1)_4 = \langle 2K^2NTVZ\{NZ^2 + L\}mh_2(1+2mh_1) + 2KN^2TVXYZmh_2(1+2mh_1) + KN^2TVYZ^2(1+2mh_1)$$
$$+ N^2TVXY^2(1+2mh_1) + 2KLNTVY(1+2mh_1) + 2K^2NTV^2Zmh_1\{NZ^2 + L\}(1+2mh_1)$$
$$+ 2KN^2TV^2XYZmh_1(1+2mh_1) - 4K^2N^2TVZ^3m^2h_1h_2\rangle e^{mh_1}e^{4mh_2}e^{-mH}$$

$$(Num\,C_1)_5 = \langle 2KLN^2T^2YZmh_2(1+2mh_1) + LN^2T^2Y^2(1+2mh_1) + 8K^2LN^2T^2XZm^3h_2^3(1+2mh_1)$$
$$+ 4KLN^2T^2XYm^2h_2^2(1+2mh_1) + KLN^2STVXY(1+2mh_1) + KLN^2V^2XY(1+2mh_1)$$
$$+ 8K^2LN^2T^2VXZm^3h_1h_2^2(1+2mh_1) - 6K^2LN^2STVXZm^2h_1h_2 + 2K^2LN^2V^3XZmh_1(1+2mh_1)$$
$$+ 4KLN^2T^2VYZmh_1(1+2mh_1) + 2K^2LN^2V^2XZ(1+4mh_1) - 4KLN^2T^2VXYm^2h_1h_2(1+2mh_1)$$
$$+ KSTVX + T^2Y + 4KT^2Xm^2h_2^2 + 4K^2N^3V^3XZ^3m^2h_1^2 + 2KN^3V^2XYZ^2mh_1$$
$$+ 4K^2N^3V^2XZ^3m^2h_1h_2 + 4K^2LN^2VXZm^2h_2^2 - 2KLN^2STXYmh_2 - 4K^2LN^2STXZm^2h_2^2$$
$$+ 2KLN^2VXYmh_2 - KLN^2VYZ\rangle e^{mh_1}e^{4mh_2}e^{-3mH}$$

$$(Num\,C_1)_6 = \langle 2K^2LN^2TVYZmh_2(1+2mh_1) + KLN^2TVY^2(1+2mh_1) + 2K^2LN^2TV^2YZmh_1(1+2mh_1)\rangle$$
$$* e^{mh_1}e^{6mh_2}e^{-3mH}$$

$$(Num\,C_1)_7 = \Big\langle 4K^3TV\{NZ^2+L\}m^2h_2^2(1+2mh_1)+4K^2NTVYZmh_2(1+2mh_1)+K^3SV^2\{NZ^2+L\}(1+2mh_1)$$
$$-4KNTVXZmh_2(1+2mh_1)+KTV\{NZ^2+L\}(1+2mh_1)+2KNSV^2X^2(1+2mh_1)+KNTVY^2(1+2mh_1)$$
$$+4KNTVX^2m^2h_2^2(1+2mh_1)+KST^2\{NZ^2+L\}(1+2mh_1)+NST^2XY(1+2mh_1)+NTVXY(1+2mh_1)$$
$$+2K^2NST^2YZmh_2(1+2mh_1)+KNST^2Y^2mh_2(1+2mh_1)-16KNT^3X^2m^4h_1h_2^3(1+2mh_1)$$
$$-4NT^3XYm^2h_1h_2(1+2mh_1)-8KNTV^2X^2m^2h_1h_2(1+2mh_1)-4KNTVX^2m^2h_2^2(1+4mh_1)$$
$$+4KNST^2X^2m^2h_2^2(1+4mh_1)+4KNST^2X^2m^2h_2^2(1+2mh_1)+24KNT^3XZm^3h_1h_2^2(1+2mh_1)$$
$$+2NT^3YZmh_1(1+2mh_1)+2KNTV^2XZmh_1(1+2mh_1)+2KNTVXZmh_2(1+4mh_1)-2KNST^2XZmh_2(1+4mh_1)$$
$$+2K^2NTV^2YZmh_1(1+2mh_1)-4K^3TV\{NZ^2+L\}m^2h_2^2(1+2mh_1)-4K^3TV\{NZ^2+L\}m^2h_1h_2(1+2mh_1)$$
$$-16K^3T^3\{NZ^2+L\}m^2h_1h_2(1+2mh_1)-16K^2NT^3YZ\{NZ^2+L\}m^3h_1h_2^2(1+2mh_1)$$
$$-4KNT^3Y^2m^2h_1h_2(1+2mh_1)+4K^3ST^2\{NZ^2+L\}m^3h_1h_2^2(1+2mh_1)-16KNT^3X^2m^4h_1h_2^3(1+2mh_1)$$
$$-4KT^3\{NZ^2+L\}m^2h_1h_2(1+2mh_1)+2K^2NST^2YZmh_2(1+4mh_1)-2K^2NTVYZmh_2(1+4mh_1)$$
$$+2KNST^2XZmh_2(1-4mh_1)+2KNTVXZmh_2(1+2mh_1)-4KNS^2TX^2mh_2+KNS^2TXZ$$
$$+K^2NSVYZ-2K^3NS^2TZ^2mh_2-16KNTVX^2m^3h_1h_2^2-8KNTX^2m^3h_2^3-K^3LS^2Tmh_2$$
$$+2K^3SV\{NZ^2+L\}mh_2+4KNSVX^2mh_2-KNSVX^2-K^2NS^2TYZ\Big\rangle e^{mh_1}e^{-2mh_2}e^{mH}$$

$$(Num\,C_1)_8 = \Big\langle KV^2X(1+2mh_1)-4KT^2VXmh_1(1+2mh_1)-2KSTXmh_2+8KT^2Xm^3h_1h_2^2+2KSTVXmh_1$$
$$+2T^2Ymh_1\Big\rangle * e^{mh_1}e^{-2mh_2}e^{3mH}$$

$$(Num\,C_1)_9 = \Big\langle KN^2STVXZ^2(1+2mh_1)+2KLNSTVX(1+2mh_1)+N^2STVX^2Y(1+2mh_1)$$
$$-4KNT^2VX\{NZ^2+L\}m^2h_1h_2(1+2mh_1)-4N^2T^2VX^2Ym^2h_1h_2(1+2mh_1)$$
$$+2KNT^2VZ\{NZ^2+L\}mh_1(1+2mh_1)+2N^2T^2VXYZmh_1(1+2mh_1)-4KLNT^2VXm^2h_1h_2(1+2mh_1)$$
$$+32KN^2T^2VX^2Zm^4h_1^2h_2^2-8KN^2STVX^2Zm^2h_1h_2+2KN^2STVXZ^2mh_1-16KN^2T^2VXZ^2m^3h_1^2h_2$$
$$* e^{mh_1}e^{-2mh_2}e^{-mH}$$

$$(Num\,C_1)_{10} = \Big\langle K^2STV\{NZ^2+L\}(1+2mh_1)+2KNSTVXY(1+2mh_1)$$
$$-4K^2T2Vm^2h_1h_2\{NZ^2+L\}(1+2mh_1)-8KNT^2VXYm^2h_1h_2(1+2mh_1)+2KNT^2VYZmh_1(1+2mh_1)\Big\rangle$$
$$-4K^2NSTVXZm^2h_1h_2+16K^2NT^2VXZm^4h_1^2h_2^2\Big\rangle e^{mh_1}e^{-4mh_2}e^{mH}$$

$$(Num\,C_1)_{11} = \Big\langle 4K^2TVXm^2h_2^2(1+2mh_1)+K^2SV^2X(1+2mh_1)+KTVY(1+2mh_1)+KST^2Y(1+2mh_1)$$
$$-16K^2T^3Xm^4h_1h_2^3(1+2mh_1)-4KT^3Ym^2h_1h_2(1+2mh_1)-4K^2TV^2Xm^2h_1h_2(1+2mh_1)$$
$$+4K^2ST^2Xm^2h_2^2(1+4mh_1)-4K^2TVXm^2h_2^2(1+4mh_1)-2K^2STXmh_2\Big\rangle e^{mh_1}e^{-4mh_2}e^{3mH}$$

$$(Num\,C_1)_{12} = \Big\langle K^2STVY(1+2mh_1)-4K^2T^2VYm^2h_1h_2(1+2mh_1)\Big\rangle e^{mh_1}e^{-6mh_2}e^{3mH}$$

$$(Num\,C_1)_{13} = \langle 6KNT^2YZmh_2(1+2mh_1) + 2NT^2Y^2(1+2mh_1) + 4K^2T^2\{NZ^2+L\}m^2h_2^2(1+2mh_1)$$
$$+ K^2STV\{NZ^2+L\}(1+2mh_1) - 4NT^2XZmh_2(1+2mh_1) + T^2\{NZ^2+L\}mh_1(1+2mh_1)$$
$$+ NSTVX^2(1+2mh_1) + K^2V^2\{NZ^2+L\}(1+2mh_1) + KNV^2XY(1+2mh_1) + 2K^2NSTVXZmh_2(1+2mh_1)$$
$$+ 8K^2NT^2XZm^3h_2^3(1+2mh_1) + KNSTVXY(1+2mh_1) + 4KNT^2XYm^2h_2^2(1+2mh_1) + NV^2X^2(1+2mh_1)$$
$$- 4KNT^2VXYm^2h_1h_2(1+2mh_1) - 4K^2T^2Vm^2h_1h_2\{NZ^2+L\}(1+2mh_1) + 8K^2NT^2VXZm^3h^1h_2^2(1+2mh_1)$$
$$+ 2K^2NV^3XZmh_1(1+2mh_1) + 2NT^2VXZmh_1(1+2mh_1) - 4NT^2VX^2m^2h_1h_2(1+2mh_1)$$
$$+ 4NT^2X^2m^2h_2^2 - 2K^2ST\{NZ^2+L\}mh_2 + 8K^2NT^2Z^2m^3h_1h_2^2 - 2KNSTXYmh_2$$
$$+ 4KT^3XYm^2h_2^2(1+4mh_1) + 8KNV^2XZm^2h_1h_2 + 4KNVXZm^2h_2^2 - 8KNSTVXZm^2h_1h_2$$
$$+ K^2NS^2VXZ + KNVYZ - 2NSTX^2mh_2 + NSTXZ + 2K^2V\{NZ^2+L\}mh_2 + 2KNVXYmh_2$$
$$- 4K^2NSTXZm^2h_2^2 - K^2NS^2VXZ - KNSTYZ + 2NVX^2mh_2$$
$$- NVXZ - KNT^2VYZ(1-2mh_1) + 2K^2NV^2XZmh_2 - 2K^2NSTVXZmh_2\rangle e^{mh_1}e^{mH}$$

$$(Num\,C_1)_{14} = \langle TVX(1+2mh_1)\rangle e^{mh_1}e^{3mH}$$

$$(Num\,C_1)_{15} = \langle 4K^2NTVX\{NZ^2+L\}m^2h_2^2 - 2K^2N^2TVXZ^2m^2h_2^2 + 2KN^2TVXYZmh_2$$
$$+ K^2NSV^2X\{NZ^2+L\}mh_1(1+2mh_1) - 2N^2TVX^2Zmh_2 + NTVX\{NZ^2+L\}(1+2mh_1)$$
$$+ N^2SV^2X^3(1+2mh_1) + N^2TVXY^2(1+2mh_1) + K^2LNSV^2X(1+2mh_1) + 2K^2N^2SV^2XZmh_1$$
$$+ KLNTVY(1+2mh_1) + 2K^2NST^2Z\{NZ^2+L\}mh_2(1+2mh_1) - 2K^2NST^2Z\{NZ^2+L\}mh_2(1+4mh_1)$$
$$+ 2KN^2ST^2XYZmh_2(1+2mh_1) + KNST^2Y(1+2mh_1) + N^2ST^2XY^2(1+2mh_1) + LNST^2X(1+2mh_1)$$
$$+ N^2ST^2XZ^2(1-4mh_1) - 8K^2LNT^3Xm^3h_2^3(1+4m^2h_1^2) + 8K^2NT^3Xmh_2\{NZ^2+L\}mh_2(1-2mh_1)$$
$$- 8K^2NTV^2X\{NZ^2+L\}m^3h_1h_2^2 - 4K^2LNTV^2Xm^2h_1h_2 - 8K^2N^2TV^2XZ^2m^3h_1^2h_2$$
$$+ 2K^2NTV^2X\{NZ^2+L\}mh_2(1-2mh_1) + K^2LNST^2Xmh_2(1+4mh_1) - 2KLNT^2Ymh_2(1+4m^2h_1^2)$$
$$+ 4KN^2T^3YZ^2mh^2(1+4m^2h_1^2) - 4KN^2T^3YZ^2mh_2(1-2mh_1) + 2KLNT^3Ymh_2(1-2mh_1)$$
$$+ 4KN^2TVXYZm^2h_1h_2 - K^2NTV^2Z\{NZ^2+L\}(1-2mh_1) + 2KN^2TV^2XYZmh_1(1+2mh_1)$$
$$- N^2TV^2X^3mh_2 - 2N^2TV^2X^3m^2h_1h_2(1+4m^2h_1^2) - 16K^2N^2TVXZ^2m^3h1h_2^2$$
$$- 2K^2NTV^2X\{NZ^2+L\}mh_2(1+4m^2h_1^2) - 8K^2NT^3Xm^3h_2^3\{NZ^2+L\}(1+4m^2h_1^2)$$
$$+ 8N^2T^3X^2Zm^2h_2^2(1+4m^2h_1^2) - 4N^2T^3X^2Zm^2h_2^2(1-2mh_1) - 16KN^2T^3XYZm^2h_2^2(1+2mh1)$$
$$+ 4K^2NST^2X\{NZ^2+L\}m^2h_2^2(1+4mh_1) - 16N^2T^3X^3m^3h_2^3(1+2mh_1) - 4NT^3X\{NZ^2+L\}mh_2(1+2mh_1)$$
$$+ 2KN^2ST^2XYZmh_2(1+4mh_1) - 8KN^2TVXYZm^2h_1h_2 - 16N^2ST^2X^2Zm^2h_1h_2 - N^2ST^2X^2Zmh_2$$
$$+ 4N^2T^3XZ^2mh_2(1-2mh_1) + 2N^2TVX^2Zmh_2(1+2mh_1) - 4K^2LNTVXm^2h_2^2(1+4mh_1)$$
$$+ 4N^2ST^2X^3m^2h_2^2(1+4mh_1) + 2N^2TV^2X^2Zmh_1(1+2mh_1) + 2K^2NTVZ\{NZ^2+L\}mh_2(1+4mh_1)$$
$$+ 4K^2NT^3Z\{NZ^2+L\}m^2h_2^2(1+4mh_1) - 4K^2NT^3Z\{NZ^2+L\}(1-2mh_1) + 2N^2T^3Y^2Zmh_1(1+2mh_1)$$
$$- 4N^2T^3X^2Zm^2h_2^2(1-4mh_1) + 16N^2T^3X^2Zm^4h_1^2h_2^2 + 2NT^3Z\{NZ^2+L\}mh_1(1+2mh_1)$$
$$- KN^2ST^2YZ^2(1+4mh_1) + KN^2TVYZ^2(1+4mh_1) - N^2TVXZ^2(1+2mh_1) - 2K^2LNS^2TXmh_2$$
$$+ KN^2SVXYZ - 2N^2T^3XY^2(1+4mh_1) - 2K^2N^2S^2TXZ^2mh_2 - K^2LNS^2TXmh_2 - 16N^2TVX^3m^3h_1h_2^2$$
$$- 8N2TX3m3h_2^3 - 2N^2S^2TX^2mh_2 - 4N^2T^3XZ^3mh_2(1+4mh_1) + 4N^2TX^2Zm^2h_2^2 + N^2S^2TX^2Z$$
$$+ 2N^2SVX^3mh_2 + 2K^2NSVXmh_2\{NZ_2+L\} - N^2SVX^2Z + 2K^2LNSVXmh_2 + 2KLNTYmh_2$$
$$- KN^2S^2TXYZ + 2N^2T^3XYmh_2 + 8K^2LNT^3Xm^3h_2^3(1-2mh_1) - 4K^2LNT^3Zm^2h_2^2(1-2mh_1)$$
$$+ 4K^2LNT^3Zm^2h_2^2(1-2mh_1) - K^2NTV^2Z\{NZ^2+L\}(1-2mh_1)\rangle e^{mh_1}e^{-mH}$$

$$(Num\,C_1)_{16} = \langle LN^2STVX^2(1+2mh_1) - 4LN^2T^2VX^2m^2h_1h_2(1+2mh_1) + 2LN^2T^2VXZmh_1(1+2mh_1)$$
$$- 8N^3T^2VX^2Z^2m^3h_1^2h_2 + 16N^3T^2VX^3Zm^4h_1^2h_2^2 - 4N^3STVX^3Zm^2h_1h_2 + 4N^3T^2VXZ^3m^2h_1^2$$
$$- 8N^3T^2VX^2Z^2m^3h_1^2h_2 + 2N^2STVX^2Z^2mh_1\rangle e^{mh_1}e^{-3mH}$$

$$(Num\,C_1)_{17} = \langle -4KN^2TVX^2Zm^2h_2^2\rangle e^{3mh_1}e^{2mh_2}e^{-mH}$$

$$(Num\,C_1)_{18} = \langle 8KNT^2X^2m^3h_2^3\rangle e^{3mh_1}e^{-2mh_2}e^{mH}$$

$$(Num\,C_1)_{19} = \langle 4KTVXmh_2\rangle e^{3mh_1}e^{-2mh_2}e^{3mH}$$

$$(Num\,C_1)_{20} = \langle 8N^2T^2X^3m^3h_2^3 - 4N^2T^2X^2Zm^2h_2^2\rangle e^{3mh_1}e^{-mH}$$

$$(Num\,C_1)_{21} = \Big\langle -2NSTXY - 2NT^2VXY(1+2mh_1) - 2KNSTVXZmh_1 - KT^2V\{NZ^2+L\}(1+2mh_1)$$
$$-2KNT^2VXZmh_2(1+2mh_1) - KST\{NZ^2+L\} + 4KNT^2Z^2m^2h_1h_2 - 2KNSTXZmh_2\Big\rangle e^{-mh_1}e^{2mh_2}e^{mH}$$

$$(Num\,C_1)_{22} = \Big\langle -4K^2N^2TVYZ^2mh^2(1+2mh_1) - 4K^2NTVY\{NZ^2+L\}m^2h_1h_2 - 2K^2LNTVYmh_2(1-2mh_1)$$
$$-4K^3NTVZ\{NZ^2+L\}m^2h_2^2(1-2mh_1) - 16K^3NTVZ\{NZ^2+L\}m^3h_1h_2^2 - 2KNTV^2X\{NZ^2+L\}mh_1(1-2mh_1)$$
$$-KNTV^2X\{NZ^2+L\}(1+4m^2h_1^2) - 2KNTV^2Xmh_1\{NZ^2+L\}(1-2mh_1) - KLNTV^2X$$
$$-KN^2TVY^2Z(1+4m^2h_1^2) + 2KN^2TVY^2Zmh_1 + 2KN^2SV^2X^2Zmh_1 + 2KN^2TVXZ^2mh_2$$
$$-2KNTVX\{NZ^2+L\}m^2h_1h_2 + 10KN^2TVXZ^2m^2h_1h_2 - 2KLNTVXmh_2 + 2KNTVZ\{NZ^2+L\}mh_1$$
$$-4KN^2TVX^2Zm^2h_2^2(1+2mh_1) + 2KNST^2X\{NZ^2+L\}mh_2(1-2mh_1) + 8KLNST^2Xm^2h_1h_2$$
$$-4KN^2ST^2XZ^2mh_2 + 2N^2ST^2X^2Ymh_2(1-2mh_1) - 2KNST^2Z\{NZ^2+L\}mh_1 - N^2ST^2XYZ(1+2mh_1)$$
$$+4K^2NST^2Y\{NZ^2+L\}m^2h_1h_2 + 2K^2NST^2Y\{NZ^2+L\}mh_2 + 2K^2N^2ST^2YZ^2mh_2(1-2mh_1)$$
$$-2N^2TV^2X^2Y(1+2mh_1) - 4KLNT^3Xm^2h_2^2(1+2mh_1) - LNT^3Y(1-2mh_1) + N^2TVXYZ(1-4mh_1)$$
$$-K^2LNTV^2Y(1+2mh_1) - K^2NTV^2Y\{NZ^2+L\}(1+2mh_1) - 2KN^2TV^2X^2Zmh_2(1+2mh_1)$$
$$-2K^3NTV^2Z\{NZ^2+L\}mh_2(1+2mh_1) - 8K^3NT^3Z\{NZ^2+L\}m^3h_2^3(1+4m^2h_1^2)$$
$$-16K^3NT^3Zm^2h_1h_2\{NZ^2+L\}(1-2mh_1) + 8KN^2T^3XZ^2m^2h_2^2(1+2mh_1) - 8K^2N^2T^3YZ^2m^2h_2^2(1+2mh_1)$$
$$-4K^2NT^3Y\{NZ^2+L\}m^2h_2^2(1+4m^2h_1^2) - 2KN^2T^3Y^2Zmh_2(1+2mh_1) + 8K^3NST^2Z\{NZ^2+L\}m^3h_1h_2^2$$
$$+4K^3NST^2Z\{NZ^2+L\}(1-2mh_1) - 8KN^2T^3X^2Zm^3h_2^3(1+2mh_1) - 2KNT^3Z\{NZ^2+L\}mh_2(1+2mh_1)$$
$$+4KN^2ST^2X^2Zm^2h_2^2 + 4N^2T^3XYZmh_2(1+2mh_1) - 4KN^2T^3Y^2mh_2(1+2mh_1) - N^2T^3Y^2(1+2mh_1)$$
$$-4N^2T^3X^2Ym^2h_2^2(1+2mh_1) - NT^3Y\{NZ^2+L\}(1+2mh_1) + 2KN^2ST^2Y^2Z - 2KN^2ST^2Y^2Zmh_1$$
$$-2N^2TVX^2Ymh_2 - 2K^3NSV^2Z\{NZ^2+L\}mh_1 - N^2SVX^2Y - KLNSVX - KLNS^2TX - 4KLNTXm^2h_2^2$$
$$-K^2LNSVY - 8K^2N^2TYZ^2m^2h_2^2 - 8K^3NTZ\{NZ^2+L\}m^3h_2^3 + 8KN^2TXZ^2m^2h_2^2 - 2KN^2TZ^3mh_2$$
$$-KLNTZmh_2 - 8KN^2TX^2Zm^2h_2^2 - 2KN^2TY^2Zmh_2 - 4KN^2TY^2Zmh_2 - 4K^2N^2TYZ^2m^2h_2^2$$
$$+4N^2TXYZmh_2 - NTY\{NZ^2+L\} - 4N^2TX^2Ym^2h_2^2 - 4K^2LNTYm^2h_1h_2 + 8KN^2ST^2X^2Ym^2h_1h_2$$
$$-N^2S^2TX^2Y - N^2TY^3 - K^2LNS^2TY - K^2N^2SVYZ^2 - 2K^3NSVZ\{NZ^2+L\}mh_2 - 2KN^2SVX^2mh_2$$
$$+KN^2S^2TXZ^2 - 4KNTVXZ^2m^2h_1h_2 - 8K^2NT^2Ymh_1\{NZ^2+L\}(1-2mh_1) + 4K^2N^2TVYZm^2h_1h_2\Big\rangle$$
$$*\,e^{-mh_1}e^{2mh_2}e^{-mH}$$

$$(Num\,C_1)_{23} = \Big\langle -4KLN^2T^2VX^2m^2h_2^2(1+2mh_1) - KLN^2V^3X^2(1+2mh_1) - LN^2T^2VXY(1+2mh_1)$$
$$+ 2KLN^2STVX^2mh_2(1-2mh_1) - 2KLN^2V^2X^2mh_2 - 16KLN^2T^2X^2m^4h_1h_2^3$$
$$+ 4LN^2T^2XYm^2h_1h_2 - 8KLN^2T^2XZm^3h_1h_2^2 - 2LN^2T^2YZmh_1 - 2KLN^2V^2XZmh_1$$
$$- 2KLN^2STVXZmh_1 - 2KLN^2T^2VXZmh_2(1+2mh_1) - LN^2T^2VXY(1+2mh_1)$$
$$- 4KLN^2STX^2m^2h_2^2 - 2KLN^2VXZmh_2 + 8KN^3T^2VX^2Z^2m^3h_1h_2^2 + 4N^3T^2VX^2YZm^2h_1h_2$$
$$- 4KN^3T^2VXZ^3m^2h_1h_2 - 2N^3T^2VXYZ^2mh_1 - 6KN^3V^3X^2Z^2mh_1 + 8KLN^2STVX^2m^2h_1h_2$$
$$- 2N^3V^2X^2YZmh_1 - 4KN^3V^2X^2Z^2m^2h_1h_2 - KLN^2S^2VX^2 - 8KN^2T^2VXZ^3m^3h_1^2h_2$$
$$+ 16KN^3T^2VX^2Z^2m^4h_1^3h_2 - 4KN^3STVX^2Z^2m^2h_1h_2 - 4N^3T^2VXYZ^2m^2h_1^2$$
$$- LN^2STXY + 8N^3T^2VX^2YZm^3h_1^2h_2 - 2N^3STVX^2Zmh_1\Big\rangle e^{-mh_1}e^{2mh_2}e^{-3mH}$$

$$(Num\,C_1)_{24} = \Big\langle -2K^2NSTVZmh_1 - 2KN^2STVXYZmh_1 - 2KN^2T^2VXYZmh_2(1+2mh_1)$$
$$- 2K^2NT^2VZ\left\{NZ^2+L\right\}mh_2(1+2mh_1) - KNT^2VY\left\{NZ^2+L\right\}(1+2mh_1) - N^2T^2VXY^2(1+2mh_1)$$
$$- KLNT^2VY(1+2mh_1) - 2K^2NSTZ\left\{NZ^2+L\right\}mh_2 + 2K^2N^2T^2Z^3m^3h_1h_2^2 - 2KN^2STXYZmh_2$$
$$- KNSTY\left\{NZ^2+L\right\} + KN^2T^2YZ^2m^2h_1h_2 - N^2STXY^2 - KLNSTY\Big\rangle e^{-mh_1}e^{4mh_2}e^{-mH}$$

$$(Num\,C_1)_{25} = \Big\langle 4K^2LN^2ST^2XZm^2h_2^2 - 2K^2LN^2SV^2XZmh_1 - KLN^2ST^2YZ(1+2mh_1)$$
$$- 8K^2LN^2T^3XZm^3h_2^3(1+2mh_1) - 2K^2LN^2TV^2XZmh_2(1+2mh_1) - 8K^2N^3TV^2XZ^3m^3h_1^2h_2$$
$$- 2KLN^2T^3YZmh_2(1+2mh_1) - 4K^2LN^2TVXZm^2h_2^2(1-2mh_1) - 4KLN^2T^3XYm^2h_2^2(1+2mh_1)$$
$$- KLN^2TV^2XY(1+2mh_1) - 2KN^3TV^2XYZ^2mh_1(1+2mh_1) - LN^2T^3Y^2(1+2mh_1)$$
$$+ 4KLN^2ST^2XYm^2h_1h_2 - 2KLN^2TVXYmh_2 - 4KN^3TVXYZ^2m^2h_1h_2 - KLN^2TV^2XY(1+2mh_1)$$
$$- 2KLN^2TVYZmh_1 - 2K^2LN^2SVXZmh_2 - 4K^2N^3TV^2XZ^3m^2h_1h_2 - 4KN^3TVXYZ^2m^2h_1h_2$$
$$- 8K^2N^2TVXZ\left\{NZ^2+L\right\}m^3h_1h_2^2 - 8K^2LN^2TVXZm^3h_1h_2^2 - 8K^2LN^2TXZm^3h_2^3$$
$$- 2N^3TVXY^2Zmh_1 - KLN^2S^2TXY - 4KLN^2TXYm^2h_2^2 - KLN^2SVXY\Big\rangle e^{-mh_1}e^{4mh_2}e^{-3mH}$$

$$(Num\,C_1)_{26} = \Big\langle -2K^2LN^2STVYZmh_1 - 2K^2LN^2T^2VYZmh_2(1+2mh_1) - KLN^2T^2VY^2(1+2mh_1)$$
$$- 2K^2LN^2STYZmh_2 - KLN^2STY^2\Big\rangle e^{-mh_1}e^{6mh_2}e^{-3mH}$$

$$(Num\,C_1)_{27} = \Big\langle 2K^3STV\{NZ^2+L\}mh_2(1+2mh_1)+16K^2NT^2YZm^3h_1h_2^2+8K^3T^2\{NZ^2+L\}m3h_2^3$$
$$-8K^3T^2\{NZ^2+L\}mh_2(1-2mh_1)+2KNT^2VXZm^2h_1h_2(1+4mh_1)+4KNT^2VXZmh_2(1+4m^2h_1^2)$$
$$+8KNT^2VXZmh_2(1-2mh_1)+4KNT^2Y^2m^2h_1h_2+4KNSTVX^2mh_2(1+2mh_1)-24KNT^2XZm^3h_1h_2^2$$
$$+4KT^2\{NZ^2+L\}m^2h_1h2+32KNT^2X^2m^4h_1h_2^3+4NT^2XYm^2h_1h_2-KNSTVXZ-8KNSTVXZmh_1$$
$$-2NT^2YZmh_1-K^2NV^2YZ(1+2mh_1)-KT^2V\{NZ^2+L\}mh_1(1+2mh_1)-2NT^2VXY(1+2mh_1)$$
$$-8KNT^2VX^2m^2h_2^2(1+2mh_1)-2KNV^3X^2(1+2mh_1)-2KNV^2X^2mh_2(1+4mh_1)$$
$$-2K^2NT^2VYZmh_2(1+4mh_1)-8K^2NT^2VYZm^2h_1h_2(1-2mh_1)-4K^2NSTYZmh_2$$
$$-2KNT^2VY^2(1+2mh_1)-2K^3V^2\{NZ^2+L\}mh_2(1+2mh_1)-2K^3V^3\{NZ^2+L\}$$
$$-4K^3T^2V\{NZ^2+L\}m^2h_2^2(1+4m^2h_1^2)-8K^3T^2V\{NZ^2+L\}mh_1(1-2mh_1)-2K^2NT^2VYZ(1+4m^2h_1^2)$$
$$-2K^2NT^2VYZ(1+2mh_1)-KT^2V\{NZ^2+L\}(1+2mh_1)+K^2NSTVYZ-2K^2NVYZmh_2$$
$$-KST\{NZ^2+L\}-NSTXY-KNS^2VX^2-NVXY-KNSTY^2-K^3S^2V\{NZ^2+L\}-KV\{NZ^2+L\}$$
$$-KNS^2VX^2-KNVY^2-4K^3ST\{NZ^2+L\}m^2h_2^2-8KNSTX^2m^2h_2^2+KNV^2XZ(1-2mh_1)\Big\rangle$$
$$*e^{-mh_1}e^{-2mh_2}e^{mH}$$

$$(Num\,C_1)_{28} = \Big\langle 2KST^2Xmh_2(1+2mh_1)-2KTV^2X(1+2mh_1)-4KT^3Xm^2h_2^2(1+2mh_1)$$
$$-T^3Y(1+2mh_1)-2KTVXmh_2-KS^2TX-TY-KSVX\Big\rangle e^{-mh_1}e^{-2mh_2}e^{3mH}$$

$$(Num\,C_1)_{29} = \Big\langle -KNTV^2X\{NZ^2+L\}(1+2mh_1)-2KN^2TV^2XZ^2mh_1(1+2mh_1)$$
$$-2KLNTV^2Xmh_1(1-2mh_1)-N^2TV^2X^2Y(1+2mh_1)+4KNTVX\{NZ^2+L\}m^2h_1h_2-4KLNTVXm^2h_1h_2$$
$$+4N^2TVX^2Ym^2h_1h_2-KLNTV^2X(1+4mh_1)-2KNTVZmh_1-2N^2TVXYZmh_1+6KN^2TV^2X^2Zm^2h_1h_2$$
$$-4KN^2SV^2X^2Zmh_1-KNSVX\{NZ^2+L\}-KLNSVX+16KN^2TV^2X^2Zm^3h_1^2h_2-N^2SVX^2Y\Big\rangle$$
$$*e^{-mh_1}e^{-2mh_2}e^{-mH}$$

$$(Num\,C_1)_{30} = \Big\langle -2KNTV^2XY(1+2mh_1)+8KNTVXYm^2h_1h_2-K^2TV^2\{NZ^2+L\}(1+2mh_1)$$
$$+4K^2TV\{NZ^2+L\}m^2h_1h_2-2KNTVYZmh_1-2K^2NSV^2XZmh_1-K^2SV\{NZ^2+L\}$$
$$+12K^2NTV^2XZm^2h_1h_2-2KNSVXY\Big\rangle e^{-mh_1}e^{-4mh_2}e^{mH}$$

$$(Num\,C_1)_{31} = \Big\langle -4K^2T^2VXm^2h_2^2(1+2mh_1)-K^2V^3X(1+2mh_1)-2KT^2VY(1+2mh_1)$$
$$-2K^2V^2Xmh_2+2K^2STVXmh_2(1+2mh_1)+16K^2T^2Xm^4h_1h_2^3+4KT^2Ym^2h_1h_2-4K^2STXm^2h_2^2$$
$$-K^2S^2VX-KVY-KSTY\Big\rangle e^{-mh_1}e^{-4mh_2}e^{3mH}$$

$$(Num\,C_1)_{32} = \Big\langle -K^2TV^2Y(1+2mh_1)+4K^2TVYm^2h_1h_2-K^2SVY\Big\rangle e^{-mh_1}e^{-6mh_2}e^{3mH}$$

$$(Num\,C_1)_{33} = \Big\langle 2K^2ST^2\{NZ^2+L\}mh_2(1+2mh_1) + 2KNST^2XYmh_2(1+2mh_1) - 2K^2NSV^2$$
$$- 4K^2NTVXZm^2h_2^2(1+2mh_1) + 2NST^2X^2mh_2(1+2mh_1) - NST^2XZ(1+2mh_1) - KNTVYZ(1+2mh_1)$$
$$- 2KNTV^2XY(1+2mh_1) - 2K^2TV^2\{NZ^2+L\}(1+2mh_1) + 4K^2NTVZ^2m^2h_1h_2 - 2K^2TV\{NZ^2+L\}mh_2$$
$$- 8K^2NT^3XZm^3h_2^3(1+2mh_1) - 6KNT^3YZmh_2(1+2mh_1) - 2K^2NTV^2XZmh_2(1+2mh_1)$$
$$+ 4K^2NST^2XZm^2h_2^2 - 4KNT^3XYm^2h_2^2(1+2mh_1) - 2NT^3Y^2(1+2mh_1) - 2KNTVXYmh_2$$
$$- 2NTV^2X^2(1+2mh_1) - 4K^2T^3\{NZ^2+L\}m^2h_2^2(1+4m^2h_1^2) - 8K^2T^3\{NZ^2+L\}mh_1(1-2mh_1)$$
$$+ 4NT^3XZmh_2(1+2mh_1) - 4NT^3X^2m^2h_2^2(1+2mh_1) - T^3\{NZ^2+L\}(1+2mh_1) + KNST^2YZ$$
$$- 2NTVX^2mh_2 + NTVXZ(1-2mh_1) - K^2SV\{NZ^2+L\} - KNSVXY - 2K^2NTXZm^3h_2^3 - 2KNTYZmh_2$$
$$- 4KNTXYm^2h_2^2 - KNS^2TXY - 2NTY^2 - NSVX^2 - K^2S^2T\{NZ^2+L\} - 4KNTYZmh_2$$
$$- 4K^2T\{NZ^2+L\}mh_2 + 4NTXZmh_2 - T\{NZ^2+L\} - 4NTX^2m^2h_2^2 - NS^2TX^2 - 2K^2NSVXZmh_2\Big\rangle$$
$$* e^{-mh_1}e^{mH}$$

$$(Num\,C_1)_{34} = \Big\langle -T^2VX(1+2mh_1) - STX\Big\rangle e^{-mh_1}e^{3mH}$$

$$(Num\,C_1)_{35} = \Big\langle 2K^2NSTVX\{NZ^2+L\}mh_2(1+2mh_1) + 2K^2LNSTVXmh_2(1+2mh_1)$$
$$-4K^2N^2STVXZ^2m^2h_1h_2 + 16KN^2T^2XYZm^3h_1h_2^2 + 8K^2NT^2Xm^3h_2^3\{NZ^2+L\}$$
$$-8K^2NT^2X\{NZ^2+L\}mh_2(1-2mh_1) + 16K^2LNT^2Xm^3h_2^3 + 4N^2T^2VX^2Z(1-2mh_1)$$
$$+8N^2T^2VX^2Zm^2h_1h_2 + 4N^2T^2VX^2Zmh_2(1+4m^2h_1^2) + 4N^2T^2XY^2m^2h_1h_2$$
$$+2N^2STVX^3mh_2(1+2mh_1) - 8N^2T^2X^2Zm^2h_2^2 - 8N^2T^2X^2Zm^2h_2^2(1-2mh_1)$$
$$+4NT^2X\{NZ^2+L\}m^2h_1h_2 + 8N^2T^2XZ^2m^2h_1h_2 + 18N^2T^2X^3m^4h_1h_2^3 - 2K^2NSTVZ\{NZ^2+L\}mh_1$$
$$-8KN^2T^2YZ^2m^2h_1h_2 + 4KLNT^2Ym^2h_1h_2 - 4K^2NT^2Z\{NZ^2+L\}m^2h_2^2 + 4K^2NT^2Z\{NZ^2+L\}(1-2mh_1)$$
$$-2NT^2VX\{NZ^2+L\}mh_1 - LNT^2VX - 4N^2T^2VXZ^2m^2h_1^2 - 2NT^2VX\{NZ^2+L\}mh_1(1-2mh_1)$$
$$-2N^2T^2Y^2Zmh_1 - N^2STVX^2Z - 8N^2STVX^2Zmh_1 - 2NT^2Z\{NZ^2+L\}mh_1$$
$$+8K^2N^2T^2VXZ^2m^3h_1h_2^2(1+2mh_1) - 4K^2LNT^2VXm^2h_2^2(1-2mh_1)$$
$$-4K^2NT^2VX\{NZ^2+L\}m^2h_2^2(1+4m^2h_1^2) - 8K^2NT^2VXmh_1\{NZ^2+L\}(1-2mh_1)$$
$$-8K^2LNT^2VXm^3h_1h_2^2(1-2mh_1) - 6KN^2T^2VXYZmh_2(1+2mh_1) - 4KN^2T^2VXYZm^2h_1h_2(1-2mh_1)$$
$$-2K^2NV^2Z\{NZ^2+L\}mh_1 - NT^2VX\{NZ^2+L\}(1+4m^2h_1^2) - K^2NV^3X\{NZ^2+L\}(1-2mh_1)$$
$$-2K^2NV^3X\{NZ^2+L\}mh_1(1+2mh_1) - K^2LNV^3X + 4K^2LNV^3Xm^2h_1^2 - KN^2V^2XYZ$$
$$-KLNT^2VY(1+2mh_1) - 2K^2NV^2X\{NZ^2+L\}mh_2(1+2mh_1) - 2K^2LNV^2Xmh_2(1-2mh_1)$$
$$-2K^2NT^2VZ\{NZ^2+L\}mh_2(1+2mh_1) - 4KN^2STXYZmh_2 - KNT^2VY\{NZ^2+L\}(1+2mh_1)$$
$$+KN^2STVXYZ(1-4mh_1) - 2N^2T^2VXY^2(1+2mh_1) - N^2V^3X^3(1+2mh_1)$$
$$-4N^2T^2VX^3m^2h_1h_2(1+2mh_1) + 2KN^2STVXYZmh_1 - 4KN^2VXYZmh_1 - 4KN^2XYZmh_2$$
$$+2KN^2VXYZmh_2 - 2N^2V^2X^3mh_2 - K^2LNS^2VX - KLNSTY - N^2STXY^2 - LNSTX$$
$$-K^2NS^2VX\{NZ^2+L\} - LNVX - N^2SVX^3 - N^2VXY^2 - 4K^2NSTX\{NZ^2+L\}m^2h_2^2$$
$$-4K^2LNSTXm^2h_2^2 - 4N^2STX^3m^2h_2^2 - 2N^2STX^2Zmh_2 - KN^2VYZ^2 - 2K^2NVZ\{NZ^2+L\}mh_2$$
$$+N^2V^2X^2Z(1-2mh_1) + 2N^2STX^2Zmh_2 + N^2STXZ^2\Big\rangle e^{-mh_1}e^{-mH}$$

$$(Num\,C_1)_{36} = \Big\langle -LN^2TV^2X^2(1+2mh_1) + 4LNTVX^2m^2h_1h_2 - 2LN^2TVXZmh_1 + 4N^3TV^2X^3Zm^2h_1h_2$$
$$-2N^3TV^2X^2Z^2mh_1 - 4N^3TV^2X^2Z^2m^2h_1^2 - LN^2SVX^2 + 8N^3TV^2X^3Zm^3h_1^2h_2 - 2N^3SV^2X^3Zmh_1\Big\rangle$$
$$*\,e^{-mh_1}e^{-3mH}$$

$$(Num\,C_1)_{37} = \Big\langle 2NST^2XY + KST^2\{NZ^2+L\} + 2KNST^2XZmh_2\Big\rangle e^{-3mh_1}e^{2mh_2}e^{mH}$$

$$(Num\,C_1)_{38} = \Big\langle 2K^3NSTVZ\{NZ^2+L\}mh_2 + 8K_3NT^2Z\{NZ^2+L\}m^3h_2^3 + 2KNT^2Z\{NZ^2+L\}mh_2$$
$$+4K^2NT^2Y\{NZ^2+L\}m^2h_2^2 + KNSTVX\{NZ^2+L\} + K^2NSTVY\{NZ^2+L\} + 8K^2N^2T^2YZ^2m^2h_2^2$$
$$+NT^2Y\{NZ^2+L\} + 8KN^2T^2VXZ^2m^2h_1h_2 + 6KN^2T^2Y^2Zmh_2 + 2KN^2STVX^2Zmh_2 - 8KN^2T^2XZ^2m^2h_2^2$$
$$+8KN^2T^2X^2Zm^3h_2^3 + 4N^2T^2VXYZmh_1 + N^2T^2Y^3 + N^2STVX^2Y - 4N^2T^2XYZmh_2 + 4N^2T^2X^2Ym^2h_2^2$$
$$+N^2ST^2X^2Y + LNT^2Y + KLNSTVX + 4KLNT^2Xm^2h_2^2 + K^2LNSTVY\Big\rangle e^{-3mh_1}e^{2mh_2}e^{-mH}$$

$$(Num\,C_1)_{39} = \left\langle 8KN^3TV^2X^2Z^2m^2h_1h_2 + 2LN^2TVXY + 4N^3TV^2X^2YZmh_1 + KLN^2SV^2X^2 \right.$$
$$\left. + 4KLN^2TVX^2m^2h_2^2 + 2KLN^2TVXZmh_2 \right\rangle e^{-3mh_1}e^{2mh_2}e^{-3mH}$$

$$(Num\,C_1)_{40} = \left\langle 2K^2N^2ST^2Z^3mh_2 + 2KN^2ST^2XYZmh_2 + 2KLNST^2Zmh_2 + KN^2ST^2YZ^2 + N^2ST^2XY^2 \right.$$
$$\left. + LNST^2Y + KLNST^2Y \right\rangle e^{-3mh_1}e^{4mh_2}e^{-mH}$$

$$(Num\,C_1)_{41} = \left\langle 2KLN^2STVXY + 4K^2N^3T^2VXZ^3m^3h_1h_2^2 + 4KN^3T^2VXYZ^2m^2h_1h_2 + 2KLN^2T^2YZmh_2 \right.$$
$$+ 2K^2LN^2STVXZmh_2 + 8K^2LN^2T^2XZm^3h_2^3 + 4KN^3T^2VXYZ^2m^2h_1h_2 + 2N^3T^2VXY^2Zmh_1$$
$$\left. + LN^2T^2Y^2 + 4KLN^2T^2XY \right\rangle e^{-3mh_1}e^{4mh_2}e^{-3mH}$$

$$(Num\,C_1)_{42} = \left\langle 2K^2LN^2ST^2YZmh_2 + KLN^2ST^2Y^2 \right\rangle e^{-3mh_1}e^{6mh_2}e^{-3mH}$$

$$(Num\,C_1)_{43} = \left\langle 2KNSV^2X^2 + 2NTVXY + 2KNTVY^2 + 6K^2NTVYZmh_2 + 8KNTVX^2m^2h_2^2 \right.$$
$$+ 2KTV\left\{NZ^2 + L\right\} + 4KNTV^2XZmh_1 + 4K^3TV\left\{NZ^2 + L\right\}m^2h_2^2 + K^2SV^2\left\{NZ^2 + L\right\} - 4KNTVXZmh_2 \Big\rangle$$
$$* e^{-3mh_1}e^{-2mh_2}e^{mH}$$

$$(Num\,C_1)_{44} = \left\langle 2KSTVX + T^2Y + 4KT^2Xm^2h_2^2 \right\rangle e^{-3mh_1}e^{-2mh_2}e^{3mH}$$

$$(Num\,C_1)_{45} = \left\langle 4KN^2V^3X^2Zmh_1 + 2KLNV^2X + KN^2V^2XZ^2 + N^2V^2X^2Y \right\rangle e^{-3mh_1}e^{-2mh_2}e^{-mH}$$

$$(Num\,C_1)_{46} = \left\langle 2KNV^2XY + K^2V^2\left\{NZ^2 + L\right\} + 2K^2NV^3XZmh_1 \right\rangle e^{-3mh_1}e^{-4mh_2}e^{mH}$$

$$(Num\,C_1)_{47} = \left\langle 2KTVY + K^2SV^2X + 4K^2TVXm^2h_2^2 \right\rangle e^{-3mh_1}e^{-4mh_2}e^{3mH}$$

$$(Num\,C_1)_{48} = \left\langle K^2V^2Y \right\rangle e^{-3mh_1}e^{-6mh_2}e^{3mH}$$

$$(Num\,C_1)_{49} = \left\langle 2NSTVX^2 + 2NT^2Y^2 + 2KNSTVXY + 2K^2NSTVZ^2 + 6KNT^2YZmh_2 \right.$$
$$+ 2K^2LSTV + 4K^2T^2\left\{NZ^2 + L\right\}m^2h_2^2 + 2NT^2VXZmh_1 - 4NT^2XZmh_2 + T^2\left\{NZ^2 + L\right\}$$
$$\left. + 4NT^2X^2m^2h_2^2 + 2K^2NSTVXZmh_2 + 8K^2NT^2XZm^3h_2^3 + 4KNT^2XYm^2h_2^2 \right\rangle e^{-3mh_1}e^{mH}$$

$$(Num\,C_1)_{50} = \left\langle ST^2X \right\rangle e^{-3mh_1}e^{3mH}$$

$$(Num\,C_1)_{51} = \Big\langle 2N^2TVXY^2 + 4N^2TV^2X^2Zmh_1 + NTVX\left\{NZ^2 + L\right\} + LNTVX$$
$$+ 8K^2N^2TV^2XZ^2m^2h_1h_2 + 4KN^2TV^2XYZmh_1 + 6KN^2TVXYZmh_2 + K^2NSV^2X\left\{NZ^2 + L\right\}$$
$$+ K^2LNSV^2X + 4K^2NTVXZ^2m^2h_2^2 - 4N^2TVX^2Zmh_2 + 4N^2TVX^3m^2h_2^2 + 8K^2LNTVXm^2h_2^2$$
$$\Big\langle + 2K^2N^2TVZ^3mh_2 + KNTVY\left\{NZ^2 + L\right\}\Big\rangle e^{-3mh_1}e^{-mh}$$

$$(Num\,C_1)_{52} = \Big\langle 2N^3V^3X^3Zmh_1 + LN^2V^2X^2\Big\rangle e^{-3mh_1}e^{-3mH}$$

A.1.2 The list of Denominator C_1

$$(Denom\,C_1)_1 = \Big\langle -2NVXY - KV\left(NZ^2 + L\right) - 2KNV^2XZmh_1 - 2KNVXZmh_2\Big\rangle e^{2mh_1}e^{2mh_2}e^{mH}$$

$$(Denom\,C_1)_2 = \Big\langle -2LNTY - 2KLNSVX - 4KNTV\left(NZ^2 + L\right)mh_1 - 2K^2LNSVY - 2N^2SVX^2Y$$
$$+ 4KNTVX\left(NZ^2 + L\right)m^2h_1h_2 - 4K^2NTY\left(NZ^2 + L\right)m^2h_2^2 - 8K^3NTVZ\left(NZ^2 + L\right)m^3h_1h_2^2$$
$$- 8K^2N^2TVYZ^2m^2h_1h_2 - 2K^3NSV^2Z\left(NZ^2 + L\right)mh_1 - 8KN^2TVXZ^2m^2h_1h_2$$
$$- 2KN^2SV^2X^2Zmh_1 - 2KN^2TVY^2Zmh_1 - 8KN^2TVX^2Zm^3h_1h_2^2 - 8K^3NTZ\left(NZ^2 + L\right)m^3h_2^3$$
$$- 8K^2N^2TYZ^2m^2h_2^2 - 2K^3NSVZ\left(NZ^2 + L\right)mh_2 + 8KN^2TXZ^2m^2h_2^2 - 2KNTZ\left(NZ^2 + L\right)mh_2$$
$$- 2KN^2SVX^2Zmh_2 - 2KN^2TY^2Zmh_2 - 8KN^2TX^2Zm^3h_2^3 - 4KN^2TY^2Zmh_2 - K^2N^2SVYZ^2$$
$$+ 4N^2TXYZmh_2 - N^2TYZ^2 - N^2TY^3 - 4N^2TX^2Ym^2h_2^2 + 4N^2TVX^2Ym_2h_1h_2$$
$$- 2N^2TVXYZmh_1 - KN^2SVXZ^2 - 4KLNTXm^2h_2^2 + 4K^2LNTVYm_2h_1h_2\Big\rangle e^{2mh_1}e^{4mh_2}e^{-mH}$$

$$(Denom\,C_1)_3 = \Big\langle -2LN^2STXY - 4KLN^2STVXZmh_1 + 16KLN^2T^2X^2m^4h_1h_2^3$$
$$+ 4KLN^2STVX^2m^2h_1h_2 + 4LN^2T^2XYm^2h_1h_2 - 8KLN^2T^2XZm^3h_1h_2^2 - 8KLN^2T^2XZm^3h_1h_2^2$$
$$- 2LN^2T^2YZmh_1 - 4KLN^2STX^2m^2h_2^2 - KLN^2S^2VX^2 - 2KLN^2STXZmh_2\Big\rangle e^{2mh_1}e^{2mh_2}e^{-3mH}$$

$$(Denom\,C_1)_4 = \Big\langle -2KLNVY - 2K^2NV^2Z\left(NZ^2 + L\right)mh_1 - 2KN^2V^2XYZmh_1$$
$$- 2K^2NVZ\left(NZ^2 + L\right)mh_2 - 2KN^2VXYZmh_2 - KN^2VYZ^2 - N^2VXY^2\Big\rangle e^{2mh_1}e^{4mh_2}e^{-mH}$$

$$(Denom\,C_1)_5 = \Big\langle -2KLN^2SVYZ - 4KLN^2TVYZmh_1 - 8K^2LN^2TVXZm^3h_1h_2^2 - 2K^2LN^2SV^2XZmh_1$$
$$- 8K^2LN^2TXZm^3h_2^3 - 2K^2LN^2SVXZmh_2 - 2KLN^2TYZmh_2 - 4KLN^2TXYm^2h_2^2 - LN^2TY^2$$
$$+ 4KLN^2TVXYm^2h_1h_2\Big\rangle e^{2mh_1}e^{4mh_2}e^{-3mH}$$

$$(Denom\,C_1)_6 = \Big\langle -2K^2LN^2V^2YZmh_1 - 2K^2LN^2VYZmh_2 - KLN^2VY^2\Big\rangle e^{2mh_1}e^{6mh_2}e^{-3mH}$$

$$(Denom\,C_1)_7 = \langle -2KST(NZ^2+L) - 2KNSTY^2 + 32KNT^2X^2m^4h_1h_2^3 - 2NSTXY$$
$$+ 8KNSTVX^2m^2h_1h_2 - 8KNSTX^2m^2h_2^2 - 2KNS^2VX^2 - 24KNT^2XZm^3h_1h_2^2 - 6K^2NSTYZmh_2$$
$$- 16K^3T^2(NZ^2+L)m^4h_1h_2^3 + 16K^2NT^2YZm^3h_1h_2^2 + 4K^3STV(NZ^2+L)m^2h_1h_2$$
$$+ 4KT^2(NZ^2+L)m^2h_1h_2 + 4KNT^2Y^2m^2h_1h_2 - 4K^3ST(NZ^2+L)m^2h_2^2 + K^3S^2V(NZ^2+L)$$
$$+ 4KNSTXZmh_2 + 4NT^2XYm^2h_1h_2 - 2KNSTVXZmh_1 - 2NT^2YZmh_1 - 2K^2NSTVYZmh_1\rangle$$
$$* e^{2mh_1}e^{-2mh_2}e^{mH}$$

$$(Denom\,C_1)_8 = \langle -2KSVX - 4KTXm^2h_2^2 + 4KTVXm^2h_1h_2\rangle e^{2mh_1}e^{-2mh_2}e^{3mH}$$

$$(Denom\,C_1)_9 = \langle 4KNST^2X(NZ^2+L)m^2h_1h_2 - KS^2TX(NZ^2+L) + 4N^2ST^2X^2Ym^2h_1h_2$$
$$- 2KNST^2Z(NZ^2+L)mh_1 - 2N^2ST^2XYZmh_1 - N^2S^2TX^2Y + 4KLNST^2Xm^2h_1h_2 - KLNS^2TX\rangle$$
$$* e^{2mh_1}e^{-2mh_2}e^{-mH}$$

$$(Denom\,C_1)_{10} = \langle -2KNS^2TXY + 8KNST^2XYm^2h_1h_2 + 4K^2ST^2(NZ^2+L)m^2h_1h_2$$
$$- K^2S^2T(NZ^2+L) - 2KNST^2YZmh_1\rangle e^{2mh_1}e^{-4mh_2}e^{mH}$$

$$(Denom\,C_1)_{11} = \langle -2KSTY + 4K^2STVXm^2h_1h_2 + 4K^2T^2Ym^2h_1h_2 + 16K^2T^2Xm^4h_1h_2^3 - K^2S^2VX$$
$$- 4K^2STXm^2h_2^2\rangle e^{2mh_1}e^{-4mh_2}e^{3mH}$$

$$(Denom\,C_1)_{12} = \langle 4K^2ST^2Ym^2h_1h_2 - K^2S^2TY\rangle e^{2mh_1}e^{-6mh_2}e^{3mH}$$

$$(Denom\,C_1)_{13} = \langle -2NSVX^2 - 2NTY^2 - 2KNSVXY - 6KNTYZmh_2 - 2K^2SV(NZ^2+L)$$
$$- 4K^2T(NZ^2+L)m^2h_2 + 4NTXZmh_2 - T(NZ^2+L) - 4NTX^2m_2h_2^2 + 4K^2TV(NZ^2+L)m^2h_1h_2$$
$$+ 4KNTVXYm^2h_1h_2 - 2K^2NSV^2XZmh_1 - 2KNTVYZmh_1 - 8K^2NTVXZm^3h_1h_2^2 - 2K^2NSVXZmh_2$$
$$- 8K^2NTXZm^3h_2^3 - 4KNTXYm^2h_2^2 + 4NTVX^2m^2h_1h_2 - 2NTVXZmh_1\rangle e^{2mh_1}e^{mH}$$

$$(Denom\,C_1)_{14} = \langle -VX\rangle e^{2mh_1}e^{3mH}$$

$$(Denom\,C\,)_{15} = \langle -2NSTX\left(NZ^2+1\right)-2N^2STXY^2-KNSTY\left(NZ^2+L\right)-6KN^2STXYZmh_2$$
$$+16K^2NT^2X\left(NZ^2+L\right)m^4h_1h_2^3-4K^2NSTX\left(NZ^2+L\right)m^2h_2^2-K^2NS^2VX\left(NZ^2+L\right)$$
$$-4K^2NSTVZ\left(NZ^2+L\right)mh_1+4K^2NSTVX\left(NZ^2+L\right)m^2h_1h_2+16KN^2T^2XYZm^3h_1h_2^2$$
$$-16N^2T^2X^2Zm^3h_1h_2^2+4NT^2X\left(NZ^2+L\right)m^2h_1h_2+4N^2STVX^3m^2h_1h_2+4N^2T^2XY^2m^2h_1h_2$$
$$+16N^2T^2X^3m^4h_1h_2^3-8K^2NT^2Z\left(NZ^2+L\right)m^3h_1h_2^2-8KN^2T^2YZ^2m^2h_1h_2+8N^2T^2XZ^2m^2h_1h_2$$
$$-2NT^2Z\left(NZ^2+L\right)mh_1-2N^2STVX^2Zmh_1-2N^2T^2Y^2Zmh_1-8N^2T^2X^2Zm^3h_1h_2^2+4N^2STX^2Zmh_2$$
$$-N^2S^2VX^3-4N^2STX^3m^2h_2^2+16K^2LNT^2Xm^4h_1h_2^3+4K^2LNSTVXm^2h_1h_2+4KLNT^2Ym^2h_1h_2$$
$$-4K^2LNSTXm^2h_2^2-K^2LNS^2VX-KLNSTY-2KN^2STVXYZmh_1-2K^2NSTZ\left(NZ^2+L\right)mh_2\rangle$$
$$*\,e^{2mh_1}e^{-mH}$$

$$(Denom\,C_1)_{16} = \left\langle 4LN^2ST^2X^2m^2h_1h_2-2LN^2ST^2XZmh_1-LN^2S^2TX^2\right\rangle e^{2mh_1}e^{-3mH}$$

$$(Denom\,C_1)_{17} = \langle -3NSTXY-2NT^2VXY\left(1+4m^2h_1^2\right)-4KNSTXZmh_2+4KNST^2X\left(NZ^2+L\right)m^2h_1h_2$$
$$+4N^2ST^2X^2Ym^2h_1h_2-2KNST^2Z\left(NZ^2+L\right)mh_1-2N^2ST^2XYZmh_1-KNS^2TX\left(NZ^2+L\right)$$
$$-N^2S^2TX^2Y-2KNSTVXZmh1-KT2V\left(NZ2+L\right)\left(1+4m^2h_1^2\right)-KST\left(NZ^2+L\right)-4KNT^2Z^2m^2h_1h_2$$
$$-2KNT^2VXZmh_1\left(1+4m^2h_1^2\right)\rangle e^{-2mh_1}e^{2mh_2}e^{mH}$$

$$(Denom\,C_1)_{18} = \langle -2NTY\left(NZ^2+L\right)-2KLNSVX-4KNTZ\left(NZ^2+L\right)mh_2-8K^2NTY\left(NZ^2+L\right)m^2h_2^2$$
$$+8N^2TXYZmh_2-6N^2TVXYZmh_1-K^2NSVY\left(NZ^2+L\right)-2N^2TY^3-2N^2SVX^2Y-12N^2TX^2Ym^2h_2^2$$
$$-10KN^2TY^2mh_2-24KN^2TX^2Zm^3h_2^3+16KN^2TXZ^2m^2h_2^2-8KLNTXm^2h_2^2$$
$$-16K^3NTZ\left(NZ^2+L\right)m^3h_2^3-16K^2N^2TYZ^2m^2h_2^2-2N^2S^2TX^2Y+12K^2LNST^2Ym^2h_1h_2$$
$$-2K^2LNS^2TY-2KNTV^2X\left(NZ^2+L\right)\left(1+4m^2h_1^2\right)-2KNSTZ\left(NZ^2+L\right)mh_1-2LNT^3Y\left(1+4m^2h_1^2\right)$$
$$-N^2T^3YZ^2\left(1+4m^2h_1^2\right)-2N^2TV^2X^2Y\left(1+4m^2h_1^2\right)-16K^2N^2TVYZ^2m^2h_1h_2$$
$$+16K^2N^2ST^2YZ^2m^2h_1h_2-6N^2ST^2XYZmh_1-2K^3NSV^2Z\left(NZ^2+L\right)mh_1-8K^2N^2TVYZ^2m^2h_1h_2$$
$$-8K^3NTVZm^3h_1h_2^2-4KN^2TV^2XZ^2m^2h_1^2-2KNTVZ\left(NZ^2+L\right)mh_1-8KN^2TVX^2Zm^3h_1h_2^2$$
$$-2KN^2TVY^2Zmh_1-2KN^2SV^2X^2Zmh_1-2K^3NSVZ\left(NZ^2+L\right)mh_2-2KN^2SVX^2Zmh_2$$
$$+4KNST^2X\left(NZ^2+L\right)m^2h_1h_2+4KLNST^2Xm^2h_1h_2+4KLNST^2Xm^2h_1h_2-KNS^2TX\left(NZ^2+L\right)$$
$$-2N^2TVXYZmh_1-LNTY-KN^2SVXZ^2-4KLNT^3Xm^2h_2^2\left(1+4m^2h_1^2\right)+8KLNST^2Xm^2h_1h_2$$
$$-8KLNTVXm^2h_1h_2-KLNS^2TX-K^2LNSVY-K^2LNTV^2Y\left(1+4m^2h_1^2\right)$$
$$-2KN^2TV^2X^2Zmh_2\left(1+4m^2h_1^2\right)-16K^3NTVZ\left(NZ^2+L\right)m^3h_1h_2^2$$
$$-2K^3NTV^2Zmh_2\left(NZ^2+L\right)\left(1+4m^2h_1^2\right)-8K^3NT^3Zm^3h_2^3\left(NZ^2+L\right)\left(1+4m^2h_1^2\right)$$
$$+8KN^2T^3XZ^2m^2h_2^2\left(1+4m^2h_1^2\right)-8K^2N^2T^3YZ^2m^2h_2^2\left(1+4m^2h_1^2\right)-KN^2T^3Y^2Zmh2\left(1+4m^2h_1^2\right)$$
$$+16K^3NST^2Zm^3h_1h_2^2-2K^3N^2S^2TZ^3mh_2-8KN^2T^3X^2Zm^3h_2^3\left(1+4m^2h_1^2\right)$$
$$-2KNT^3Zmh_2\left(NZ^2+L\right)\left(1+4m^2h_1^2\right)-8KN^2ST^2XZ^2m^2h_1h_2-16KN^2TVX^2Zm^3h_1h_2^2$$
$$+4KNTVXZm^2h_1h_2+16KN^2ST^2X^2Zm^3h_1h_2^2-2KNS^2TX^2Zmh_2-2KN^2TY^2Zmh_2$$
$$-2K^2LNS^2TZmh_2-K^2NTV^2Y\left(NZ^2+L\right)\left(1+4m^2h_1^2\right)-4K^2NT^3Ym^2h_2^2\left(NZ^2+L\right)\left(1+4m^2h_1^2\right)$$
$$+4N^2T^3XYZmh_2\left(1+4m^2h_1^2\right)-4KN^2T^3Y^2Zmh_2\left(1+4m^2h_1^2\right)-N^2T^3Y^3\left(1+4m^2h_1^2\right)$$
$$-K^2N^2S^2TYZ^2-4N^2T^3X^2Ym^2h_2^2\left(1+4m^2h_1^2\right)+4KN^2ST^2Y^2Zmh_1-4KN^2TVY^2Zmh_1$$
$$-8N^2TVX^2Ym^2h_1h_2-8K^2LNTVYm^2h_1h_2+8N^2ST^2X^2Ym^2h_1h_2\rangle e^{-2mh_1}e^{2mh_2}e^{-mH}$$

$$(Denom\,C_1)_{19} = \langle 16KN^2T^2X^2\left(NZ^2+L\right)m^4h_1h_2^3+16N^3T^2VX^2YZm^3h_1^2h_2-2LN^2STXY$$
$$-2LN^2T^2VXY\left(1+4m^2h_1^2\right)-8N^3T^2VXYZ^2m^2h_1^2+12KLN^2STVX^2m^2h_1h_2$$
$$-8KN^3V^3X^2Z^2m^2h_1^2-16KN^3T^2VXZ^3m^3h_1^2h_2-4N^3STVX^2YZmh_1-2KLN^2S^2VX^2$$
$$-4N^3V^2X^2YZmh_1-8KN^2V^2X^2Z^2m^2h_1h_2-8KN^3STVX^2Z^2m^2h_1h_2+4LN^2T^2XYm^2h_1h_2$$
$$-2LN^2T^2YZmh_1-2KLN^2STVXZmh_1-8KLN^2T^2XZm^3h_1h_2^2-4KLN^2STX^2m^2h_2^2$$
$$-2KLN^2V^2XZmh_1-2KLN^2VXZmh_2-LN^2VXY-4KLNT^2VXm^2h_2^2\left(1+4m^2h_1^2\right)$$
$$-KLN^2V^3X^2\left(1+4m^2h_1^2\right)-8KLN^2V^2X^2m^2h_1h_2-4KLN^2VX^2m^2h_2^2$$
$$-2KLN^2T^2VXZmh_2\left(1+4m^2h_1^2\right)-2KLN^2STXZmh_2+16KN^3T^2VX^2Z^2m^4h_1^2h_2^2\rangle$$
$$*\,e^{-2mh_1}e^{2mh_2}e^{-3mH}$$

$$(Denom\,C1)_{20} = \langle -2KLNSTY - 2KNSTY\left(NZ^2 + L\right) - 4K^2NSTZ\left(NZ^2 + L\right)mh_2$$
$$-4KN^2STXYZmh_2 - 2N^2STXY^2 - 2K^2NSTVZ\left(NZ^2 + L\right)mh_1 - 2KN^2STVXYZmh_1$$
$$-2KN^2T^2VXYZmh_2(1+4m^2h_1^2) - 2K^2NT^2VZ\left(NZ^2 + L\right)mh_2(1+4m^2h_1^2)$$
$$+8K^2N^2T^2Z^3m^3h_1h_2^2 - N^2T^2VXY^2(1+4m^2h_1^2) - KNT^2VY\left(NZ^2 + L\right)(1+4m^2h_1^2)$$
$$+4KN^2T^2YZ^2m^2h_1h_2 - KLNT^2VY(1+4m^2h_1^2)\rangle e^{-2mh_1}e^{4mh_2}e^{-mH}$$

$$(Denom\,C_1)_{21} = \langle -2KLN2S2TXY - 8KLN^2TXYm^2h_2^2 - 2KLN^2SVXY + 12KLN^2ST^2XYm^2h_1h_2$$
$$-8K^2N^2TVXZ\left(NZ^2 + L\right)m^3h_1h_2^2 - 16K^2LN^2TXZm^3h_2^3 - 16KN^3TVXYZ^2m^2h_1h_2$$
$$-4N^3TVXY^2Zmh_1 - 8KN^3TV^2XYZ^2m^2h_1^2 - 16K^2N^3TV^2XZ^3m^3h_1^2h_2 - 8KLN^2TVXYm^2h_1h_2$$
$$-KLN^2TVXY\left(1+4m^2h_1^2\right) - 2KLN^2TVYZmh_1 - 2K^2LN^2SV^2XZmh_1 - 2KLN^2TYZmh_2$$
$$-2K^2LN^2SVXZmh_2 - LN^2TY^2 - 2KLN^2ST^2YZmh_1 - 8K^2LN^2T^3XZm^3h_2^3\left(1+4m^2h_1^2\right)$$
$$-2K^2LN^2TV^2XZmh_2\left(1+4m^2h_1^2\right) + 16K^2LN^2ST^2XZm^3h_1h_2^2 - 2KLN^2T^3YZmh_2\left(1+4m^2h_1^2\right)$$
$$-8K^2N^3TVXZ^3m^3h_1h_2^2 - 16K^2LN^2TVXZm^3h_1h_2^2 - 2K^2LN^2S^2TZmh_2$$
$$-4KLN^2T^3XYm^2h_2^2\left(1+4m^2h_1^2\right) - KLN^2TV^2XY\left(1+4m^2h_1^2\right) - LN^2T^3Y^2\left(1+4m^2h_1^2\right)\rangle$$
$$*\,e^{-2mh_1}e^{4mh_2}e^{-3mH}$$

$$(Denom\,C_1)_{22} = \langle -2KLN^2STY^2 - 4K^2LN^2STYZmh_2 - 2K^2LN^2STVYZmh_1$$
$$-2K^2LN^2T^2VYZmh_2\left(1+4m^2h_1^2\right) - KLN^2T^2VY^2\left(1+4m^2h_1^2\right)\rangle e^{-2mh_1}e^{6mh_2}e^{-3mH}$$

$$(Denom\,C_1)_{23} = \langle 2KV\left(NZ^2+L\right) - 2NSTXY - 4KNSTVXZmh_1 - 2KST\left(NZ^2 + L\right)$$
$$-8KNSTX^2m^2h_2^2 - 6KNSTVXZmh_1 - 2NVXY - 2KNS^2VX^2 - 2KNVY^2 - 2K^3S^2V\left(NZ^2 + L\right)$$
$$-2KNS^2VX^2 + 12KNSTVX^2m^2h_1h_2 - 2KNSTY^2 + 8K^3STV\left(NZ^2 + L\right)m^2h_1h_2$$
$$-NT^2VXY(1+4m^2h_1^2) - 24KNT^2XZm^3h_1h_2^2 - 6K^2NVYZmh_2 - 6K^2NV^2YZmh_1$$
$$-8KNT^2VX^2m^2h_2^2(1+4m^2h_1^2) - 2KNV^3X^2(1+4m^2h_1^2) - 12KNVX^2m^2h_2^2$$
$$-4K^3V\left(NZ^2 + L\right)m^2h_2^2 + 16K^2NT^2YZmh_2 + 16K^3T^2\left(NZ^2 + L\right)m^4h_1h_2^3 + 8KNT^2VXZm^3h_1^2h_2$$
$$+4KT^2\left(NZ^2 + L\right)m^2h_1h_2 + 32KNT^2X^2m^4h_1h_2^3 + 4KNT^2Y^2m^2h_1h_2 - 4K^2NSTYZmh_2$$
$$-4K^3ST\left(NZ^2 + L\right)m^2h_2^2 + 4KNSTXZmh_2 + 4KNSTVX^2m^2h_1h_2 + 4NT^2XYm^2h_1h_2$$
$$-2NT^2YZmh_1 - KT^2V\left(NZ^2 + L\right)(1+4m^2h_1^2) + 8KNT^2VXZm^3h_1^2h_2 - 8K^2NV^2X^2m^2h_1h_2$$
$$+8KNSTVX^2m^2h_1h_2 - 2K^2NT^2VYZmh_2(1+4m^2h_1^2) - 2K^2NSTYZmh_2 - KNT^2VY^2(1+4m^2h_1^2)$$
$$-8K^3V^2\left(NZ^2 + L\right)m^2h_1h_2 - K^3V^3\left(NZ^2 + L\right)(1+4m^2h_1^2) - 4K^3T^2V\left(NZ^2 + L\right)m^2h_2^2(1+4m^2h_1^2)$$
$$+4KNT^2VXZmh_2(1+4m^2h_1^2) - KNT^2VY^2(1+4m^2h_1^2) - 4KNT^2VX^2m^2h_2^2(1+4m^2h_1^2)$$
$$-KT^2V\left(NZ^2 + L\right)(1+4m^2h_1^2) + 4K^2NSTVYZmh_1 + 4KNVXZmh_2 - 8KNV^2X^2m^2h_1h_2\rangle$$
$$*\,e^{-2mh_1}e^{-2mh_2}e^{mH}$$

$$(Denom\,C_1)_{24} = \langle -2KSVX - 2TY + 12KST^2Xm^2h_1h_2 - 2KS^2TX - 8KTXm^2h_2^2$$
$$-2KTV^2X(1+4m2h_1^2) - 4KT^3Xm^2h_2^2(1+4m2h_1^2) - T^3Y(1+4m2h_1^2) - 8KTVXm^2h_1h_2\rangle$$
$$* e^{-2mh_1}e^{-2mh_2}e^{3mH}$$

$$(Denom\,C_1)_{25} = \langle 32KN^2TV^2X^2Zm^3h_1^2h_2 - 2KNSVX\{NZ^2+L\} - 2KLNSVX - 2N^2SVX^2Y$$
$$+8KNTVX\{NZ^2+L\}m^2h_1h_2 - 8KN^2SV^2X^2Zmh_1 - KNTV^2X\{NZ^2+L\}(1+4m^2h_1^2)$$
$$-4KNTV^2X\{NZ^2+L\}m^2h_1^2 - KLNTV^2X + 4N^2TVX^2Ym^2h_1h_2 - N^2TV^2X^2Y(1+4m^2h_1^2)$$
$$-2KNTVZ\{NZ^2+L\}mh_1 - 2N^2TVXYZmh_1\rangle * e^{-2mh_1}e^{-2mh_2}e^{-mH}$$

$$(Denom\,C_1)_{26} = \langle -3KNSVXY - 2KNTV^2XY(1+4m^2h_1^2) + 8KNTVXYm^2h_1^2 + 16K^2NTV^2XZm^3h_1^2h_2$$
$$+4K^2TV\{NZ^2+L\}m^2h_1h_2 - 2KNTVYZmh_1 - K^2TV^2\{NZ^2+L\}(1+4m^2h_1^2) - 2K^2NSV^2XZmh_1$$
$$-K^2SV\{NZ^2+L\}\rangle * e^{-2mh_1}e^{-4mh_2}e^{mH}$$

$$(Denom\,C_1)_{27} = \langle -2KSTY - 2KVY - 2KT^2VY(1+4m^2h_1^2) + 12K^2STVXm^2h_1h_2 - 2K^2S^2VX$$
$$+4KT^2Ym^2h_1h_2 + 16K^2T^2Xm^4h1h_2^3 - 4K^2STXm^2h_2^2 - 4K^2T^2VXm^2h_2^2(1+4m^2h_1^2) - K^2V^3X(1+4m^2h_1^2)$$
$$-8K^2V^2Xm^2h_1h_2 - 4K^2VXm^2h_2^2\rangle * e^{-2mh_1}e^{-4mh_2}e^{3mH}$$

$$(Denom\,C_1)_{28} = \langle -2K^2SVY + 4K^2TVYm^2h_1h_2 - K^2TV^2Y(1+4m^2h_1^2)\rangle * e^{-2mh_1}e^{-6mh_2}e^{3mH}$$

$$(Denom\,C_1)_{29} = \langle -2T\{NZ^2+L\} - 12NTX^2m^2h_2^2 - 4NTY^2 - 2K^2SV\{NZ^2+L\} - 2KNSVXY$$
$$-2NSVX^2 - 2NS^2TX^2 - 2KNS^2TXY - 2K^2S^2T\{NZ^2+L\} - 6KNTYZmh_2 - 4K^2T\{NZ^2+L\}m^2h_2^2$$
$$+8NTXZmh_2 + 12KNST^2XYm^2h_1h_2 + 12K^2ST^2\{NZ^2+L\}m^2h_1h_2 - 2KNTV^2XY(1+4m^2h_1^2)$$
$$-4K^2NTVZ^2m^2h_1h_2 - 2K^2TV^2\{NZ^2+L\}(1+4m^2h_1^2) - 2NT^3Y^2(1+4m^2h_1^2)$$
$$-6NST^2XZmh_1 + 12NST^2X^2m^2h_1h_2 - 8KNTXYm^2h_2^2 - 24K^2NTVXZm^3h_1h_2^2$$
$$-2K^2NTV^2XZmh_2(1+4m^2h_1^2) - 2K^2NSV^2XZmh_1 - 2KNTVYZmh_1 - 2K^2NSVXZmh_2$$
$$-2KNTYZmh_2 - 16K^2NTXZm^3h_2^3 - 6KNT^3YZmh_2(1+4m^2h_1^2) - NTV^2X^2(1+4m^2h_1^2)$$
$$-8NTVX^2m^2h_1h_2 - 4KNTVYZmh_1 - 4KNTYZmh_2 - 8K^2NT^3XZm^3h_2^3$$
$$+16K^2NST^2XZ - 2K^2NS^2TXZ - 4KNT^3XYm^2h_2^2(1+4m^2h_1^2) - 8KNTVXYm^2h_1h_2$$
$$-NTV^2X^2(1+4m^2h_1^2) - 4K^2T^3\{NZ^2+L\}m^2h_2^2(1+4m^2h_1^2) + 4NT^3XZmh_2(1+4m^2h_1^2)$$
$$-4NT^3X^2m^2h_2^2(1+4m^2h_1^2) - T^3\{NZ^2+L\}(1+4m^2h_1^2) + 4KNST^2YZmh_1 - 8K^2LTVm^2h_1h_2\rangle$$
$$* e^{-2mh_1}e^{mH}$$

$$(Denom\,C_1)_{30} = \langle -2STX - T^2VX(1+4m^2h_1^2)\rangle * e^{-2mh_1}e^{3mH}$$

$$(Denom\,C_1)_{31} = \langle -NSTX\{NZ^2+L\} - LNSTX - NVX\{NZ^2+L\} - LNVX - 2N^2S^2VX^3$$
$$-2N^2STXY^2 - KNSTY\{NZ^2+L\} - KLNSTY - 2K^2NS^2VX\{NZ^2+L\} - 2K^2LNS^2VX$$
$$-2N^2VXY^2 + 8K^2NSTVX\{NZ^2+L\}m^2h_1h_2 - 4K^2N^2STVXZ^2m^2h_1h_2 + 8K^2LNSTVXm^2h_1h_2$$
$$-6KN^2T^2VXYZmh_2(1+4m^2h_1^2) - 4K^2NSTX\{NZ^2+L\}m^2h_2^2 - 4K^2LNSTXm^2h_2^2$$
$$-4KN2STVXYZmh_1 + 32K^2N^2T^2VXZ^2m^4h_1^2h_2^2 + 16KN^2T^2VXYZm^3h_1^2h_2$$
$$+16K^2NT^2X\{NZ^2+L\}m^4h_1h_2^3 + 16K^2LNT^2Xm^4h_1h_2^3 - 4K^2NT^2VX\{NZ^2+L\}m^2h_2^2(1+4m^2h_1^2)$$
$$-4K^2LNT^2VXm^2h_2^2(1+4m^2h_1^2) - 4K^2NVX\{NZ^2+L\}m^2h_2^2 - 4K^2LNVXm^2h_1h_2$$
$$-12K^2NV^2X\{NZ^2+L\}m^2h_1h_2 - 4K^2LNV^2Xm^2h_1h_2 - 6KN^2V^2XYZmh_1 + 16N^2T^2VX^2Zm^3h_1^2h_2$$
$$-2N^2T^2VXY^2(1+4m^2h_1^2) - 8K^2N^2V^3XZ^2m^2h_1^2 - 8NT^2VX\{NZ^2+L\}m^2h_1^2 - NT^2VX\{NZ^2+L\}$$
$$-LNT^2VX - 2KN^2VXYZmh_2 - 2KN^2V^2XYZmh_1 + 16KN^2T^2XYZm^3h_1h_2^2 - 16N^2T^2X^2Zm^3h_1h_2^2$$
$$+4NT^2X\{NZ^2+L\}m^2h_1h_2 + 16N^2T^2X^3m^4h_1h_2^3 + 4N^2T^2XY^2m^2h_1h_2 + 4N^2STVX^3m^2h_1h_2$$
$$-2K^2NSTVX\{NZ^2+L\}mh_1 - 8KN^2T^2YZ^2m^2h_1h_2 - 8K^2NT^2Z\{NZ^2+L\}m^3h_1h_2^2$$
$$-4N^2T^2VXZ^2m^2h_1^2 + 8N^2T^2XZ^2m^2h_1h_2 - 2NT^2Z\{NZ^2+L\}mh_1 - 8N^2T^2X^2Zm^3h_1h_2^2$$
$$-2N^2T^2Y^2Zmh_1 - 2N^2STVX^2mh_1 - 4KN^2STXYZmh_2 - 2N^2STVX^2Zmh_1 + 4N^2STXZmh_2$$
$$-4N^2STX^3m^2h_2^2 + 4KLNT^2Ym^2h_1h_2 - 2K^2NV^2Z\{NZ^2+L\}mh_1 - 2KN^2V^2XYZmh_1$$
$$-2K^2NVZ\{NZ^2+L\}mh_2 - 4K^2N^2V^2XZ^2mh_2 - KNVY\{NZ^2+L\} - K^2LNV^3X(1+4m^2h_1^2)$$
$$+8K^2LNSTVXm^2h_1h_2 - KLNT^2VY(1+4m^2h_1^2) - 2K^2NT^2VZ\{NZ^2+L\}mh_2(1+4m^2h_1^2)$$
$$-2K^2NSTZ\{NZ^2+L\}mh_2 - 2KN^2STXYZmh_2 - KNT^2VY\{NZ^2+L\}(1+4m^2h_1^2)$$
$$-2KN^2STVXYZmh_1 - 2N^2STVX^2Zmh_1 - N^2V^3X^3(1+4m^2h_1^2)$$
$$-K^2NV^3X\{NZ^2+L\}(1+4m^2h_1^2) + 4N^2T^2VX^2Z(1+4m^2h_1^2)$$
$$-4N^2T^2VX^3m^2h_2^2(1+4m^2h_1^2) + 4K^3N^2STVXZ^2mh_1 - 4KN^2VXYZmh_2$$
$$+4N^2VX^2Zmh_2 - 4N^2STVXZmh_1 - 8N^2V^2X^3m^2h_1h_2 - 8N^2VX^3m^2h_2^2$$
$$+8N^2STVX^3m^2h_1h_2\rangle e^{-2mh_1}e^{-mH}$$

$$(Denom\,C_1)_{32} = \langle -2LN^2SVX^2 - 4N^2TV^2X^2\{NZ^2+L\}m^2h_1^2 - 4N^3SV^2X^3Zmh_1$$
$$+16N^3TV^2X^3Zm^3h_1^2h_2 + 4LN^2TVX^2m^3h_1h_2^2 - 4N^3TV^2X^2Z^2m^2h_1^2 - 2LN^2TVXZmh_1\rangle * e^{-2mh_1}e^{-3mH}$$

$$(Denom\,C_1)_{33} = \langle 2NST^2XY + KST^2\{NZ^2+L\} + 2KNST^2XZmh_2\rangle * e^{-4mh_1}e^{2mh_2}e^{mH}$$

$$(Denom\,C_1)_{34} = \langle KNSTVX\{NZ^2+L\} + NT^2Y\{NZ^2+L\} + K^2NSTVY\{NZ^2+L\}$$
$$+4N^2T^2VXYZmh_1 + 8KN^2T^2VXZ^2m^2h_1h_2 + 2N^2STVX^2Y - 8KN^2T^2XZ^2m^2h_2^2$$
$$+4KLNT^2Xm^2h_2^2 + 2K^3NSTVZ\{NZ^2+L\}mh_2 + 8K^2N^2T^2YZ^2m^2h_2^2$$
$$+8K^3NT^2Z\{NZ^2+L\}m^3h_2^3 + 2KN^2T^2Z^3mh_2 + 8KN^2T^2X^2Zm^3h_2^3 + 2KN^2T^2Y^2Zmh_1$$
$$+2KN^2STVX^2Zmh_2 + 4KN^2T^2Y^2Zmh_2 + 4K^2NT^2Y\{NZ^2+L\}m^2h_2^2 - 4N^2T^2XYZmh_2$$
$$+4N^2T^2X^2Ym^2h_2^2 + N^2T^2Y^3 + LNT^2Y + KLNSTVX\rangle e^{-4mh_1}e^{2mh_2}e^{-mH}$$

$$(Denom\,C_1)_{35} = \langle 2LN^2TVXY + 4N^3TV^2X^2YZmh_1 + 8KN^3TV^2X^2Z2m^2h_1h_2 + KLN^2SV^2X^2 + 4KLN^2TVX^2m^2h_2^2 + 2KLN^2TVXZmh_2 \rangle e^{-4mh_1}e^{2mh_2}e^{-3mH}$$

$$(Denom\,C_1)_{36} = \langle KNST^2Y\{NZ^2 + L\} + KLNST^2Y + 2K^2N^2ST^2Z^3mh_2 + 2KN^2ST^2XYZmh_2 + 2K^2LNST^2Zmh_2 + N^2ST^2XY^2 \rangle e^{-4mh_1}e^{4mh_2}e^{-mH}$$

$$(Denom\,C_1)_{37} = \langle 2KLN^2STVXY + 8KN^3T^2VXYZ^2m^2h_1h_2 + 8K^2N^3T^2VXZ^3m^3h^1h_2^2 + 2KLN^2T^2YZmh_2 + 2K^2LN^2STVXZmh_2 + 8K^2LN^2T^2XZmh_2 + 2N^3T^2VXY^2Zmh_1 + LN^2T^2Y^2 + 4KLN^2T^2XYm^2h_2^2 \rangle e^{-4mh_1}e^{4mh_2}e^{-3mH}$$

$$(Denom\,C_1)_{38} = \langle 2K^2LN^2ST^2YZmh_2 + KLN^2ST^2Y^2 \rangle e^{-4mh_1}e^{6mh_2}e^{-3mH}$$

$$(Denom\,C_1)_{39} = \langle 2KNTVY^2 + 2KTV\{NZ^2 + L\} + 2NTVXY + 2KNSV^2X^2 + 4KNTV^2XZmh_1 + 6K^2NTVYZmh_2 + 8KNTVX^2m^2h_2^2 + K^3SV^2\{NZ^2 + L\} + 4K^3TV\{NZ^2 + L\}m^2h_2^2 - 4KNTVXZmh_2 \rangle * e^{-4mh_1}e^{-2mh_2}e^{mH}$$

$$(Denom\,C_1)_{40} = \langle 2KSTVX + T^2Y + 4KT^2Xm^2h_2^2 \rangle e^{-4mh_1}e^{-2mh_2}e^{3mH}$$

$$(Denom\,C_1)_{41} = \langle 4KN^2V^3X^2Zmh_1 + KNV^2X\{NZ^2 + L\} + N^2V^2X^2Y + KLNV^2X \rangle e^{-4mh_1}e^{-2mh_2}e^{-mH}$$

$$(Denom\,C_1)_{42} = \langle 2KNV^2XY + K^2V^2\langle NZ^2 + L\rangle + 2K^2NV^3XZmh_1 \rangle e^{-4mh_1}e^{-4mh_2}e^{mH}$$

$$(Denom\,C_1)_{43} = \langle 2KTVY + K^2SV^2X + 4K^2TVXm^2h_2^2 \rangle e^{-4mh_1}e^{-4mh_2}e^{3mH}$$

$$(Denom\,C_1)_{44} = \langle K^2V^2Y \rangle e^{-4mh_1}e^{-6mh_2}e^{3mH}$$

$$(Denom\,C_1)_{45} = \langle 2KNSTVXY + 2NSTVX^2 + 2NT^2Y^2 + 2K^2STV\{NZ^2 + L\} + 6KNT^2YZmh_2 + 4K^2T^2\{NZ^2 + L\}m^2h_2^2 + 2NT^2VXZmh_1 - 4NT^2XZmh_2 + T^2\{NZ^2 + L\} + 4NT^2X^2m^2h_2^2 + 2KNSTVXZmh_2 + 8K^2NT^2XZm^3h_2^3 + 4KNT^2XYm^2h_2^2 \rangle e^{-4mh_1}e^{mH}$$

$$(Denom\,C_1)_{46} = \langle ST^2X \rangle e^{-4mh_1}e^{3mH}$$

$$(Denom\,C_1)_{47} = \langle NTVX\{NZ^2 + L\} + LNTVX + 2N^2TVXY^2 + 2KLNTVY + K^2NSV^2X\{NZ^2 + L\} + K^2LNSV^2X + 8K^2N^2TV^2XZ^2m^2h_1h_2 + 4N^2TV^2X^2Zmh_1 + 4KN^2TV^2XYZmh_1 + 6KN^2TVXYZmh_2 + 4K^2NTVX\{NZ^2 + L\}m^2h_2^2 + 4K^2LNTVXm^2h_2^2 - 4N^2TVX^2Zmh_2 + 4N^2TVX^3m^2h_2^2 + N^2SV^2X^3 + 2K^2NTVZ\{NZ^2 + L\}mh_2 + KN^2TVYZ^2 \rangle e^{-4mh_1}e^{-mH}$$

$$(Denom\,C_1)_{48} = \langle 2N^3V^3X^3Zmh_1 + LN^2V^2X^2 \rangle e^{-4mh_1}e^{-3mH}$$

$$(Denom\,C_1)_{49} = \Big[2NTVXY + 4KNTVXZ\left(1+2m^2h_1^2\right) + KTV\left\{NZ^2+L\right\} + 2NTVXY\left(1+4m^2h_1^2\right)$$
$$+ KTV\left\{NZ^2+L\right\}\left(1+4m^2h_1^2\right) + KS\left\{NZ^2+L\right\} - 4KNTZ^2m^2h_1h_2 + 2NSXY$$
$$+ 2KNTV^2XZmh_1\left(1+4m^2h_1^2\right) + 4KNSVXZmh_1 + 2KNSXZmh_2\Big\rangle e^{2mh_2}e^{mH}$$

$$(Denom\,C_1)_{50} = \Big\langle 2N^2T^2Y^3\left(1+2m^2h_1^2\right) + 2N^2V^2X^2Y\left(1+2m^2h_1^2\right) - 8N^2T^2XYZmh_2\left(1+2m^2h_1^2\right)$$
$$+ 8N^2T^2X^2Ym^2h_2^2\left(1+2m^2h_1^2\right) + 2N^2STVX^2Y\left(1+2m^2h_1^2\right) + 2N^2S^2X^2Y + 2K^2LNS^2Y$$
$$- 12K^2LNSTYm^2h_1h_2 + 2LNT^2Y\left(1+2m^2h_1^2\right) + 8KLNT^2Xm^2h_2^2 + 16KLNT^2Xm^4h_1^2h_2^2$$
$$+ 2KN^2T^2Y^2Zmh_2 - 8KNSTX\left\{NZ^2+L\right\}m^2h_1h_2 - 4KLNSTXm^2h_1h_2 + 8KN^2STXZ^2m^2h_1h_2$$
$$+ 24K^3NVZ\left\{NZ^2+L\right\}m^3h_1h_2^2 + 4KN^2T^2Y^2Zmh_2 - 16KN^2T^2XZ^2m^2h_2^2\left(1+2m^2h_1^2\right)$$
$$+ 2KN^2STVX^2Zmh_2 - 16KN^2STVX^2Zm^3h_1^2h_2 + 16K^2N^2T^2YZ^2m^2h_2^2\left(1+2m^2h_1^2\right)$$
$$+ 2KN^2T^2Y^2Zmh_2\left(1+2m^2h_1^2\right) + 2KN^2T^2Y^2Zmh_2 + 6KN^2VY^2Zmh_1 + 24K^2N^2VYZ^2m^2h_1h_2$$
$$+ 6KN^2Y^2Zmh_2 + 12K^2N^2YZ^2m^2h_2^2 - 16K^2N^2STYZ^2m^2h_1h_2 + 2K^3NT^2Z\left\{NZ^2+L\right\}m^3h_2^3$$
$$+ 6K^3LNT^2Zm^3h_2^3 + 2K^3NSTVZ\left\{NZ^2+L\right\}mh_2 + 2KNT^2Zmh_2\left\{NZ^2+L\right\}mh_2$$
$$+ 2KN^2T^2X^2Zm^3h_2^3 + 4K^2NT^2YZ^2m^2h_2^2 + K^2NSTVY\left\{NZ^2+L\right\} + NT^2\left\{NZ^2+L\right\}$$
$$+ 4K^2LNTYm^2h_2^2 + KNV^2X\left\{NZ^2+L\right\} + KLNSTVX + K^2LNV^2Y - 4N^2T2VX^2Ym^2h_1h_2\left(1+4m^2h_1^2\right)$$
$$- 4KNT^2VX\left\{NZ^2+L\right\}m^2h_1h_2\left(1+4m^2h_1^2\right) + 16KN^2T^2XZ^2m^4h_1^2h_2^2 - 4N^2STX^2Ym^2h_1h_2$$
$$+ 2N^2T^2VXYZmh_1\left(1+4m^2h_1^2\right) + 2KNT^2VZ\left\{NZ^2+L\right\}mh_2\left(1+4m^2h_1^2\right) + 2KN^2STZ^3mh_1$$
$$- 8KN^2T^2Z^3m^3h_1^2h_2 + 2N^2STXYZmh_1 + 2KLNSTZmh_1 + KNSTVX\left\{NZ^2+L\right\}\left(1+4m^2h_1^2\right)$$
$$+ KN^2S^2XZ^2 + KLNS^2X + KLNV^2X\left(1+4m^2h_1^2\right) + 2N^2VXYZmh_1 + 8KLNVXm^2h_1h_2$$
$$+ KLNS^2X + 4KLNXm^2h_2^2 - 4K^2LNT^2VYm^2h_1h_2\left(1+4m^2h_1^2\right) + K^2LNSTVY\left(1+4m^2h_1^2\right)$$
$$+ 2KN^2V^3X^2Zmh_1\left(1+4m^2h_1^2\right) + 16K^3N^2V^2Z^3m^3h_1^2h_2 + 2K^3NV^3Z\left\{NZ^2+L\right\}mh_1\left(1+4m^2h_1^2\right)$$
$$+ 8K^3NT^2VZ\left\{NZ^2+L\right\}m^3h_1h_2^2\left(1+4m^2h_1^2\right) - 8KN^2T^2VXZ^2m^2h_1h_2\left(1+4m^2h_1^2\right)$$
$$+ 8K^2N^2T^2VYZ^2m^2h_1h_2\left(1+4m^2h_1^2\right) + 2KN^2T^2VY^2Zmh_1\left(1+4m^2h_1^2\right) - 8K^3N^2STVZ^3m^3h_1^2h_2$$
$$- 2K^3N^2S^2VZ^3mh_1 + 8KN^2T^2VX^2Zm^3h_1h_2^2\left(1+4m^2h_1^2\right) + 2KNT^2VZ\left\{NZ2+L\right\}m^2h_2h_1\left(1+4m^2h_1^2\right)$$
$$- 8K^2N^2STVYZ^2m^2h_1^2 + 8K^2N^2V^2YZ^2m^2h_1^2 - 8KN^2VXZ^2m^2h_1h_2 + 2KNVZ\left\{NZ^2+L\right\}mh_1$$
$$+ 8KN^2STVXZ^2m^2h_1^2 + 16KN^2V^2X^2Zm^3h_1^2h_2 + 16KN^2VX^2Zm^3h_1h_2^2 + 16K^3LNV^2Z^3m^3h_1^2h_2$$
$$+ 2KNS^2VX^2Zmh_1 - 16K^3LNSTVZmh_1 + 2K^3LNS^2VZmh_1 + 2KN^2V^2X^2Zmh_2\left(1+4m^2h_1^2\right)$$
$$+ 16K^3N^2VZ^3m^3h_1h_2^2 + 2K^3NV^2Z\left\{NZ^2+L\right\}mh_2\left(1+4m^2h_1^2\right) + 8K^3NT^2Z\left\{NZ^2+L\right\}m^3h_2^2\left(1+4m^2h_1^2\right)$$
$$- 16K^3N^2STZ^3m^3h_1h_2^2 + 2K^3N^2S^2Z^3mh_2 + 8KN^2T^2X^2Zm^3h_2^2\left(1+4m^2h_1^2\right)$$
$$+ 2KNT^2Z\left\{NZ^2+L\right\}mh_2\left(1+4m^2h_1^2\right) + 8K^3N^2Z^3m^3h_2^3 - 8KN^2XZ^2m^2h_2^2 + 2KNZ\left\{NZ^2+L\right\}mh_2$$
$$+ 16KN^2VX^2Zm^3h_1h_2^2 + 16KN^2X^2Zm^3h_2^3 + 8K^3LNZm^3h_2^3 - 16KN^2STX^2Zm^3h_1h_2^2$$
$$+ 2KN^2S^2X^2Zmh_2 - 16K^3LNSTZm^3h_1h_2^2 + 2K^3LNS^2Zmh_2 + K^2NV^2Y\left\{NZ^2+L\right\}\left(1+4m^2h_1^2\right)$$
$$+ 4K^2NT^2Y\left\{NZ^2+L\right\}m^2h_2^2\left(1+4m^2h_1^2\right) + K^2N^2S^2YZ^2 + NT^2Y\left\{NZ^2+L\right\}\left(1+4m^2h_1^2\right)$$
$$- 4KN^2STY^2Zmh_1 - 4N^2XYZmh_2 + N^2YZ^2 + LNY + 4N^2STXYZmh_1 + 8N^2VX^2Ym^2h_1h_2$$
$$+ 8N^2X^2Ym^2h_2^2 - 2N^2VXYZmh_1 + 8K^2LNVYm^2h_1h_2 + 4K^2LNYm^2h_2^2 - 8N^2STX^2Ym^2h_1h_2$$
$$+ N^2Y^3\Big\rangle e^{2mh_2}e^{-mH}$$

$$(Denom\,C_1)_{51} = \langle 2LN^2TVXY(1+2m^2h_1^2) - 16KN^2TV^2X^2\{NZ^2+L\}m^4h_1^2h_2^2 - 4KLN^2TV^2X^2m^2h_1h_2$$
$$- 24KN^2TVX^2\{NZ^2+L\}m^4h_1^2h_2^2 - 8KLN^2TVX^2m^4h_1^2h_2^2 - 4KN^2SV^2X^2\{NZ^2+L\}m^2h_1^2$$
$$- KLN^2SV^2X^2 - 4KN^2SVX^2\{NZ^2+L\}m^2h_1h_2 - 4KLN^2SVX^2m^2h_1h_2 - 8KN^2TVXZm^3h_1^2h_2$$
$$- 8KLN^2TVXZm^3h_1^2h_2 - 16KN^3TV^2X^2Z^2m^4h_1^3h_2 - 16N^3TVX^2YZm^3h_1^2h_2 - 4LN^2ST^2XYm^2h_1^2$$
$$+ 4KLN^2TVX^2m^2h_2^2 + KLN^2SV^2X^2 + 2KLN^2ST^2XZmh_2 - 16KLN^2T^3X^2m^4h_1h_2^3(1+4m^2h_1^2)$$
$$+ 32KLN^2ST^2X^2m^4h_1^2h_2^2 - 4LN^2T^3XYm^2h_1h_2(1+4m^2h_1^2) - 4KLN^2STX^2m^2h_1h_2$$
$$- 16KLN^2TX^2m^4h_1h_2^3 - 8KLN^2T^3XZm^3h_1h_2^2(1+4m^2h_1^2) - 8KN^2TV^2XZ\{NZ^2+L\}m^3h_1^3$$
$$- 2KLN^2TV^2XZmh_1 + 16KLN^2ST^2XZm^3h_1^2h_2 - 2LN^2T^3YZmh_1(1+4m^2h_1^2)$$
$$- 2KLN^2S^2TXZmh_1 - 8KLN^2TXZm^3h_1h_2^2 - KLN^2ST^2X^2m^2h_2^2(1+4m^2h_1^2) + 8KLN^2S^2TX^2m^2h_1h_2$$
$$- KLN^2S^3X^2 - 4KLN^2SX^2m^2h_2^2 + 8KN^2TV^2XZ\{NZ^2+L\}m^3h_1^3 + 2KLN^2TV^2XZmh_1$$
$$+ 2KLN^2SVXZmh_1 + 4KN^3SV^2X^2Z^2m^2h_1^2 + 8KN^2TVXZ^3m^3h_1^2h_2 + KLN^2TVXZmh_2(1+4m^2h_1^2)$$
$$+ 2KLN^2SXZmh_2 + 4KN^3SVX^2Z^2m^2h_1h_2 + LN^2SXY\rangle e^{2mh_2}e^{-3mH}$$

$$(Denom\,C_1)_{52} = \langle 2KLNSY + 2KNTVY\{NZ^2+L\}(1+2m^2h_1^2) + 2KLNTVY(1+2m^2h_1^2)$$
$$+ 2N^2TVXY^2(1+2m^2h_1^2) + 4K^2NTVZ\{NZ^2+L\}mh_2(1+2m^2h_1^2) + 4KN^2TVXYZmh_2(1+2m^2h_1^2)$$
$$+ 2KN^2TV^2XYZmh_1(1+4m^2h_1^2) + 2K^2NTV^2Z\{NZ^2+L\}mh_1(1+4m^2h_1^2) + 2K^2NSVZmh_1\{NZ^2+L\}$$
$$- 8K^2N^2TVZ^3m^3h_1^2h_2 + 2KN^2SVXYZmh_1 + 2K^2NSZ\{NZ^2+L\}mh_2 - 8K^2N^2TZ^3m^3h_1h_2^2$$
$$+ 2KN^2SXYZmh_2 + KN^2SYZ^2 - 4KN^2TYZ^2m^2h_1h_2 + N^2SXY^2\rangle e^{4mh_2}e^{-mH}$$

$$(Denom\,C_1)_{53} = \langle 2KLN^2S^2XY + 4KLN^2T^2YZ\{NZ^2+L\}mh_2(1+4m^2h_1^2) - 4KLN^2STXYm^2h_1h_2$$
$$+ KLN^2STVXY(1+4m^2h_1^2) + 8KLN^2T^2XYm^2h_2^2(1+2m^2h_1^2) + 2K^2LN^2STVXZmh_2$$
$$- 16K^2LN^2STVXZm^3h_1^2h_2 + 16K^2LN^2STVXZm^3h_1^2h_2 + 16K^2LN^2VXZm^3h_1h_2^2 + 2K^2LNS^2VXZmh_1$$
$$+ 2K^2LN^2S^2XZmh_2 + 8K^2N^2VXZ\{NZ^2+L\}m^3h_1h_2^2 + 8KN^3V^2XYZ^2m^2h_1^2 + 16K^2N^3V^2XZ^3m^3h_1^2h_2$$
$$+ 4KLN^2T^2VYZmh_1(1+4m^2h_1^2) + 16K^2LN^2T^2XZm^3h_2^2(1+2m^2h_1^2) + 2KLN^2V^2XY(1+2m^2h_1^2)$$
$$+ KLN^2T^2Y^2 + 8K^2LN^2T^2VXZm^3h_1h_2^2(1+4m^2h_1^2) + 8K^2N^2V^3XZ\{NZ^2+L\}m^3h_1^2$$
$$+ 2K^2LN^2V^3XZmh_1 + 2K^2LN^2V^2XZmh_2(1+4m^2h_1^2) - 16K^2LN^2STXZm^3h_1h_2^2$$
$$+ 4KN^3VXYZ^2m^2h_1h_2 + 8K^2LN^2XZm^3h_2^3 - 8KLN^2STXYm^3h_1h_2^2 + LN^2T^2Y^2(1+4m^2h_1^2)$$
$$+ 2N^3VXY^2Zmh_1 + 4KN^3VXYZ^2m^2h_1h_2 + 4KLN^2XYm^2h_2^2 + 8KLN^2VXYm^2h_1h_2$$
$$- 4KLN^2T^2VXY(1+4m^2h_1^2) + 2KLN^2STYZmh_1\rangle * e^{4mh_2}e^{-3mH}$$

$$(Denom\,C_1)_{54} = \langle 4K^2LN^2TVYZmh_2(1+2m^2h_1^2) + 2KLN^2TVY^2(1+2m^2h_1^2) + 2KLN^2SVYZmh_1$$
$$+ 2K^2LN^2TV^2YZmh_1(1+4m^2h_1^2) + 2K^2LN^2SYZmh_2 + KLN^2SY^2\rangle e^{6mh_2}e^{-3mH}$$

$$(Denom\,C_1)_{55} = \langle 2KNSY^2 + 2NTVXY(1+2m^2h_1^2) + 2NSXY + 12KNSX^2m^2h_2^2 + 2KNS^3X^2$$
$$+ 2NST^2XY(1+2m^2h_1^2) + 2KNSV^2X^2(1+2m^2h_1^2) + KNSV^2X^2 + 2KNTVY^2(1+2m^2h_1^2)$$
$$+ 16KNSVX^2m^2h_1h_2 - 16KNS^2TX^2m^2h_1h_2 + 16KNTVXZm^3h_1^2h_2 + 64KNST^2X^2m^4h_1^2h_2^2$$
$$- 8KNS^2TX^2m^2h_1h_2 - 48KNTX^2m^4h_1h_2^3 - 8KNTV^2X^2m^2h_1h_2(1+4m^2h_1^2)$$
$$- 16KNT^3X^2m^4h_1h_2^3(1+2m^2h_1^2) - 16KNT^3X^2m^2h_2^2(1+4m^2h_1^2) + 24KNT^3XZm^3h_1h_2^2(1+4m^2h_1^2)$$
$$+ 24KNTXZm^3h_1h_2^2 + 6KNS^2TXZmh_1 + 2K^2NTVYZmh_2(1+4m^2h_1^2) - 16K^2NTVYZm^3h_1^2h_2$$
$$+ 6K^2NSVYZmh_1 + 6K^2NSYZmh_2 + 8KNST^2X^2m^2h_2^2(1+4m^2h_1^2) + 6K^2NST^2YZmh_2$$
$$+ 2KNST^2Y2(1+2m^2h_1^2) + 4K^3TV\{NZ^2+L\}m^2h_2^2 + 4K^2NTVYZmh_2 + K^3SV^2\{NZ^2+L\}$$
$$- 4KNTVXZmh_2 + KTV\{NZ^2+L\} + 4KNTVX^2m^2h_2^2 + KST^2\{NZ^2+L\} + 4KNTVX^2m^2h_2^2$$
$$+ KTV\{NZ^2+L\}(1+4m^2h_1^2) + KS\{NZ^2+L\} - 4NT^3XYm^2h_1h_2(1+4m^2h_1^2)$$
$$- 32KNTVX^2m^4h_1^2h_2^2 - 4NTXYm^2h_1h_2 + 2NT^3YZmh_1(1+4m^2h_1^2) + 2KNTV^2XZmh_1(1+4m^2h_1^2)$$
$$- 16KNSTXZm^3h_1^2h_2 + 2NTYZmh_1 + 2K^2NTV^2YZmh_1(1+4m^2h_1^2) - 32K^3TV\{NZ^2+L\}m^4h_1h_2^3$$
$$- 4K^3TV^2m^2h_1h_2\{NZ^2+L\}(1+4m^2h_1^2) - 16K^3T^3\{NZ^2+L\}m^4h_1h_2^3(1+4m^2h_1^2)$$
$$- 16K^2NT^3YZm^3h_1h_2^2(1+4m^2h_1^2) + 32K^3ST^2\{NZ^2+L\}m^4h_1^2h_2^2 - 4K^3NS^2TZ^2$$
$$- 4KT^3m^2h_1h_2\{NZ^2+L\}(1+4m^2h_1^2) + 16K^2NST^2YZm^3h_1^2h_2 - 16K^2NTYZm^3h_1h_2^2$$
$$- 16K^3T\{NZ^2+L\}m^4h_1^2h_2^2 - 4KT\{NZ^2+L\}m^2h_1h_2 - 16KNST^2XZm^3h_1^2h_2$$
$$- 32KNTVX^2m^4h_1^2h_2^2 - KNTY^2m^2h_1h_2 - 4K^3LS^2Tm^2h_1h_2 + KNSV^2X^2(1+4m^2h_1^2)$$
$$+ 8K^3NS^2TZ^2m^2h_1h_2 + K^3SV^2\{NZ^2+L\}(1+4m^2h_1^2) + 4K^3ST^2\{NZ^2+L\}m^2h_2^2(1+4m^2h_1^2)$$
$$- 4KNST^2XZmh_2(1+4m^2h_1^2) - 8K^3NS^2TZ^2m^2h_1h_2 + K^3S^3\{NZ^2+L\}$$
$$+ KST^2\{NZ^2+L\}(1+4m^2h_1^2) - 4K^2NS^2TYZmh_1 + 4K^3NSZ^2m^2h_2^2 - 4KNSXZmh_2$$
$$+ KS\{NZ^2+L\} + 8K^3LSVm^2h_1h_2 + 4K^2LSm^2h_1h_2 - 8K^3LS^2Tm^2h_1h_2\rangle e^{-2mh_2}e^{mH}$$

$$(Denom\,C_1)_{56} = \langle 2KV^2X(1+2m^2h_1^2) + 2KS^2X + 2KSTVX + 2T^2Y(1+2m^2h_1^2) - 12KSTXm^2h_1h_2$$
$$+ 8KT^2Xm^2h_2^2(1+2m^2h_1^2) + 8KVXm^2h_1h_2 + 4KXm^2h_2^2 + Y - 4KT^2VXm^2h_1h_2(1+4m^2h_1^2)\rangle e^{-2mh_2}e^{3mH}$$

$$(Denom\,C_1)_{57} = \langle 2KLNSTVX(1+2m^2h_1^2) + 2KNSTVX\{NZ^2+L\}(1+2m^2h_1^2) - 16KN^2STVX^2Zm^3h_1^2h_2$$
$$+ 4KN^2S^2VX^2Zmh_1 + 8KN^2STVXZ^2m^2h_1^2 - 16KN^2STVX^2Zm^3h_1^2h_2 + 64KN^2T^2VX^2Zm^5h_1^3h_2^2$$
$$- 4KNSTX\{NZ^2+L\}m^2h_1h_2 - 4KLNSTXm^2h_1h_2 - 32KN^2T^2VXZ^2m^4h_1^3h_2 - 4N^2STX^2Ym^2h_1h_2$$
$$- 4N^2STX^2Ym^2h_1^2 - 4KNT^2VXm^2h_1h_2\{NZ^2+L\}(1+4m^2h_1^2) - 4N^2T^2VX^2Ym^2h_1h_2(1+4m^2h_1^2)$$
$$+ 2KNT^2VZmh_1\{NZ^2+L\}(1+4m^2h_1^2) + KN^2STZ^3mh_1 + 2KLNSTZmh_1 + 2N^2T^2VXYZmh_1(1+4m^2h_1^2)$$
$$+ 2N^2STXYZmh_1 + KNS^2X\{NZ^2+L\} - N^2S^2X^2Y - 4KLNT^2VXm^2h_1h_2(1+4m^2h_1^2) + KLNS^2X\rangle$$
$$* e^{-2mh_2}e^{-mH}$$

$$(Denom\,C_1)_{58} = \langle 2KNS^2XY + 2KNSTVXY(1+4m^2h_1^2) + 2KNSTVXY - 8KNSTXYm^2h_1h_2$$
$$- 8KNT^2VXYm^2h_1h_2(1+4m^2h_1^2) - 16K^2NSTVXZm^3h_1^2h_2 + 2K^2STV\{NZ^2+L\}(1+2m^2h_1^2)$$
$$- 4K^2T^2Vm^2h_1h_2\{NZ^2+L\}(1+4m^2h_1^2) - 4K^2ST\{NZ^2+L\}m^2h_1h_2 + 32K^2NT^2VXZm^5h_1^3h_2^2$$
$$+ 2K^2NS^2VXZmh_1 + K^2S^2\{NZ^2+L\} + 2KNT^2VYZmh_1(1+4m^2h_1^2) + 2KNSTYZmh_1\rangle e^{-4mh_2}e^{mH}$$

$$(Denom\,C_1)_{59} = \langle 2KSY + 2KTVY\left(1+2m^2h_1^2\right) + 2K^2SV^2X\left(1+2m^2h_1^2\right) - 12K^2S^2TXm^2h_1h_2$$
$$+ 2KST^2Y\left(1+2m^2h_1^2\right) + 4K^2TVXm^2h_2^2 - 4K^2TV^2Xm^2h_1h_2\left(1+4m^2h_1^2\right) + 32K^2ST^2Xm^4h_1^2h_2^2$$
$$+ 4K^2ST^2Xm^2h_2^2\left(1+4m^2h_1^2\right) - 16K^2T^3Xm^4h_1h_2^3\left(1+4m^2h_1^2\right) - 4KT^3Ym^2h_1h_2\left(1+4m^2h_1^2\right)$$
$$- 32K^2TVXm^4h_1^2h_2^2 - 16K^2TXm^4h_1h_2^3 - 4KTYm^2h_1h_2 + 8K^2SVXm^2h_1h_2 + 4K^2SXm^2h_2^2 + K^2S^3X\rangle$$
$$* e^{-4mh_2}e^{3mH}$$

$$(Denom\,C_1)_{60} = \langle 2K^2STVY\left(1+4m^2h_1^2\right) - 4K^2T^2VYm^2h_1h_2\left(1+4m^2h_1^2\right) - 4K^2STYm^2h_1h_2 + K^2S^2Y\rangle$$
$$* e^{-6mh_2}e^{3mH}$$

$$(Denom\,C_1)_{61} = \langle 2K^2S^2\left\{NZ^2+L\right\} + 2KNS^2XY + 4NT^2Y^2\left(1+2m^2h_1^2\right) + 2NY^2 - 8K^2ST\left\{NZ^2+L\right\}m^2h_1h_2$$
$$- 4K^2NSTZ^2m^2h_1h_2 + 12KNT^2YZmh_2\left(1+2m^2h_1^2\right) - 8NT^2XZmh_2\left(1+2m^2h_1^2\right) + 2KNV^2XY\left(1+2m^2h_1^2\right)$$
$$+ 6KNVYZmh_1 + 2KNSTVXY\left(1+2m^2h_1^2\right) - 12KNSTXYm^2h_1h_2 + 8K^2T^2\left\{NZ^2+L\right\}m^2h_2^2\left(1+2m^2h_1^2\right)$$
$$+ 16K^2NT^2Z^2m^4h_1^2h_2^2 + 16K^2NT^2XZm^3h_2^3\left(1+2m^2h_1^2\right) + 6NSTXZmh_1 + 2NS^2X^2$$
$$+ 8KNT^2XZm^2h_2^2\left(1+2m^2h_1^2\right) - 4KNT^2VXYm^2h_1h_2\left(1+4m^2h_1^2\right) + 2KNYZmh_2 + 2K^2NSTVXZmh_2$$
$$- 16K^2NSTVXZm^3h_1^2h_2 + 2K^2V^2\left\{NZ^2+L\right\}\left(1+2m^2h_1^2\right) + 2K^2STV\left\{NZ^2+L\right\}\left(1+2m^2h_1^2\right)$$
$$+ 2T^2\left\{NZ^2+L\right\}\left(1+2m^2h_1^2\right) + NSTV^2 + 4NT^2X^2m^2h_2^2 + NV^2X^2 - 4K^2T^2V\left\{NZ^2+L\right\}m^2h_1h_2\left(1+4m^2h_1^2\right)$$
$$+ 8K^2NT^2VXZm^3h_1h_2^2\left(1+4m^2h_1^2\right) + 2KNT^2VYZmh_1\left(1+4m^2h_1^2\right) + 2K^2NV^3XZmh_1\left(1+4m^2h_1^2\right)$$
$$+ 16K^2NV^2XZm^3h_1^2h_2 + 8K^2NVXZm^3h_1h_2^2 + 2K^2NS^2VXZmh_1 + 2K^2NV^2XZmh_2\left(1+4m^2h_1^2\right)$$
$$+ 8K^2NXZm^3h_2^3 - 16K^2NSTXZm^3h_1h_2^2 + 16K^2NVXZm^3h_1h_2^2 + 2K^2NS^2XZmh_2 + 8KNVXYm^2h_1h_2$$
$$+ 4KNXYm^2h_2^2 - 4NT^2VX^2m^2h_1h_2\left(1+4m^2h_1^2\right) - 4NSTX^2m^2h_1h_2 + 2NT^2XZmh_1\left(1+4m^2h_1^2\right)$$
$$+ NSTVX^2\left(1+4m^2h_1^2\right) + NV^2X^2\left(1+4m^2h_1^2\right) + 8K^2NVZ^2m^2h_1h_2 + 4NT^2X^2m^2h_2^2\left(1+4m^2h_1^2\right)$$
$$- 4KNSTYZmh_1 + 4K^2\left\{NZ^2+L\right\}m^2h_2^2 - 4NXZmh_2 + \left\{NZ^2+L\right\} + 8NVX^2m^2h_1h_2$$
$$+ 8NX^2m^2h_2^2 - 2NVXZmh_1 + 8K^2LVm^2h_1h_2 - 8NSTX^2m^2h_1h_2\rangle e^{mH}$$

$$(Denom\,C_1)_{62} = \langle 2TVX\left(1+2m^2h_1^2\right) + SX\rangle e^{3mH}$$

$$
\begin{aligned}
(Denom\,C_1)_{63} = \Big\langle & -16K^2N^2TV^2XZm^4h_1^3h_2 - 16K^2N^2TVXZm^4h_1^2h_2^2 + 4K^2NSV^2X\left\{NZ^2+L\right\}\left(1+4m^2h_1^2\right) \\
& + K^2LNSV^2X - 4K^2NS^2TX\left\{NZ^2+L\right\}m^2h_1h_2 - 8K^2LNS^2TXm^2h_1h_2 + KNST^2Y\left\{NZ^2+L\right\} \\
& + KLNST^2Y\left(1+4m^2h_1^2\right) + K^2NSV^2X\left\{NZ^2+L\right\} + K^2LNSV^2X + 6K^2NSVX\left\{NZ^2+L\right\}m^2h_1h_2 \\
& + 2K^2LNSVXm^2h_1h_2 - 32K^3NTV^2X\left\{NZ^2+L\right\}m^4h_1^3h_2 - 4K^3NTV^2Xm^2h_1h_2\left\{NZ^2+L\right\} \\
& - 4K^2LNTV^2Xm^2h_1h_2 - 16K^2NT^3X\left\{NZ^2+L\right\}m^4h_1h_2^3\left(1+4m^2h_1^2\right) - 16K^2LNT^3Xm^4h_1h_2^3\left(1+4m^2h_1^2\right) \\
& + 32K^2NST^2X\left\{NZ^2+L\right\}m^4h_1^2h_2^2 + 4K^2LNST^2Xm^2h_2^2\left(1+4m^2h_1^2\right) + NSX\left\{NZ^2+L\right\} + LNSX \\
& + 32N^2TX^2Zm^3h_1h_2^2 - 32K^2LNTXm^4h_1h_2^3 + 16N^2TVX^2Zm^3h_1^2h_2 + NTVX\left\{NZ^2+L\right\}\left(1+4m^2h_1^2\right) \\
& + LNTVX - 4N^2TVXZ^2m^2h_1^2 - NST^2X\left\{NZ^2+L\right\}\left(1+4m^2h_1^2\right) + LNST^2X - N^2T^3XZ^2mh_1\left(1+4m^2h_1^2\right) \\
& - 4NT^3X\left\{NZ^2+L\right\}m^2h_1h_2\left(1+4m^2h_1^2\right) + 4K^2NTVX\left\{NZ^2+L\right\}m^2h_2^2 + 4K^2LNTVXm^2h_2^2 \\
& + KLNTVY + KNTVY\left\{NZ^2+L\right\}\left(1+4m^2h_1^2\right) + 8KN^2TVYZ^2m^2h_1^2 + 2N^2TVXY^2\left(1+2m^2h_1^2\right) \\
& - 16N^2ST^2X^2Zm^3h_1^2h_2 - 4N^2ST^2X^2Z\left(1+4m^2h_1^2\right) + 2N^2ST^2XY^2\left(1+2m^2h_1^2\right) + 4KN^2SVXYZmh_1 \\
& + K^2NS^3X\left\{NZ^2+L\right\} + K^2LNS^3X - 8KN^2TVXYZm^3h_1^2h_2 + 2KN^2TV^2XYZmh_1\left(1+4m^2h_1^2\right) \\
& + 4K^2NSX\left\{NZ^2+L\right\}m^2h_2^2 + 4K^2N^2SV^2XZ^2m^2h_1^2 + K^2NSV^2X\left\{NZ^2+L\right\}\left(1+4m^2h_1^2\right) \\
& + 2K^2NSVZ\left\{NZ^2+L\right\}mh_1 + 8K^2LNSVXm^2h_1h_2 + 2K^2NTVZmh_2\left\{NZ^2+L\right\}\left(1+4m^2h_1^2\right) \\
& + 16K^2NTVZ\left\{NZ^2+L\right\}m^3h_1^2h_2 - 32K^2NTVX\left\{NZ^2+L\right\}m^4h_1^2h_2^2 - 8K^2N^2TVXZ^2m^4h_1^2h_2^2 \\
& + 16N^2T^3X^2Zm^2h_1h_2\left(1+4m^2h_1^2\right) + 8N^2T^3X^2Zm^3h_1h_2^2\left(1+4m^2h_1^2\right) + 4KN^2TVXYZmh_2 \\
& - 4N^2TVX^2mh_2 + N^2SV^2X^3 + 4N^2TVX^3m^2h_2^2 + 2K^2NST^2Z\left\{NZ^2+L\right\}mh_2 \\
& + 2KN^2ST^2XYZmh_2 - 4KLNT^3Ym^2h_1h_2\left(1+4m^2h_1^2\right) + 2K^2NTV^2Zmh_1\left\{NZ^2+L\right\}\left(1+4m^2h_1^2\right) \\
& + 2K^2NSZ\left\{NZ^2+L\right\}mh_2 + 2KN^2TVXYZmh_2\left(1+4m^2h_1^2\right) + 2KN^2SXYZmh_2 \\
& + 2KN^2SVXYZmh_1 + KNSY\left\{NZ^2+L\right\} - 8KN^2TVXYm^3h_1^2h_1 + 2N^2SXY^2 \\
& - 4N^2TV^2X^3m^2h_1h_2\left(1+4m^2h_1^2\right) - 16KN^2T^3XYZm^3h_1h_2^2\left(1+4m^2h_1^2\right) - 4N^2T^3XY^2m^2h_1h_2\left(1+4m^2h_1^2\right) \\
& - 16N2T3X3m4h1h_2^3\left(1+4m2h1\right) + 16KN2ST2XYZm3h_1^2h2 - 16KN2TVXYZm3h_1^2h2 \\
& - 16KN2TXYZm3h1h_2^2 - 16K2N2TXZ2m4h1h_2^3 - 4NTX\left\{NZ2+L\right\}m2h1h2 - 16N2ST2X2Zm3h_1^2h2 \\
& - 32N2TVX3m4h_1^2h_2^2 - 32N2TX3m4h1h_2^3 - 32K2LNTVXm4h_1^2h_2^2 + 32N2STX3m4h_1^2h_2^2 \\
& - 4N^2S^2TX^3m^2h_1h_2 - 4N^2TXY^2m^2h_1h_2 + 32K^3LNST^2Xm^4h_1^2h_2^2 - K^2LNS^2TXm^2h_1h_2 \\
& + 2N^2TV^2X^2Zmh_1\left(1+4m^2h_1^1\right) + 2K^2NTV^2Zmh_1\left\{NZ^2+L\right\}\left(1+4m^2h_1^2\right) \\
& + 8K^2NT^3Z\left\{NZ^2+L\right\}m^3h_1h_2^2\left(1+4m^2h_1^2\right) + 8KN^2T^3YZ^2m^2h_1h_2\left(1+4m^2h_1^2\right) \\
& + 2N^2T^3Y^2Zmh_1\left(1+4m^2h_1^2\right) - 16K^2NST^2Z\left\{NZ^2+L\right\}m^3h_1^2h_2 + 2K^2NS^2TZ\left\{NZ^2+L\right\}mh_1 \\
& - 2NT^3Z\left\{NZ^2+L\right\}mh_1\left(1+4m^2h_1^2\right) - 8KN^2ST^2YZ^2m^2h_1^2 + 8KN^2TYZ^2m^2h_1h_2 \\
& + 8K^2NTZ\left\{NZ^2+L\right\}m^3h_1^2h_2 - 8N^2TXZ2m^2h_1h_2 + 2NTZ\left\{NZ^2+L\right\}mh_1 + 8N^2ST^2XZ^2m^2h_1^2 \\
& + 2N^2S^2TX^2Zmh_1 + N^2TY^2Zmh_1 + N^2SV^2X^3\left(1+4m^2h_1^2\right) + 8K^2NSVXZ^2m^2h_1h_2 \\
& + 4K^2NST^2X\left\{NZ^2+L\right\}m^2h_2^2\left(1+4m^2h_1^2\right) + 4KNST^2XYZmh_2\left(1+4m^2h_1^2\right) \\
& - 8K^2NS^2TX\left\{NZ^2+L\right\}m^2h_1h_2 + 4N^2ST^2X^3m^2h_2^2\left(1+4m^2h_1^2\right) - 4KN^2S^2TXYZmh_1 \\
& + 4KN^2SVXYZmh_1 + 4KN^2SXYZmh_2 - 4N^2SX^2Zmh_2 + 4N^2S^2TX^2Zmh_1 \\
& + 8N^2SVX^3m^2h_1h_2 + 8N^2SX^3m^2h_2^2 + 4K^2LNSXm^2h_1h_2 - 8N^2S^2TX^3m^2h_1h_2 \\
& + N^2S^3X^3\Big\rangle e^{3mH}
\end{aligned}
$$

$$(Denom\,C_1)_{64} = \langle 2LN^2STVX^2(1+2m^2h_1^2) - 32N^3T^2VX^2Z^2m^4h_1^3h_2 - 16N^3STVX^3Zm^3h_1^2h_2 - 4LN^2T^2VX^2m^2h_1h_2(1+4m^2h_1^2) - 4LN^2STX^2m^2h_1h_2 + 32N^3T^2VX^3Zm^5h_1^3h_2^2 + 8N^3T^2VXZ^3m^3h_1^3 + 2LN^2T^2VXZmh_1(1+4m^2h_1^2) + 2LN^2STXZ + 4N^3STVX^2Z^2m^2h_1^2 + 4N^3STVX^2Z^2m^2h_1^2 + LN^2S^2X^2 + 2N^3S^2VX^3Zmh_1\rangle e^{-3mH}$$

A.2 Final terms of constant D_1

$$D_1m = \frac{Numerator\ D_1}{Denominator\ D_1} = \left\{ \frac{-\left(\sum_{i=1}^{18}(Num\ D_1)_i\right)}{\sum_{i=1}^{27}(Denom\ D_1)_i} \right\}$$

A.2.1 The list of Numerator D_1

$$(Num\ D_1)_1 = \langle -4KNTYZmh_2 - 4K^2NTZ^2m^2h_2^2 - K^2NSVZ^2 - K^2LSV + 4NTXZmh_2 - NTZ^2 - 4K^2LTm^2h_2^2 - NSVX^2 - LT - NTY^2\rangle e^{mh1}$$

$$(Num\ D_1)_2 = \langle -KNVZ^2 - NVXY - KLV\rangle e^{mh_1}e^{2mh_2}$$

$$(Num\ D_1)_3 = \langle -KLNSVX - 4KLNTXm^2h_2^2 - LNTY\rangle e^{mh_1}e^{2mh_2}e^{-2mH}$$

$$(Num\ D_1)_4 = \langle -KLNVY\rangle e^{mh_1}e^{4mh_2}e^{-2mH}$$

$$(Num\ D_1)_5 = \langle -KNSTZ^2 - KLST - NSTXY\rangle e^{mh_1}e^{-2mh_2}$$

$$(Num\ D_1)_6 = \langle -4KTXm^2h_2^2 - KSVX - TY\rangle e^{mh_1}e^{-2mh_2}e^{2mH}$$

$$(Num\ D_1)_7 = \langle -KSTY\rangle e^{mh_1}e^{-4mh_2}e^{2mH}$$

$$(Num\ D_1)_8 = \langle -VX\rangle e^{mh_1}e^{2mH}$$

$$(Num\ D_1)_9 = \langle -LNSTX\rangle e^{mh_1}e^{-2mH}$$

$$(Num\ D_1)_{10} = \langle 4NT^2X^2m^2h_2^2(1-2mh_1) - 4NT^2XZmh_2(1-2mh_1) + T^2(NZ^2+L)(1-2mh_1) + K^2V^2(NZ^2+L)(1-2mh_1) + 4K^2T^2(NZ^2+L)(1-2mh_1) + 4KNT^2YZmh_2(1-2mh_1) + KNSTYZ + NT^2Y^2(1-2mh_1) + 2K^2NSTZ^2mh_2 - KNVYZ - 2K^2NVZ^2mh_2 + NV^2X^2(1-2mh_1) - 2NVX^2mh_2 + NVXZ - 2K^2LVmh_2 + 2NSTX^2mh_2 + NSTXZ + 2K^2LSTmh_2\rangle e^{-mh1}$$

$$(Num\ D_1)_{11} = \left\langle KTV\left(NZ^2 + L\right)(1-2mh_1) + NTVXY(1-2mh_1)\right\rangle e^{-mh_1} e^{2mh_2}$$

$$(Num\ D_1)_{12} = \left\langle KLNT^2 Xm^2 h_2^2 (1-2mh_1) + KLNV^2 X(1-2mh_1) + LNT^2 Y(1-2mh_1) + 2KLNSTXmh_2 - 2KLNVXmh_2\right\rangle e^{-mh_1} e^{2mh_2} e^{-2mH}$$

$$(Num\ D_1)_{13} = \left\langle KLNTVY(1-2mh_1)\right\rangle e^{-mh_1} e^{4mh_2} e^{-2mH}$$

$$(Num\ D_1)_{14} = \left\langle KTV\left(NZ^2 + L\right)(1-2mh_1) + NTVXY(1-2mh_1)\right\rangle e^{-mh_1} e^{-2mh_2}$$

$$(Num\ D_1)_{15} = \left\langle 4KT^2 Xm^2 h_2^2 (1-2mh_1) + KV^2 X(1-2mh_1) + T^2 Y(1-2mh_1) - 2KVXmh_2 + 2KSTXmh_2\right\rangle e^{-mh_1} e^{-2mh_2} e^{2mH}$$

$$(Num\ D_1)_{16} = \left\langle KTVY(1-2mh_1)\right\rangle e^{-mh_1} e^{-4mh_2} e^{2mH}$$

$$(Num\ D_1)_{17} = \left\langle TVX(1-2mh_1)\right\rangle e^{-mh_1} e^{2mH}$$

$$(Num\ D_1)_{18} = \left\langle LNTVX(1-2mh_1)\right\rangle e^{-mh_1} e^{-2mH}$$

A.2.2 The list of Denominator D_1

$$(Denom\ D_1)_1 = \left\langle 4K^2 NTZ^2 m^2 h_2^2 + 4KNTYZmh_2 + K^2 NSVZ^2 + K^2 LSV - 4NTXZmh_2 + T\left(NZ^2 + L\right) + NSVX^2 + NTY^2 + 4NTX^2 m^2 h_2^2 + 4K^2 LTm^2 h_2^2\right\rangle e^{2mh_1}$$

$$(Denom\ D_1)_2 = \left\langle KV\left(NZ^2 + L\right) + NVXY\right\rangle e^{2mh_1} e^{2mh_2}$$

$$(Denom\ D_1)_3 = \left\langle 4KLNTXm^2 h_2^2 + KLNSVX + LNTY\right\rangle e^{2mh_1} e^{2mh_2} e^{-2mH}$$

$$(Denom\ D_1)_4 = \left\langle KLNVY\right\rangle e^{2mh_1} e^{4mh_2} e^{-2mH}$$

$$(Denom\ D_1)_5 = \left\langle KST\left(NZ^2 + L\right) + NSTXY\right\rangle e^{2mh_1} e^{-2mh_2}$$

$$(Denom\ D_1)_6 = \left\langle KSVX + TY + 4KTXm^2 h_2^2\right\rangle e^{2mh_1} e^{-2mh_2} e^{2mH}$$

$$(Denom\ D_1)_7 = \left\langle KSTY\right\rangle e^{2mh_1} e^{-4mh_2} e^{2mH}$$

$$(Denom\ D_1)_8 = \left\langle VX\right\rangle e^{2mh_1} e^{2mH}$$

$$(Denom\ D_1)_9 = \left\langle LNSTX\right\rangle e^{2mh_1} e^{-2mH}$$

$$(Denom\ D_1)_{10} = \left\langle K2SV\left(NZ^2+L\right)+4KNTYZmh_2+4K^2T\left(NZ^2+L\right)m^2h_2^2+NTY^2+NSVX^2 \right.$$
$$\left. -4NTXZmh_2+T\left(NZ^2+L\right)+4NTX^2m^2h_2^2\right\rangle e^{-2mh_1}$$

$$(Denom\ D_1)_{11} = \left\langle KST\left(NZ^2+L\right)+NSTXY\right\rangle e^{-2mh_1}e^{2mh_2}$$

$$(Denom\ D_1)_{12} = \left\langle 4KN^2TVXZ^2m^2h_1h_2+2N^2TVXYZmh_1+LNTY+KLNSVX+4KLNTXm^2h_2^2\right\rangle$$
$$*\,e^{-2mh_1}e^{2mh_2}e^{-2mH}$$

$$(Denom\ D_1)_{13} = \left\langle KLNSTY\right\rangle e^{-2mh_1}e^{4mh_2}e^{-2mH}$$

$$(Denom\ D_1)_{14} = \left\langle KV\left(NZ^2+L\right)+2KNV^2XZmh_1+NVXY\right\rangle e^{-2mh_1}e^{-2mh_2}$$

$$(Denom\ D_1)_{15} = \left\langle KSVX+TY+4KTXm^2h_2^2\right\rangle e^{-2mh_1}e^{-2mh_2}e^{2mH}$$

$$(Denom\ D_1)_{16} = \left\langle KVY\right\rangle e^{-2mh_1}e^{-4mh_2}e^{2mH}$$

$$(Denom\ D_1)_{17} = \left\langle STX\right\rangle e^{-2mh_1}e^{2mH}$$

$$(Denom\ D_1)_{18} = \left\langle 2N^2V^2X^2Zmh_1+LNVX\right\rangle e^{-2mh_1}e^{-2mH}$$

$$(Denom\ D_1)_{19} = \left\langle -NTVXY\left(1+4m^2h_1^2\right)-KTV\left(NZ^2+L\right)\left(1+4m^2h_1^2\right)-KS\left(NZ^2+L\right)\right.$$
$$\left. +4KNTZ^2m^2h_1h_2-NSXY\right\rangle e^{2mh_2}$$

$$(Denom\ D_1)_{20} = \left\langle -4KLNT^2Xm^2h_2^2\left(1+4m^2h_1^2\right)-4KN^2V^2XZ^2m^2h_1^2-KLNV^2X\left(1+4m^2h_1^2\right)\right.$$
$$+8KLNSTXm^2h_1h_2-LNT^2Y\left(1+4m^2h_1^2\right)-2N^2VXYZmh_1-4KN^2VXZ^2m^2h_1h_2$$
$$\left. -8KLNVXm^2h_1h_2-KLNS^2X-4KLNXm^2h_2^2\right\rangle e^{2mh_2}e^{-2mH}$$

$$(Denom\ D_1)_{21} = \left\langle -KLNSY-KLNTVY\left(1+4m^2h_1^2\right)\right\rangle e^{4mh_2}e^{-2mH}$$

$$(Denom\ D_1)_{22} = \left\langle -KTV\left(NZ^2+L\right)\left(1+4m^2h_1^2\right)-2KNSVXZmh_1-KS\left(NZ^2+L\right)\right.$$
$$\left. +8KNTVXZm^3h_1^2h_2-NTVXY\left(1+4m^2h_1^2\right)-NSXY\right\rangle e^{-2mh_2}$$

$$(Denom\ D_1)_{23} = \left\langle -4KT^2Xm^2h_2^2\left(1+4m^2h_1^2\right)-T^2Y\left(1+4m^2h_1^2\right)-KV^2X\left(1+4m^2h_1^2\right)\right.$$
$$\left. -8KVXm^2h_1h_2-4KXm^2h_2^2+8KSTXm^2h_1h_2-KS^2X-Y\right\rangle e^{-2mh_2}e^{2mH}$$

$$(Denom\ D_1)_{24} = \left\langle -KTVY\left(1+4m^2h_1^2\right)-KSY\right\rangle e^{-4mh_2}e^{2mH}$$

$$(Denom\ D_1)_{25} = \left\langle -TVX\left(1+4m^2h_1^2\right)-SX\right\rangle e^{2mH}$$

$$(Denom\ D_1)_{26} = \langle -4N^2TVXZ^2m^2h_1^2 - LNTVX\left(1+4m^2h_1^2\right) - LNSX + 8N^2TVX^2Zm^3h_1^2h_2$$
$$-2N^2SVX^2Zmh_1\rangle e^{-2mH}$$

$$(Denom\ D_1)_{27} = \langle -NV^2X^2\left(1+4m^2h_1^2\right) - 8K^2V\left(NZ^2+L\right)m^2h_1h_2 - K^2V^2\left(NZ^2+L\right)\left(1+4m^2h_1^2\right)$$
$$-4K^2T^2\left(NZ^2+L\right)m^2h_2^2\left(1+4m^2h_1^2\right) + 4NT^2XZmh_2\left(1+4m^2h_1^2\right) - 4KNT^2YZmh_2\left(1+4m^2h_1^2\right)$$
$$-NT^2Y^2\left(1+4m^2h_1^2\right) + 8K^2ST\left(NZ^2+L\right)m^2h_1h_2\left(1+4m^2h_1^2\right) - K^2S^2\left(NZ^2+L\right)$$
$$-4NT^2X^2m^2h_2^2\left(1+4m^2h_1^2\right) - T^2\left(NZ^2+L\right)\left(1+4m^2h_1^2\right) + 4KNSTYZmh_1 - 4KNVYZmh_1$$
$$-4KNYZmh_2 - 4K^2\left(NZ^2+L\right)m^2h_2^2 + 4NXZmh_2 - \left(NZ^2+L\right) - 4NSTXZmh_1 - 8NVX^2m^2h_1h_2$$
$$-4NX^2m^2h_2^2 + 2NVXZmh_1 + 8NSTX^2m^2h_1h_2 - NS^2X^2 - NY^2\rangle$$

APPENDIX B

LIST OF PAPERS RELATED WITH THIS STUDY

B.1 Publication in Journal

S/N	Paper Title	Year	Name of Journal
1	Evaluation of Backcalculation Methods for Nondestructive Determination of Concrete Properties	2006	Transportation Research Record Volume 1949, pp. 83-97
2	Consideration of Finite Slab Size in Backcalculation Analysis of Jointed Concrete Pavements	2007	Transportation Research Record Volume 2005, pp. 124-142
3	Examining k-E Relationship of Pavement Subgrade Based on Load-Deflection Consideration	2009	Journal of Transportation Engineering Volume 135, Issue 3, pp. 140-148

B.2 Presented in Conference

S/N	Paper Title	Year	Name of Conference
1	Statistical Evaluation for Backcalculation of Concrete Pavement Properties	2007	Special International Conference on Pavement Technology (ICPT) on Road Construction and Maintenance Technology Beijing, China.
2	Backcalculation Analysis of Rigid Pavement Properties Considering Presence of Subbase Layer	2008	The 87th Annual Meeting, Transportation Research Board Washington D.C.
3	Influence of Slab Thickness Variation on Backcalculation of Concrete Pavement Properties	2008	the 1st International Conference on Transportation and Infrastructure (ICTI) Beijing, China
4	Estimating Modulus of Subgrade Reaction for Rigid Pavement Design	2009	The 8th Eastern Asia Society for Transportation Studies (EASTS) Surabaya, Indonesia